DEVELOPMENT OF ENVIRONMENTALLY FRIENDLY EPOXY RESIN COMPOSITES

Doctoral thesis
Hungarian Academy of Sciences

Toldy Andrea

Department of Polymer Engineering
Budapest University of Technology and Economics

2017

Toldy Andrea

Doctoral thesis

Hungarian Academy of Sciences

Development of environmentally friendly epoxy resin composites

ISBN 978-963-313-262-3

Budapest University of Technology and Economics
Department of Polymer Engineering

Budapest University of Technology and Economics

Department of Polymer Engineering

Development of environmentally friendly epoxy resin composites

Doctoral thesis

Hungarian Academy of Sciences

Toldy Andrea

2017

CONTENTS

ABBREVIATIONS

APP	ammonium polyphosphate
AR917	methyltetrahydrophthalic anhydride
ATR-IR	attenuated total reflection infrared spectrometry
BAMPO	bis(3-aminophenyl)methylphosphine oxide
BAPP	bis(4-aminophenyl)phenylphosphonate
BPA	bisphenol A
CE	cyanate ester
CF	carbon fibre
DDM	4,4'-diaminodiphenylmethane
DDS	4,4'-diaminodiphenylsulphone
DETDA	diethyl-methylbenzene-diamine
DFT	density functional theory
DGEBA	diglycidyl ether of bisphenol A
DGEBF	diglycidyl ether of bisphenol F
DMA	dynamic mechanical analysis
DOPO	9,10-dihydro-9-oxa-10-phosphaphenanthrene-10-oxide
DSC	differential scanning calorimetry
dTG_{max}	maximum mass loss rate
DTGS	deuterated triglycine sulphate
DY070	1-methylimidazole
EAS	epoxidized allyl soyate
ECO	epoxidized castor oil
EDA	ethylenediamine
EHC	average effective heat of combustion
EHO	epoxidized hemp oil
ELO	epoxidized linseed oil
EMS	epoxidized methyl soyate
EP	epoxy resin
ESO	epoxidized soybean oil
EVO	epoxidized vegetable oil
FIGRA	fire growth rate
FR	flame retardant
FTIR	Fourier transform infrared spectrometry
GER	triglycidyl ether of glycerol
GFTE	glucofuranoside triglycidyl ether
GPBE	glucopyranoside biglycidyl ether
GPQE	glucopyranoside tetraglycidyl ether
GPTE	glucopyranoside triglycidyl ether
IFSS	interfacial shear strength
IPN	interpenetrating polymer network
LOI	limiting oxygen index
LP-FTIR	laser pyrolysis - Fourier transform infrared spectrometry coupled method

MALDI TOF	matrix assisted laser desorption/ionization technique
MARHE	maximum of average rate of heat emission
N	nitrogen
NaOH	sodium hydroxide
NHF	non-modified hemp fabric
NMR	nuclear magnetic resonance
P	phosphorus
PER	tetraglycidyl ether of pentaerythritol
PFR	phosphorus-containing flame retardants
phr	parts per hundred
pHRR	peak of heat release rate
PT-30	cyanated phenol-formaldehyde oligomer
*p*TsOH	*p*-toluenesulfonic acid
R	universal gas constant [8.314 J/mol K]
RDP	resorcinol bis(diphenyl phosphate)
RTM	resin transfer moulding
Si	silicone
SiTHF	silane and thermotex-treated hemp fabric
SPE	sorbitol polyglycidyl ether
$T_{-5\%}$	temperature at 5% mass loss
$T_{-50\%}$	temperature at 50% mass loss
T58	3,3'-dimethyl-4,4'-diaminodicyclohexylmethane
tan δ	loss factor, ratio of loss modulus to storage modulus
TAPP	tris-(3-aminophenyl)-phosphate
TBBPA	tetrabromobisphenol A
T_{dTGmax}	temperature belonging to maximum mass loss rate
TEDAP	*N,N',N"*-tris(2-aminoethyl)-phosphoric triamide
TEP	triethyl phosphate
TETA	triethylenetetramine
T_g	glass transition temperature
TGA	thermogravimetric analysis
TGDDM	4,4'-tetraglycidyldiaminodiphenylmethane
THF	thermotex-treated hemp fabric
THR	total heat released
TMPDAP	*N,N',N"*-tris(3-aminophenyl)-phosphoric triamide
TMS	tetramethylsilane
TOPDAP	*N,N',N"*-tris(2-aminophenyl)-phosphoric triamide
TPSA	topological polar surface area
TTI	time to ignition
V/V%	volume percent
VRTM	vacuum-assisted resin transfer moulding

1. INTRODUCTION, AIMS

Epoxy resins (EPs), as typical representatives of thermosetting polymers, have found use in numerous industrial applications since their commercialization in 1946, including surface coatings, castings, laminates, adhesives and polymer composites. They provide an exceptional balance of mechanical and chemical properties, such as high strength, toughness, chemical and electrical resistance, low shrinkage on cure and high adhesion to many substrates, combined with outstanding processing versatility [1,2,3]. Due to these properties they are also of particular interest in structural polymer composite applications, where their technical advantages balance their relatively high price level compared to other commodity thermosetting matrices.

The tendency towards replacement of mineral oil based polymers and reinforcements by bio-based ones has emerged also in polymer composite industry. Depleting mineral oil sources initiated increasing environmental awareness and legislations aiming at fostering the use of renewable resources, which is reflected in rapidly increasing need for bio-based polymers and composites. By definition, bio-based composites are those composites, in which at least one of the components is originating from biological products issued from biomass [4]. This means that polymer composites, in which either the matrix or the reinforcement is bio-based, can be already considered as bio-based, nevertheless, it is essential to distinguish these “partial bio-based” materials from the “completely bio-based” or “all-bio” composites. Also, it has to be noted, that bio-based polymer composites are not necessarily biodegradable, as the ability of being degraded by biological activity depends not on the origin, but rather on the chemical structure. In the case of polymer products the end of the use must be predictable, providing structural and functional stability during their entire service time, which requires controlled degradation even by biological activity. As the biodegradable feature is only relevant in the case of all-bio composites, where both the polymer matrix and the reinforcement are biodegradable, other end of life options have to be considered as well. Besides reuse and energy recovery, recycling should be addressed [5]. In the case of thermosetting bio-based composites, if only the polymer matrix is biodegradable, the conventional routes as mechanical and thermal (with energy and/or material recovery) recycling are available [6]. In the case of natural fibre reinforcement the recovery of the fibres is not possible by thermal processes; however composites made from biofibres can be completely burnt, which is a clear advantage over conventional glass or carbon fibres. Furthermore, the use of biofibres offers the advantage of becoming fully biodegradable by combining natural fibres with a biodegradable thermosetting polymer matrix.

The main deficiency of these bio-based composites, similarly to mineral oil based ones, is their flammability during their use. The thermal stability and flammability of epoxy resins depends on the structure of the epoxy monomer, of the curing agent, on the crosslink density achieved, as well as on the applied modifiers used to provide specific physical, mechanical and other properties both in uncured and cured resins [7]. In order to meet the strict safety requirements of more demanding sectors as automotive and aircraft industries, the flame retardant (FR) properties of epoxy resins have to be improved, possibly by maintaining other important characteristics as mechanical and thermal properties, and also considering environmental issues as risks for human life and environment, waste treatment and recycling. The application of halogenated components is a highly effective method for the preparation of flame retarded systems. However, the increasing focus on health and environmental compatibility of FRs has led to a massive decline in the acceptance of these products. The concept of sustainable development applied to this field involves that FRs should have low impact on health and environment during the entire life cycle. According to the directives of the European Parliament from July 2006 the most used halogenated flame retardants are banned from the market [8]. Considering all these issues tremendous amount of research and development has been dedicated to replace these halogen-containing FRs by halogen-free products e.g. by phosphorus-containing flame retardants (PFRs). Phosphorus, depending on the molecular structure of the FR, can act both in gas phase, predominantly at the beginning of degradation, and later in solid phase, providing advantageous FR effect for polymers by this combined mechanism. Environmental studies were recently carried out on additive type PFRs [9]. The reactive type FRs, being bonded to polymer macromolecules, have probably no adverse effect, as they do not migrate to the matrix surface either during high temperature processing or application. Furthermore, compared to the additive approach less FR is needed to achieve same level of flame retardancy, which also leads to the reduction of toxic gas emission. Additionally, multifunctional reactive FRs can be cost-effectively integrated into the production process as well.

In the case of biocomposites, the use of natural reinforcement is a reasonable solution. The natural fibre reinforcement represents a green and suitable alternative to the glass and carbon fibres (produced with high energy consumption) in several fields of application; however, their low thermal stability and flammability represents a major drawback. In order to decrease their flammability, FR fibre treatments have to be applied, in such a way, that the achieved FR properties do not decrease the fibre–matrix adhesion and the mechanical properties of the biocomposites.

In the light of all these reflected issues, the current work aimed at the development of environmentally friendly epoxy resin composites in the following ways:

1. Synthesis of novel bio-based epoxy monomers capable of replacing the currently most used mineral oil based benchmark materials in terms of glass transition temperature, mechanical and thermal properties.
2. Synthesis of phosphorus-containing epoxy monomers and crosslinking agents providing environmentally friendly, reactive flame retardancy solutions for epoxy resins and their composites.
3. Development and characterization of partially and fully bio-based epoxy resin systems capable of replacing mineral oil based benchmark systems in terms of glass transition temperature, mechanical and thermal properties.
4. Development and characterization of carbon fibre and natural fibre reinforced composites from partially and fully bio-based epoxy resin systems, capable of replacing mineral oil based composites in terms of glass transition temperature, mechanical and thermal properties.
5. Elaboration of green flame retardancy solutions both for benchmark and bioepoxy resins using phosphorus-containing flame retardants in additive and reactive form.
6. Elaboration of green flame retardancy solutions for carbon fibre and natural fibre reinforced composites, including the flame retardancy of the natural fibres itself.
7. Testing the applicability of the developed solutions for industrial purposes, in particular in non-structural and structural aircraft applications.

2. LITERATURE OVERVIEW

This chapter summarizes state of the art on the development of environmentally friendly epoxy resin composites. First, synthesis and application possibilities of bio-based epoxy monomers are overviewed, followed by recent achievements in the field of all-bio epoxy resin composites. Finally, green flame retardancy solutions for epoxy resin composites, including synthesis of phosphorus-containing epoxy monomers and crosslinking agents, as well as fire retardant modifications of bioepoxy resins and biofibres, are summarized.

2.1. Bio-based epoxy monomers

In the past few years intensive research work has been carried out on the partial or full replacement of the mineral oil based epoxy monomers, such as diglycidyl ether of bisphenol A (DGEBA), with renewable ones in thermosetting polymers [10]. Decreasing amount of mineral oil stock, increasing environmental awareness and legislations aiming at fostering the use of renewable resources all supported this direction of development. Besides the fossil origin, the recognized estrogenic properties of bisphenol A (BPA) also intensify the research activities in this field [11]. Bio-based epoxy resin components are currently produced from different bio-based sources [12], such as vegetable oils, lignin, tannin, cardanol, terpene and carbohydrate, which are summarized in the followings.

2.1.1. Vegetable oil based bioepoxy monomers

One of the most common solutions to prepare bio-based epoxy resins is the epoxidation of different vegetable oils, which are basically fatty acid esters of glycerol [13,14,15]. Among these plant oil derivatives, epoxidized soybean oil (ESO) is probably the most investigated one in polymer composite applications, as it is used in large quantities mostly in polyvinyl chloride manufacturing as plasticizer.

To receive epoxy-functionalized vegetable oils, the carbon-carbon double bonds have to be epoxidized. There are four general methods for the epoxidization of oils: epoxidation with percarboxylic acids; with inorganic or organic peroxides; with halohydrines; or with molecular oxygen [16]. According to the assumption of Rangarajan et al. [17], the mechanism of the epoxidation comprises three steps. The formation of the peracetic acid is the first step, followed by the reaction between the percarboxylic acid and the double bonds, and, finally, hydrolysing side-reactions take place. The main reaction is the addition of the oxygen from the percarboxylic acid to the carbon-carbon double bond, which results in the formation of the oxirane group and is

always accompanied by side-reactions (**Figure 2.1.1**). These reactions, which lead to the opening of the oxirane group, can be induced by several different compounds, including the percarboxylic acids present in the reaction mixture, the carboxylic acids formed from the percarboxylic acids during the epoxidation, traces of moisture, and the potentially produced hydrogen peroxide. All of these components can be nucleophiles, which can cause the opening of the oxirane ring, attacking the carbon atom of the three-membered ring.

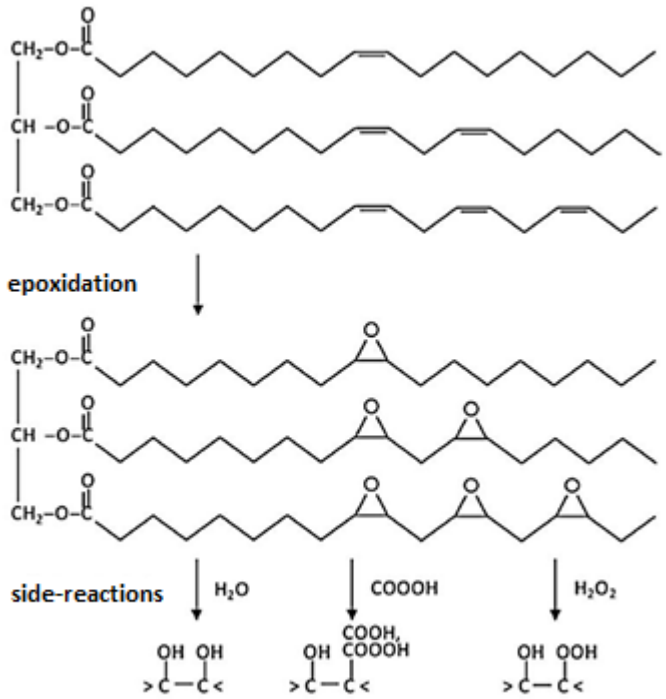

Figure 2.1.1 Epoxidation reaction of vegetable oils [17]

Kim and Sharma proposed a solvent-free method for the preparation of several epoxidized plant oils [18]. The epoxidation of linseed oil, cottonseed oil, soybean oil, peanut oil and oilseed radish oil were carried out with good conversion and high selectivity.

Ratna [19] investigated the effect of ESO on a DGEBA-based epoxy resin system cured with triethylenetetramine (TETA). With a pre-curing step, the ESO-content of 20% significantly increased the impact strength of the DGEBA system. Above this content, with 30% ESO-content, the impact strength decreased.

Zhu et al. [20] investigated epoxidized methyl soyate (EMS), epoxidized allyl soyate (EAS) and ESO with a synthetic epoxy resin component as base resin cured with *p*-amino cyclohexyl methane. With the addition of 10% of EAS, the mechanical properties and the glass transition temperature (T_g) values improved remarkably.

Amine and anhydride cured epoxidized triglycerides, epoxidized linseed oil (ELO) and DGEBA were compared by Earls et al. [21]. The epoxidized triglycerides were much tougher than the ELO and the DGEBA cured with 4,4'-diaminodiphenylmethane (DDM).

In the case of the ESO/DGEBA epoxy resin system, cured with DDM, the increasing ESO-content and higher curing temperature resulted in higher porosity, while higher amount of curing agent led to lower porosity in the specimen structure [22].

With *p*-aminobenzoic acid curing agent, the increased ESO-content improved the toughness of the DGEBA-based epoxy system and decreased its T_g values [23].

Park et al. replaced 5, 10, 15 and 20% of 4,4'-tetraglycidyldiaminodiphenylmethane (TGDDM) by ESO [24]. The T_g values decreased slightly with the increasing amount of ESO, from 277 °C of the reference TGDDM cured with DDM to 258 °C for the 20% ESO-containing resin, while the critical stress intensity factor, related to the toughness of the samples, could be increased by 150%.

Epoxidized castor oil (ECO) was blended in different ratios with DGEBA [25]. The ECO-content of the different formulations was 10, 20, 30 and 40%. The T_g decreased from 197 °C of the reference system to 169, 158, 150 and 131 °C with increasing amount of ECO, while the toughness of the samples significantly increased.

Various types of anhydrides were also used in case of bio-based epoxy resins as curing agent [26]. Some authors reported phase separation, decreased T_g values and increasing toughness of epoxidized vegetable oil (EVO) based systems compared to the neat synthetic diglycidyl ether of bisphenol F (DGEBF) [27] or DGEBA [28,29,30] epoxy resin systems.

2.1.2. Lignin based bioepoxy monomers

The main components of plant biomass are cellulose (35-50%), hemicellulose (25-35%), and lignin (15-30%), which are connected to one another via covalent bonds to form lignocellulose. After cellulose, lignin is the second most abundant macromolecule in the nature, which is produced in large quantities as a by-product of the paper industry.

Lignin itself can be considered as a cross-linked phenolic polymer structure. Due to the steric hindrance, it cannot be directly reacted to form bioresins [31], therefore lignin-based epoxy monomers are prepared from liquefied lignin. There are various thermochemical methods for the "depolymerisation" of lignin [32,33], such as fast or vacuum pyrolysis, liquefaction and solvolysis, leading to smaller phenolic molecules, which can be more easily converted to bio-based resins. During the solvolysis, the most commonly applied reagents are phenol [34,35,36], resorcinol [37,38] and the mixture of poly(ethylene glycol) and glycerol [39,40]. Usually, these molecules are

added to the lignin in 1:1 mass ratio, and the reaction takes place by applying 2-3% sulphuric acid. The received liquefied lignin is reacted with epichlorohydrin in strong basic conditions.

Hofmann and Glasser [41] reacted the pre-treated lignin first with propylene oxide, in order to improve the solubility, and then the product was reacted with ethylene oxide, resulting in primary hydroxyl groups instead of the former secondary ones. These primary hydroxyl groups were then reacted with epichlorohydrin, resulting in lignin-based epoxy monomer. Above 50% lignin content the *m*-phenylene diamine cured systems had similar mechanical properties as DGEBA. Feng and Chen [35] prepared phenolated lignin-based epoxy monomer, which was mixed with DGEBA in 10-50%, and then cured with triethylenetetramine (TETA). The application of lignin-based epoxy monomer increased the adhesive shear strength of DGEBA.

When the solvolysis was carried out using resorcinol, the resulting epoxy resins showed similar mechanical properties to DGEBA, both when cured with DDS (4,4'-diaminodiphenylsulphone) [37] or with DDM (4,4'-diaminodiphenylmethane) [38].

2.1.3. Tannin and cardanol based bioepoxy monomers

Tannins are natural polyphenolic materials [42], which are usually subdivided into two main groups based on their chemical structure: hydrolysable tannins and proanthocyanidins, often called as condensed tannins as well [43]. Among hydrolysable tannins gallotannins are esters of gallic acid and polyols (usually D-glucose), while ellagitannnins are esters of ellagic acid and polyols. Proanthocyanidins are oligomers or polymers consisting of flavonoid (flavan-3-ol) units, which are linked to each other by non-hydrolysable carbon-carbon bonds. Among tannin derivatives, the transformation of catechol and gallic acid to bioepoxy monomers has the widest literature.

Epoxy monomers have been synthesized from green tea extract [44], tara tannins [45] and catechol [46,47] by the reaction with epichlorohydrin. However, due to the different reactivity of the hydroxyl groups and some side reactions, no fully alkylated product could be obtained.

Another approach for the preparation of glycidyl ether function is to react the –OH groups with allyl bromide, followed by the epoxidation of the carbon-carbon double bonds. By applying this method, the side reactions can be avoided, and fully alkylated products can be obtained, leading to higher functionality, thus higher cross-link density, and higher T_g [48].

Cardanol (**Figure 2.1.2**), available in large quantities from vacuum distillation of cashew nut shell liquid, is mixture of 4 phenol derivatives having 15 carbon atoms long differently saturated alkyl chains in the *meta* position: 3-n-pentadecylphenol, 3-(pentadeca-8-enyl)phenol, 3-(pentadeca-8,11-dienyl)phenol and 3-(pentadeca-8,11,14-trienyl)phenol [49,50].

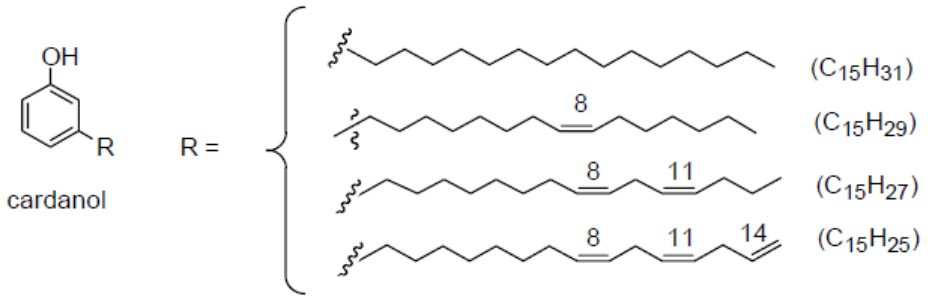

Figure 2.1.2 Structure of cardanol [based on 50]

From cardanol monoglycidyl ether can be prepared by reacting its phenolic OH-group with epichlorohydrin, while the carbon-carbon double bounds can be epoxidized, or reacted with formaldehyde to obtain novolac type epoxy resin [51,52].

Cardanol monoglycidyl ether was synthesized in the presence of NaOH by reacting the phenolic OH-group with epichlorohydrin [53], with 60% conversion due to the lower reactivity of the OH-group in cardanol than the one in phenol. The received monofunctional epoxy resin was mixed to DGEBA crosslinked with polyamine, and acted as reactive plasticizer resulting in a less rigid product.

In a two-step reaction, diepoxy monomer can be synthesized from cardanol. First, phenol was reacted with the double bonds of the unsaturated side chain in the presence of a strong acid (HBF_4), and then the received diphenol was converted to the corresponding bifunctional epoxy molecule with epichlorohydrin [54].

With the application of *Candida Antarctica* lipase enzyme, the double bonds of the side chain can also be epoxidized using H_2O_2 as oxidizing agent [55].

2.1.4. Terpene based bioepoxy monomers

Terpenes are naturally occurring unsaturated hydrocarbons consisting of isoprene units.

Among terpenes, limonene, which is a cyclic diterpene having carbon-carbon double bonds both in the 6-membered ring and in its side chains, is one of the most abundant ones. By the epoxidation of double bounds in limonene mono or bifunctional epoxy monomers can be obtained, already available as commercial products [56,57].

Xu et al. [58] synthesized epoxy monomers by linking two naphthalene moieties with limonene, reacting the received adduct with formaldehyde to give a novolac type molecule, which was further reacted with epichlorohydrin. The obtained epoxy monomer was cured with dicyandiamide, resulting in an epoxy resin with high T_g and good thermal stability.

The two main components of the rosin acids, abietic and pimaric acid (**Figure 2.1.3**) having hydrophenanthrene structures, can be converted to versatile derivatives due to the presence of carbon-carbon double bonds and acid function.

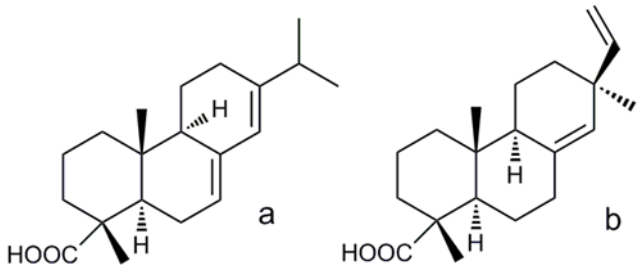

Figure 2.1.3 Structure of abietic and pimaric acid

Liu et al. [59] prepared trifunctional epoxy monomers from abietic acid by addition of maleic anhydride in Diels-Alder reaction to the double bond rearranged due to heat, and subsequent reaction of the adduct with epichlorohydrin. By using the intermediate anhydride as curing agent a fully bio-based epoxy resin was obtained, which had similar mechanical properties as the benchmark DGEBA resin.

Mantzaridis et al. [60] synthesized different epoxy functional molecules from rosin acids, both by the epoxidation of the double bonds with *m*-chloroperbenzoic acid and by esterification of the acid functions by glycidyl alcohol. The received epoxy monomers were mixed to DGEBA, and the effect of bioepoxy resins on the T_g was examined. According to their results, 40% of rosin based resin lead to the lowest decrease in T_g values.

2.1.5. Carbohydrate based bioepoxy monomers

The presence of highly reactive hydroxyl group(s) in the very common and readily available carbohydrates enables the synthesis of a wide variety of monomers suitable for making different classes of polymers [61,′62,63,64,65]. Wang et al. [66] reviewed the synthesis and application of carbohydrate-containing polymers up to 2001, summarizing the knowledge accumulated on the synthetic carbohydrate-based polymers, increasingly explored as renewable, often biodegradable and biocompatible materials. Carbohydrate-based polycondensates typically show increased hydrophilicity, lower toxicity and higher susceptibility to biodegradation, compared to those coming from petrochemical feedstock.

Cellulose and starch are biopolymers composing of D-glucose units. Examples for the epoxidation of both starch [67,68] and cellulose [69] can be found in the literature, applying different epoxidizing reagents. By enzymatic [70], acidic [71] or hydrothermal hydrolysis [72] of cellulose

and starch, D-glucose can be prepared [73]. Sorbitol is formed by the hydrogenation of glucose, and by the didehydration of sorbitol, the resulting products are dianhydrohexitols (**Figure 2.1.4**).

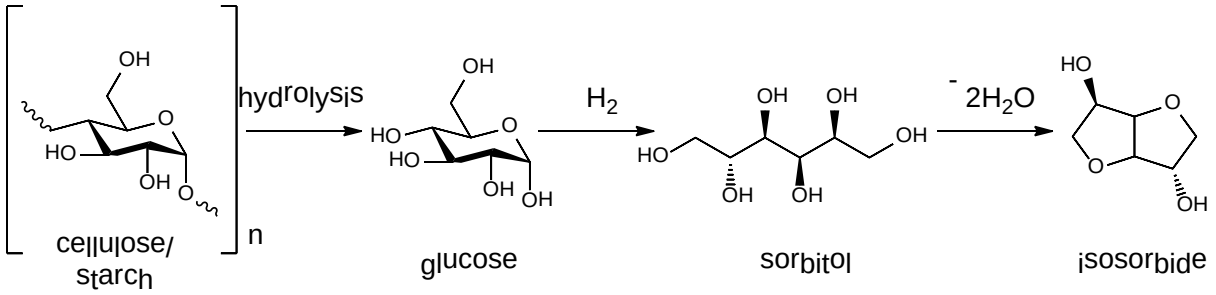

Figure 2.1.4 Synthesis of isosorbide

The epoxy monomer prepared from sorbitol is already a commercial product (sorbitol polyglycidyl ether, SPE), as well as the glycidyl ethers prepared from glycerol. Shibata et al. [74] reacted SPE with different renewable curing agents to receive fully bio-based epoxy resins. With the application of quercetin as hardener, the highest T_g reached was 85 °C, while with the application of DGEBA as epoxy monomer under the same circumstances, they reached 145 °C. When tannic acid was applied as hardener, the T_g increased to 90 °C [75], while with the use of a calixarene, synthesized from pyrogallol and vanillin, the T_g increased to nearly 150 °C [76].

One of the most promising sugar based starting materials to form engineering plastics is the group of dianhydrohexitols (isosorbide, isomannide and isoidide) [77], which are produced from D-glucose, D-mannose, and L-fructose, respectively.

The synthesized diglycidyl ether of isosorbide (1,4:3,6-dianhydro-D-sorbitol) was successfully incorporated into thermosets and thermoplastics in several cases. Several research groups synthesized epoxy monomers from isosorbide and its diastereomers, both by the reaction with epichlorohydrin and by allylation followed by epoxidation (**Figure 2.1.5**) [78,79,80]. Some isosorbide-based thermosets had mechanical properties comparable to DGEBA [78,79], however, the glass transition temperatures of the amine-cured networks are still lower than expected [80].

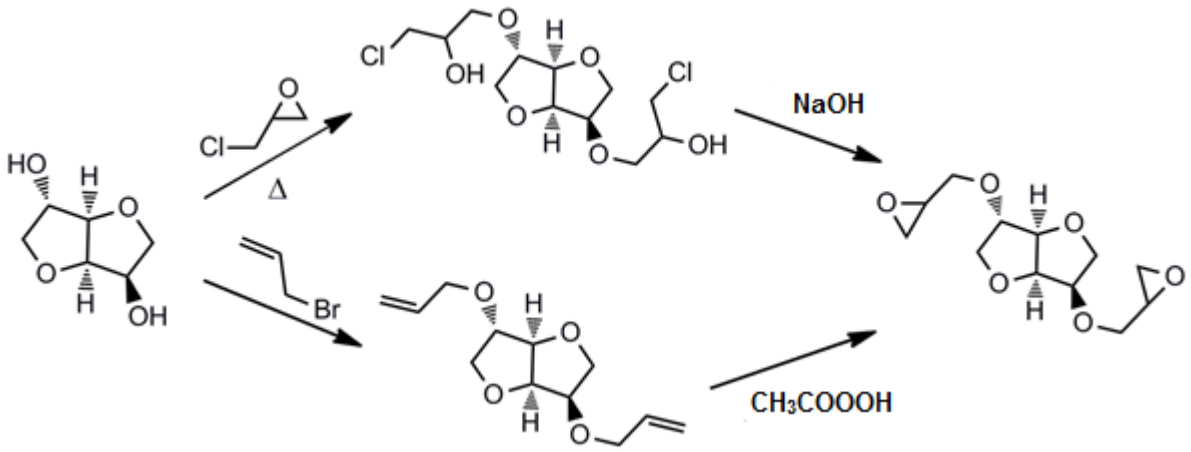

Figure 2.1.5 Possible reaction routes to synthesize diglycidyl ether of isosorbide [78]

2.2. All-bio epoxy resin composites

The tendency towards substitution of mineral oil based polymers by bio-based ones has emerged also in the polymer composite industry, including such demanding sectors as aeronautical and automotive [81]. Besides the environmental advantages, the partial or full replacement of polymer matrices and reinforcements by renewable ones can be a strategy to reduce the dependence on petrochemicals and eliminate the effect of their fluctuating price level as well.

To achieve fully bio-based composite systems, not only the matrix, but also the reinforcing fibre has to be prepared from renewable sources. Among the large variety of natural fibres available for this purpose, jute is one of the most promising renewable sourced reinforcing materials, due to its high cellulose content and relatively good mechanical properties compared to other natural fibres. According to the literature elemental jute fibres have the following characteristics: density: 1.3 g/cm^3; cellulose content: 61-71%; hemicellulose content: 14-20%; lignin content: 12-13%, wax content: 0.5%. Furthermore, jute is produced in large quantities worldwide (2300 kt/year), so its structural application is not depending from the availability [82].

In the case of natural fibres as jute the need for chemical treatment before composite preparation is an often discussed issue. Most frequently sodium hydroxide (NaOH) alkali treatment of the fibres is applied in order to improve their mechanical properties by removing the non-cellulosic materials (lignin, hemicellulose) from the fibres. Several fibre treatment methods were published in the literature, however the results are contradictory, both improvement and worsening of the mechanical properties of the fibres is reported. Saha et al. [83] have reported almost 50% increase of jute fibres' mechanical properties due to a treatment with 4% NaOH solution at room temperature for 0.5 h, but above this specific treatment time and NaOH solution concentration the mechanical properties decreased in comparison to the untreated fibres. Similar effect was observed by Roy et al. [84] with 0.5% NaOH solution at room temperature and 24 h treatment

time, the reported increment was 82% in this case. Gassan and Bledzki [85] examined the influence of alkali treatment on jute/EP unidirectional composites' mechanical properties with different NaOH solutions and treatment times. They observed 120% increment in the composites' tensile strength due to a treatment with 25% NaOH solution for 20 min at 20 °C. Doan et al. [86] investigated the effect of NaOH treatment alone and in combination 3-phenyl-aminopropyl-trimethoxy-silane and 3-aminopropyl-triethoxy-silane in jute/EP composites; the highest improvement was observed in case of the latter treatment. According to Pinto et al. [87] the mechanical properties of jute/EP composites increased due to combined fibre treatment consisting of silane pre-treatment and treatment with 5% NaOH solution for 2 h.

The reinforcing effect of jute fibres is widely investigated in different EP matrices. Hossain et al. [88] investigated the effect of the fibre reinforcing direction on the jute/EP laminates' mechanical properties, and concluded that in case of the 0°-0° reinforcing direction tensile and flexural strength were the highest compared to the 0°-45° and 0°-90° reinforcing directions. Mishra and Biswas [89] found that in case of jute/EP composites, the hardness, tensile properties and impact strength increased and the void content decreased by increasing the fibre content. Several EP composites with hybrid bio-based [90,91,92,93,94,95] or jute/synthetic reinforcement [96,97] were investigated as well.

Nevertheless, the literature on all-bio composites made from jute fibres and bioresins is limited, mainly dealing with epoxidized plant oil composites. Avancha et al. [98] prepared jute reinforced soy resin biocomposites. Best mechanical properties (tensile strength of 35 MPa and tensile modulus of 1546 MPa) were reached with composites consisting of 60% jute reinforcement and 40% soy resin compounded with 7% furfuraldehyde. Ramamoorthy et al. [99] compared the properties of acrylated epoxidized soybean oil composites reinforced with jute mat, regenerated cellulose mat and glass fibre. The jute biocomposites had a tensile strength of about 50 MPa and tensile modulus of about 10 MPa. Tensile, flexural and impact properties could be improved by hybridization with glass fibre and cellulose. Manthey et al. [100] prepared jute biocomposites from blends of epoxidized hemp oil (EHO) and epoxidized soybean oil (ESO), respectively, with DGEBA. EHO and ESO jute-based samples displayed similar tensile behaviour at a concentration of 10% bioresin, a significant reduction in mechanical properties occurred after 30% bioresin content. Campaner et al. [101] manufactured composite pipes from an EP crosslinked with a cardanol based novolac as matrix and jute fibres by filament winding technology, and carried out tensile and parallel plate compression tests on the composite pipes.

2.3. Green flame retardancy solutions for epoxy resin composites

Epoxy resins that are fire retarded with conventional additives are of poorer physical properties than the unmodified ones; therefore, in many cases, the use of reactive co-monomers is preferred. Despite their disadvantages, the additive flame retardants (FRs) dominate the market because most of the available reactive solutions are too complicated and expensive. The most versatile method involves incorporating phosphorus-containing compounds that react easily with the OH-groups of the resin, resulting in high char yield during fire. The composition of the epoxy system (e.g. the type of hardener, the presence or absence of fibres or fillers) and its application determine the amount of phosphorus needed to meet the flammability requirements (e.g. V-0 rating UL-94 standard). If anhydride hardeners are used, up to 5% P is required, while usually 3% is enough with amines. For laminates with 60% fibre content even 2% P can be sufficient. Hence an iterative optimisation must be carried out for every system. Extensive reviews on phosphorus-containing FRs for epoxy resins have been previously published by Jain et al. [102] in 2002, by Levchik and Weil [103] in 2004 and by Rakotomalala et al. [104] in 2010.

Low molecular mass organophosphorus additives are often somewhat volatile, leading to loss of phosphorus by volatilization from the polymer during high temperature processing or degradation. Evidently, there is a need to increase the permanence of the FR within the polymer; therefore the integration of the organophosphorus functionality into the polymeric structure is a reasonable progression of this field [**105**]. Reactive organophosphorus monomers built chemically into polymers can render the macromolecules inherently flame retardant. In the case of epoxy resins either the epoxy component, or the crosslinking agent or both can hold the P-containing chemical unit.

In the followings, the currently most used synthesis routes for preparation of phosphorus-containing epoxy monomers and crosslinking agents are classified by chemical reaction type [**106**].

2.3.1. Synthesis of phosphorus-containing epoxy monomers

The synthesis methods of phosphorus-containing epoxy monomers can be categorized into the following main groups based on chemical reaction type:

Reaction of phosphorus-containing co-monomers with epoxy monomers

The most common phosphorus-containing molecule, which is used to incorporate phosphorus into the epoxy monomer by reacting with its oxirane ring, is 9,10-dihydro-9-oxa-10-phosphaphenantrene-10-oxide (DOPO).

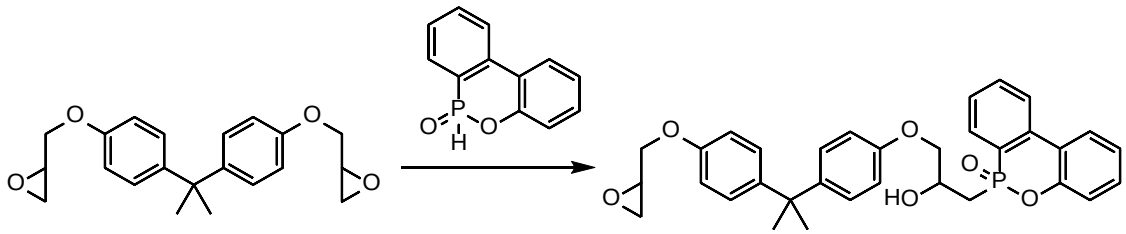

Figure 2.3.1 Reaction of DGEBA with DOPO

By incorporating DOPO into DGEBA (**Figure 2.3.1**), flame retarded epoxy resins were synthesized of 1-3% P-content [107,108].When cured with DDM, V-0 rating could be reached at 3% P-content, while the LOI value could be increased to 30.

The application of (4-[(5,5-dimethyl-2-oxide-1,3,2-dioxaphosphorinan-4-yl)oxy]-phenol) in a DGEBA/low molecular weight polyamide resin system resulted in 80% lower heat release rate, and V-0 rating at 2.5% P-content [109].

When another P-containing co-monomer, 2,8-dimethyl-phenoxaphosphin-10-oxide was used to react with novolac resin and cured with DDM, the system reached V-0 rating even at 0.75% P-content [110].

Modification of phosphorus-containing co-monomers with phenols followed by reaction with epichlorohydrin

As the incorporation of co-monomers usually decreases the reactive oxirane groups in the resin, and subsequently the crosslink density as well, the glass transition temperature (T_g) of these compositions is generally significantly lower than that of the unmodified material. As this problem is the main drawback of the application of the reactive co-monomers, new DOPO derivatives were prepared with more rigid structure to overcome this phenomenon.

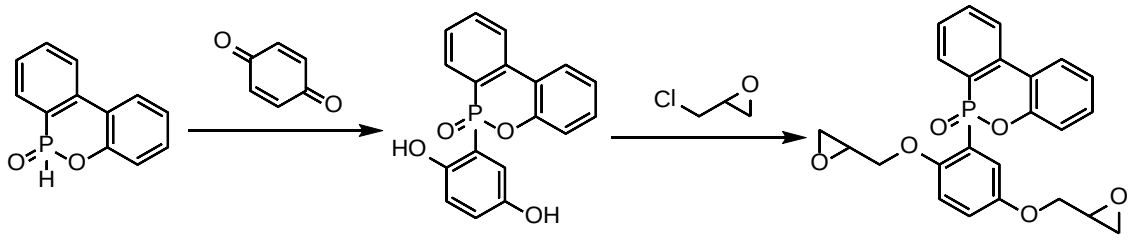

Figure 2.3.2 Reaction of DOPO with benzoquinone followed by epoxidation with epichlorohydrin

Both the benzoquinone (**Figure 2.3.2**) [111] and the naphthoquinone [112] substituted DOPO led to V-0 rating with 2% P.

Reaction of phosphorus-containing alcohols/phenols with epichlorohydrin

Epichlorohydrin, widely used as industrial reactant, easily reacts with hydroxyl groups, which allows the synthesis of P-containing epoxy monomers from P-containing alcohols/phenols.

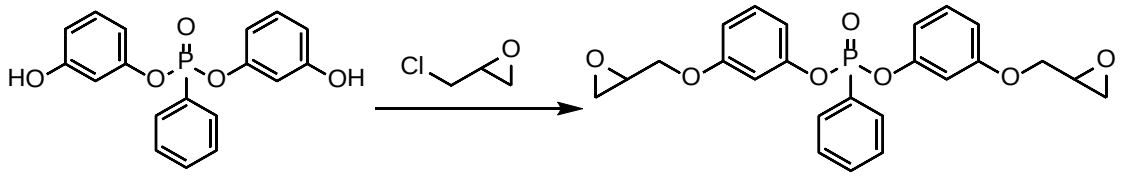

Figure 2.3.3 Reaction of bis(3-hydroxyphenoxy)phenylphosphine oxide with epichlorohydrin

The reaction product of resorcinol and phenyl phosphonic dichloride was reacted with epichlorohydrin to form the diglycidyl ether of bis(3-hydroxyphenoxy) phenylphosphine oxide (**Figure 2.3.3**) [113]. Cured with diaminodiphenylsulfone (DDS), this system reached only LOI of 34 V/V%, although the P-content was 7.8%.

Spontón et al. [114] synthesized with this method diglycidyl ether of (2,5-dihydroxyphenyl)diphenylphosphine oxide, which was cured with the P-containing bis(3-aminophenyl)methylphosphine oxide (BAMPO) leading to 8.5% total P-content, however, the obtained epoxy resin only reached an LOI value of 32 V/V%. The same result was achieved by curing it with benzoxazine with only 3.5% P-content [115].

Reaction of phosphorus (oxy)chlorides with glycidyl alcohol

A feasible way to synthesize P-containing epoxy monomers is to react phosphorus (oxy)chlorides with glycidyl alcohol (**Figure 2.3.4)**.

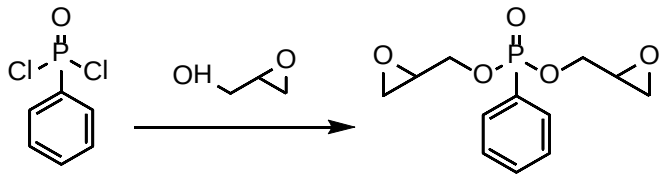

Figure 2.3.4 Reaction of phosphorus oxychloride with glycidyl alcohol

Various epoxy monomers prepared by this method were incorporated by Hergenrother et al. [116] into a tetraglycidyl methylenedianiline – diaminodiphenylsulfone (DDS) system in different concentrations. Low P-content (3%) was enough to fulfil the strict requirements of the aircraft industry.

Cyclophosphazene-based epoxy monomers were also synthesized [117,118]. By replacing 20% of DGEBA with P-containing epoxy monomer, V-0 UL-94 rate was achieved.

In the case of diglycidyl-phenylphosphate [119] cured with 2,5-bis(*p*-aminophenyl)-1,3,4-oxadiazole the P-content of the system was 7.4% and it resulted in an LOI of 47 V/V%.

2.3.2. Synthesis of phosphorus-containing crosslinking agents

Epoxy resins can be made inherently flame retardant by using P-containing crosslinking agents as well. Due to the phosphorus-nitrogen synergism in terms of flame retardancy performance, incorporation of P into amine type of curing agents is much more common than the synthesis of P-containing anhydride type crosslinking agents. Moreover, P-containing reactive amines have potential applicability not only in epoxy resins but in some other engineering plastics as well. Although the flame retardant efficacy of P-containing reactive amine hardeners in epoxy resins is well-known; most of their known synthesis methods apply hazardous, objectionable reagents in multistep, complex reactions, therefore the breakthrough in this field still awaits. The methods described in the literature for the synthesis of P-containing amines can be categorized into the following main groups based on chemical reaction type:

Reaction of phosphorus oxychlorides with aminophenols or aminoalcohols, or with nitrophenols followed by reduction to obtain the amino group (Figure 2.3.5)

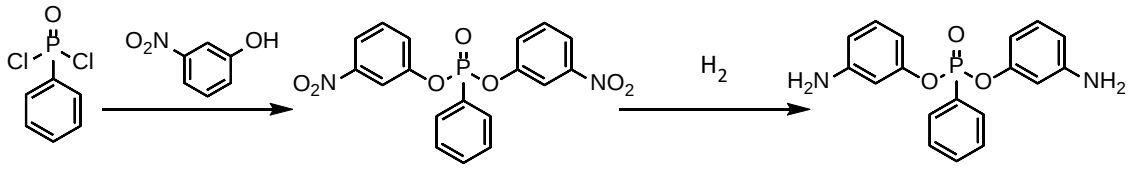

Figure 2.3.5 Reaction of phosphorus oxychloride with nitrophenol followed by reduction

The reaction of *p*-nitrophenol with methylphosphonic dichloride followed by reduction resulted in the formation of bis(4-aminophenyl)methylphosphonate. This compound has been used as a curing agent of TGDDM, yielding an immediately extinguishing resin at 3.9% P-content [115].

The same method was applied for synthesizing bis(4-aminophenyl)phenylphosphonate (BAPP) [120], which was applied in DGEBA and TGDDM EPs. A reduction of 30% of the peak heat release rate could be achieved when curing DGEBA (2.8% P-content), while in case of TGDDM the reduction was more than 50% [121].

DGEBA mixed with siliconized DGEBA in different ratios was also cured with BAPP [122].When the mixing ratio of the two EPs was 100:15, the LOI increased from 32 to 42 V/V%.

Reaction of phosphorus oxychlorides with amines (Figure 2.3.6)

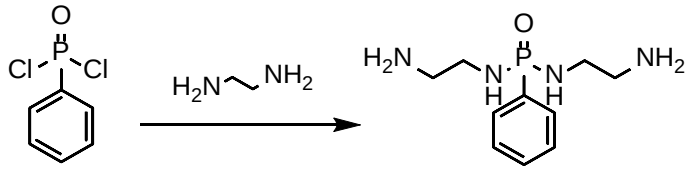

Figure 2.3.6 Reaction of phosphorus oxychloride with amine

By the reaction between phosphoryl chloride derivatives and commercially available polyetheramines, ethylenediamine and N-phenyl-1,4-phenylenediamine, series of P-containing poly(alkylene) amines with or without aromatic groups were synthesized [123] and DGEBA was cured with them. The highest P-content (i.e. 4%) could be reached when applying the reaction product of ethylenediamine and phenylphosphonic dichloride as crosslinking agent. As expected, this formulation showed the best results: an LOI of 31 V/V%, and 12.2% char yield in air at 850 °C. These values could not be further increased significantly despite the application of a P-containing epoxy component [124].

The synthesis of a cyclophosphazene-based aromatic diamine was also carried out, and showed high thermal stability with a char yield of 55.6% at 600 °C in nitrogen [125].

Transesterification of phosphate esters with aminophenols or aminoalcohols (Figure 2.3.7)

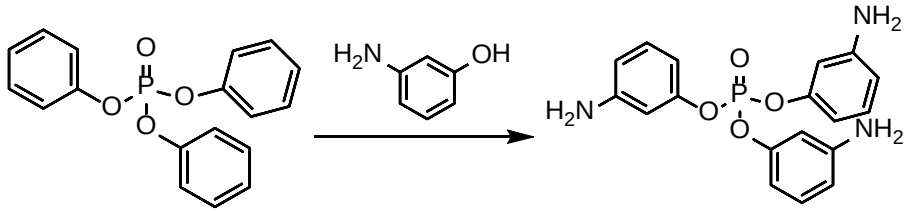

Figure 2.3.7 Transesterification of phosphate esters with aminophenols

Triphenyl phosphate can easily be transesterified with 3-aminophenol to form tris-(3-aminophenyl)-phosphate (TAPP) [126]. Similarly effective by-products (incompletely replaced starting material and oligomers) were also found in the reaction mixture, but due to lower functionality, they decrease the crosslinking density. The laminates made of novolac type epoxy resin cured with TAPP reached V-1 UL-94 rating.

Nitration of aromatic phosphine oxides followed by reduction to obtain the amino group (Figure 2.3.8)

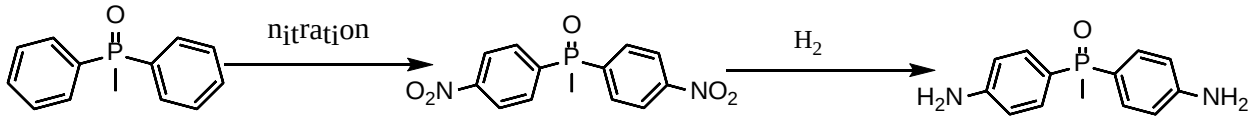

Figure 2.3.8 Nitration of aromatic phosphine oxide followed by reduction

A comparative research was carried out by Braun et al. [127] about the effect of different oxidation state of phosphorus on the flame retardancy of epoxy resins. According to their results, the best flame retardant performance was reached with the application of aromatic phosphinate-type FRs. Bis(4-aminophenyl)methylphosphine oxide was synthesized by the nitration of diphenylmethylphosphine oxide followed by reduction of the nitro groups [116]. TGDDM was cured with this new P-containing amine. The P-content of this composition was 4%, which led to an immediately extinguishing resin, with 23% char yield at 800 °C in N_2.

Reaction of 9,10-Dihydro-9-oxa-10-phosphaphenanthrene-10-oxide (DOPO) with reagents containing amine groups (Figure 2.3.9)

DOPO-based diamines can be prepared by the addition reaction of DOPO with different amine-functional reagents. The addition of DOPO can occur on oxo [128] or imine groups [129].

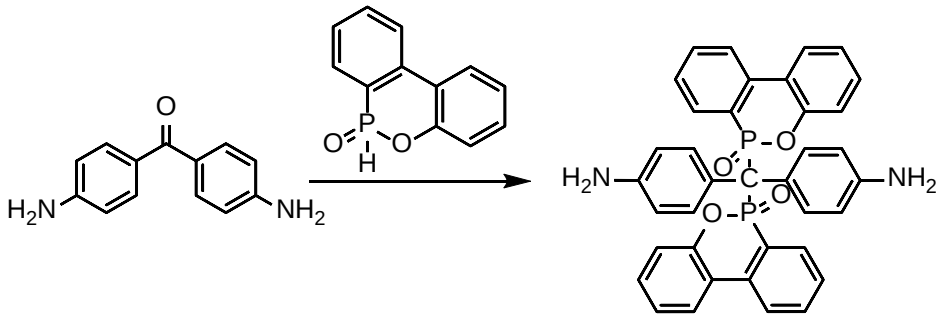

Figure 2.3.9 Reaction of 9,10-Dihydro-9-oxa-10-phosphaphenanthrene-10-oxide (DOPO) with reagents containing amine groups

When applying the reaction product of DOPO and 4,4'-diaminobenzophenone in siliconized DGEBA, an LOI value of 35 V/V% could be reached with 2.35% P- and 4.57% Si-content [130].

DOPO can also react with an aromatic diimine, resulting in a symmetric diamine which can be used as co-curing agent in DGEBA – DDM system. At 1.5% P-content, V-0 UL-94 rating was reached, while the LOI was 37 V/V%.

By the nitration and then reduction of the aromatic rings of DOPO, a P-containing curing agent can be gained, which can increase the LOI by 13 V/V% [131].

New organophosphorus oligomer, poly(DOPO-substituted hydroxyphenyl methanol pentaerythritol diphosphonate) was synthesized by Wang et al. [132]. Incorporating it into an EP cured by DDM, significantly increased char yield, accompanied with higher T_g was achieved compared to the reference.

Transamidation of phosphate esters with diamines

An alternative, halogen-free route to produce P-containing reactive amine curing agents, which can be used instead of reaction of phosphorous oxychlorides with amines was elaborated and patented by the author and her co-workers (**Figure 2.3.10**) [**133**].

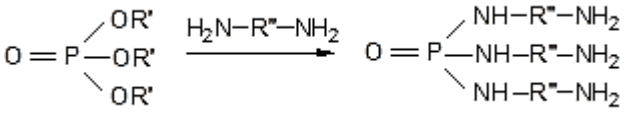

where
R' = any aliphatic or aromatic hydrocarbon structure including the unsaturated or/and arbitrarily substituted structures
R" = any aliphatic or aromatic hydrocarbon structure including the unsaturated or/and arbitrarily substituted structures
H2N-R"-NH2 = aliphatic or aromatic amine at least with two amine functionalities per molecule

Figure 2.3.10 General scheme for transamidation of phosphate esters with diamines

Prior to this invention, the reaction between tertiary phosphoric ester and diamines has not yet been described. Although an article of Michaelis from 1903 contains a hint that if monoamide-diester of phosphoric acid is heated together with benzylamine for a long time it will be converted into phosphine oxide, however the reaction conditions are not defined and the product is not characterized by any means of analytics (also the exact name and chemical formula of the compound is missing) [134]. Also, according to the article of O. Mauerer [126], which gives an example for transesterification of phosphate esters with aminophenols or aminoalcohols, the reaction between a tertiary ester and amine function does not take place. In the reaction of a tertiary ester of phosphoric acid and an aminophenol, only transesterification reaction between the triester and phenol functions occurred, resulting in variously substituted esters, however the amine group remained intact.

2.3.3. Fire retardant modifications of bioepoxy resins

As the synthesis of bio-based thermosetting polymers is a relatively new research area in the field of polymer chemistry, only a few articles deal with the flame retardancy of such biopolymers.

Das and Karak [135] determined the FR properties of vegetable oil-based epoxy formulations applying tetrabromobisphenol A (TBBPA)-based epoxy monomer as FR. In their work, they reached high LOI values (up to 45 V/V%) and UL-94 V-0 rating.

Similarly, TBBPA was applied as FR together with melamine polyphosphate in the study of Zhan and Wool [136], reaching V-0 rating. However, the application of brominated FRs deteriorates the environmentally friendly character of the bio-based polymers, since HBr is released during combustion, which is corrosive and toxic.

As a greener alternative, silicon-containing vegetable oil-based polyurethanes have been synthesized in order to enhance the FR properties of the biopolymer [137]. With the incorporation of 9% of Si into the matrix by the reaction between methyl 10-undecenoate and phenyl tris (dimethylsiloxy)silane, the LOI value increased from 18.2 V/V% of the reference system to 23.6 V/V%.

Pillai and co-workers reacted the free OH-group of cardanol with ortophosphoric acid, in order to prepare a FR starting material [138]. Based on their experience, oligomerization of cardanol occurred by the reaction of the carbon-carbon double bonds present in the side chain, proposing new potential fields of application.

Lligadas et al. synthesized phosphorus-containing flame retarded epoxidized fatty acids [139,140]. ω-Unsaturated undecenoyl chloride was used as a model fatty acid precursor, which can be later exchanged to natural-based unsaturated fatty acids. The P-content of the prepared system was provided by 9,10-dihydro-9-oxa-10-phosphaphenantrene-10-oxide, which is an extensively used commercially available FR for EPs. DOPO was reacted with hydroquinone by its active hydrogen. The product of this reaction was then reacted with undecenoyl chloride, followed by epoxidation with *m*-Cl-perbenzoic acid (**Figure 2.3.11)**.

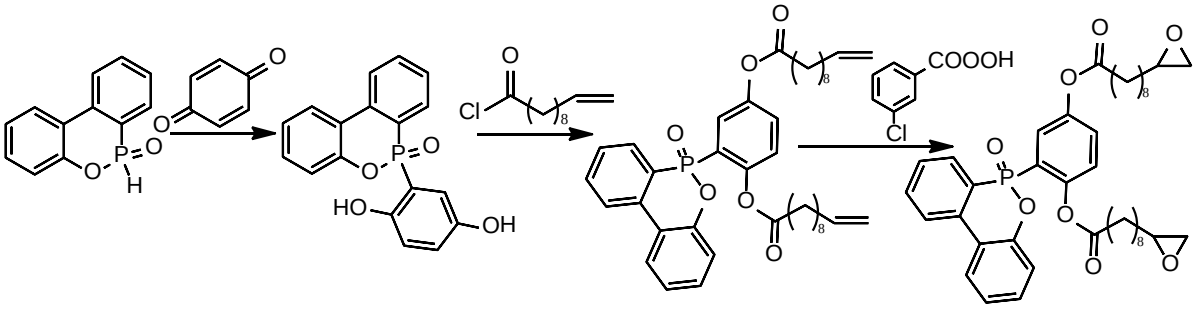

Figure 2.3.11 Preparation of flame retarded epoxidized fatty acids [139]

The epoxy component produced was cured with 4,4'-diaminodiphenylmethane (DDM) and bis(*m*-aminophenyl)methylphosphine oxide (BAMPO), respectively. The cured samples were analysed by DSC and DMA measurements, and tested to determine their limiting oxygen index. According to the results, contrary to the expectations, the application of BAMPO did not notably increase the LOI of the resin (from 31 to 32 V/V%), and that the T_g decreased compared to the DDM-cured sample (from 108 to 95 °C).

Itaconic acid was reacted with DOPO to form a P-containing dicarboxylic acid [141]. In a second step, diglycidyl esters of this molecule were prepared two ways. On the one hand, the acid was reacted directly with epichlorohydrin, and on the other hand, allyl bromide was added to form allyl ester, followed by the epoxidation of the double bonds with *m*-chloroperbenzoic acid. The received epoxy monomer was then cured with methyltetrahydrophthalic anhydride. The cured samples having 4.4% phosphorus content, reached V-0 rating in the UL-94 test, however, the LOI of this sample was only 22.8 V/V%. When DGEBA was added to the system, decreasing the P-content to 2%, a LOI of 31.4 V/V% was reached.

A possible interpenetrating polymer network (IPN) structure was proposed by Alagar and co-workers [142] for the flame retardancy of soy-based epoxy resins. Several bismaleimides were synthesized, which were then mixed to the bio-based EP before curing. Besides the crosslinking of the EP, the homopolymerization of the bismaleimide molecules also took place through their carbon-carbon double bonds. The resulted IPN system provided improved thermal stability, and when the P-containing bismaleimide was applied in 20 phr concentration, the LOI value of the reference system increased from 21 V/V% to 30 V/V%.

A new class of P-containing renewable thermosetting polymers was synthesized through aza- and phospha-Michael additions on α,β-unsaturated ketone derived from high oleic vegetable oils [143,144]. When the phospha-Michael addition was carried out with the monofunctional diphenyl phosphine oxide [143], a LOI of 35 V/V% was reached, however, the crosslink density of the polymer decreased. To overcome this negative effect, a bifunctional reagent (1,3-bis(phenylphosphino)propane oxide) was applied [144], and in this case the LOI further increased to 38 V/V%.

2.3.4. Fire retardant modification of biofibres

Natural fibres represent an obvious choice as reinforcement for bio-based polymer matrix materials, as with their combination all-bio composites can be prepared. Lower density, renewability and biodegradability, as well as lower price and composite processing costs make them promising alternatives to the commonly applied synthetic carbon, glass or aramid fibres

[145]. Kenaf, hemp, flax, jute, and sisal have attained commercial success in designing biocomposites. Among their disadvantages, such as fluctuating fibre quality, high moisture uptake, limited processing temperature range, low impact strength and durability, their flammability represents a major drawback, especially in more demanding sectors as aeronautical, automotive and electronic industries.

The flammability of bio-based fibres depends mainly on their chemical composition (determining their thermal degradation), but also on their structure, degree of polymerization and fibrillar orientation. The thermal degradation of the natural fibres is a well-described phenomenon [146,147,148]. It involves several processes as desorption of adsorbed water; dehydration of cellulose leading to dehydrocellulose and water; decomposition of the formed dehydrocellulose to char and volatiles; depolymerisation of cellulose resulting in levoglucosan (a non-volatile liquid intermediate) and its decomposition to flammable and non-flammable gases, tar and char. The main characteristics of the thermal degradation behaviour of the major natural fibre components and their effect on flammability are summarized in **Table 2.3.1**.

Table 2.3.1 Thermal degradation characteristics of natural fibre main components

main component	**temperature range of the main thermal degradation***	**major decomposition products**	**effect on flammability by increasing its ratio**
cellulose	315-400 °C	flammable gases incombustible gases tars less char than in the case of hemicellulose	increased flammability
hemicellulose	220-315 °C	incombustible gases less tar than in the case of cellulose	decreased flammability
lignin	160-900 °C	flammable gases aromatic char	higher decomposition temperature lower resistance to oxidation

*based on thermogravimetric analysis in nitrogen atmosphere, from 25 to 900 °C, at 10 °C/min heating rate [149]

As for the chemical composition of fibres, lower cellulose content and higher lignin content reduce their flammability. Concerning the fine structure of fibres, the high crystallinity of cellulose leads to formation of high amount of levoglucosan during pyrolysis and consequently to increased flammability, so from this point of view lower cellulose content is preferred. On the other hand, as more energy is required to decompose the crystalline structure of the cellulose, it results in higher ignition temperature. As for the degree of polymerization and orientation of the fibrillar structure higher molecular weight and orientation (resulting in lower oxygen permeability) is favourable.

The flammability of natural fibres and composites made thereof can be decreased with flame-retardant fibre treatments. Inorganic phosphorous compounds (such as phosphoric acid, monoammonium phosphate and diammonium phosphate), tributyl phosphate, triallyl phosphate,

triallyl phosphoric triamide have been used to flame retard cellulose based fibres [150,151,152,153]. P-containing FRs can efficiently initiate the charring of fibres, which is favourable in terms of flame retardancy [150,**154**], however, the application of these treatments decreases the initial decomposition temperature of natural fibres significantly (even by 90 °C) [**154**,155]. The reduced thermal stability can be a major issue, both from mechanical and aesthetic point of view, when the natural fibres are intended to be used as fillers or reinforcements in polymer composites. The presence of water, acids and oxygen catalyses the thermal degradation of cellulose, therefore natural fibres usually turn brown during fibre treatments. Low thermal stability is critical in case of thermoplastic matrices with processing temperatures above 140 °C (such as polypropylene, polyamide, polyethylene terephthalate and also polylactic acid), but also in case of high glass temperature thermosetting matrices requiring elevated curing temperature (e.g. high-tech epoxy resins, cyanate esters). Surface treatment with silane compounds is a possible solution to increase the thermal stability of cellulosic fibres [156,157]. Recently, the layer by layer assembly came to the forefront for rendering textiles flame retardant [158,159].

According to the literature, when bio-based fibres are used as reinforcements (without adding FRs to the polymer matrix) in polymer matrices to form biocomposites, the heat conductivity increases while the apparent stability of the polymer decreases, therefore the ignition of the composite is facilitated [160]. This, so-called candlewick effect of natural fibres makes the flame retardancy of the natural fibre reinforced biocomposites rather challenging [161,162]. Thus the flame retardant treatment of biofibres was found to be essential from this respect as well.

Bocz et al. elaborated a novel one-step reactive flame-retardant treatment for natural fibres: Phosphorus-containing silanes were synthesized from commercial phosphorus-containing polyol and 3-(triethoxysilyl)-propyl isocyanate, and the adduct was used to treat flax fibres used for the reinforcement of polylactic acid /thermoplastic starch composites [163]. These P-containing silanes did not decrease the initial temperature of thermal degradation as the treatment with diammonium phosphate, and lead to improved fire retardant properties. These results can be explained by the known synergistic effect of P and Si atoms [164,165].

In the case of thermosetting matrices, e.g. in EPs, the silane treatment can be combined with the alkali surface treatment of the natural fibres [86], aiming at improving the relatively poor interaction at the fibre - matrix interphase [166,85]. Fibre treatment with silanes having reactive functionalities (e.g. amine) leads to covalent bonds between the fibre and the matrix resulting in improved mechanical properties as well [167]. However, it has to be taken into account that the surface treatment of the reinforcement with reactive species can influence the curing kinetics of the applied epoxy resin [168].

2.4. Conclusions of the literature overview

The development of renewable epoxy resins has attracted considerable attention in the last few years. According to the literature review, although there are some promising results, the breakthrough leading to massive application of bioepoxy composites in more demanding sectors as aircraft industry is yet to come.

Among the bioepoxy monomers epoxidized plant oils are currently mainly used in combination with commodity mineral oil based epoxy resin components. Considering their low glass transition temperature and that the composition of plant oil based polymers is not as exact as that of the synthetic ones, this step-by-step replacement approach is easily understandable, especially in the case of advanced applications with strict safety standards, e.g. aeronautical and electrical industry. The related literature focuses on combinations with DGEBA, other epoxy resins are rarely examined, furthermore a comparative, systematic study to characterize the effect of epoxidized plant oils on curing and rheological behaviour, glass transition temperature, thermal and mechanical properties of various epoxy resin systems and their composites is not available.

The epoxy monomer prepared from sorbitol, sorbitol polyglycidyl ether, is already a widely used commercial product. Nevertheless, due to the long aliphatic segment present in the molecule, SPE provides much lower glass transition temperature than the benchmark DGEBA epoxy resin, therefore its use is still limited to non-structural composite applications.

Considering the use of other carbohydrates as starting materials in the synthesis of bioepoxy resins, it has to be noted, that although D-glucose is an inexpensive, easily available and renewable starting material, having the potential to be used as an alternative to petroleum-based polymers, it has not yet been applied as epoxy monomer precursor. The development of new high value products and new concepts in sugar manufacturing could be an answer [169] to the challenge of both oversupply and low prices in this field [170].

Natural fibres offer an evident possibility for reinforcing bioepoxy resins, as their combination results in all-bio composites. However, their major disadvantages, as low thermal stability, leading to limited processing temperatures, and flammability needs to be addressed. Due to the so-called candlewick effect of natural fibres, the ignition of their composites is facilitated, which makes the flame retardancy of the natural fibre reinforced biocomposites a rather challenging task. Concerning the most applied sodium hydroxide alkali treatment of the fibres contradictory results on the mechanical properties of the fibres were published, therefor further investigations are necessary.

Literature on all-bio composites, in particular composites made from jute fibres and bioresins is limited, mainly dealing with epoxidized plant oil composites.

As for the flame retardancy solutions currently available for epoxy resins, the additive types of flame retardants are still dominating the market, but their disadvantages facilitate the progress of the reactive approach.

Among the reactive solutions, 9,10-dihydro-9-oxa-10-phosphaphenantrene-10-oxide (DOPO) is one of the few flame retardants commercially available. The flame retardant effect of DOPO and its various derivatives (both epoxy monomers and crosslinking agents) are widely investigated, but mainly in DGEBA based aromatic epoxy resins only. Despite the relatively rigid structure, DOPO-based FRs usually decrease the glass transition temperature of the epoxy resins due to low functionality. Also, because of their low phosphorus-content, generally high amounts are needed to reach appropriate flame retardant effect, which leads to further decrease in glass transition temperature, thermal stability and mechanical properties as well.

As for other available reactive solutions, their synthesis mostly means complicated, multistep reactions, applying expensive, often hazardous reagents. Alternative, halogen-free synthesis methods taking into account the principles of green chemistry (as the ones previously elaborated by the author and her co-workers [**133**]) may offer solution for these issues.

3. APPPLIED MATERIALS AND METHODS

In this chapter the applied materials and methods are briefly summarized. Their choice was driven by practical applicability in high-tech composite industries.

3.1. Applied materials

The materials applied in syntheses, as well as polymer components, flame retardants and the applied fibre reinforcements and their surface treatments are presented in this chapter.

3.1.1. Materials applied in syntheses

The materials used in the organic syntheses were purchased from Sigma-Aldrich. If not mentioned otherwise in the description of the synthesis methods (see 4.1), the reagents were used as received, without further purification.

3.1.2. Polymer components

The characteristics of the applied epoxy monomers are summarized in **Table 3.1.1**, while their chemical structures are shown in **Figure 3.1.1**.

Table 3.1.1 Characteristics of the applied epoxy monomers

epoxy monomer	main component	supplier	trade name	viscosity [Pa·s; at 25 °C]	density [g/cm^3; at 25 °C]	molecular mass [g/mol]	epoxy equivalent [g/eq]
ESO	epoxidized soybean oil	Emery Oleochemicals Ltd. (Shah Alam, Malaysia)	Edenol D81	0.53	0.99	935	246
SPE	sorbitol polyglycidyl ether	Emerald Performance Materials (Moorestown, USA)	ERYSIS GE-60	7-9.5	1.27-1.30	294	160-190
GER	triglycidyl ether of glycerol	IPOX Chemicals Ltd. (Budapest, Hungary)	MR3012	0.16-0.2	1.22	274	140-150
PER	tetraglycidyl ether of pentaerythritol	IPOX Chemicals Ltd. (Budapest, Hungary)	MR3016	0.9-1.2	1.24	360	156-170
DGEBA	diglycidyl ether of bisphenol A	IPOX Chemicals Ltd. (Budapest, Hungary) DOW Chemical Company (Midland, USA)	ER1010 DER330	10-14 7-10	1.13 1.16	340 340	180-196 176-185
GPTE	glucopyranoside triglycidyl ether	synthesized at Budapest University of Technology and Economics	-	solid	n.a.	436	160
GFTE	glucofuranoside triglycidyl ether	synthesized at Budapest University of Technology and Economics	-	3.76	1.20	388	160

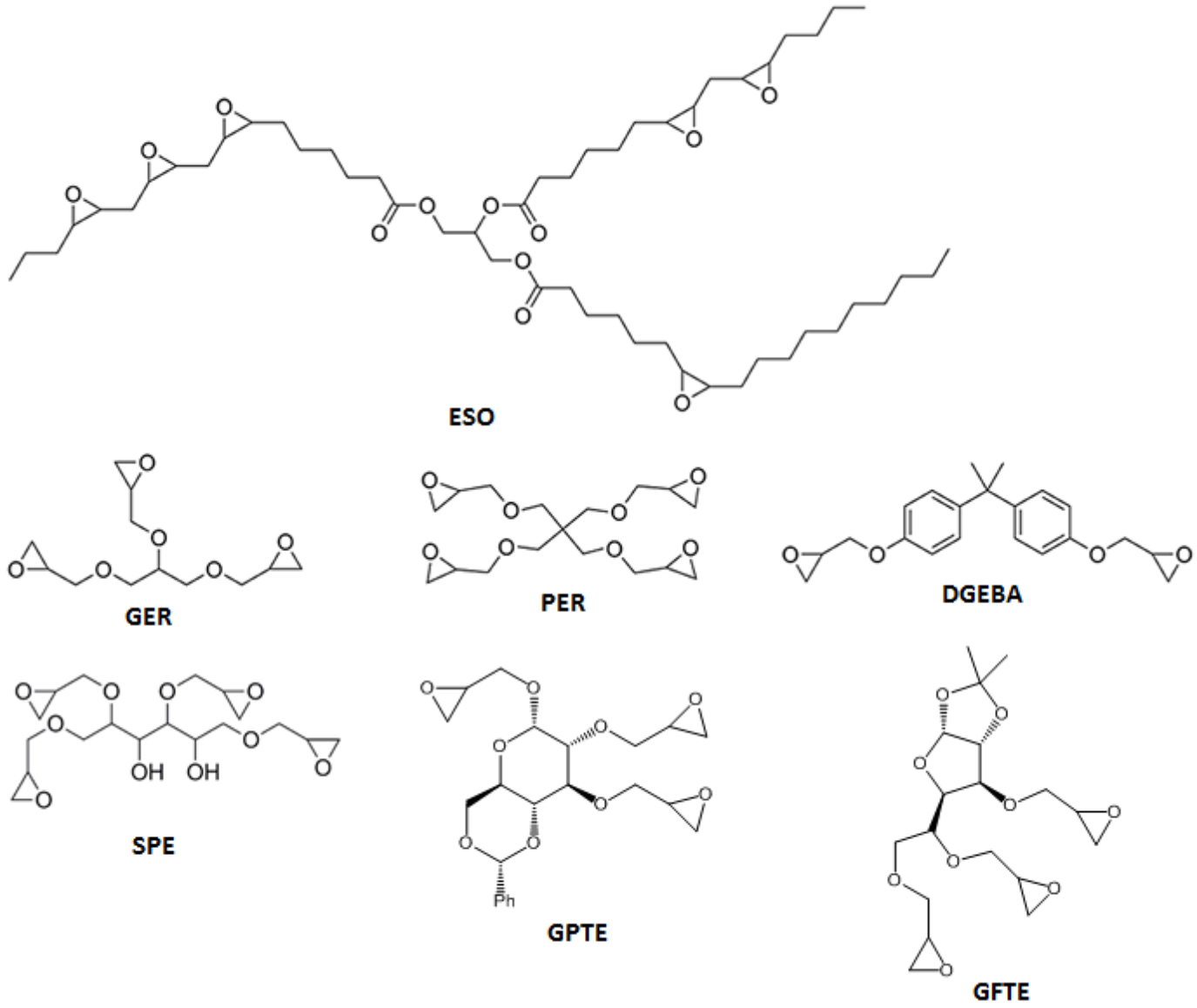

Figure 3.1.1 Chemical structures of the applied epoxy monomers

The characteristics of the applied crosslinking agents are summarized in **Table 3.1.2**, while their chemical structures are shown in **Figure 3.1.2**. PT-30 type cyanate ester was also listed among the crosslinking agents, as it was used in this work as a multifunctional reagent both to crosslink epoxy resins instead of anhydride type hardeners and to increase their glass transition temperature.

Table 3.1.2 Characteristics of the applied crosslinking agents

crosslinking agent	main component	supplier	trade name	viscosity [mPa·s; at 25 °C]	density [g/cm^3; at 25 °C]	amine/anhydride equivalent [g/eq]
DDM	4,4'-diaminodiphenyl methane	Sigma-Aldrich (Saint Louis, USA)	-	1.25	solid	49.6
T58	3,3'-dimethyl-4,4'-diaminodicyclohexyl-methane	IPOX Chemicals Ltd. (Budapest, Hungary)	MH 3122	80-120	0.94	60
TETA	triethylenetetramine	Dow Chemical Company (Midland, USA)	DEH 24	19.5-22.5	0.98	24
DETDA	diethyl-methylbenzene-diamine	Lonza Ltd. (Basel, Switzerland)	DETDA80	200	1.02	45
AR917	methyl-tetrahydrophthalic anhydride	Huntsman Advanced Materials (Basel, Switzerland)	Aradur 917	50-100	1.20-1.25	160
DY070 (catalyst)	1- methylimidazole	Huntsman Advanced Materials (Basel, Switzerland)	DY070	≤ 50	0.95-1.05	- (2% related to AR917)
PT-30	cyanated phenol-formaldehyde oligomer	Lonza Ltd. (Basel, Switzerland)	PT-30	0.3-0.5 at 80 °C	1.25	-

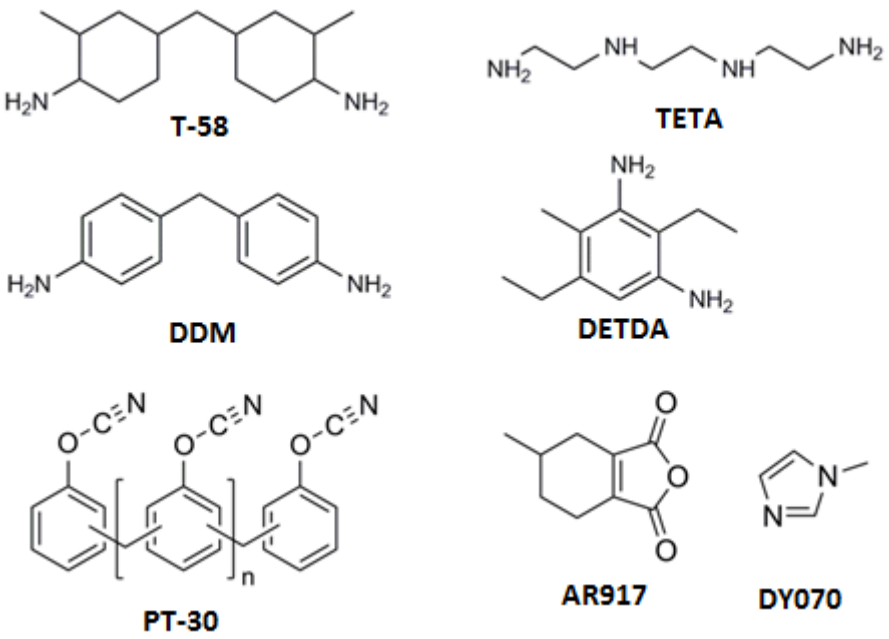

Figure 3.1.2 Chemical structures of the applied crosslinking agents

3.1.3. Flame retardants

The characteristics of the applied flame retardants are summarized in **Table 3.1.3**, while their chemical structures are shown in **Figure 3.1.3**.

Table 3.1.3 Characteristics of the applied flame retardants

flame retardant	main component	supplier	trade name	P-content [%]	other characteristics
APP	ammonium polyphosphate	Nordmann Rassmann (Hamburg, Germany)	NORD-MIN JLS APP	31-32	average particle size: 15 µm
RDP	resorcinol bis(diphenyl phosphate	ICL Industrial Products (Beer Sheva, Israel)	Fyrolflex RDP	10.7	density at 25 °C: 1.298 viscosity at 25 °C: 600 mPa·s
DOPO	9,10-dihydro-9-oxa-10-phosphaphenantrene-10-oxide	Struktol GmbH (Hamburg, Germany)	Struktol Polydis 3710	14.3	molecular mass: 216 g/mol melting point: 116 °C
TEDAP	*N,N′,N″*-tris(2-aminoethyl)-phosphoric acid triamide	synthesized at Budapest University of Technology and Economics	-	13.8	amine number: 510–530 mg KOH/g viscosity at 20 °C: 400 mPa·s

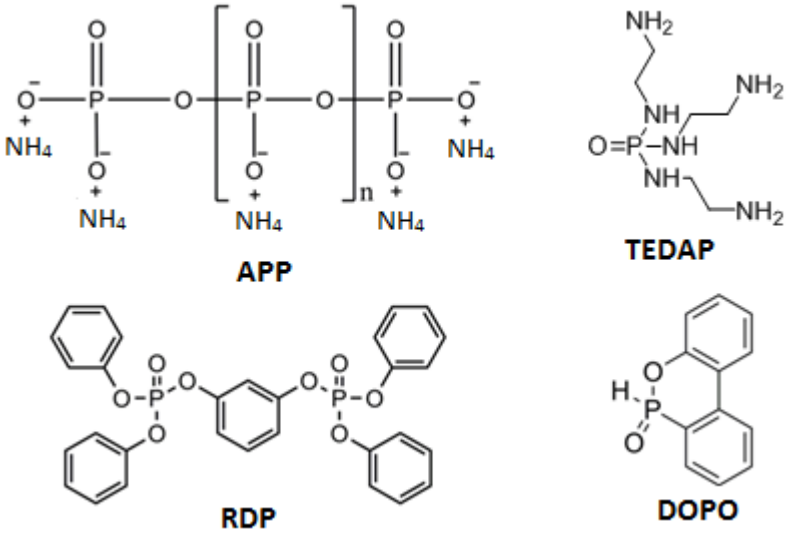

Figure 3.1.3 Chemical structures of the applied flame retardants

3.1.4. Fibre reinforcements and their surface treatment

Raw linen woven jute fabric with 270 g/m^2 surface mass was provided by Műszaki Konfekció Kft. (Szeged, Hungary). Before the composite preparation the fabrics were dried in 80 °C for 2 h under 50 mbar vacuum in Sheldon Manufacturing (Cornelius, USA) 1465 vacuum oven.

For the alkali treatment of jute fibres NaOH was acquired from Sigma Aldrich in form of pellets with ≥97% purity. 0.5; 1; 2; 4 and 8 mass% NaOH solutions were prepared by dissolving NaOH pellets in distilled water. 5-5 pieces of jute fabric (stored at 25 °C, 53% relative humidity) were immersed into NaOH solutions and the pieces were removed subsequently after 0.5; 1; 2; 4 and 8 h. The removal was followed by a three-step washing with distilled water to adjust the pH. The washed jute fabric pieces were dried for 1 week at 25 °C, 53% relative humidity, and for 1 day at 80°C under 50 mbar vacuum. The dried samples were consequently kept for 1 week at 25 °C, 53% relative humidity in order to reach saturation.

As core material for the jute reinforced sandwich composite structure Rohacell XT110 type polymethacrylimide foam (obtained from Evonik Industries (Essen, Germany)) with 110 kg/m^3 density was used in two different thicknesses (6.5 and 20 mm).

Twill woven hemp fabric (surface mass: 580 g/m^2) was received from the Institute of Natural Fibres and Medicinal Plants (Poznan, Poland). For the surface treatment of the fabrics, phosphoric acid (75%, Azúr Vegyszerbolt Kft., Hungary), ammonium hydroxide (25% solution) and Geniosil GF-9 (N-(3-(trimethoxysilyl)propyl)ethylenediamine), provided by Wacker Chemie AG (Germany), were used. Prior to surface treatment hemp fabrics (HF) were washed with water to remove dust and impurities and then dried in oven at 70 °C for 12 h. Two kinds of treatments were applied:

In the case of the so-called thermotex procedure [171] the fabrics were preheated at 120 °C for 2 h, and then immersed into a cold 17% phosphoric acid solution for 5 min. The ratio of fabric to the phosphoric acid solution was 1 g fabric to 10 ml solution. As the acid may trigger long-term degradation in cellulose fibre structure, the fabrics were immersed into 5% ammonium hydroxide solution. The excess of the treating and neutralizing solutions were removed by pressing the fabrics in a foulard. After treatment, the fabrics were dried in air. The amount of the absorbed phosphorus was determined by the mass increase. It was set to 1.7% of P.

The sol-gel treatment (combined with the thermotex-modification) of the fabrics was carried out using Geniosil GF-9 amine-type silane. The fabrics were immersed into 10% aminosilane solution in toluene. The ratio of fabric to the aminosilane solution was 1 g fabric to 10 ml solution. After the addition of the catalyst (3 droplets of dibutyl tin dilaurate to 100 ml solution), the fabrics were refluxed at 110 °C for 1 h. After cooling to room temperature, the excess was removed in a foulard, and then the fabrics were dried in air at 50 °C. As the next step, thermotex treatment with phosphoric acid solution was carried out. The amount of the adsorbed/chemically bound Si, determined by the mass increase, was set to 4.9%. As the silylation did not affect the effectiveness of the thermotex treatment, the P-content of the fibres/fabric was set to 1.7%.

As carbon fibre reinforcement Zoltek Panex 35 type unidirectional carbon weave with 300 g/m^2 surface mass provided by Zoltek Ltd. (Nyergesújfalu, Hungary) and UDO® MX CST 200 type biaxial CF fabric with 200 g/m^2 surface mass (from SGL Technologies GmbH (Wiesbaden, Germany)) were used (The biaxial type was used in GFTE and reference composites in 4.3.2.1.).

3.2. Applied methods

In this chapter the methods used for the characterization of the synthesized polymer components, as well as preparation of polymer and composite specimens, and their characterization methods are briefly summarized.

3.2.1. Characterization of the synthesized components

The ^{31}P nuclear magnetic resonance (NMR) spectra of the synthesized amines were recorded in a Bruker-300 NMR spectrometer at 25 MHz. ^{1}H and ^{13}C NMR spectra were recorded on a Bruker 300 and a Bruker DRX-500 instrument in $CDCl_3$ with tetramethylsilane (TMS) as the internal standard. Infrared spectra (4000–400 cm^{-1} or 4000–650 cm^{-1}, depending on the physical state) were recorded using a Bruker Tensor 37 type Fourier transform infrared (FTIR) spectrometer with resolution of 4 cm^{-1}, and equipped with deuterated triglycine sulphate (DTGS) detector.

Mass spectroscopic measurements applying fast atom bombardment ionization technique (MS FAB) were performed on ZAB-2SEQ spectrometer. Mass spectroscopic measurements applying matrix assisted laser desorption/ionization technique (MALDI TOF) measurements were taken on Bruker BiFlex III MALDI-TOF apparatus and evaluated with XMASS 5.0 software.

Amine number was determined by titration according to EN ISO 9702:1998 with 0.1 M perchloric acid solution in glacial acetic acid and crystal violet indicator.

Epoxy equivalent was determined by titration according to ASTM D 1652 – 04 with 0.1 M perchloric acid solution in glacial acetic acid and crystal violet indicator in the presence of an excess of tetraethylammonium bromide.

3.2.2. Preparation of polymer and composite specimens

During the specimen preparation the polymer components were mixed in a glass beaker in order to obtain a homogenous mixture. If not mentioned otherwise, stoichiometric ratio of epoxy monomer and hardener was used. Specimens were either cured in appropriately sized heat resistant silicone moulds, or in the case of specimens for mechanical testing resin moulding between two steel plates (with appropriately thick spacing elements to avoid resin leaking) was applied. The applied isothermal curing procedure was determined on the basis of differential scanning calorimetry (DSC) and gel time tests.

The composite laminates were made by hand lamination in a press mould. Each reinforcing layer was separately impregnated, in case of high viscosity matrices the polymer and the mould were heated to 80 °C. The prepared laminates were put under compression with 200 bar hydraulic pressure in T30 type platen press (Metal Fluid Engineering s. r. l., Verdello Zingonia, Italy) to

achieve high and uniform fibre content in the composites. The heat treatment of the laminates (same as in the case of polymer matrix samples) was carried out during the pressing. The measured fibre content was in the range of 59-61 mass%. (In the case of carbon fibre reinforced composites reactively flame retarded with TEDAP in **4.5.1.4** and **4.5.1.5**, as well as in the case of hemp reinforced composites in **4.5.2.2** hand lay-up was used, and fibre content of 40 and 30%, respectively, was achieved). The specimens were cut to appropriate dimensions with diamond disc.

In the case of the sandwich composites consisting of GFTE or DGEBA matrix, cured with AR917 and reinforced with jute fabric, a spacer element was placed between the pressing platens to avoid the unnecessary compression of the core foam material. For the top and the bottom composite layer, two jute fabric layers were impregnated with the epoxy resin systems.

3.2.3. Characterization of polymers and composites

Differential scanning calorimetry (DSC)

DSC tests were carried out in order to investigate the curing of epoxy resins with Q2000 device of TA Instruments (New Castle, DE, USA) in 50 ml/min nitrogen flow. Tzero type aluminium pans were used, the sample mass was 5-20 mg. The applied three-step temperature program consisted of heat/cool/heat cycles: after a linear ramp from 25 to 250 °C (in the case of pure cyanate ester sample up to 400 °C) at 1-5°C/min heating rate (first cycle), the sample was cooled down to 0 °C with 50 °C/min cooling rate, followed by a second linear heating ramp from 0-250 °C (in case of pure CE sample up to 400 °C) at 1-5 °C/min heating rate (second cycle) to ensure the proper conversion. The glass transition temperature (T_g) values were determined from the second heating scan and were defined as the inflection point of the transition curve according to EN ISO 11357-1:1999. In some cases isothermal measurements were carried out as well to determine proper curing circumstances for macro-scaled specimen preparation. After carrying out the specific curing cycles on macro-scaled samples, determined on the basis of DSC results and gel time, the conversion of the specimens was checked by applying a linear heating ramp from 0 to 250 °C at 5 °C/min heating rate. If no postcuring was detected, the conversion was considered as complete.

Thermogravimetric analysis (TGA)

TA Q5000 device of TA Instruments (New Castle, DE, USA) and Setaram Labsys TG DTA/DSC instrument (Caluire, France) was used for thermogravimetric analysis. TGA measurements were carried out in the temperature range of 25-800 °C (if not marked otherwise in the discussion of the results) at a heating rate of 10 °C/min under nitrogen gas flow rate of 30 ml/min. Platinum-HT

sample pan and Setaram type 400 µl aluminium oxide pan were used, the sample size was about 15 mg.

Parallel plate rheometry

Viscosity was determined by parallel plate rheometry using AR2000 device from TA Instruments (New Castle, DE, USA) in the range of 25-80 °C, at 5 °C/min temperature ramp, applying 40 mm diameter plate and 150 µm gap between the plates.

Gel time was determined with 25 mm diameter plate and 200 µm gap between the plates. The test frequency was 10 Hz, the applied temperature was 100 °C. The gel time was determined from the crossing of the recorded shear storage and shear loss modulus values.

Raman spectrometry

Raman spectra were collected with Horiba Jobin-Yvon LabRAM system (Villeneuve d'Ascq, France) coupled with an external 785 nm diode laser source and an Olympus BX-40 optical microscope.

Completion of the curing was monitored in the spectral range of 200-2000 cm^{-1} and 3 cm^{-1} resolution. Objectives of 10× for the starting materials and 50× magnification for the cured sample were used for spectrum acquisition.

For Raman mapping objectives of 100× magnification were used for optical imaging and spectrum acquisition. The spectrograph was set to provide a spectral range of 290-1540 cm^{-1} with 1.25 cm^{-1} resolution. The measured area was 20 µm x 20 µm in each case. Step size of 1 µm x 1 µm was chosen. The spectrum acquisition time was 10 s per spectrum. 4 spectra were accumulated and averaged at each measured point to achieve acceptable signal-to-noise ratio. The distributions were determined using the reference spectra of pure materials with the Classical Least Squares algorithm modeling software.

Scanning electron microscopy (SEM)

SEM images were taken with JEOL JSM 6380LA (JEOL Ltd., Tokyo, Japan) type device from the fracture surfaces of the specimens, which were gold spur coated with a Jeol JPC1200 device before examination to prevent charge build-up on their surface.

Characterization of the fire behaviour

The fire behaviour of the reference and flame retarded systems was characterized by limiting oxygen index measurements (LOI, according to ASTM D-2863, specimen size: 150 mm x 10 mm x 4

mm). The LOI value expresses the minimum volume fraction of oxygen in a mixture of oxygen and nitrogen that supports flaming combustion of a material under specified test conditions.

Standard UL-94 flammability tests (according to ASTM D3081 and ASTM D-635, respectively) were also carried out in order to classify the samples based on their flammability in horizontal and vertical test setups. The increasing values of UL-94 ratings are as follows: HB, V-2, V-1, V-0.

Mass loss calorimeter tests of polymer and composite specimens were carried out by an instrument made by FTT Inc. according to the ISO 13927 standard method. Specimens (100 mm × 100 mm × 4 mm) were exposed to a constant heat flux of 50 kW/m^2 (equivalent to 780 °C cone temperature) and ignited with a spark igniter (In the case of flame retarded SPE and GFTE 2 mm thick samples were subjected to 25 kW/m^2 (equivalent to 605 °C) to avoid excessive charring). Heat release values and mass reduction were continuously recorded during burning. Hemp fabrics were tested according to ASTM E 906 standard method. One ply of the differently treated and untreated fibres (approx. 6 g) was exposed to a constant heat flux of 50 kW/m^2 and ignited.

Laser pyrolysis – Fourier transform infrared analysis

Laser pyrolysis – Fourier transform infrared (LP-FTIR) [172] method was used for investigating the pyrolytic degradation products of samples, and so the possible gas phase effect of the different flame retardants. The system comprises of a CO_2 pyrolyser laser (10.6 nm, SYNRAD 48-1) (Mukilteo, WA, USA) unit coupled with Bruker Tensor 37 type FTIR spectrometer (Billerica, MA, USA) (detector: deuterated triglycine sulphate, gas cell: KRS5 type thallium bromo-iodide window, resolution: 4 cm^{-1}). The pyrolysis of the samples was carried out with 1 W laser power for 1 min, and the formed gases were subjected to FTIR analysis.

Attenuated total reflection infrared (ATR-IR) analysis of the charred residues

IR spectra of the charred residues received after mass loss type cone calorimeter tests were recorded in ATR mode in wavenumber region of 4000-600 cm^{-1}, using the same Bruker Tensor 37 FTIR spectrometer as above.

Char strength determination

The mechanical resistance of the chars obtained after combustion of a round specimen (diameter of 25 mm and thickness of 2 mm) in the mass loss type cone calorimeter (set to 50 kW/m^2 heat flux) was examined through compression tests carried out in a TA AR2000 rheometer (New Castle, DE, USA) with plate–plate geometry, with a constant squeeze rate of 30 μm/s. During the test the normal force transduced by the charred layer was constantly detected and registered [**173**].

Hardness

Shore-D hardness of cured epoxy networks was investigated using a Zwick Roell H04.3150 (Ulm, Germany) type hardness tester according to ISO 868.

Dynamic mechanical analysis (DMA)

For the investigations of the dynamic mechanical properties and for the determination of the glass transition temperature (T_g) values DMA tests were carried out in three point bending setup with TA Q800 device of TA Instruments (New Castle, DE, USA). The temperature range was 25-200 °C (or in high thermal stability samples up to 260 °C or 400 °C) at 3 °C/min heating rate. The frequency was 1 Hz. The size of the specimens was 55x10x2 mm (length x width x thickness), and the support span was 50 mm. The amplitude was strain controlled with 0.1% relative strain. From the results, the storage modulus and tan δ curves, storage modulus values at different temperatures and T_g values were determined by TA Instruments Universal Analysis 2000 4.7A version software.

Tensile test

Tensile tests were carried out to determine the tensile strength and modulus of matrix and composite specimens according to EN ISO 527-4:1999 with Zwick Z020 (Ulm, Germany) type computer controlled universal tester, equipped with a 20 kN capacity load cell. During the test, force and displacement values were recorded and the tensile parameters were calculated according to the standard. In each case 5 parallel tests were carried out.

Bending test

Bending tests were carried out in three point bending setup to determine the flexural strength and modulus of the matrix (according to EN ISO 178:2003) and the composite (according to EN ISO 14125:1999) specimens using Zwick Z020 (Ulm, Germany) type computer controlled universal tester, equipped with a 20 kN capacity load cell with standard three point bending fixtures. During the test, force and deflection values were recorded and the bending parameters were calculated according to the standard. In each case 5 parallel tests were carried out.

Charpy impact test

Charpy impact tests were carried out according to EN ISO 179-1 by a normal impact on unnotched specimens with a Ceast Resil Impactor Junior (Torino, Italy) instrumented pendulum equipped with a 2 J hammer with 150° starting angle and 62 mm support span. The force–time curves were

registered by a Ceast DAS 8000 data acquisition unit and the Charpy impact energy was calculated and compared. In each case 5 parallel tests were carried out.

Interlaminar shear test

According to EN ISO 14130 interlaminar shear tests were carried out by a Zwick Z020 (Ulm, Germany) universal tester. From the registered force-displacement results apparent interlaminar shear strength was calculated and compared. In each case 5 parallel tests were carried out.

Microbond test

Microbond tests were carried using a microbond device fixed onto a Zwick Z005 instrumented tester, with a test speed of 2 mm/min. Matrix droplets were placed on 50 mm long elemental fibres, and the interfacial shear strength (IFSS) between the fibres and the matrices was determined from the maximum force measured during the pull out of the fibre.

Strip tensile test

Strip tensile tests were carried out to determine the effect of alkali treatment on the mechanical properties of jute fabric. 300 mm long samples containing 20 yarns in warp direction were tested according to the ISO 13934-1:2013 standard using Zwick Z020 (Ulm, Germany) instrumented tensile tester. The applied force was parallel to the warp direction of the fabrics. The measured maximal force values were divided by the number of yarns, resulting in specific maximal force values, which were used for the comparison of the differently treated fabrics.

4. EXPERIMENTAL RESULTS AND THEIR DISCUSSION

This chapter summarizes the synthesis of bioepoxy monomers, phosphorus-containing epoxy monomers and curing agents, as well as the development of bio-based epoxy matrices and composites, and last but not least the flame retardancy of epoxy resins and their composites.

4.1. Synthesis of polymer components

To achieve the desired properties, as high glass temperature resins, with an optimum between flame retardancy and mechanical performance, the choice of starting materials and synthesis methods was based on structure-property relationships presented in **Table 4.1.1** (based on [174] and own experience].

Table 4.1.1 Structure-property relationships for tailored synthesis epoxy monomers and hardeners

structure	**property**
high functionality (at least two functional groups per molecule)	increased crosslinking density better mechanical properties
rigid, cycloaliphatic or aromatic backbone	higher glass transition temperature
long aliphatic chains	lower thermal stability lower crosslinking density
aromatic backbone	higher thermal stability increased charring, favourable in terms of flame retardancy
high P-content	flame retardancy is proportional with P-content as a general rule, at least 2% is necessary in polymer composition
high N-content	acts as spumific agent in intumescent FR formulations P-N synergism is favourable in terms of flame retardancy
high OH-content	acts as charring component in intumescent FR formulations easily functionalizable
oligomeric or polymeric form	due to higher molecular mass, limited migration to the surface of the polymer, more stable effect

4.1.1. Synthesis of sugar based epoxy monomers

In this chapter, the syntheses of α-D-glucopyranoside- and glucofuranoside-based epoxy monomers derived from D-glucose, an inexpensive, easily available, renewable starting material, not yet been applied as epoxy monomer precursor, are presented. Our aim was to prepare bioepoxy monomers with high functionality, whose application results in high glass temperature epoxy resins. The detailed recipes of the synthetic procedures are disclosed in [**175**]. Curing properties, glass transition temperature and thermal stability of the synthesized monomers are compared in order to choose the best performing ones for epoxy resin and composite preparation.

4.1.1.1. *Synthesis of glucopyranoside-based bifunctional epoxy monomer (GPBE)*

Methyl 4,6-*O*-benzylidene-α-D-glucopyranoside (**1**) was prepared by condensing methyl-α-D-glucoside (commercially available product, obtained by the condensation of D-glucose with methanol in the presence of cation-exchange resin as catalyst [176]) with benzaldehyde using zinc chloride as catalyst. After a reaction of 4 h at room temperature, the intermediate **1** was obtained in a yield of nearly 72% by crystallization [177]. Treatment of compound **1** with an excess of allyl bromide and solid potassium hydroxide in refluxing toluene gave diallyl ether **2**, after crystallization in a yield of 90%. [178]. Diallyl ether **2** was converted by treatment with hydrogen peroxide into diglycidyl ether derivative **3** in methanol in the presence of K_2CO_3 and benzonitrile by the method of Holmberg [179]. The reaction temperature was kept at room temperature by external cooling. After chromatography the yield of the solid crystalline product **3** was 40% (**Figure 4.1.1**).

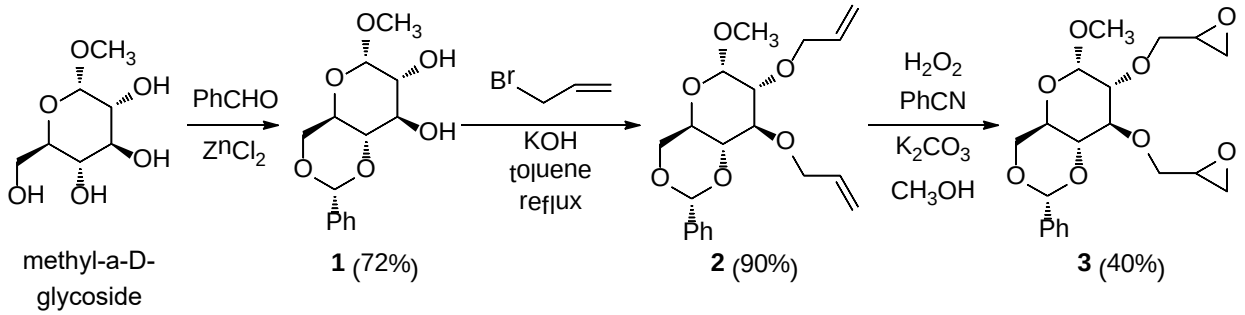

Figure 4.1.1 Synthesis of glucopyranoside-based bifunctional epoxy monomer (GPBE)

4.1.1.2. *Synthesis of glucopyranoside-based trifunctional epoxy monomer (GPTE)*

The synthesis of compound **7** having three glycidyl ether groups was carried out using two methods (**Figure 4.1.2**). Preparation of allyl-α-D-glucopyranoside (**4**) was performed by the reaction of D-glucose and allyl alcohol in the presence of boron trifluoride diethyl etherate ($BF_3{\cdot}Et_2O$) as catalyst in 26% yield (5 h, reflux, column chromatography) [180]. Selective protection of the 4- and 6-hydroxyl groups of the allyl-α-D-glucopyranoside with benzaldehyde dimethylacetal using *p*-toluenesulfonic acid (*p*TsOH) as catalyst was accomplished in DMF resulting in compound **5** in good yield (76%). The one pot method for preparation of compound **5** proved to be simpler [181]. D-glucose was refluxed in allyl alcohol in the presence of CF_3SO_3H for 48 h. After the removal of the alcohol and the acid, the residue was reacted in DMF with benzaldehyde dimethylacetal using *p*TsOH as catalyst (40 °C, 5 h). Mixture of α and β isomers of allyl-4,6-*O*-benzylidene-α- D-glucopyranoside (**5**) was obtained with 45% yield. The reaction of compound **5** with allyl bromide in toluene in the presence of potassium hydroxide gave the corresponding 1,2,3-tri-*O*-allyl derivative **6** [182]. Epoxidation of **6** with *m*-chloroperbenzoic acid in toluene

resulted in (2',3'-epoxypropyl)-2,3-di-*O*-(2',3'-epoxypropyl)-4,6-*O*-benzylidene-α-D-glucopyranoside (**7**) after chromatography with 72% yield of the crystalline product.

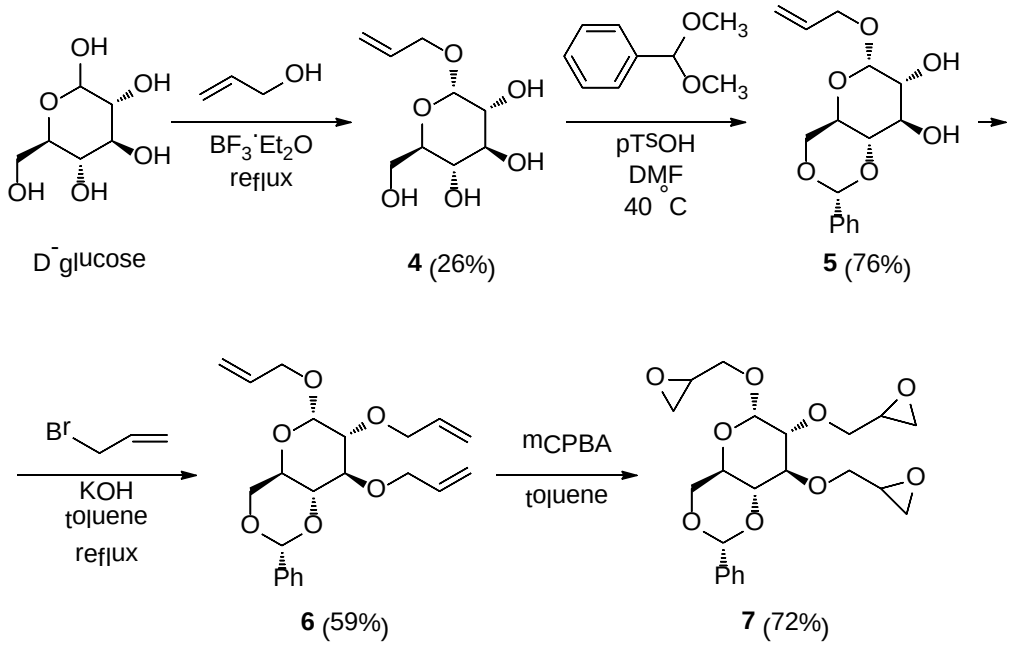

Figure 4.1.2 Synthesis of glucopyranoside-based trifunctional epoxy component (GPTE)

4.1.1.3. *Synthesis of glucopyranoside-based tetrafunctional epoxy monomer (GPQE)*

The preparation of the tetraallyl-derivative (**8**) was carried out by the reaction of methyl-α-D-glucoside and allyl bromide in 1,4-dioxane in the presence of potassium hydroxide. After chromatography the yield of product **8** was 40%. The tetraepoxy-glucopyranoside-derivative (**9**) was obtained by the oxidation of compound **8** with *m*-chloroperbenzoic acid in toluene after stirring at room temperature for 24 h. The yield of the crystalline product **9** was 50% (**Figure 4.1.3**) [183].

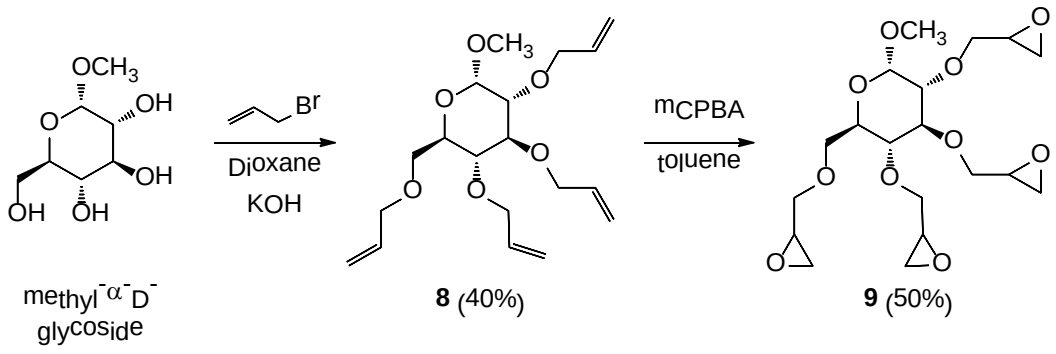

Figure 4.1.3 Synthesis of glucopyranoside-based tetrafunctional epoxy component (GPQE)

4.1.1.4. *Synthesis of glucofuranoside-based trifunctional epoxy monomer (GFTE)*

D-Glucose was also the starting material of the isopropylidene-α-D-glucofuranoside-based epoxy monomer. The key compound was the 1,2-di-*O*-isopropylidene-α-D-glucofuranoside (**11**) (**Figure 4.1.4**), which could be obtained by two methods. The reaction of D-glucose with acetone (reagent and solvent) in the presence of iodine (as catalyst) lead to 1,2:5,6-di-*O*-isopropylidene-α-D-

glucofuranoside (**10**) in good yield (59%) after purification by crystallization [184]. Selective removal of the 5,6-*O*-isopropylidene group of the intermediate was carried out with diluted sulfuric acid in methanol (24 h, room temperature, yield after crystallization was 65%) [184]. The one pot method for the preparation of compound **11** proved to be more effective [185]. First, D-glucose was treated with acetone in the presence of sulfuric acid, then after neutralization and evaporation of the reaction mixture, the crude product (1,2:5,6-di-*O*-isopropylidene-α-D-glucofuranoside) was treated with hydrochloric acid giving intermediate **11** in a yield of 43% after recrystallization. The reaction of compound **11** with mixture of potassium hydroxide and allyl bromide in toluene gave the corresponding 3,5,6-tri-*O*-allyl derivative **12** in a yield of 74% applying a modification of Bullock's method [186]. Epoxidation of allyl ether **12** with *m*-chloroperbenzoic acid in toluene resulted in 3,5,6-tri-*O*-(2',3'-epoxypropyl)-1,2-*O*-isopropylidene-α-D-glucofuranoside (**13**) in a yield of 76% after purification by chromatography. The product is yellow oil, with a viscosity of 3.77 Pa·s at room temperature.

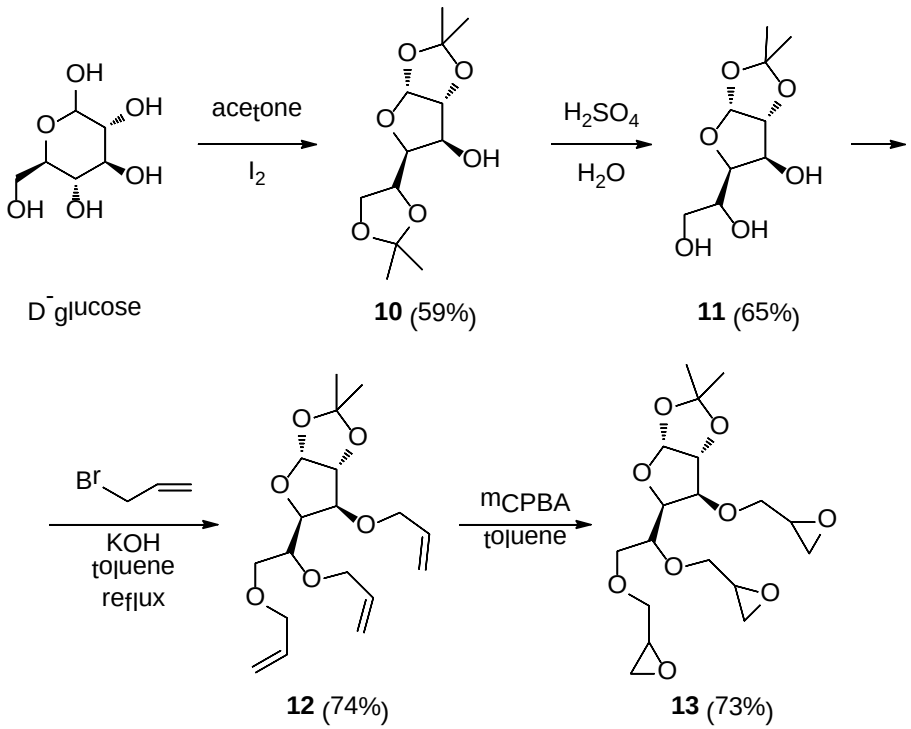

Figure 4.1.4 Synthesis of glucofuranoside-based trifunctional epoxy component (GFTE)

As among the synthesized glucose-based epoxy monomers the liquid, trifunctional glucofuranoside-based epoxy monomer provided the highest glass transition temperature, the synthesis of this product was scaled-up. During the initial synthesis both the allyl- derivative and the epoxy monomer were purified by chromatography, which is an uneconomical and extremely time-consuming procedure. During the scale-up the number of purification steps was attempted to be reduced and alternative reaction pathways were elaborated as follows:

1,2-di-*O*-isopropylidene-α-D-glucofuranoside (**11**) was synthesized with the already described one-pot method. The precipitate was filtered from the mother liquor after evaporation, and after the evaporation of the secondary mother liquor, **11** was received with 55% yield. The product contains in each case minor pollutants (e.g. disaccharides), but they can be easily removed in the next step of the reaction by filtration, as they are not soluble in toluene, just the formed KBr and the eventually unreacted KOH base. The excess allyl bromide was removed from the reaction mixture during evaporation. The received product was dissolved in toluene again, washed with water to remove traces of KBr and KOH. After drying and evaporation the allyl derivative (**12**) was received with nearly 100% yield without purification. The crude product of the previous step was dissolved in toluene and epoxidation was carried out with *m*-chloroperbenzoic acid (*m*CPBA). The reaction by-product, *m*-chlorobenzoic acid (*m*CBA) precipitated from toluene, so it could be removed by filtration. The up-scaled synthesis required cooling to avoid side reactions above 45 °C e.g. oxidation of the backbone or opening of the acetal ring. After filtering, the mother liquor was washed with Na_2CO_3 solution in order to remove the excess *m*CPBA and unfiltered *m*CBA. After evaporation, the epoxidized product, having an epoxy equivalent of 160 g/eq, was received with nearly 80% yield, without any further purification.

4.1.1.5. *Preliminary testing of the synthesized sugar based bioepoxy monomers*

Curing properties

For investigating the applicability of the synthesized glucose-based epoxy monomers DSC measurements were carried out with 4,4'-diaminodiphenyl methane (DDM) hardener. As the synthesized components were prepared in >95% purity, their epoxy equivalents could be determined from their molecular mass (**Table 4.1.2**), which were in good agreement with the values determined by titration.

The onset point of the curing is about 120 °C in most cases. The peak temperatures are also in the same temperature range for GPBE, GPQE, and GFTE, while GPTE showed somewhat lower values. From the curing enthalpy measured in DSC (J/g), the enthalpy in kJ/mol epoxy groups was calculated and compared to the theoretical value (105 kJ/mol per epoxy groups, independently from the molecular structure of epoxy resin and amine reacted [187,188]) to determine the degree of cure. In the case of the oily GFTE bioepoxy monomer, the calculated enthalpy is in good accordance with the theoretical value, similarly to the reference DGEBA – DDM system. It can be stated, that the reaction between the glucopyranoside-based epoxy components and the hardener was not complete, which can be explained by their solid state: during the mixing with solid DDM, no molecular level homogenization was reached, thus, no full curing could be

achieved. (Neither the solutions of the components, nor the mixtures of the melted molecules are suitable for determining the curing by the DSC method. The presence of the solvent, or the already started reaction between the components would falsify the results.)

Table 4.1.2 Curing behaviour of the synthesized bioepoxy components and the DGEBA reference

epoxy monomer	GPBE	GPTE	GPQE	GFTE	DGEBA
epoxy equivalent [g/eq]	197	145	104	129	180
onset temperature of curing [°C]	127	98	118	128	121
peak temperature of curing [°C]	164	127	143	158	149
measured enthalpy of curing [J/g]	258	395	535	531	432
calculated enthalpy of curing [kJ/mol epoxy groups]	63.7	77.2	82.7	95.1	99.2
degree of cure [%]	60.7	73.5	78.8	90.6	94.5
glass transition temperature [°C]	76	154	130	177	174

The glass transition temperatures (T_g) of the glucose-based epoxy networks (**Table 4.1.2**) show various values. As expected, the lowest T_g was measured for the bifunctional glucopyranoside-based component (GPBE), due to the low functionality and low degree of cure. When comparing the glucopyranoside-based tri- and tetrafunctional resins, in contrast to the expectations, the lower functionality provided the higher T_g. This can be explained by the higher flexibility of GPQE structure, as the rigid bicyclic part is missing in this case, the segmental movements are less limited. The highest T_g value (177 °C), even higher than that for the reference DGEBA (174 °C), was reached using GFTE, owing to the compact structure of the molecule.

The completion of the curing in the case of GFTE was also investigated by Raman spectrometry (**Figure 4.1.5**).

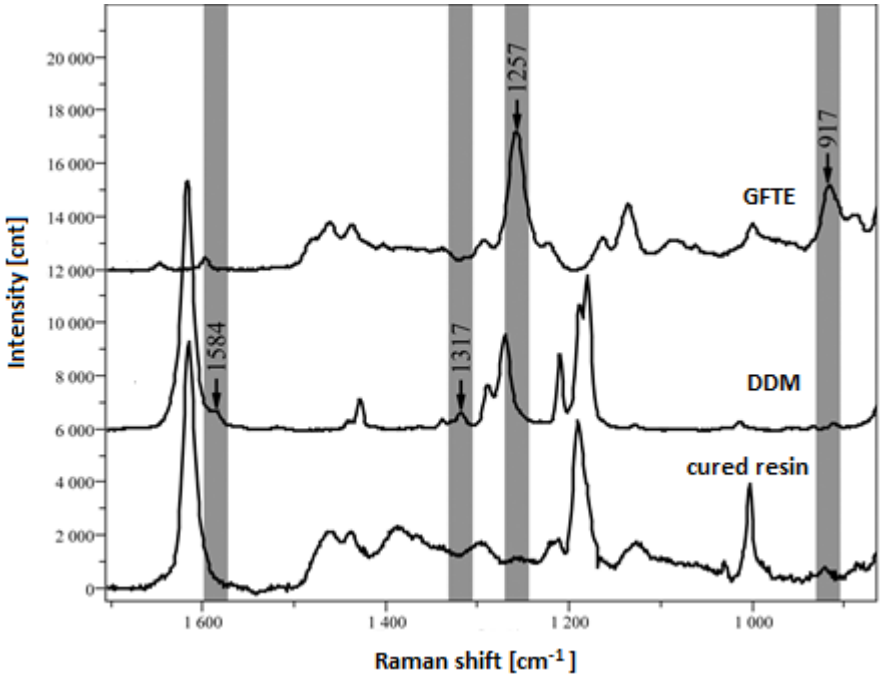

Figure 4.1.5 Raman spectra of GFTE epoxy component, DDM curing agent and the cured resin

The characteristic bands of the epoxy ring can be seen at 917 and at 1257 cm^{-1} in the spectrum of GFTE. At this region, the vibrations of the NH_2 groups appear as weak peaks at 1317 and at 1584 cm^{-1} in the spectrum of DDM. In the spectrum of the cured resin neither the epoxy component nor the amine-type hardener has characteristic peaks, which indicates the complete reaction between the two components.

Thermal stability

The thermal stability of the cured bioepoxy networks was determined by TGA (**Table 4.1.3**).

Table 4.1.3 TGA results of the different bioepoxy resins and DGEBA reference cured with DDM

component	$T_{-5\%}$ [°C]	$T_{-50\%}$ [°C]	dTG_{max} [%/°C]	T_{dTGmax} [°C]	char yield at 800 °C [%]
GPBE	330	467	0.76	375	42.7
GPTE	336	398	1.15	363	26.6
GPQE	367	426	1.24	385	34.0
GFTE	293	416	0.54	359	34.6
DGEBA	368	424	1.34	384	34.8

$T_{-5\%}$: temperature at 5% mass loss; $T_{-50\%}$: temperature at 50% mass loss, dTG_{max}: maximum mass loss rate; T_{dTGmax}: temperature belonging to dTG_{max}

The degradation of the trifunctional glucofuranoside-based resin (GFTE) starts at the lowest temperature among the investigated systems, as the 1,2-*O*-isopropylidene group of the molecule can easily split off, releasing acetone. The further decomposition of this sample is relatively slow. The bi- and trifunctional glucopyranoside-based resins (GPBE and GPTE) start to degrade at about 330 °C, with the leaving of the 4,6-*O*-benzylidene protecting group. GPQE and DGEBA have no easily cleaveable protecting groups, so the highest thermal stability can be reached (up to 360 °C), however, their degradation rate is also high. The relatively high char yields of the synthesized bioepoxy compositions are promising in terms of flame retardancy.

4.1.2. Synthesis of phosphorus-containing epoxy monomer

P-containing epoxy monomers were synthesized from aromatic DGEBA and aliphatic PER by adduct formation with 9,10-dihydro-9-oxa-10-phosphaphenantrene-10-oxide (DOPO). These syntheses were based on the method previously published by Wang and Lin [107].

4.1.2.1. *Synthesis of DGEBA-DOPO adduct*

In order to form an aromatic P-containing epoxy monomer DOPO was reacted with DGEBA in 1:1 molar ratio (**Figure 4.1.6**) [**189**,**190**]. Prior to the reaction DOPO was kept at 85 °C for 12 h, in order to remove the traces of moisture. DGEBA was kept in under vacuum at 110 °C to remove air and traces of moisture, and after adding DOPO, the mixture was stirred at 160 °C for 5 h. After cooling

to room temperature a solid adduct was obtained, which was used for reactive flame retardancy of DGEBA (see **4.4.4**).

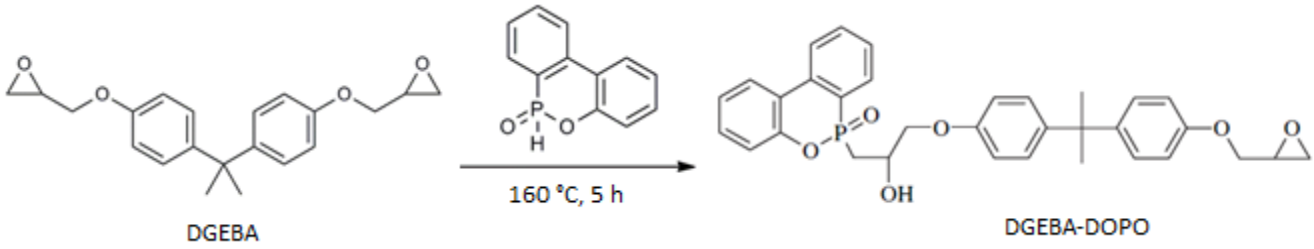

Figure 4.1.6 Synthesis of DGEBA-DOPO adduct

4.1.2.2. *Synthesis of PER-DOPO adduct*

In order to form an aliphatic P-containing epoxy monomer, DOPO was reacted with PER in 1:1 molar ratio (**Figure 4.1.7**) [**191**]. Prior to the reaction DOPO was kept at 85 °C for 12 h, in order to remove the traces of moisture. The mixture of PER and DOPO was stirred at 160 °C for 8 h. After cooling to room temperature a solid adduct was obtained, which was used for reactive flame retardancy of PER (see **4.4.1**).

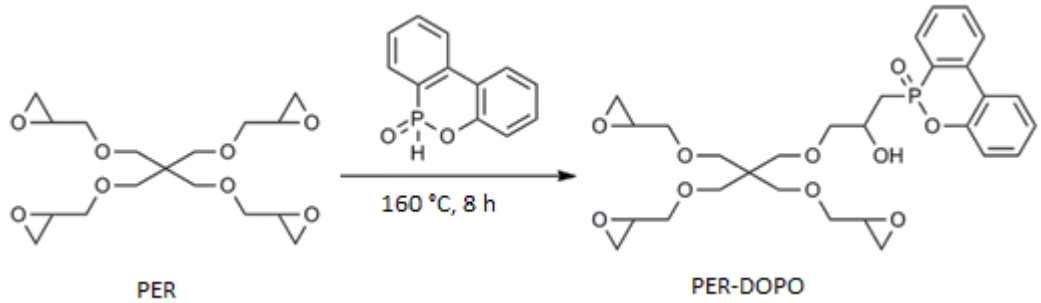

Figure 4.1.7 Synthesis of PER-DOPO adduct

4.1.3. Synthesis of phosphorus-containing crosslinking agents

In this chapter, a simple, cost-effective and environmentally friendly method (patented by the author and co-workers [**133**]) was used for the synthesis of phosphorylated amines with high P-content, which can act as FR crosslinking agent in epoxy resins. Reaction of triethyl phosphate with an aliphatic diamine, ethylene diamine and two aromatic diamines, *o*- and *m*-phenylenediamine was carried out. Concerning the choice of amine reagents, it can be noted that short chained aliphatic amines are widely applied as crosslinking agents in epoxy resins and are produced in large quantities, and choosing them as a reactant in this synthesis, high P-content of the hardener and the epoxy resin system can be achieved. As the P-content is proportional to the FR effect, this was an important aspect. On the other hand although the P-content which can be achieved using aromatic amines is lower than in case of short chained aliphatic amines, the aromatic backbone offers numerous advantages as high char yield, higher thermal stability, more rigid structure

leading to higher glass transition temperature. The curing properties, glass transition temperature, thermal stability and FR performance of the synthesized amines were compared.

4.1.3.1. *Synthesis of N,N',N''-tris(2-aminoethyl) phosphoric triamide (TEDAP)*

Transamidation of triethyl phosphate (TEP) was carried out with ethylene diamine (EDA) according to **Figure 4.1.8**.

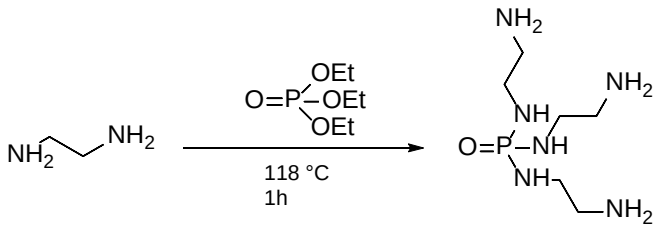

Figure 4.1.8 Synthesis of TEDAP

EDA and TEP were reacted in 10:1 molar ratio instead of the necessary 3:1 to shift the equilibrium in the direction of the required trisubstituted product. After TEP was added dropwise to EDA, the mixture was stirred at the boiling point of EDA, at 118 °C for 1 h. The excess of EDA was removed by vacuum distillation to give the liquid, yellowish brown product with amine number of 500±5 mg KOH/g in 93% yield. The FTIR spectra confirmed the formation of P-N-C bonds [**192**]. According to MALDI-TOF spectra the product mainly contained monomers, but possible fragments of dimers, trimers and tetramers were also detected. For detailed results see [**193**].

4.1.3.2. *Synthesis of N,N',N''-tris(3-aminophenyl) phosphoric triamide (TMPDAP)*

An aromatic diamine, *m*-phenylenediamine was used in the transamidation reaction according to **Figure 4.1.9.**

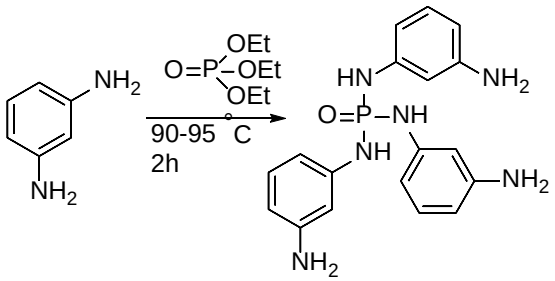

Figure 4.1.9 Synthesis of TMPDAP

7.136 g (0.066 mol) of *m*-phenylenediamine was heated in a round flask until melting (64-66 °C). When the amine was completely melted, 3.72 ml (0.022 mol) of TEP was added dropwise, and then stirred at 90-95 °C for 2 h. The formed ethanol was removed from the reaction mixture by vacuum evaporation to give the liquid, dark green product with amine number of 655±5 mg KOH/g in 90% yield. For detailed results see [**193**].

4.1.3.3. *Synthesis of N,N',N''-tris(2-aminophenyl) phosphoric triamide (TOPDAP)*

The transamidation reaction was also carried out with another aromatic diamine, *o*-phenylenediamine according to **Figure 4.1.10.**

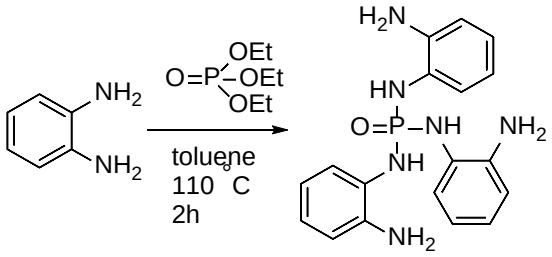

Figure 4.1.10 Synthesis of TOPDAP

To the solution of 70 ml toluene and 7.136 g (0.066 mol) of *o*-phenylenediamine 3.72 ml (0.022 mol) of TEP was added and the mixture was stirred at the boiling point of toluene, at 110 °C for 7 h. After cooling, the dark violet solid product with amine number of 307±5 mg KOH/g was filtered out, with a yield of 90%. For detailed results see [**193**].

4.1.3.4. *Preliminary testing of the synthesized phosphorus-containing amines*

Curing properties of the synthesized amines

For investigating the applicability of the synthesized P-containing amines as curing agents for epoxy resins, DSC measurements were carried out (**Table 4.1.4**). The pentaerythritol-based model epoxy monomer (PER) and the synthesized amines, as well as the reference cycloaliphatic diamine (T58), were mixed in an appropriate ratio. The highest enthalpy of curing was measured in the case of the latter one. The difference between the measured values of the two P-containing aromatic amines (TMPDAP and TOPDAP) is negligible; the peak of curing appears at somewhat higher temperature in case of the *o*-phenylene diamine-based molecule, which can be explained by steric hindrance of the amine groups in *ortho* position compared to that of the *meta* one. The aliphatic P-containing TEDAP showed the lowest curing enthalpy, so the least exothermic reaction, which can be beneficial at large scale curing. As for the glass transition temperatures (T_g), the cycloaliphatic reference hardener had the highest value, as the rigidity of the cycloaliphatic rings hinders the segmental movements in the crosslinked resin. In the case of the two aromatic, P-containing amines, the T_g is somewhat lower, as the rings are bound together via the more flexible N-P-N bonds compared to the one atom distance between the cycloaliphatic rings. TEDAP showed the lowest glass transition temperature among the investigated resin systems, as both the epoxy component and the hardener have flexible aliphatic chains, which allow easy segmental movements and thus relatively low T_g.

Table 4.1.4 Curing behaviour of the synthesized amines and glass transition temperature of PER crosslinked with them

curing agent	onset temperature of curing [°C]	peak temperature of curing [°C]	enthalpy of curing [J/g]	glass transition temperature [°C]
T58 reference	65	100	402	98
TEDAP	44	77	283	40
TMPDAP	56	84	337	79
TOPDAP	71	93	337	77

Thermal stability

The degradation of PER cured with reference cycloaliphatic hardener starts with a sharp mass decrease at 295 °C, and a very high decomposition rate (**Table 4.1.5**). The residue at 500 °C is less than 10%, as no charring agent is present in the system. When the P-containing hardeners are applied, the decomposition starts at lower temperatures, which can be explained by the evolved PO radicals at the early stage of the degradation slowing down the further degradation steps [**173**]. The degradation of the TOPDAP-cured resin shows a two-step curve, with almost the same decomposition rates. This double degradation can be explained by the lower stability of the amine starting material itself due to the $–NH_2$ groups in *o*-position. The residue of the TOPDAP-cured resin is less than that of its stereoisomer, TMPDAP: 28.9% compared to 41.8%. The TMPDAP-cured system shows elongated and relatively slow degradation. The highest decomposition rate appears at 280 °C, between the values of the two steps of TOPDAP. The amount of charred residue for the aliphatic P-containing hardener (26.6%) is somewhat lower than that for the aromatic ones, which is related to the beneficial effect of the aromatic rings in char formation. Also the rate of decomposition is higher in the case of TEDAP; however this maximum is reached at higher temperature.

Table 4.1.5 TGA results of PER cured with different amines

curing agent	$T_{-5\%}$ [°C]	$T_{-50\%}$ [°C]	dTG_{max} [%/°C]	T_{dTGmax} [°C]	char yield at 500 °C [%]
T58 reference	294	326	2.47	296	8.6
TEDAP	264	326	0.88	289	26.6
TMPDAP	266	391	0.75	280	41.8
TOPDAP	256	350	0.70 0.68	263 325	28.9

$T_{-5\%}$: temperature at 5% mass loss; $T_{-50\%}$: temperature at 50% mass loss, dTG_{max}: maximum mass loss rate; T_{dTGmax}: temperature belonging to dTG_{max}

Flame retardancy

For the comparison of the FR efficiency of the synthesized P-containing amines, LOI and UL-94 measurements were carried out (**Table 4.1.6**). The P-containing hardeners result in decreased flammability compared PER, LOI values are above 30 V/V% in all cases, which indicates the

beneficial effect of P in terms of decreasing the ignitability of the resins. The reference system reached only HB UL-94 classification with a relatively high flame spreading rate (32 mm/min), while the P-containing resins passed the horizontal test, no flame spreading rates could be measured. The significance of the P-content is doubtless: the TMPDAP-cured resin contains less than 2% P and reaches only V-1 classification (the difference between the P-content of the two aromatic amines is caused by the difference of their amine values requiring different mixing ratios for achieving the same level of crosslinking), while the samples with more than 2% P-content could reach the best, V-0 classification.

Table 4.1.6 Comparison of LOI and UL-94 results of reference and FR epoxy resin matrices

curing agent	P-content [%]	LOI [V/V%]	UL-94*
reference	0	23	HB (32 mm/min)
TEDAP	2.8	33	V-0
TMPDAP	1.7	31	V-1
TOPDAP	3.0	30	V-0

* in parenthesis the horizontal burning rate is showed, where measurable

4.1.4. Summary on synthesis methods

Bioepoxy monomers were synthesized from an inexpensive, renewable and easily available **starting material, D-glucose**. By protecting the hydroxyl groups in the 4 and 6 positions, **bi- and trifunctional glucopyranoside-based epoxy monomers (GPBE and GPTE)** were prepared via allylation of the free hydroxyl groups, followed by the epoxidation of the carbon-carbon double bond with m-chloroperbenzoic acid, having a relatively rigid, bicyclic backbone. By removing the 4,6-O-benzylidene protecting group, a **tetrafunctional epoxy monomer (GPQE)** was synthesized. Besides the glucopyranoside-based components, a **glucofuranoside-based trifunctional monomer (GFTE)** was also prepared: glucose was reacted with acetone, followed by the selective removing of the 5,6-O-isopropylidene group. The formed free hydroxyl groups were reacted first with allyl bromide, and then the allyl functions were epoxidized. Among the prepared components, the **glucopyranoside-based tri- and tetrafunctional molecules have not yet been synthesized earlier**, while the other two compounds have not yet been cured to form epoxy resins. The applicability of the synthesized compounds as epoxy monomers was investigated by **curing probes with a model aromatic amine-type hardener (DDM)**. The curing enthalpy of the bioepoxy resins were examined and compared to theoretical values, as well as the glass transition temperature, which is a crucial parameter when determining the potential fields of application of the bioresins. The **highest glass transition temperature (175 °C)** was reached with the **glucofuranoside-based trifunctional**

monomer, as the easy accessibility of the epoxy groups is combined with a relatively rigid bicyclic backbone. The thermal stability of the cured resins was investigated by TGA measurements. The **degradation** of the samples **starts between 293 and 367 °C**, while all the synthesized resins have relatively **high char yields at 800 °C,** promising in terms of flame retardancy. Among the synthesized bi- tri- and tetrafunctional D-glucose-based bioepoxy monomers the **glucopyranoside- and glucofuranoside-based trifunctional** ones proved to be the **most promising for high-tech applications**.

P-containing epoxy monomers were prepared in the reaction of **DOPO with aromatic DGEBA and aliphatic PER**, respectively, for reactive flame retardancy of the latter epoxy resins.

Environmental-friendly and cost-effective one-pot synthesis method was used for the synthesis of **P-containing amines**. The starting material, **triethyl phosphate** is commercially available and produced in large quantities for other purposes, is not harmful to the environment and during the reaction no harmful by-products are formed. In the case of the aliphatic amine, the excess of **ethylenediamine** serves also as solvent in the reaction, which can be recycled during the production. When the aromatic ***o*-phenylene diamine** is used as starting material, the formed product is crystalline, which can be easily filtered out from the toluene solution. **The *m*-phenylene diamine** can react with the phosphorylating agent even in molten phase, so the application of solvents can be avoided. Based on the DSC results all the tested molecules can cure the resins, and thus, **can be used as crosslinking agents**. The FR efficacy was also tested. The resins with more than 2% P-content could reach the best, **V-0** classification in the **UL-94 test**, while all the investigated FR systems have **LOI values higher than 30 V/V%.**

4.2. Development and characterization of bio-based polymer matrices

In this chapter the results on a partially bio-based epoxy resin system consisting of epoxidized vegetable oil and mineral oil based epoxy monomers, and sugar based bioepoxy resins are summarized.

Epoxidized plant oils are currently mainly used in combination with commodity mineral oil based epoxy resin components. Considering that the composition of plant oil based polymers is not as exact as that of synthetic ones, this **step-by-step replacement approach** is easily understandable. Therefore in order to facilitate the application of bio-based resins in more demanding advanced sectors, a **systematic study** was carried out to characterize the **effect of epoxidized soybean oil (ESO)**, one of the most commonly used bio-based resins, **on curing and rheological behaviour, glass transition temperature, mechanical and thermal properties** in various epoxy resin systems.

Besides the conventional, widely investigated **aromatic diglycidyl ether of bisphenol-A (DGEBA)** resin, a **glycerol- (GER)** and **a pentaerythritol-based (PER) aliphatic resin** was chosen as base resin, whose **synthesis is feasible from renewable materials as well** (glycerol is available in large quantities from natural fatty acids, while pentaerythritol can be produced from bio-based methanol as well), in the end leading to full replacement of mineral oil based epoxy monomers by the ones from renewable sources. As hardener a **phthalic anhydride** based component was used, which can be **potentially** also **synthesized from natural sources** [194], offering the possibility of a fully bio-based matrix material. In the hybrid resin system the ESO-content was systematically increased from 0 to 100%. The expected outcome of this study was to define the composition along with its curing characteristics, which contains the **highest amount of ESO with acceptable reduction in the T_g and stiffness** compared to those of the neat epoxy resin.

As **renewable** epoxy resin components two glucose-based components, synthesized previously by our research group [**175**], were used: a **solid glucopyranoside based trifunctional** epoxy resin component **(GPTE)** and a **liquid glucofuranoside based trifunctional** epoxy resin component **(GFTE)**. The **curing and rheological behaviour, glass transition temperature, mechanical and thermal properties** of these two novel glucose-based EP components were compared to the conventional, widely investigated bifunctional aromatic DGEBA resin, to a trifunctional glycerol- and a tetrafunctional pentaerythritol-based aliphatic resin. The expected outcome of this study was to determine the **potential application areas**, where these newly developed glucose-based EP components are **capable of replacing the mineral oil based commodity resins**.

4.2.1. Development of vegetable oil based epoxy resin matrices

Blends of epoxidized soybean oil (ESO) with a glycerol- (GER) and a pentaerythritol-based (PER) aliphatic epoxy resins and aromatic DGEBA epoxy resin were tested. In each case 25, 50 and 75% ESO was added to the synthetic resin. The effect of ESO on curing and rheological behaviour, glass transition temperature, mechanical and thermal properties was determined [**195**].

Curing behaviour

The curing process of the three basic epoxy resins as a function of the ESO-content was monitored by DSC (**Figure 4.2.1**).

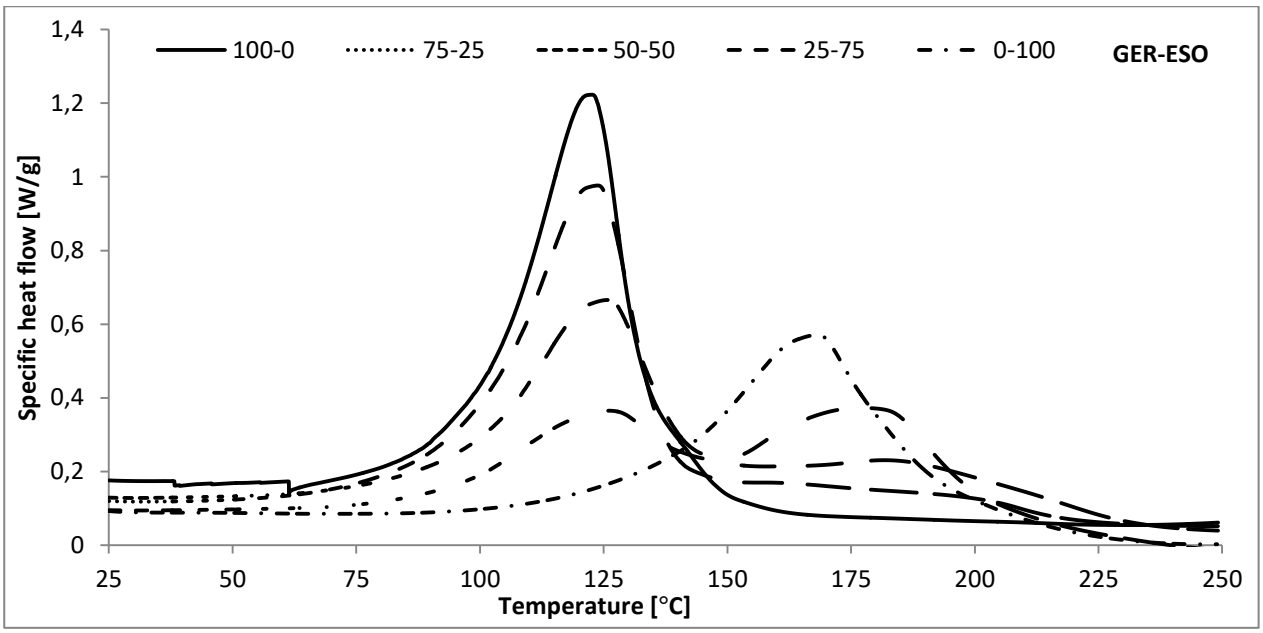

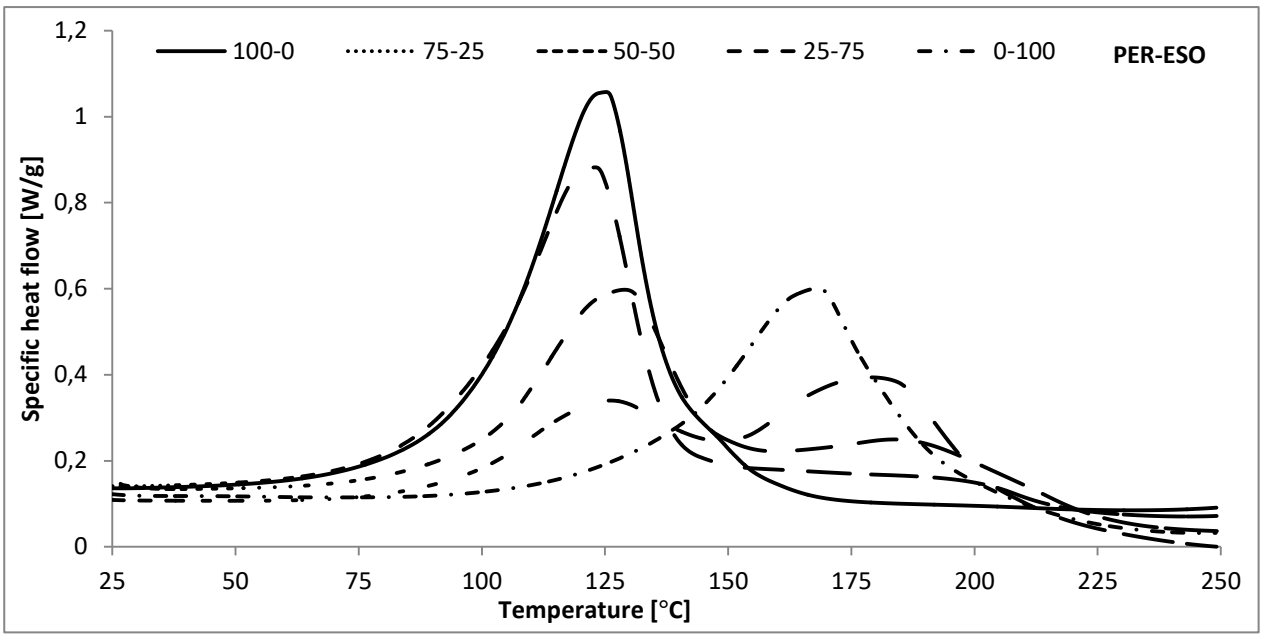

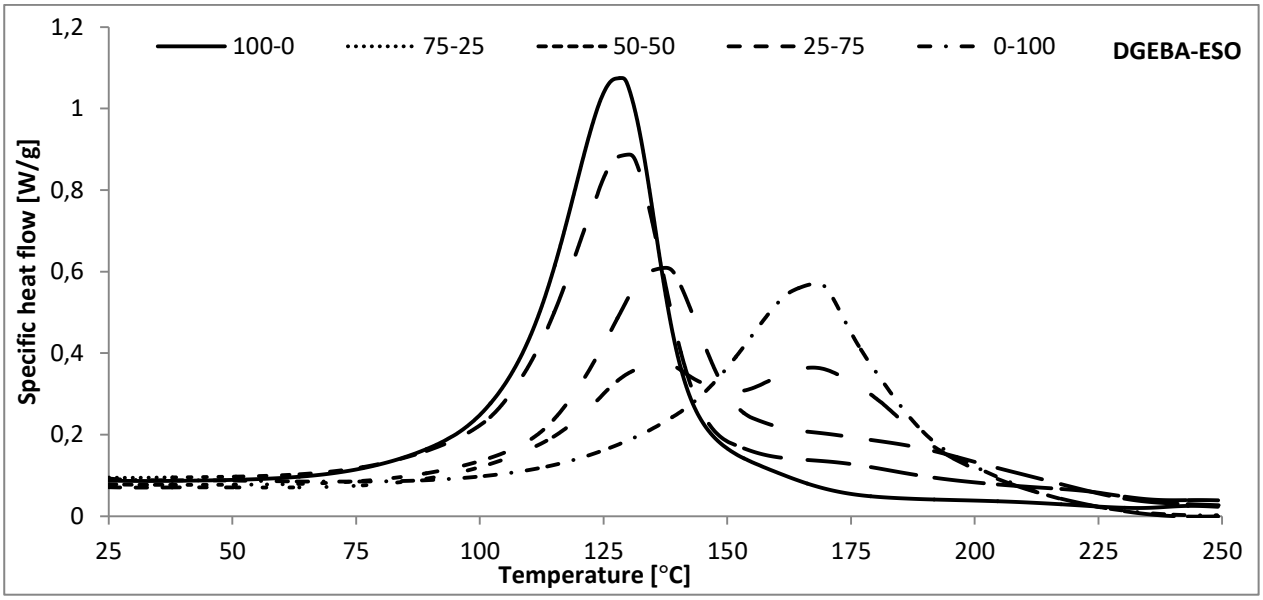

Figure 4.2.1 DSC curves of the different EP/ESO systems

In the case of the aliphatic systems, a second peak appeared on the DSC curves when the samples contained 50 and 75% ESO, while in the case of DGEBA there was a second peak only at 75% ESO content. This peak doubling can refer to phase separation, which is usually explained by the fact that the internal oxirane rings in ESO have lower reactivity than the terminal ones in GER/PER/DGEBA [13]. The total calculated specific reaction enthalpy values, the temperatures related to the first and second heat flow peaks are shown in **Table 4.2.1**.

Table 4.2.1 Specific reaction enthalpy values and temperatures related to the first and second heat flow peaks of the different EP/ESO systems

	base resin	**ESO content [%]**				
		0	**25**	**50**	**75**	**100**
total specific reaction enthalpy [J/g]	GER	372	399	367	344	287
	PER	388	378	353	328	287
	DGEBA	381	346	311	309	287
temperature of first heat flow peak [°C]	GER	123	124	126	126	168
	PER	125	123	129	126	168
	DGEBA	129	130	138	137	168
temperature of second heat flow peak [°C]	GER	-	-	182	177	-
	PER	-	-	184	179	-
	DGEBA	-	-	-	167	-

By adding 25% ESO the temperature of the first heat flow peak was only negligibly influenced, while 50 and 75% shifted it to higher temperatures. This effect was more pronounced in the aromatic DGEBA system. As for the second heat flow peaks, in aliphatic systems with 50 and 75% ESO, they appeared at higher temperatures than in neat ESO itself suggesting slower crosslinking reaction, while in the case of the DGEBA with 75% ESO content the second peak appeared nearly at the same temperature as the ESO heat flow peak. By increasing the ESO content the total specific enthalpy decreased practically in all cases. These results suggest that higher curing temperature and/or longer curing cycles may be necessary when ESO is used to reach complete conversion than in the case of the neat resins.

For proper specimen preparation, isothermal DSC measurements were carried out to check the conversion with all of the resin mixtures for 2 h on 140 °C. According to the heat flow curves of the second heating cycle (0-250 °C with 5 °C/min heating rate), no post-curing could be detected both in a case of aliphatic and aromatic hybrid systems, proving that the chosen curing cycle (2 h at 140 °C) provided appropriate conversion in each case. Consequently, the glass transition temperatures (T_g) could be determined from the second heat flow curves. These results are discussed later in **Table 4.2.4** in comparison with the T_g values determined by DMA.

Gelling

In order to estimate the processability of different EP/ESO blends gel time was determined by parallel plate rheometry (**Table 4.2.2).** The gel time, consequently the pot life of the epoxy resins significantly increased with the ESO content, as expected from decreased specific heat flow values of curing reaction as well.

Table 4.2.2 Gel times of the different EP/ESO systems

base resin		**gel time[s]**		
		GER	**PER**	**DGEBA**
ESO content [%]	**0**	769	532	935
	25	854	616	1088
	50	939	686	1200
	75	946	862	1879
	100			6366

Storage modulus and glass transition temperature

Storage modulus and tan δ curves of EP/ESO blends are displayed in **Figure 4.2.2.** In the case of aliphatic systems the 25% ESO addition significantly improved the storage modulus values in both cases (below (25, 50, 75 °C) and above (160 °C) the T_g) compared to the neat epoxy resin systems (**Table 4.2.3**). At all temperatures the highest improvements could be detected in the case of PER with 25% ESO. The increased storage modulus values may be explained with the similar chemical structure of aliphatic resins and ESO. In the case of DGEBA the ESO addition decreased the storage modulus at every temperature. Crosslinking between DGEBA and ESO is more probable in those positions, where the aromatic and the aliphatic segments are as far from each other as possible; while in aliphatic resins the similar structure allows steric proximity, leading to increase in crosslink density. At low ESO-content most probably the co-crosslinking is more dominant than the phase separation. Above 50% ESO content a significant softening effect appears in all epoxy resin systems. Peak doubling in case of tan δ curves of samples containing 75% ESO suggests as well that at higher ESO content the phase separation prevails over the co-crosslinking.

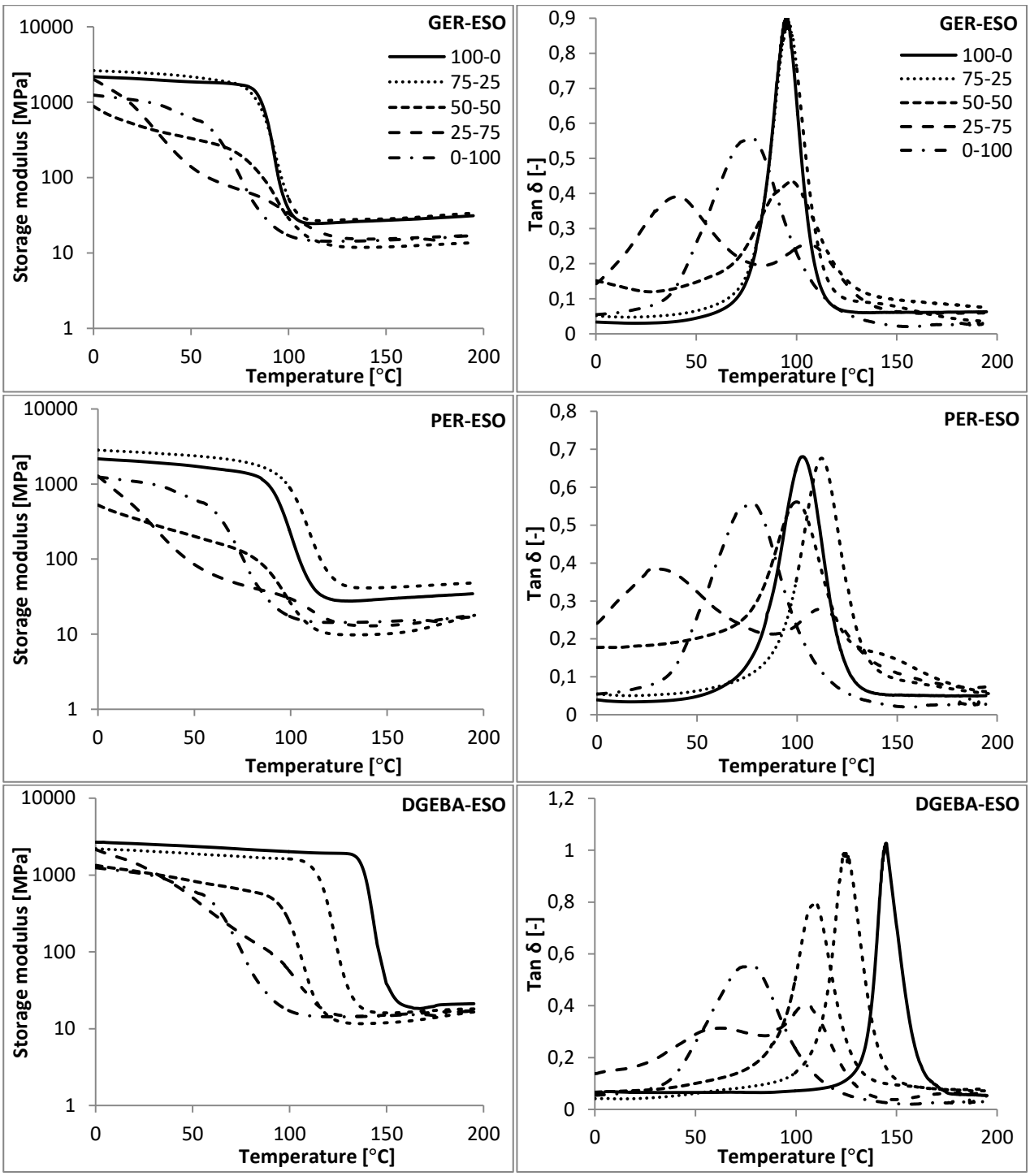

Figure 4.2.2 Storage modulus and tan δ curves of the different EP/ESO systems

Table 4.2.3 Storage modulus of all neat resins in comparison with the EP/ESO blends containing 25% ESO at 25, 50, 75 and 160 °C

		base resin	storage modulus [MPa]		relative value [-]
			ESO content [%]		
			0	25	
temperature [°C]	25	GER	2029	2452	1.21
		PER	1974	2621	1.33
		DGEBA	2525	2055	0.81
	50	GER	1862	2175	1.17
		PER	1733	2380	1.37
		DGEBA	2361	1891	0.80
	75	GER	1704	1697	1.00
		PER	1434	1992	1.39
		DGEBA	2172	1738	0.80
	160	GER	28	29	1.04
		PER	31	43	1.39
		DGEBA	20	16	0.80

* relative value: ratio of values of EP with 25% ESO-content and the corresponding neat EP system

Table 4.2.4 shows the effect of ESO addition on the T_g values determined both by DSC and DMA tests in all EP/ESO systems. Among the neat resins, the aromatic DGEBA has the highest T_g due to its more rigid structure. Among the aliphatic resins the tetrafunctional PER has much higher T_g than the trifunctional GER, which can be explained by the higher crosslinking density. By increasing the amount of ESO, the T_g of the DGEBA systems decreases, while the ESO addition has a synergistic effect on the T_g of the hybrid aliphatic blends, as their T_g is higher than both that of the neat aliphatic resins and that of ESO as well. This synergistic effect can be explained by the increase in crosslink density due to the similar chemical structure of the aliphatic resins and ESO. Another possible explanation is that aliphatic resins cure at lower temperatures according to DSC, and the already cured aliphatic parts apply pressure on the uncured ESO parts. This pressure shifts the beginning of segmental movements in the cured ESO parts to higher temperature leading to higher T_g. When comparing the T_g values measured by DSC and DMA method, it has to be noted, that although the peak doubling in DSC suggests phase separation, no separate T_g value could be determined by DSC for the EP-rich and ESO-rich phases. This may be again explained by the delayed segmental movements of the uncured ESO parts described above.

Table 4.2.4 Comparison of glass transition temperature values of the EP/ESO systems with ESO addition determined by DSC and DMA tests

base resin		GER				PER				DGEBA				ESO
method	ESO content [%]	0	25	50	75	0	25	50	75	0	25	50	75	-
DSC	glass transition temperature	94	104	105	120	110	118	120	129	140	138	131	121	75
DMA	[°C]	95	96	98	41, 106	103	112	100	29, 112	145	124	110	62, 105	79

Mechanical characterization

Based on the DMA test results, specimens were prepared from the neat basic epoxy resins and with 25% ESO content only, where the softening effect of ESO was only moderate. To determine the effect of ESO addition to the different basic epoxy resins on the mechanical properties, tensile, bending and Charpy impact tests were carried out (**Table 4.2.5**).

Table 4.2.5 Tensile, flexural and Charpy impact properties of the neat epoxy resin systems and their blends with 25% ESO content

	base resin	ESO content [%]		relative value [-]
		0	25	
tensile strength [MPa]	GER	66.92±0.34	55.18±1.03	0.82
	PER	64.69±0.78	51.75±1.86	0.80
	DGEBA	77.61±0.79	47.77±1.56	0.62
tensile modulus [GPa]	GER	2.66±0.07	2.22±0.04	0.83
	PER	2.66±0.05	2.29±0.04	0.86
	DGEBA	2.54±0.04	2.43±0.01	0.96
flexural strength [MPa]	GER	94.41±0.21	78.23±1.93	0.83
	PER	91.67±0.52	81.26±0.54	0.89
	DGEBA	94.87±0.77	85.64±0.52	0.90
flexural modulus [GPa]	GER	3.01±0.02	2.52±0.01	0.84
	PER	3.12±0.02	2.59±0.01	0.83
	DGEBA	2.88±0.03	2.61±0.02	0.91
Charpy impact energy [kJ/m^2]	GER	1.33±0.17	1.15±0.09	0.86
	PER	1.11±0.07	0.91±0.07	0.82
	DGEBA	1.73±0.07	1.44±0.12	0.83

Even with 25% ESO content the mechanical properties of the neat resins decreased considerably. The decrease of tensile strength was the most pronounced in the case of DGEBA (38% compared to the neat system). Although the aliphatic systems initially have lower tensile strength than DGEBA, their blends with ESO overperformed DGEBA in terms of tensile strength. In the case of Young's modulus, flexural strength and flexural modulus, ESO caused less deterioration than in aliphatic resins, but in all cases the decrease was less than 20%. In terms of Charpy impact energy there was no significant difference between the aromatic and aliphatic resins, the values decreased by approx. 15% due to the addition of 25% ESO in each case.

Scanning electron microscopy (SEM)

To reveal the effect of ESO on the T_g and storage modulus and to explain the decreased mechanical properties, scanning electron microscopy (SEM) examinations were carried on the fracture surfaces of the specimens. **Figure 4.2.3** suggests that in aliphatic resins phase separation occurred already with 25% ESO content. This effect did not appear in the case of DGEBA. As DGEBA is aromatic and ESO contains relatively long aliphatic chains, the decreased mechanical properties can be explained with the molecule structure of the latter one.

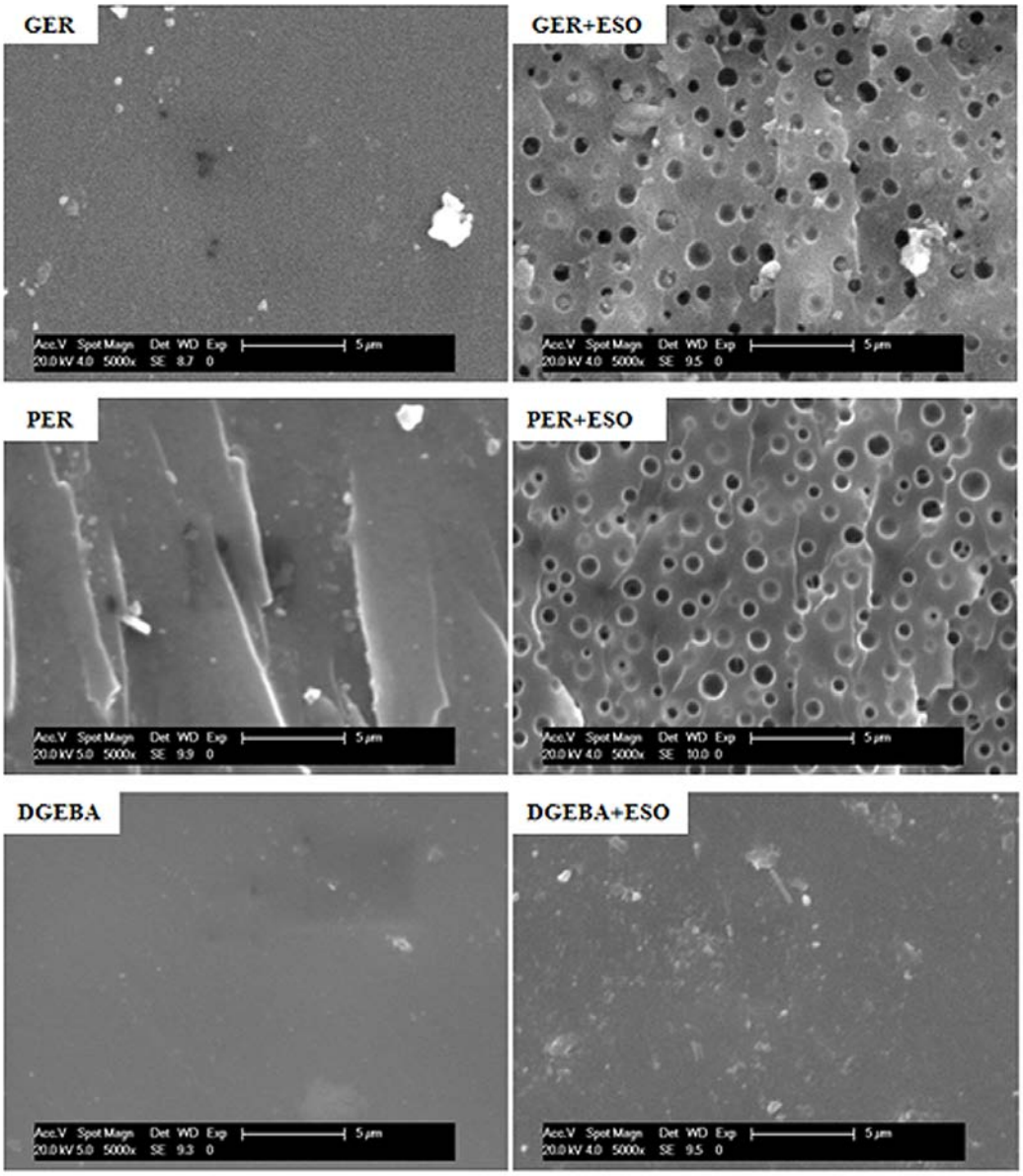

Figure 4.2.3 SEM micrographs of the neat and mixed basic epoxy resins with 25% ESO

Raman mapping

In order to get more detailed information on the extent of phase separation Raman mapping of 25% ESO containing samples was carried out (**Figure 4.2.4**). As reference spectra for Raman mapping spectra of cured GER, PER and DGEBA samples were used. These results were in good agreement with the SEM images, namely the DGEBA-ESO system showed the most homogenous distribution of the two components, while in case of GER and PER phase separation occurred.

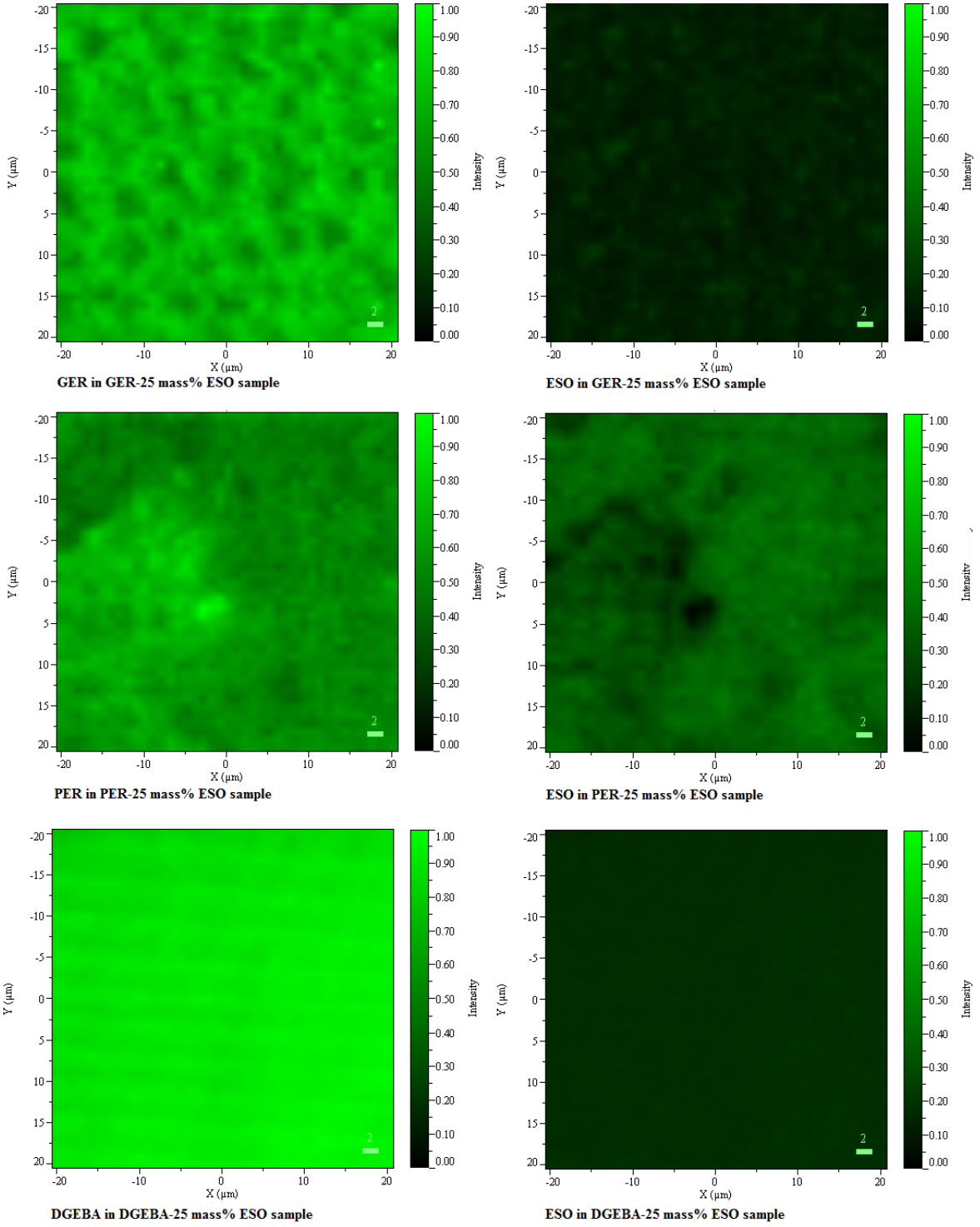

Figure 4.2.4 Raman maps of 25% ESO containing EP/ESO samples

Thermal behaviour

To determine the thermal stability of the different EP/ESO systems TGA measurements were carried out. TGA results are displayed in **Table 4.2.6.**

Table 4.2.6 TGA results of the different EP/ESO systems

base resin	GER				PER				DGEBA				ESO
ESO content [%]	**0**	**25**	**50**	**75**	**0**	**25**	**50**	**75**	**0**	**25**	**50**	**75**	**100**
$T_{-5\%}$ [°C]	285	269	208	188	294	252	227	193	348	252	216	188	183
$T_{-50\%}$ [°C]	331	330	350	363	333	332	339	363	408	401	398	382	366
dTG_{max} [%/°C]	1.91	1.63	0.83	0.66	1.88	1.44	0.99	6.10	1.56	1.36	1.08	0.82	0.87
T_{dTGmax} [°C]	327	327	327	398	325	329	326	329	409	409	412	412	355
char yield at 700 °C [%]	15.8	8.2	4.1	1.9	15.9	10.6	4.8	2.3	10.3	7.2	5.4	2.7	0.3

$T_{-5\%}$: temperature at 5% mass loss $T_{-50\%}$: temperature at 50% mass loss; dTG_{max}: maximum mass loss rate; T_{dTGmax}: the temperature belonging to maximum mass loss rate

The increasing ESO content resulted in a prolonged decomposition in a wider temperature range. In the case of the aliphatic systems, although the initial decomposition temperature becomes lower, the main decomposition is shifted to higher temperatures. In the case of DGEBA, both the initial degradation temperature and the main degradation step is shifted to lower temperatures with increasing ESO content. Nevertheless, in both aliphatic and aromatic resins the ESO content significantly decreased the decomposition rate. Regarding the char yield, the aliphatic glycerol- and pentaerythritol-based resins are often used as charring components in intumescent FR formulations; the aromatic structure also tends to result in high char yield. The long aliphatic chains of ESO are not favourable in this aspect, consequently by increasing the ESO-content, the char yield of the samples decreased.

4.2.2. Development of cycloaliphatic sugar based epoxy resin matrices

The curing and rheological behaviour, glass transition temperature, mechanical and thermal properties of two novel glucose-based EP components: a solid glucopyranoside based trifunctional epoxy resin component (GPTE) and a liquid glucofuranoside based trifunctional epoxy resin component (GFTE) (cured with diethyl-methylbenzene-diamine (DETDA) and with methyl-tetrahydrophthalic anhydride (AR917)) were investigated and compared to bifunctional aromatic bisphenol-A based DGEBA and two aliphatic components, the trifunctional glycerol-based GER and the tetrafunctional pentaerythritol-based PER [**196**].

Curing behaviour

To study the curing behaviour of the novel glucose-based epoxy resin components and compare them to the mineral oil based ones, DSC measurements were carried out (**Table 4.2.7).**

Table 4.2.7 DSC results of the EP systems with DETDA and AR917 curing agents

base resin	**GPTE**		**GFTE**		**DGEBA**		**PER**		**GER**	
curing agent	**DETDA**	**AR917**	**DETDA**	**AR917**	**DETDA**	**AR917**	**DETDA**	**AR917**	**DETDA**	**AR917**
total specific reaction enthalpy [J/g]	366	396	333	414	296	381	328	388	419	372
temperature of heat flow peak [°C]	179	133	190	130	190	129	164	125	162	123
T_g [°C]	210	178	173	157	179	155	98	116	76	99

Both novel glucose-based resins could be successfully cured both with amine and anhydride type curing agents. In the case of AR917 no significant difference could be noticed between the heat flow profile of the different EPs, the curing occurred in a rather narrow temperature zone, with a peak temperature around 130 °C. The curing process was significantly slower in the case of DETDA and the EP systems needed higher curing temperature than with AR917. The aliphatic resins cured at lower temperature, while the heat flow curve of the aromatic DGEBA and cycloaliphatic glucose-based resins was shifted to higher temperatures. The aromatic and glucose-based systems had higher T_g with the aromatic amine type DETDA than with anhydride type AR917 curing agent, while the aliphatic ones had lower T_g with DETDA. GPTE type glucose-based EP systems showed the highest T_g values among all investigated resins, followed by glucose-based cycloaliphatic GFTE and aromatic DGEBA, while the aliphatic ones had the lowest values, as expected.

Gelling

Prior to specimen moulding the gel time of the EP systems was determined as well (**Table 4.2.8)**. The applied temperature during the measurement was determined on the basis of DSC results: with DETDA a constant temperature of 175 °C, while with AR917 100 °C was applied.

Table 4.2.8 Gel times of the EP systems with DETDA and AR917 curing agents

gel time [s]	**curing agent**	**base resin**				
		GPTE	**GFTE**	**DGEBA**	**PER**	**GER**
	DETDA	586	552	862	448	420
	AR917	955	908	935	532	769

Curing with amine type DETDA leads to shorter gel times than curing with the anhydride type AR917 in all EP systems. In the case of AR917 the glucose-based EP systems had similar gel times as DGEBA, while with DETDA the glucose-based EP components have significantly lower gel times

than the DGEBA. With both curing agents the aliphatic resins showed the highest reactivity. According to these results, the gel times of the novel glucose-based resins are appropriate for processing and can be well-adopted to the requirements of the common composite preparation methods by choosing the type of the curing agent.

Storage modulus and glass transition temperature

The storage modulus as a function of temperature can be seen in **Figure 4.2.5**. **Table 4.2.9** shows the storage modulus at 0, 25, 50 and 75 °C and compares the T_g values determined by DSC and DMA.

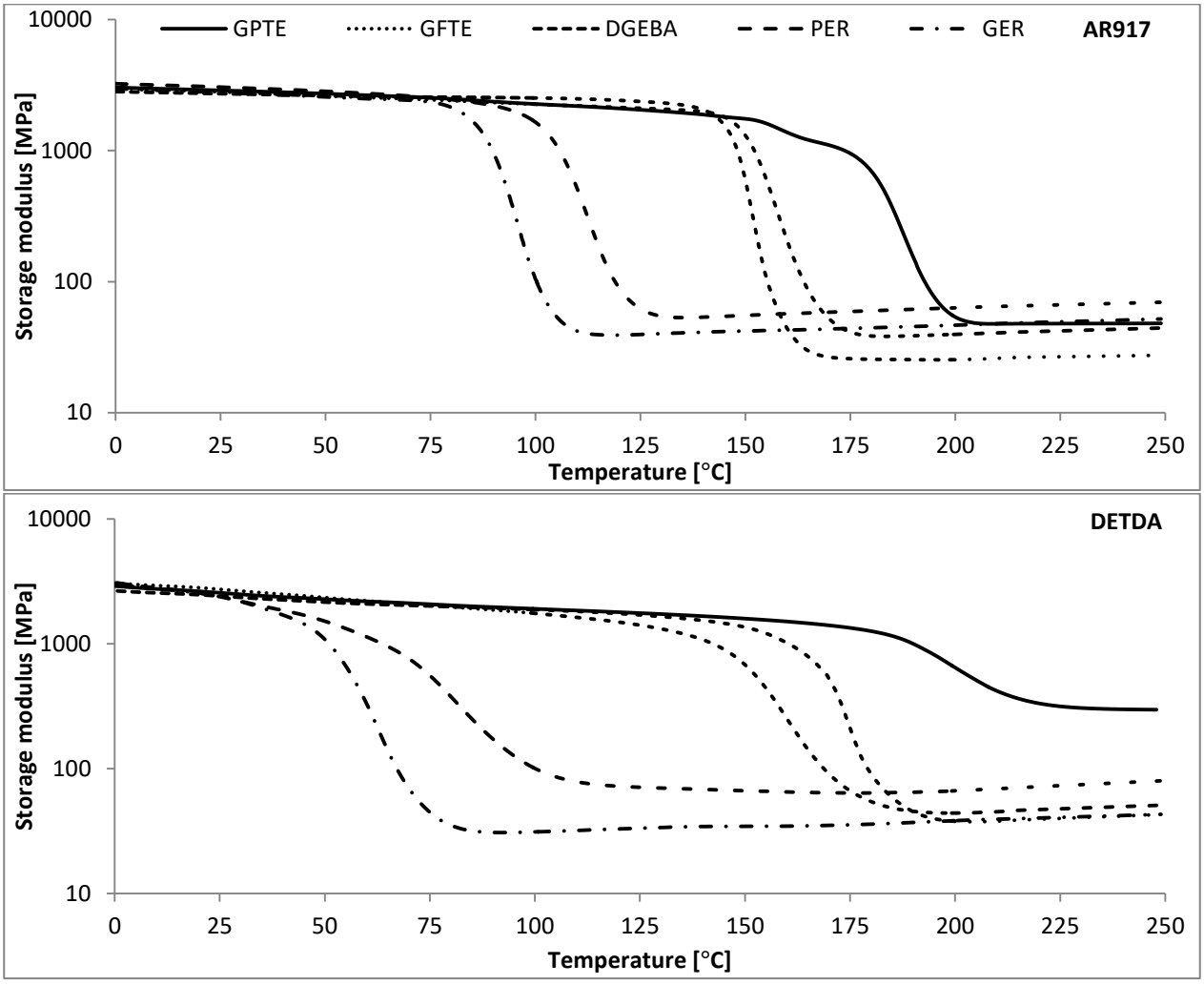

Figure 4.2.5 Storage modulus curves of EP systems with DETDA and AR917 curing agents

Table 4.2.9 Storage modulus measured by DMA and glass transition temperature values determined by DSC and DMA in EP systems cured with DETDA and AR917 curing agents

		storage modulus [MPa]									
base resin		GPTE		GFTE		DGEBA		PER		GER	
curing agent		DETDA	AR917	DETDA	AR917	DETDA	AR917	DETDA	AR917	DETDA	AR917
temperature [°C]	0	2895	3032	3058	2999	2648	2817	3078	3239	2965	2970
	25	2558	2877	2727	2804	2409	2716	2376	3049	2386	2767
	50	2274	2716	2341	2611	2155	2627	1512	2832	1076	2567
	75	2072	2528	2034	2440	2005	2559	555	2532	45	2343
	glass transition temperature [°C]										
method	DMA	213	188	178	161	177	154	86	115	65	98
	DSC	210	178	173	157	179	155	98	116	76	99

There was no significant difference between the storage modulus values of the EP systems below the T_g. The storage modulus of the novel glucose-based resins at lower temperatures is higher than the values of DGEBA, above 50 °C it is still in the same region of the storage modulus of DGEBA. In the case of PER and GER 75 °C is close to the T_g of these aliphatic systems, which explains the low storage modulus values at this temperature. The T_g values determined by DMA showed similar tendency than the ones determined by DSC: GPTE had much higher T_g than DGEBA both with DETDA and AR917, while the T_g values of GFTE were in the same range as DGEBA.

Mechanical characterization

In order to compare the mechanical properties and hardness of the glucose-based EPs to those of the mineral oil based ones, tensile, bending and Shore-D type hardness tests were carried out (**Table 4.2.10**).

DGEBA has the highest tensile strength both with DETDA and AR917 curing agent. Noteworthy worsening in the tensile strength was detected in the case of the glucose-based EP components (GPTE, GFTE) compared to the mineral oil based ones. All EP systems have lower tensile strength with amine type DETDA than with anhydride type AR917, which may be explained with the high temperature heat treatment (2h at 175 °C) necessary for proper conversion, probably causing already degradation in the crosslinked resin. Despite the tendency in tensile strength values, the GPTE and GFTE with AR917 have almost the highest tensile modulus value. Similar trend can be seen in the case of the flexural properties. The flexural strength of the glucose-based EP systems is lower than that of the synthetic resins except the GPTE with AR917. The flexural modulus values are the lowest in the case of the glucose-based epoxy components with DETDA. Basically the glucose-based and the mineral oil based epoxy components' modulus values are comparable with

each other using the same curing agent. According to the hardness tests, the glucose-based epoxy components have the highest hardness among all the five examined EP components.

Table 4.2.10 Comparison of the mechanical properties and hardness of glucose-based EP resins to mineral oil based ones with DETDA and AR917 curing agents

base resin	GPTE		GFTE		DGEBA		PER		GER	
curing agent	DETDA	AR917	DETDA	AR917	DETDA	AR917	DETDA	AR917	DETDA	AR917
tensile strength [MPa]	14.67 ±4.01	24.90 ±4.08	29.02 ±8.75	37.58 ±9.13	44.80 ±14.18	77.6 ±10.79	34.88 ±9.97	64.69 ±0.78	46.8 ±10.32	66.92 ±0.34
tensile modulus [GPa]	2.23 ±0.06	2.50 ±0.07	2.48 ±0.05	2.66 ±0.11	2.26 ±0.07	2.54 ±0.04	2.27 ±0.02	2.66 ±0.05	2.33 ±0.04	2.66 ±0.07
flexural strength [MPa]	49.11 ±10.07	86.86 ±25.82	62.84 ±8.02	68.86 ±5.71	86.84 ±1.39	94.87 ±0.77	85.85 ±0.59	91.67 ±0.52	85.81 ±1.79	94.41 ±0.21
flexural modulus [GPa]	2.29 ±0.12	2.61 ±0.12	2.31 ±0.47	2.51 ±0.16	2.12 ±0.10	2.88 ±0.03	2.50 ±0.01	3.12 ±0.02	2.30 ±0.28	3.01 ±0.02
hardness [Shore-D]	105.72 ±2.52	107.82 ±1.94	107.28 ±1.59	109.06 ±1.05	103.98 ±1.93	106.20 ±0.57	99.64 ±2.18	107.12 ±0.53	99.32 ±2.05	105.84 ±0.65

Thermal behaviour

Thermal stability of the synthesized bio-based epoxy resins, GPTE and GFTE was compared to the stability of the applied aliphatic and aromatic synthetic resins (DGEBA, PER, GER) both in case of anhydride (AR917) and aromatic amine type hardener (DETDA) (**Table 4.2.11**).

Table 4.2.11 TGA results the EP systems with DETDA and AR917 curing agents

base resin	GPTE		GFTE		DGEBA		PER		GER	
curing agent	DETDA	AR917	DETDA	AR917	DETDA	AR917	DETDA	AR917	DETDA	AR917
$T_{-5\%}$ [°C]	314	330	334	229	370	348	291	294	284	285
$T_{-50\%}$ [°C]	373	384	354	367	398	408	347	333	353	331
dTG_{max} [%/°C]	1.52	2.11	5.55	1.31	2.44	1.56	2.87	1.88	1.36	1.92
T_{dTGmax} [°C]	345	387	339	374	387	409	293	325	289	327
char yield at 700 °C [%]	13.3	0.2	16.8	0.5	2.9	10.3	12.6	15.9	10.1	15.8

$T_{-5\%}$: temperature at 5% mass loss $T_{-50\%}$: temperature at 50% mass loss; dTG_{max}: maximum mass loss rate; T_{dTGmax}: the temperature belonging to maximum mass loss rate

Based on these results, the aromatic DGEBA had the highest thermal stability, the stability of the synthesized GPTE and GFTE is between the aliphatic resins and DGEBA. In the case of the glucose-based resins, the char yield values are significantly higher with DETDA than with AR917, which may be explained by the high amount of ether type linkages derived from hydroxyl groups, which leads to the formation of an intumescent system when amine type hardeners are used [197].

4.2.3. Summary on the development of bio-based matrices

Blends of epoxidized soybean oil (ESO) with a glycerol-based (GER) and a pentaerythritol-based (PER) aliphatic epoxy resin and with a bisphenol-A based aromatic epoxy resin (DGEBA) were

investigated by DSC, DMA, parallel plate rheometry, tensile, bending and Charpy impact tests, SEM and Raman mapping. The application of **ESO decreases the reaction enthalpy of curing** in almost all cases and **increases the gel time**. Based on the DSC results, among the neat resins, the aromatic DGEBA has the highest T_g, from the aliphatic ones the tetrafunctional PER has much higher T_g than the trifunctional GER, which can be explained by the higher crosslink density. By **increasing the amount of ESO**, the **T_g of the DGEBA systems decreases**, while the **T_g of the aliphatic systems increases**, showing a synergistic effect. This can be explained by the increase in crosslink density due to the similar chemical structure of the aliphatic resins and ESO. Furthermore, **aliphatic resins cure at lower temperatures**, and the already **cured short aliphatic parts apply pressure on the uncured ESO parts**, leading to higher T_g. As for the mechanical properties of epoxy resin systems, the stiffness in the glassy state of the EP/ESO compositions decreased with increasing amount of ESO. A **significant softening** effect occurs in the case of all epoxy resin systems **above 50% ESO content**. When only **25% ESO** was applied, there was a **storage modulus increase in** the case of the **aliphatic resins**, but the aromatic DGEBA's storage modulus decreased with this ESO content. Based on the **SEM** and **Raman mapping** results, the systems containing **aliphatic resins** showed **phase separation already at 25% ESO-content**, while the DGEBA-ESO system showed a more homogenous distribution. The increasing ESO content resulted in a **prolonged decomposition** in a wider temperature range with significantly **decreased decomposition rate**. In aliphatic systems although the initial decomposition temperature becomes lower, the main decomposition is shifted to higher temperatures, while in DGEBA both the initial degradation temperature and the main degradation step is shifted to lower temperatures with increasing ESO content. Based on these results, the **highest T_g (138° C)** could be achieved in **DGEBA system with 25% ESO**, which allows its use as partially bio-based composite matrix in aircraft interior applications (which require higher T_g than 120 °C). Further increase of the ratio of bio-based/or potentially bio-based components i. e. application of more ESO and/or aliphatic epoxy resins can be also feasible, taking into account the limitations of the systems.

The curing and rheological behaviour, glass transition temperature, mechanical and thermal properties of novel **glucopyranoside (GPTE)** and **glucofuranoside (GFTE) based EP monomers** were investigated. GPTE and GFTE could be **successfully cured both with amine and anhydride type curing agents**. In all investigated EPs the curing process was significantly slower and therefore higher curing temperatures were necessary with amine type hardener. As for the T_g values, **GPTE** showed the **highest T_g** values among all investigated resins, **followed by** glucose-based cycloaliphatic **GFTE** and aromatic **DGEBA,** while the aliphatic ones had the lowest values, as expected. The glucose-based EPs had similar gel times with anhydride curing agent as DGEBA,

while with amine hardener their gel time was significantly lower than in the case of DGEBA. The **storage modulus** of the novel glucose-based resins is **higher or above 50 °C** it is in the **same** region as the storage modulus of DGEBA. The glucose based EP systems have **lower tensile and flexural strength**, but the **tensile modulus** values are **similar** to the synthetic EPs. The **thermal stability** of GPTE and GFTE is **between the aliphatic resins and DGEBA**. In the case of the glucose-based resins, the **char yield** values are significantly **higher with DETDA** than with AR917, which may be explained by the high amount of ether type linkages derived from hydroxyl groups, which leads to the formation of an **intumescent system** when amine type hardeners are used. Based on the results, the newly synthesized glucopyranoside- and glucofuranoside-based bioepoxy monomers are promising candidates to replace the commodity mineral oil based ones. Their **major advantages** are the **high T_g** (in some cases **above 200 °C**), adjustable gel time by choosing appropriate curing agent, high storage modulus values and hardness. In applications where bending stresses are dominant over the tensile ones, and outstanding T_g is required, these sugar based resins offer a feasible renewable choice.

4.3. Development and characterization of bio-based polymer composites

In this chapter the results on jute fibre reinforced composites made from epoxidized vegetable oil and mineral oil based epoxy monomers, as well as results on sugar based bioepoxy composites reinforced with jute or carbon fibres are summarized.

First, in order to map the application possibilities of bio-based resins in the composite industry, a systematic research was performed to describe **the effect of epoxidized soybean oil (ESO) addition in various EP systems reinforced by jute fibres**. As base resins, the aromatic DGEBA, glycerol (GER)- and a pentaerythritol-based (PER) aliphatic resins were chosen. The expected outcome of this work was to define the composition of a potentially fully bio-based jute fibre reinforced composite, which contains the **highest amount of ESO**, with **acceptable reduction in the T_g and mechanical properties** compared to those of the neat EP composites.

Besides the partially bio-based ESO systems, **glucofuranoside based bioepoxy (GFTE) composites reinforced with jute and carbon fibres** were investigated as well. The aim of this work was to compare the thermomechanical and mechanical properties of GFTE biocomposites to mineral oil based benchmark (DGEBA, PER, GER) composites and to **define applications areas**, where GFTE can successfully replace them.

4.3.1. Development of all-bio epoxy resin composites

The applicability of natural sourced matrix and reinforcing materials instead of synthetic ones in structural composite applications is a widely investigated area, as in order to achieve fully bio-based composite systems, not only the matrix, but also the reinforcing fibre must be renewable. Given that the composition and therefore the properties of commonly applied plant oil based polymers and natural fibres is less constant than in case of synthetic ones, usually partial replacement is applied, especially in high-tech applications with strict safety standards. Other possibility is to apply these fully bio-based composites at first in less demanding areas of these advanced sectors, as aircraft interior applications.

4.3.1.1. *Development of vegetable oil based jute fibre reinforced composites*

Jute fibre reinforced composites were prepared from epoxy resin blends consisting of epoxidized soybean oil (ESO) and glycerol-based (GER), pentaerythritol-based (PER) aliphatic EP or bisphenol-A based aromatic EP (DGEBA) cured with DETDA or AR917 hardener. In each case 25, 50 and 75% ESO was added to the synthetic resin. Composite laminates were prepared by hand lamination followed by hot pressing to achieve high (59-61%) and uniform fibre content. The effect of ESO on storage modulus, glass transition temperature, mechanical properties and morphology was determined [**198**].

Effect of the alkali treatment on the mechanical properties of the reinforcing fabric

Prior to composite preparation, a systematic study [**199**,] was carried out to select the optimal fibre treatment conditions resulting in the best fibre mechanical properties, based on the literature on the alkali treatment of elementary fibres [83,84]. The maximal force values per fibre determined from strip tensile tests of differently treated jute fabrics are displayed in **Table 4.3.1.**

Table 4.3.1 Effect of alkali concentration and treatment time on maximal force values per fibre [N] determined from strip tensile tests of jute fabrics

maximal force [N]		NaOH concentration [mass%]					
		0	0.5	1	2	4	8
treatment time [h]	0	567±56					
	0.5		496±36	523±45	522±50	460±55	395±35
	1		506±71	538±63	560±54	518±47	363±30
	2		569±24	534±38	544±38	523±62	373±25
	4		579±77	574±46	527±29	507±36	399±24
	8		554±50	596±17	559±60	520±48	349±43

From the 25 different alkali treatment conditions only 4 resulted in a modest increase in the maximal force values (marked with grey background), in all other cases the tensile strength of the

fabric decreased. The highest increase in maximal force was detected when the fabric was immersed into 1% NaOH solution for 8 h, however the increase is only around 5%, which taking into account the standard deviation cannot be considered as a significant amelioration. According to Kabir et al. [200] the non-cellulosic materials (hemicellulose and lignin) can be partially dissolved from natural fibres with the applied alkali treatment. As hemicellulose and lignin act as binding material in the elementary jute fibres, less force is sufficient to move the elementary fibres from each other, resulting in a decrease in the maximal force values.

On the other hand, the removal of hemicellulose and lignin leads to a rougher and bigger fibre surface, consequently better interfacial properties and higher glass transition temperatures [**199**,201,202]. The ultimate mechanical properties of the composites are therefore influenced both by the decreased tensile strength of the fibres and by the better fibre-matrix adhesion, leading to contrary results in the literature on the effect of the alkali treatment. According to our experience, the composite mechanical properties deteriorated due to the alkali treatment [**199**].

Additionally, it has to be noted that although the alkali treatment partially removes the components thermally less stable than cellulose, according to Sebestyén et al. due to the residual alkali ions the thermal degradation of the cellulose fraction is shifted to lower temperatures [203], all together leading to fibres with lower thermal stability. Furthermore, it is supposed that above a certain residual alkali ion concentration, the alkalisation process continues inside the fibres in an uncontrollable way leading to swollen and highly porous composites [201].

Based on these results we did not consider the alkali treatment of the jute fabric justified, consequently untreated fabric was used for the preparation of composite specimens.

Storage modulus and glass transition

Storage modulus curves of reference and EP/ESO jute fibre reinforced composites as a function of temperature are shown in **Figure 4.3.1**. **Table 4.3.2** shows the storage modulus values at 0 °C (below T_g) and 150 °C (beyond T_g) and T_g determined by the tan δ peaks.

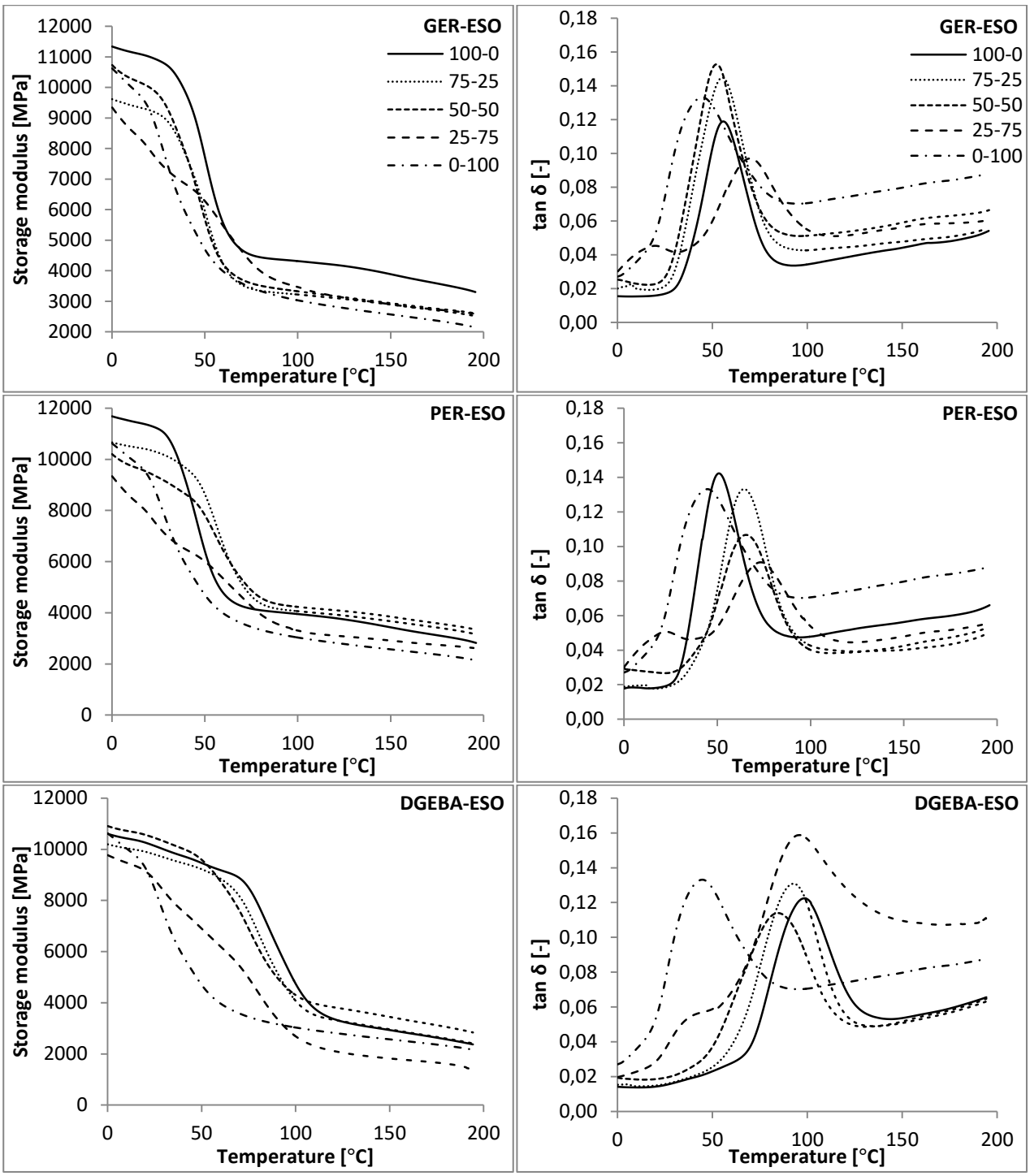

Figure 4.3.1 Storage modulus curves of the jute reinforced EP/ESO composites

In most cases the storage modulus decreased with ESO addition. Three exceptions occurred: in the case of PER with 25 and 50% ESO in glass transition range and in rubbery state, as well in the case of DGEBA with 50% ESO in glassy and rubbery states the storage modulus values were higher than in the case of the neat synthetic systems. The T_g values of the composites decreased by 40 °C compared to the corresponding neat EP systems (see **4.2.1**). In the literature this effect is attributed to the reaction of hydroxyl groups of the jute reinforcement and anhydride type curing agent [194]. As for the effect of ESO-addition on the T_g values of the composites, in aliphatic matrices, the T_g rather increases when the amount of ESO is increased, in good correspondence

with the behaviour of the neat EP systems. Also in good agreement with the neat resin, in aromatic DGEBA the T_g values rather show a decreasing tendency, yet these values are higher than in the aliphatic systems due to the more rigid aromatic backbone of DGEBA. Also, similarly to the neat resins, the observed peak doubling in tan δ curves of samples containing 75% ESO suggests that at higher ESO content phase separation occurred. In these cases dual T_g values were determined as well (**Table 4.3.2**).

Table 4.3.2 Storage modulus and T_g values of jute reinforced EP/ESO composites

base resin		**GER**				**ESO**
ESO content [%]		**0**	**25**	**50**	**75**	**100**
storage modulus [MPa]	**0 °C**	11338	9615	10731	9342	10621
	150 °C	3886	2892	2937	2902	2568
glass transition temperature [°C]		56	55	52	20, 70	45

base resin		**PER**			
ESO content [%]		**0**	**25**	**50**	**75**
storage modulus [MPa]	**0 °C**	11682	10659	10202	9338
	150 °C	3428	3668	3847	2911
glass transition temperature [°C]		51	64	65	22, 73

base resin		**DGEBA**			
ESO content [%]		**0**	**25**	**50**	**75**
storage modulus [MPa]	**0 °C**	10603	10194	10907	9771
	150 °C	2933	2959	3447	1819
glass transition temperature [°C]		99	93	85	40, 96

Mechanical characterization

Tensile and flexural properties of EP/ESO jute reinforced composites are shown in **Table 4.3.3**.

As the efficiency of the jute fibre reinforcement in woven structure was modest, the mechanical properties of the composites were rather determined by the mechanical properties of the matrices. It has to be emphasized that in the case of natural fibre reinforced composites matrix properties have significantly higher effect on the tensile properties than in the case of high performance fibre reinforced composites, because of the comparable fibre and matrix properties. In aliphatic matrices the tensile strength showed a decreasing tendency due to ESO-addition, above 50% ESO content the tensile strength values were lower than in neat ESO composite, which could be the result of the phase separated structure [14]. The same tendency was observed in case of tensile modulus, but the values decreased below the level of neat ESO composite only from 75% ESO content. The flexural strength was between the values of the neat aliphatic resin and neat ESO composites, in the case of PER composite with 25% ESO even a slight increase could be detected. From 75% ESO-content, the flexural modulus values decreased below the level of

neat ESO composite. In aromatic DGEBA systems all mechanical properties decreased with ESO addition, however they stayed above values of the neat ESO composites in all cases.

Table 4.3.3 Mechanical properties of the jute reinforced EP/ESO composites

base resin	GER				ESO
ESO content [%]	0	25	50	75	100
tensile strength [MPa]	96.73 ±7.54	96.41 ±4.51	67.32 ±13.77	61.42 ±12.08	70.89 ±3.28
tensile s modulus [GPa]	9.07 ±0.27	8.46 ±0.11	8.19 ±0.24	6.91 ±0.14	7.28 ±0.08
flexural strength [MPa]	129.71 ±2.94	119.02 ±4.86	116.40 ±1.12	92.18 ±4.00	92.28 ±3.41
flexural modulus [GPa]	10.75 ±0.20	9.31 ±0.11	9.80 ±0.07	7.49 ±0.22	8.23 ±0.45

base resin	PER			
ESO content [%]	0	25	50	75
tensile strength [MPa]	93.68 ±4.98	83.63 ±3.43	68.99 ±5.25	66.85 ±8.08
tensile modulus [GPa]	9.19 ±0.24	8.42 ±0.08	8.02 ±0.16	7.19 ±0.27
flexural strength [MPa]	120.82 ±3.82	126.54 ±2.70	108.46 ±3.92	95.21 ±4.10
flexural modulus [GPa]	10.41 ±0.16	10.05 ±0.12	9.06 ±0.25	7.87 ±0.25

base resin	DGEBA			
ESO content [%]	0	25	50	75
tensile strength [MPa]	100.42 ±12.12	87.44 ±0.65	93.97 ±1.67	76.37 ±6.45
tensile modulus [GPa]	9.22 ±0.36	8.35 ±0.27	8.58 ±0.03	7.87 ±0.13
flexural strength [MPa]	131.66 ±1.12	123.93 ±5.62	122.56 ±2.52	106.85 ±3.09
flexural modulus [GPa]	11.13 ±0.12	9.68 ±0.46	9.85 ±0.29	8.88 ±0.51

The mechanical properties of the 25% ESO-containing composites approach the properties of the reference DGEBA composite in the most values. In those applications where high T_g is not a crucial requirement, the jute fibre reinforced aromatic DGEBA epoxy resin composite can be replaced by 25% ESO-containing hybrid epoxy components. Given that besides the natural jute fibre and ESO, both PER, GER and the anhydride based hardener can be potentially synthesized from bio-based sources as well, this leads to a replacement by a fully bio-based composite without significant compromise in mechanical properties.

4.3.1.2. *Development of cycloaliphatic sugar based jute fibre reinforced composites*

Jute fibre reinforced composites were prepared from glucofuranoside based trifunctional EP monomer (GFTE) cured with DETDA or AR917 hardener. As reference resins conventional mineral

oil based aromatic bifunctional DGEBA, aliphatic trifunctional glycerol (GER) and tetrafunctional pentaerythritol based (PER) resins were used. Composite laminates were prepared by hand lamination followed by hot pressing to achieve high (59-61%) and uniform fibre content. Storage modulus, glass transition temperature and mechanical properties of the composites were compared [**204**].

Storage modulus and glass transition temperature

Storage modulus curves of EP composites cured with AR917 and DETDA are shown in **Figure 4.3.2**. The determined storage modulus at 0 and 200 °C (below and beyond the glass transition) and glass transition temperature (T_g) values (based on tan δ peaks) are summarized in **Table 4.3.4**

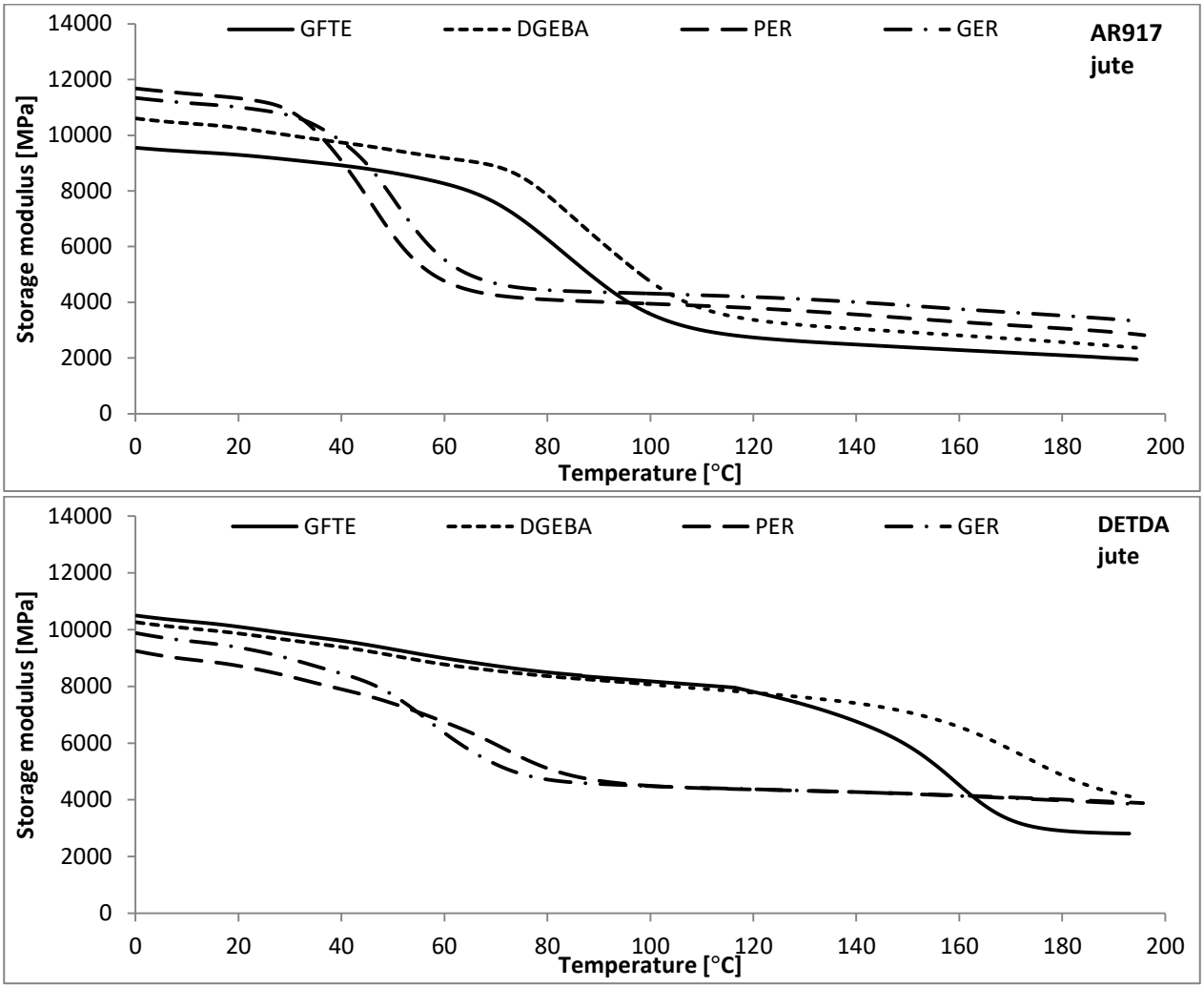

Figure 4.3.2 Storage modulus curves as a function of temperature of jute/EP composites cured with AR917 and DETDA curing agents

Table 4.3.4 Storage modulus (at 0 and 200 °C) and glass transition temperature values of jute/EP composites with AR917 and DETDA curing agents

base resin		GFTE		DGEBA		PER		GER	
curing agent		DETDA	AR917	DETDA	AR917	DETDA	AR917	DETDA	AR917
storage modulus [MPa]	0 °C	10806	9551	10257	10603	9242	11682	9874	11338
	200 °C	2812	1951	4075	2371	3885	2820	3846	3303
glass transition temperature [°C]		167	93	179	99	75	51	65	56

Below T_g, GFTE cured with DETDA had higher storage modulus than the mineral oil based composites (DGEBA, PER, GER); while above T_g and in the case of AR917, the tendency was the opposite. GFTE cured with DETDA had only 12 °C lower T_g (167 °C) than the DGEBA-based composite, which is an outstanding result for a bio-based EP (e.g. both fatty acid triglyceride [21] and isosorbide based [78] natural sourced EP systems have lower T_g, than DGEBA). In the case of AR917 the difference between the T_g of GFTE and DGEBA was even less, 6 °C. The aliphatic resins, which can be potentially synthesized from renewable materials as well, had much lower T_g, than the aromatic DGEBA or the cycloaliphatic GFTE, consequently in high temperature applications they do not represent a real bio-based alternative. These results are in good agreement with the results of the matrices (see **4.2.2**).

Mechanical characterization

Tensile strength and modulus, flexural strength and modulus of jute/EP composites cured with AR917 and DETDA are shown in **Table 4.3.5**.

Table 4.3.5 Tensile strength and modulus, flexural strength and modulus of jute/EP composites cured with AR917 and DETDA

base resin	GFTE		DGEBA		PER		GER	
curing agent	AR917	DETDA	AR917	DETDA	AR917	DETDA	AR917	DETDA
tensile strength [MPa]	61.34 ±2.16	41.83 ±1.17	100.42 ±12.12	42.31 ±4.98	93.68 ±4.98	78.49 ±4.09	96.73 ±7.54	81.80 ±0.18
tensile modulus [GPa]	6.01 ±0.32	6.29 ±0.09	9.22 ±0.36	6.78 ±0.09	9.19 ±0.24	6.11 ±0.11	9.07 ±0.27	6.05 ±0.28
flexural strength [MPa]	116.65 ±12.24	60.14 ±0.27	131.66 ±1.12	72.82 ±2.58	120.82 ±3.82	93.18 ±1.86	129.71 ±2.94	104.86 ±7.53
flexural modulus [GPa]	10.59 ±0.25	7.13 ±0.49	11.13 ±0.12	7.23 ±0.41	10.41 ±0.16	8.53 ±0.18	10.75 ±0.20	9.90 ±1.03

In the case of GFTE cured with AR917 the tensile strength and modulus were significantly lower than in the mineral oil based composites. With DETDA however, the DGEBA and the GFTE composites had similar test results. As for the flexural properties, with DETDA noteworthy difference between the composites was observed, contrary to the composites cured with AR917. Furthermore, it has to be noted that in each case composites crosslinked with DETDA were weaker

than those cured with AR917. This phenomenon may be explained by the degradation of jute fibre at 175 °C, necessary to achieve complete curing by DETDA. Namely, at this temperature the bonding agents (lignin, hemicellulose) of the cellulose based fibres can start to degrade already [200]. Typically, jute fibre has an average tensile strength of 370 MPa, according to Saha et al. [83]. This value is practically in the same order of magnitude as the tensile strength of the applied neat matrices (the average tensile strength of DGEBA is 77.6 MPa (see **4.2.1**). According to these facts, the mechanical properties of the matrices significantly influenced the mechanical properties of jute fibre reinforced composites. With the much stronger carbon fibre reinforcement, (tensile strength of 5300 MPa; tensile modulus of 276 GPa [205]) this effect can be eliminated.

4.3.2. Development of carbon fibre reinforced bioepoxy composites

Although natural fibres represent an evident choice as reinforcement for bio-based polymers, because their application leads to all-bio composites; their disadvantages, as among others fluctuating fibre quality, limited processing temperature range, low strength, represent a major drawback, as seen in case of jute fibre reinforced composites in **4.3.1.2**. As the newly developed glucofuranoside-based bioepoxy (GFTE) proved to have comparable, or in some cases even superior properties compared to the benchmark DGEBA, its applicability in carbon fibre reinforced composites was investigated as well.

4.3.2.1. *Development of cycloaliphatic sugar based carbon fibre reinforced composites*

Carbon fibre (CF) reinforced composites were prepared from glucofuranoside based EP monomer (GFTE) cured with DETDA or AR917 hardener. As reference resins conventional mineral oil based aromatic bifunctional DGEBA, aliphatic trifunctional glycerol (GER) and tetrafunctional pentaerythritol based (PER) resins were used. Composite laminates were prepared by hand lamination followed by hot pressing to achieve high (59-61%) and uniform fibre content. Storage modulus, glass transition temperature and mechanical properties of the composites were compared [**204**].

Storage modulus and glass transition

Storage modulus curves of the EP composites cured with AR917 and DETDA are shown in **Figure 4.3.3**. The determined storage modulus at 0 and 200 °C (below and beyond the glass transition) and glass transition temperature (T_g) values (based on the tan δ peaks) are summarized in **Table 4.3.6**.

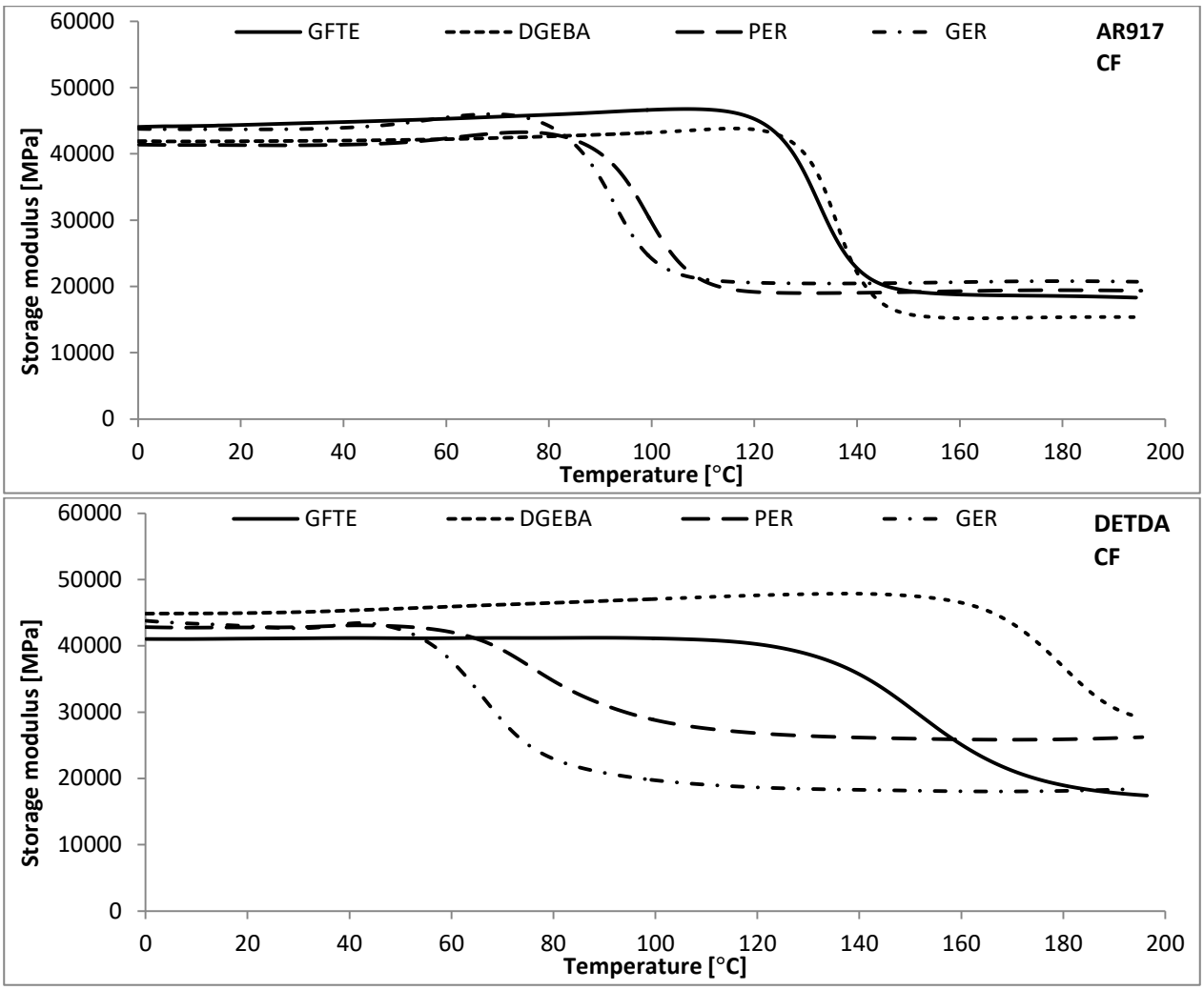

Figure 4.3.3 Storage modulus curves as a function of the temperature of the CF/EP composites cured with AR917 and DETDA curing agents

Table 4.3.6 Storage modulus (at 0 and 200 °C) and glass transition temperature values of the CF/EP composites with AR917 and DETDA curing agents

base resin		**GFTE**		**DGEBA**		**PER**		**GER**	
curing agent		**DETDA**	**AR917**	**DETDA**	**AR917**	**DETDA**	**AR917**	**DETDA**	**AR917**
storage modulus [MPa]	**0 °C**	41038	44065	44869	41919	42833	41392	43786	43770
	200 °C	17416	18308	29345	15360	26229	19358	18409	20706
glass transition temperature [°C]		161	136	184	138	82	102	70	95

Under the T_g there was no significant difference between the storage modulus of GFTE and the reference composites. As for the T_g values, in the case of DETDA, the difference between DGEBA and GFTE was higher with CF (23 °C) than with jute fibre reinforcement (12 °C), while with AR917, the difference was just 2 °C. The T_g value of GFTE DETDA composite (161 °C) is still above the results of the usual bio-based EPs, making them appropriate for some high temperature applications as well.

Mechanical characterization

Tensile strength and modulus, flexural strength and modulus of CF/EP composites cured with AR917 and DETDA are shown in **Table 4.3.7**.

Table 4.3.7 Tensile strength and modulus, flexural strength and modulus of CF/EP composites cured with AR917 and DETDA

base resin	GFTE		DGEBA		PER		GER	
curing agent	AR917	DETDA	AR917	DETDA	AR917	DETDA	AR917	DETDA
tensile strength [MPa]	498.46 ±5.88	468.91 ±29.40	471.36 ±3.26	451.48 ±36.93	482.01 ±73.43	616.13 ±8.64	496.72 ±13.99	487.67 ±19.95
tensile modulus [GPa]	14.54 ±0.47	14.29 ±1.36	13.66 ±2.51	12.92 ±1.08	14.09 ±0.65	14.43 ±0.12	14.32 ±0.38	12.58 ±0.51
flexural strength [MPa]	608.11 ±16.91	513.32 ±26.18	635.22 ±4.51	449.38 ±16.58	638.02 ±28.23	611.59 ±4.44	625.62 ±11.07	519.80 ±30.01
flexural modulus [GPa]	48.01 ±1.78	45.75 ±0.94	41.76 ±2.56	40.22 ±0.63	50.07 ±2.70	46.74 ±1.22	50.21 ±1.36	47.27 ±1.19

There was no significant difference between the mechanical properties of the sugar based and the mineral oil based composites. The GFTE/CF composites had almost in every case (except flexural strength with AR917) better mechanical properties than the DGEBA/CF composites, usually used as benchmark material in aeronautical applications. According to these results, the novel GFTE can be a potential bio-based replacement for the mineral oil based DGEBA EP component.

4.3.3. Summary on the development of bioepoxy composites

In order to facilitate the headway of natural fibre reinforced composites with bio-based resin matrix, a systematic research was performed to **characterize the effect of epoxidized soybean oil (ESO) addition on the storage modulus, glass transition temperature and mechanical properties of jute fibre reinforced composites** with a glycerol-based (GER), a pentaerythritol-based (PER) aliphatic EP and a bisphenol-A based aromatic EP (DGEBA) matrix.

Prior to composite preparation, the **effect of alkali treatment** (in particular NaOH concentration and treatment time) was **examined on raw linen woven jute fabric**. According to the results above certain concentration and treatment time a significant decrease of specific maximal force values during the strip tensile tests could be detected, as the binder in the elementary fibres was washed out. Based on these results we did not consider the alkali treatment of jute fabric justified, therefore **untreated jute fabric was used** for composite preparation.

Due to the **addition of ESO** the storage modulus decreased in almost all jute fabric reinforced composites. **In aliphatic matrices the T_g rather increases** when the amount of ESO is increased, while in aromatic DGEBA the T_g values rather show a decreasing tendency, nevertheless these

values are still higher than in the case of the aliphatic systems, due to the more rigid aromatic backbone of DGEBA. The T_g values of the composites decreased approx. by 40 °C compared to the corresponding neat epoxy resin, which is usually attributed to the decrease of crosslinking density due to the reaction of hydroxyl groups of the jute reinforcement and anhydride type curing agent.

As for the **mechanical properties**, **significant weakening effect of ESO** was detected in all composite specimens. In case of aliphatic PER and GER systems above 50% ESO-content the tensile strength values were even lower than in the case of the neat ESO composite, while the tensile modulus values decreased below the level of neat ESO composite only from 75% ESO content. The flexural strength was in the range between the values of the neat aliphatic resin and the neat ESO composites, in the case of PER composite containing 25% ESO even a slight increase could be detected. In aromatic DGEBA systems all mechanical properties decreased with ESO addition, however they stayed above values of the neat ESO composites in all cases.

According to the results, in applications where moderate glass transition temperature is acceptable, the **jute fibre reinforced aromatic DGEBA epoxy resin composite can be replaced** without significant compromise in mechanical properties **by a potentially fully bio-based composite consisting of 25% ESO-containing hybrid epoxy resin** reinforced by jute fibres.

Jute and carbon fibre reinforced composites, were prepared using a newly synthesized, renewable **glucofuranoside based epoxy resin (GFTE)** as polymer matrix. The dynamic mechanical and mechanical properties of the composites were compared to mineral oil based benchmark epoxy resin (DGEBA, PER, GER) composites.

In the case of natural **jute fibre reinforcement** the **overall mechanical performance of the GFTE composites** was somewhat **lower than** that of **DGEBA composites**, with **comparable T_g** values. The necessary curing cycle in the case of amine type DETDA hardener, used in high-tech sectors to provide high T_g, lead to the degradation of the natural fibres and consequently to lower mechanical properties than in the case of anhydride type crosslinking agent.

In order to **eliminate the drawbacks of natural fibres** (low tensile strength and thermal stability) and to get an insight into the real performance of GFTE in comparison with DGEBA, **composites with a technical carbon fibre** were tested. In this case the **tensile strength and modulus, flexural strength and modulus of the GFTE/CF composites was higher than in** the case of **DGEBA**, and the T_g values of the DGEBA/CF and the GFTE/CF composites were comparable. These results suggest that the **novel glucose-based epoxy monomer can be an alternative** to the commonly used mineral oil based diglycidyl ether of bisphenol-A (DGEBA), even **in high temperature applications up to 160 °C** using an amine type curing agent approved for aircraft composites.

4.4. Flame retardancy of epoxy resins

In this chapter the results on the flame retardancy of epoxy resins applying P-containing additive and reactive type FRs are summarized.

First, the effect of **P-based additive and reactive FRs** was **compared** in an aliphatic, **pentaerythritol-based model epoxy resin system (PER)**. Besides the commercially available **ammonium polyphosphate (APP)** additive type FR and **9,10-dihydro-9-oxa-10-phosphaphenantrene-10-oxide (DOPO)** reactive type FR, the synthesized **P-containing amine type hardener (TEDAP)** was tested as well. Among the additive type P-containing FRs APP is one of the most widely used additives, which acts in the solid phase [206]. In the case of epoxy resins mainly the fire retardancy of diglycidyl ether of bisphenol-A (DGEBA) was examined with APP [207,208]. Among the reactive FRs DOPO, along with its numerous derivatives, is one of the most investigated FRs in epoxy resins [209]. DOPO can either act in gas phase via flame inhibition, or both in gas and solid phase [210]. The FR mechanism of reactive FR TEDAP was investigated in details previously [**173**,**211**]: it acts both in gas phase (mainly at the beginning of the degradation) and in the solid phase (during high temperature degradation).

Although it is recognized, that it is **advantageous**, if the applied FR or FR combination **performs action in both gas and solid phase** [212], and it is suspected that the flame retardancy synergism of combining less volatile and more volatile phosphate FRs can be attributed to a combined phase action [206,213], to best of our knowledge no systematic study was carried out on the flame retardancy mechanism of combinations of solid and gas phase FRs. To fill this gap, fire retardancy of commercially available **sorbitol polyglycidyl ether (SPE)** and newly synthesized **glucofuranoside based trifunctional epoxy monomer (GFTE)** bioepoxy resin was investigated **using ammonium polyphosphate (APP)**, acting in solid phase and **resorcinol bis(diphenyl phosphate) (RDP)** acting mainly in gas phase through flame inhibition [214], and **their combination**. RDP has high thermal stability and low volatility [215], furthermore as it is liquid, homogenization problems, aggregation and/or filtration of FR particles e.g. in case of composite preparation by resin transfer moulding can be avoided by using RDP.

Generally, the addition of **FRs significantly influences the glass transition temperature (T_g)** of the matrix polymer, and consequently its applicability as well. A possible way to **compensate the effect of FRs** is to form blends with another polymer possessing high glass transition temperature, thermally stable backbone and outstanding mechanical properties. Instead of simple blend formation **reactive blending** resulting in primary chemical bonds between the polymers is preferred. For these reasons epoxy resins are often blended **with cyanate esters (CE)**

[216,217,218,219], which can be applied instead of the commonly applied amine or anhydride type hardeners. This way cyanate esters can be used as **multifunctional reactive modifiers** increasing the glass transition temperature, and improving the thermal stability and mechanical properties of flame retarded epoxy resins. In order to compensate the significant decrease caused by DOPO in DGEBA benchmark epoxy resin, a **hybrid system consisting of DGEBA** (diglycidyl ether of bisphenol A)**, novolac type CE and reactive DGEBA-DOPO FR** was prepared and investigated. Finally, the FR effect of the synthesized **P-containing, reactive FR, TEDAP** was compared in **aromatic DGEBA-based and aliphatic PER-based epoxy resin.**

4.4.1. Comparison of additive and reactive phosphorus-based flame retardants in epoxy resins

As a preliminary experiment, the effect of P-based additive and reactive FRs on the flammability and mechanical properties of a pentaerythritol-based model epoxy resin system (PER), cured with a cycloaliphatic diamine hardener (T58), were compared. Commercially available ammonium polyphosphate (APP) was used as additive, and DOPO, pre-reacted with PER to form P-containing epoxy monomer (PER-DOPO), was used as reactive FR besides the synthesized P-containing amine type hardener (TEDAP). APP was applied in increasing concentrations up to 5% (P)-content, while in case of reactive FRs the stoichiometry determined the maximum of introduced P, which was 4% in case of PER-DOPO and 3% in case of TEDAP [**190**].

Flame retardancy

The LOI, UL-94 and cone calorimetry results of the flame retarded PER samples are summarized in **Table 4.4.1**, the best performances among the samples are highlighted with bold letters.

Table 4.4.1 LOI, UL-94 and cone calorimetry results of flame retarded PER samples

sample	LOI [V/V%]	UL-94 (burning rate)	TTI [s]	pHRR (kW/m^2)	THR [MJ/m^2]	residue [%]
PER matrix	23	HB (32.0 mm/min)	13	706	103.5	0
APP 1%P	27	HB (-)	23	546	108.5	10
APP 2%P	32	HB (-)	25	539	71.5	14
APP 3%P	32	HB (-)	29	421	82.5	14
APP 4%P	32	V-1	23	358	76.7	18
APP 5%P	32	**V-0**	28	364	68.2	18
PER-DOPO 1%P	23	HB (14.3 mm/min)	22	704	97.2	2
PER-DOPO 2%P	23	HB (-)	26	760	102.7	7
PER-DOPO 3%P	23	HB (-)	10	682	106.0	6
PER-DOPO 4%P	24	HB (-)	26	648	92.3	11
TEDAP 1%P	25	V-2	22	668	97.5	7
TEDAP 2%P	30	V-1	17	244	59.4	26
TEDAP 3%P	**33**	**V-0**	**95**	**111**	**28.0**	**40**

LOI: limiting oxygen index, TTI: time to ignition, pHRR: peak of heat release rate, THR: total heat release

With the addition of the additive APP, the LOI value was increased with 2% P to 32 V/V%, which value could not be improved further, despite of the increasing P-content. On the other hand, self-extinguishing, V-0 UL-94 rate was achieved only with 5% P. The time to ignition (TTI) was shifted to about the double of the TTI recorded for PER independently from the APP-content. The pHRR decreased by increasing the P-content, reaching a reduction of approx. 50% in case of 4 and 5% P-content, accompanied by 25% and 35% decrease in THR, respectively, and 18% residual mass.

The application of PER-DOPO flame retarded epoxy component could not decrease the flammability of PER significantly: the LOI values practically remained the same, and although the flame spreading was reduced or ceased, the UL-94 rate remained HB due to dripping. The only positive influence is the shift of the pHRR in time by about 50 s; nevertheless the pHRR and THR values did not change considerably and the increase of the residual mass was also inferior to that of the APP-containing samples. The reason behind the poor performance of DOPO in pentaerythritol-based epoxy resin can be the incompatibility of the condensed aromatic structured DOPO with the aliphatic epoxy component. This phenomenon highlights the importance of compatibility in the flame retardancy process and the necessity of the adjustment of the structure of the FRs to the polymer matrix to be protected.

On the other hand, the application of the aliphatic P-containing hardener (TEDAP) in increasing amounts led to a continuously decreased flammability of the resin. The LOI could be increased up to 33 V/V%, and at 3% P-loading V-0 rating was reached, the TTI was shifted in time by 80 sec, the pHRR was reduced by 85% and the THR by more than 70% accompanied by 40% residual mass.

For a better comparison, the HRR curves of the reference sample and matrices containing 3% P from APP, DOPO and TEDAP are displayed in **Figure 4.4.1**. When applying DOPO, the pHRR was shifted in time by 50 s, but its value remained the same. In the case of APP, the pHRR was reduced by 40% and shifted in time by 70 s, while by the incorporation of the same amount of P by TEDAP component resulted in 85% lower pHRR value than that of the reference.

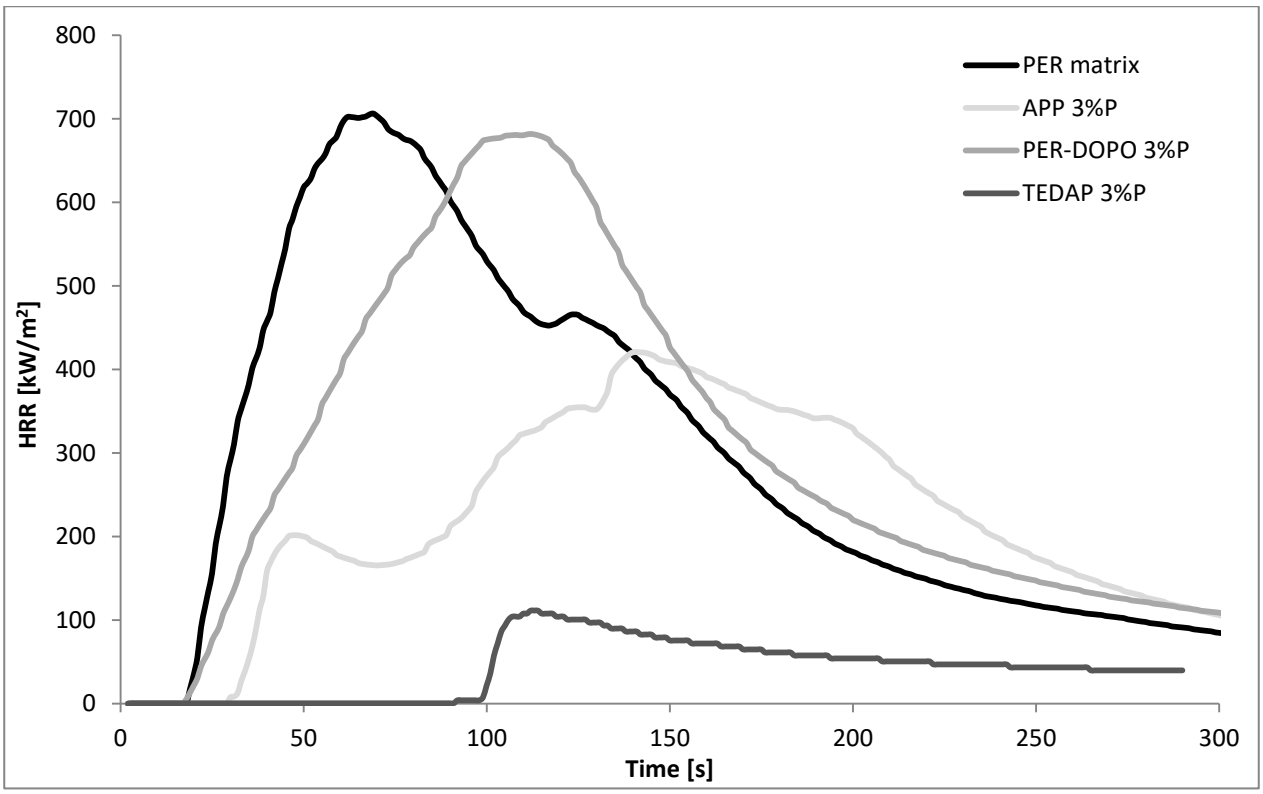

Figure 4.4.1 Comparison of the heat release rates of APP, DOPO and TEDAP in PER at 3% P-content

Mechanical characterization

In order to characterize the effect of FRs on the mechanical properties and glass transition temperature; tensile, bending and DMA tests were carried out (**Table 4.4.2**). The PER-DOPO containing formulations showed exceptional brittleness even at the removal from the silicon moulds; therefore no mechanical tests could be performed.

Table 4.4.2 Tensile, bending test results and glass transition temperature of flame retarded PER samples

sample	tensile strength [MPa]	tensile modulus [MPa]	flexural strength [MPa]	flexural modulus [GPa]	glass transition temperature [°C]
PER matrix	50.45±5.99	844.75±30.46	82.11±3.38	2.34±0.23	58
APP 1%P	41.22±7.39	830.85±23.44	78.00±6.38	1.94±0.32	78
APP 2%P	46.80±4.47	861.01±7.23	70.77±3.98	2.23±0.11	80
APP 3%P	42.95±6.63	856.21±25.92	72.71±2.73	2.38±0.16	92
APP 4%P	40.65±1.81	783.86±26.91	85.23±13.66	2.30±0.25	69
APP 5%P	41.15±1.20	776.99±39.53	87.45±7.00	2.50±0.12	61
TEDAP 1%P	49.91±2.65	726.77±34.83	84.15±7.35	2.38±0.08	53
TEDAP 2%P	35.55±1.24	98.27±9.84	75.40±2.21	1.73±0.08	44
TEDAP 3%P	32.11±3.44	65.05±5.35	52.94±5.95	1.56±0.20	40

APP-containing samples have somewhat lower tensile strength and similar flexural strength values as PER, but no significant difference could be detected between the FR concentrations applied, indicating homogenous dispersion of the additive FR particles. When 1% P was introduced by the FR crosslinking agent (TEDAP), the tensile and flexural strength was as high as that of the

reference matrix. However, at 2 and 3% P-content, the measured tensile strength was reduced by about 30%, and due to the lower crosslinking density the tensile modulus was reduced to about 10% of the original value. The 3% P-containing system had about 35% lower flexural strength and modulus than the reference system.

Up to the addition of 3% P from APP, the glass transition temperature (T_g) increased significantly, by 20-30 °C, which can be explained by the presence of the well-dispersed, rigid APP particles, which can block the segmental movements of the cross-linked epoxy matrix. At higher concentrations, this beneficial effect was compensated by the interaction of monomers with the filler particles during the polymerization process, which reduced the degree of crosslinking, and consequently the T_g. When the reference cycloaliphatic hardener was partially or fully replaced by aliphatic TEDAP, allowing faster segmental movements within the network, lower T_g values were measured: at total replacement by TEDAP, the T_g decreased by 30%, from 58 to 40 °C.

4.4.2. Flame retardancy of aliphatic sugar based epoxy resins with combination of phosphorus-containing additives

The fire retardancy of commercially available sorbitol polyglycidyl ether (SPE) bioepoxy resin cured by cycloaliphatic amine hardener (T58) was investigated using ammonium polyphosphate (APP), acting in solid phase and resorcinol bis(diphenyl phosphate) (RDP) acting mainly in gas phase, and their combination. The change of glass transition temperature, due to their effect, was determined by differential scanning calorimetry, while their fire retardancy was evaluated by limiting oxygen index (LOI), UL-94 tests and mass loss calorimetry. The anticipated combined solid- and gas phase mechanism was confirmed by thermogravimetric analysis, FTIR analysis of the gases formed during laser pyrolysis, ATR-IR analysis of the charred residues, as well as by mechanical resistance test of the chars obtained after combustion, carried out by plate-plate rheometer [220].

Glass transition temperature

The T_g of the flame retarded SPE samples determined by DSC can be seen in **Table 4.4.3**.

Table 4.4.3 Effect of the additive flame retardants on the glass transition temperature of SPE

sample	glass transition temperature [°C]
SPE matrix	124
RDP 1%P	114
RDP 2%P	108
RDP 3%P	95
APP 1%P	110
APP 2%P	110
APP 3%P	110
RDP 1%P+APP 2%P	114
RDP 1.5%P+APP 1.5%P	114
RDP 2%P+APP 1%P	114

The plasticizing effect of the additives becomes more pronounced in the case of liquid RDP: by increasing its amount, the T_g is gradually decreasing. In the case of APP, due to its higher P-content, smaller amount is needed to reach the same P-content. Furthermore, well-dispersed rigid APP particles can block the segmental movements in the cross-linked epoxy matrix and compensate the decrease of T_g caused by the reduced degree of crosslinking in the presence of filler particles (see **4.4.1**). Upon increasing its ratio in the polymer, the T_g remained uniformly 110 °C, most probably at higher APP loadings the dispersion is less efficient, therefore no increase in T_g was detected. In the mixed FR formulations independently from the origin of their P-content the T_g decreased only by 10 °C. Comparing the RDP 1%P+APP 2%P sample with the RDP 1%P sample, it can be concluded that the addition of 2% P from APP to 1% P from RDP, did not result in further decrease in T_g, both samples have a T_g of 114 °C. By increasing the ratio of RDP and decreasing the ratio of APP, the T_g remained 114 °C, which can be possibly interpreted by the lower amount of APP, which can be dispersed more efficiently, leading to the blocking of segmental movements.

Flame retardancy

The LOI and UL-94 results of the flame retarded samples can be seen in **Table 4.4.4**.

When applied alone, both the RDP and APP-containing formulations showed increased LOI values but their UL-94 ratings remained HB. P-content of 3% is generally sufficient to reach appropriate flame retardancy according to earlier experiences [116], thus, mixed FR formulations with combined RDP and APP, have been also prepared. When 1% of P was introduced from RDP and 2% from APP, the UL-94 rating remained HB, but inverting the ratio, and balancing it between the two additives lead to self-extinguishing V-0 rating with LOI values of 33-34 V/V%.

Table 4.4.4 LOI and UL-94 results of the flame retarded SPE samples

sample	LOI [V/V%]	UL-94 (burning rate)
SPE matrix	20	HB (20.0 mm/min)
RDP 1%P	25	HB (vertical 1st ignition)
RDP 2%P	27	HB (vertical 1st ignition)
RDP 3%P	28	HB (vertical 2nd ignition)
APP 1%P	27	HB (vertical 1st ignition)
APP 2%P	30	HB (vertical 1st ignition)
APP 3%P	31	HB (vertical 2nd ignition)
RDP 1%P+APP 2%P	29	HB (vertical 2nd ignition)
RDP 1.5%P+APP 1.5%P	33	V-0
RDP 2%P+APP 1%P	34	V-0

Specimens were prepared for mass loss calorimetry tests using the SPE reference, RDP 3%P, APP 3%P and 3% P-containing mixed formulations reaching V-0 UL-94. The heat release rate curves can be seen in **Figure 4.4.2**, while numerical data obtained from mass loss calorimetry results are summarized in **Table 4.4.5**, the best performances among the samples are highlighted with bold letters. In the case of combined FR samples the ignition occurred earlier, however the time to peak heat release rate (pHRR) increased compared to RDP 3%P and APP 3%P samples. From all formulations the RDP 2%P+APP 1%P sample had the lowest pHRR, FIGRA (fire growth rate), EHC (average effective heat of combustion) and MARHE (maximum of average rate of heat emission), so similarly to the conclusions of LOI and UL-94 test, this formulation can be considered as having the best overall performance.

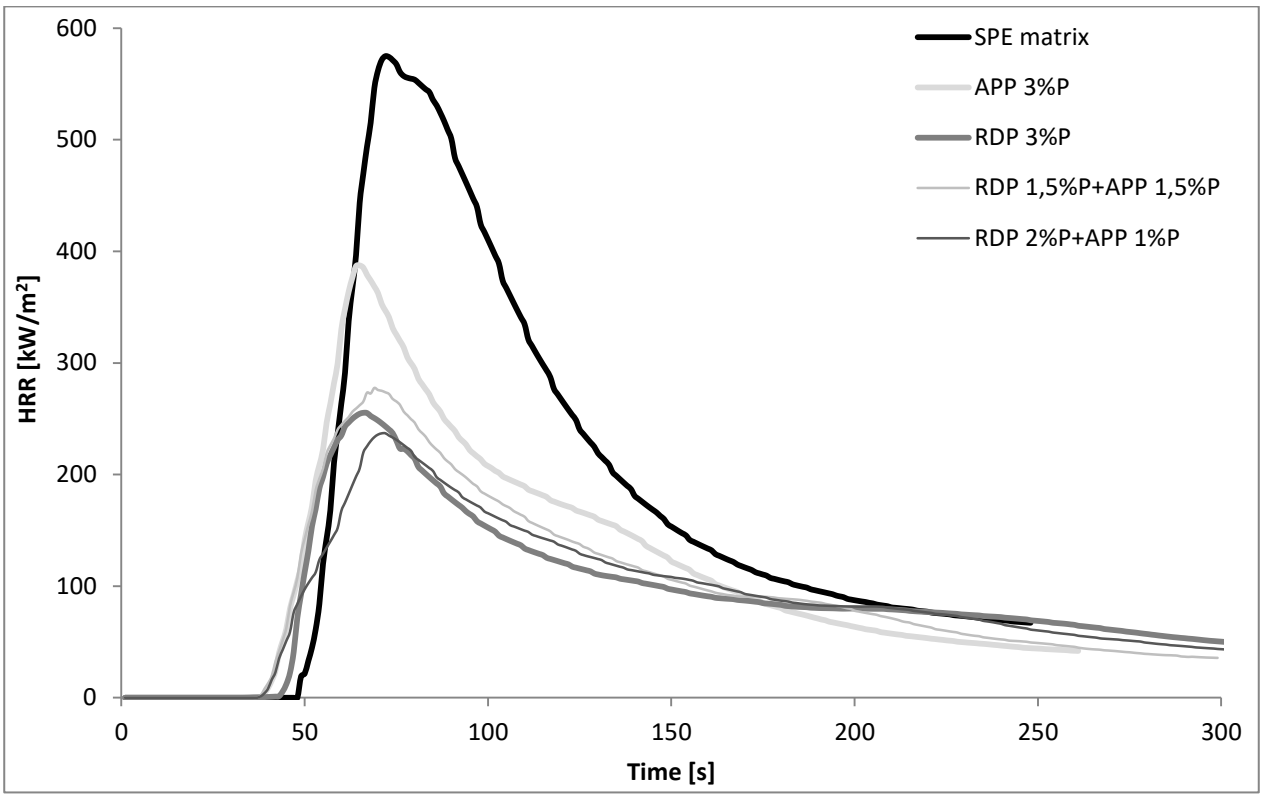

Figure 4.4.2 Heat release rate of reference and flame retarded SPE samples

Table 4.4.5 Mass loss calorimetry results of reference and flame retarded SPE samples

sample	TTI [s]	pHRR [kW/m^2]	time of pHRR [s]	FIGRA [kW/m^{2}s]	burning time [s]	THR [MJ/m^2]	EHC [MJ/kg]	MARHE [kW/m^2]	residue [%]
SPE reference	**45**	575	**72**	8.0	**105**	43.2	18.7	233.1	5
RDP 3%P	43	255	66	3.9	315	**24.5**	13.3	111.7	**28**
APP 3%P	38	387	65	6.0	146	30.1	14.7	156.6	17
RDP 1.5%P+APP 1.5%P	31	278	69	4.0	234	26.7	13.7	129.8	20
RDP 2%P+APP 1%P	35	**237**	**72**	**3.3**	282	24.7	**12.0**	**110.8**	19

(TTI: time to ignition, pHRR: peak of heat release rate, FIGRA: fire growth rate, THR: total heat released, EHC: average effective heat of combustion, MARHE: maximum of average rate of heat emission)

In order to explain the results of fire tests, the mode of action of FRs should be taken into account. The general opinion is that the ammonium polyphosphate acts in the solid phase as charring agent [206,208,207], while organophosphates act rather as radical scavenger in the gas phase [210,214]. Presumably, with the application of the combined FR formulation, a balanced solid and gas phase mechanism was reached. To confirm this hypothesis, thermogravimetric analysis was carried out; furthermore, the composition of the gas and solid phase degradation products, and the strength of the charred residue were investigated as well.

Thermogravimetric analysis

The thermal stability of the reference and flame retarded SPE samples were examined by thermogravimetric analysis. **Table 4.4.6** shows the temperature at 5% and 50% mass loss ($T_{-5\%}$; $T_{-50\%}$), the maximum mass loss rate (dTG_{max}), the temperature belonging to this value (T_{dTGmax}) and the char yield at the end of the TGA test (at 800 °C). **Figure 4.4.3** shows the TGA curves from 50 to 300 °C in order to highlight the differences at the beginning of thermal degradation.

Table 4.4.6 TGA results of flame retarded SPE samples

sample	$T_{-5\%}$ [°C]	$T_{-50\%}$ [°C]	dTG_{max} [%/°C]	T_{dTGmax} [°C]	char yield at 800 °C [%]
SPE matrix	264	322.	1.45	263	5.6
RDP 1%P	264	309	1.21	275	13.4
RDP 2%P	259	309	1.24	275	15.5
RDP 3%P	251	309	1.46	277	16.6
APP 1%P	276	310	1.81	284	16.4
APP 2%P	272	319	1.38	278	19.8
APP 3%P	263	330	0.62	276	23.2
RDP 1%P+APP 2%P	272	330	0.98	286	22.5
RDP 1.5%P+APP 1.5%P	271	331	0.99	279	22.5
RDP 2%P+APP 1%P	262	314	1.09	274	16.6

$T_{-5\%}$: temperature at 5% mass loss, $T_{-50\%}$: temperature at 50% mass loss; dTG_{max}: maximum mass loss rate; T_{dTGmax}: the temperature belonging to maximum mass loss rate

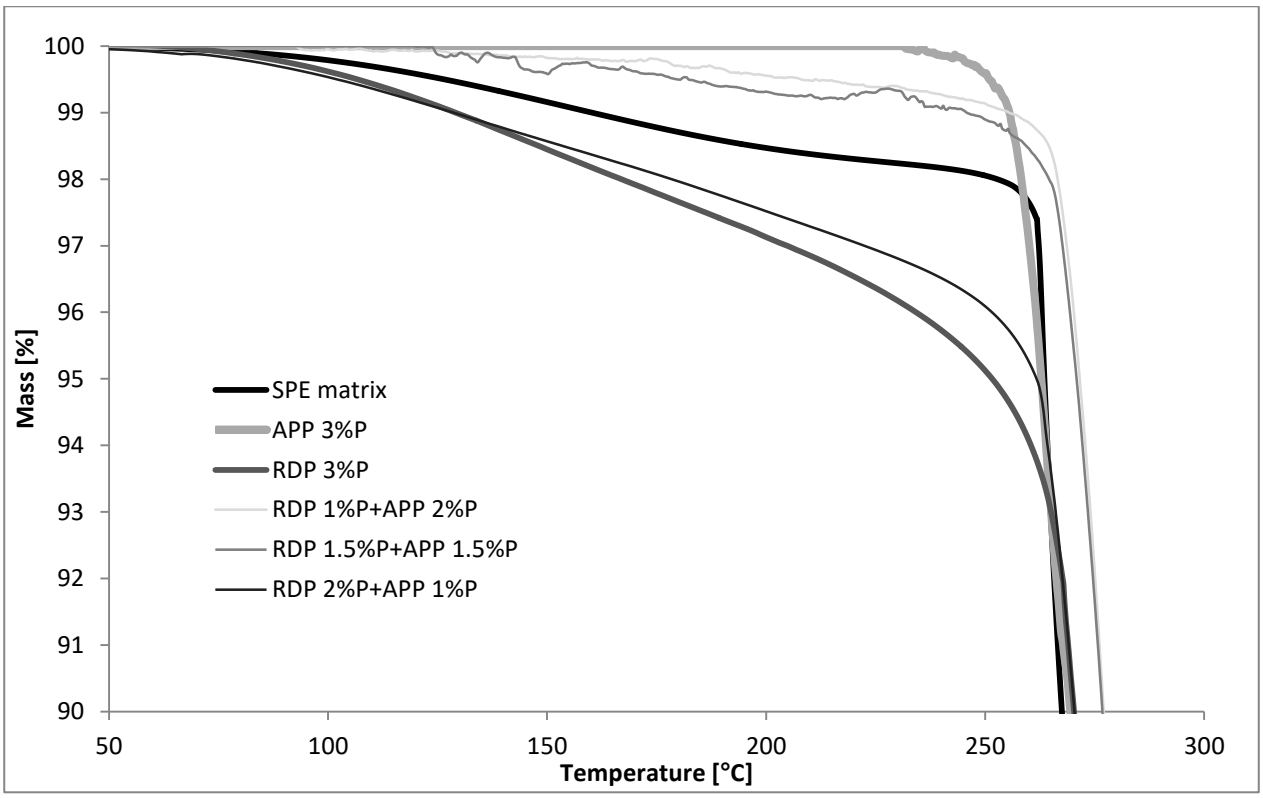

Figure 4.4.3 TGA curves of the reference and 3% P-containing SPE samples in the range of 50-300 °C

As it can be seen from **Table 4.4.6**, by increasing the amount of P introduced by RDP to 2 and 3%, the temperature belonging to 5% mass loss was gradually shifted to lower temperatures. The reason for this is that organic P FRs usually act during the early degradation step in the gas phase. The temperature belonging to 50% mass loss was around 15 °C less than in the case of the reference sample, independently from the P-content. The char yield at 800 °C increased almost by 10% by introducing only 1% of P, however, further increase of P-content did not result in significantly further improvement. In the case of APP at 1 and 2% P-content the temperature belonging to 5% mass loss increased compared to the reference, while the sample with 3% P showed similar value as the reference. The temperature belonging to 50% mass loss increased gradually with increasing P-content, while the maximum mass loss rate decreased. The char yield at 800 °C was the same in the APP-containing sample with 1% P and in the RDP-containing sample with 3% P, confirming the solid phase mechanism of APP. The char yield is gradually increasing when the P-content of APP origin is increased: at 3% P-content 23% of the initial sample mass remained as char at 800 °C. As for the samples containing both RDP and APP, formulations containing 1% and 1.5% P of RDP origin showed very similar thermal behaviour. By increasing the amount of RDP in combined samples the thermal degradation started at lower temperature and the temperature belonging to 50% mass loss decreased. On the other hand, by increasing the

amount of APP the maximum mass loss rate decreased and the char yield increased. The different phase mechanism of the two FRs could by clearly identified from the TGA results.

Investigation of gas and solid phase flame retardancy mechanisms by infrared spectrometry

Gas phase flame retardancy mechanism was examined by a coupled LP-FTIR method in the case of four samples containing 3% P: samples containing only APP and only RDP, as well as the two samples reaching V-0 UL-94 classification (RDP 1.5% P+APP 1.5% P and RDP 2% P+APP 1% P) (**Figure 4.4.4**).

Clear differences could be identified in the gas phase spectra of different formulations: the vibrations belonging to P=O and P-O-C bonds appear as sharp peaks (in the range of 1290-1190 cm^{-1} and 1050 to 950 cm^{-1}, respectively) in the case of the samples containing RDP, while the sample containing only APP showed no peaks in these intervals. For all samples CO_2 (2400-2300 cm^{-1}) and CO (2200-2080 cm^{-1}) peaks were observed in the gas phase, as well as aromatic C=C vibrations (1600 and 1490 cm^{-1}), whose intensity increased by increasing the RDP-content. Increasing the APP-content the wide peak, characteristic for N-H vibrations (3400 cm^{-1}), became more and more separated from the set of C-H vibrations (3200-2800 cm^{-1}). Based on these results, no gas phase effect could be detected in the sample containing only APP, while with increasing RDP content, the amount of P species increased among the gas phase degradation products.

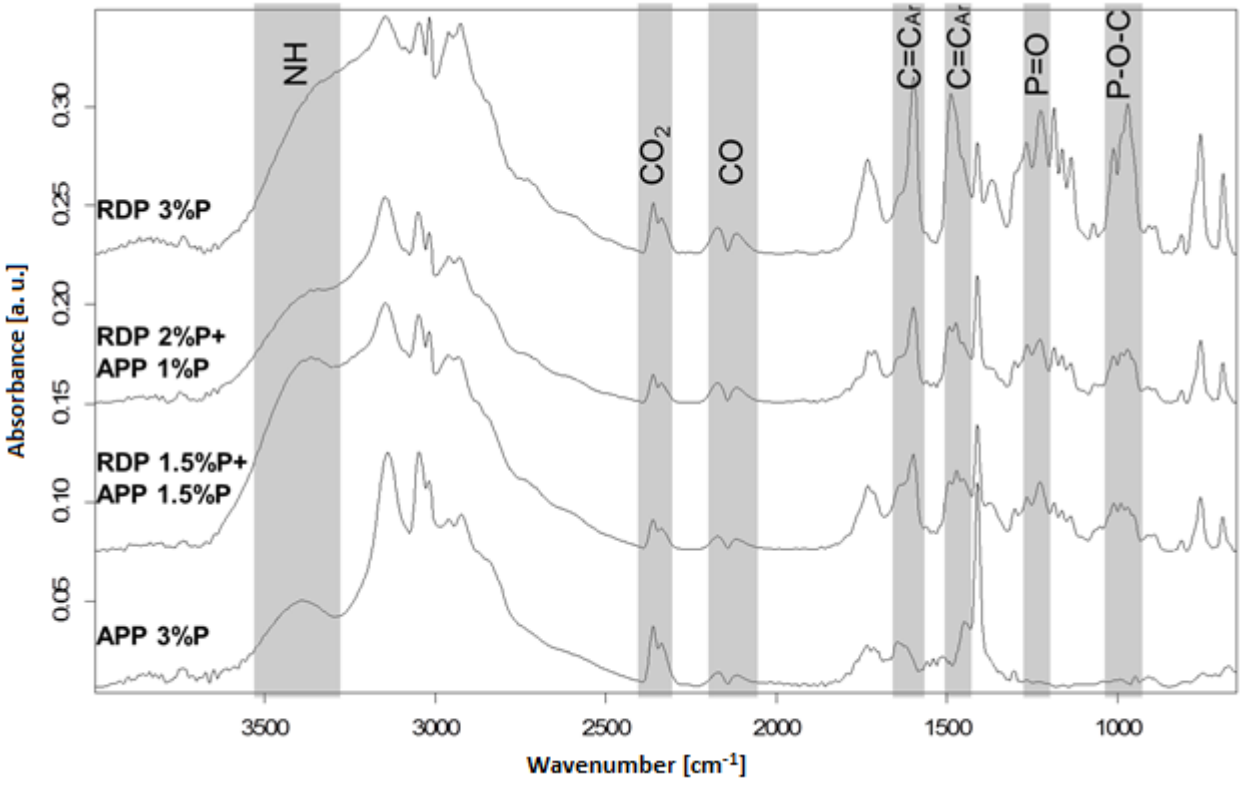

Figure 4.4.4 LP-FTIR spectra of the gas phase degradation products from 3% P-containing SPE samples

Solid residues collected after 50 kW/m^2 heat treatment in mass loss calorimeter were subjected to ATR-IR analysis (**Figure 4.4.5**).

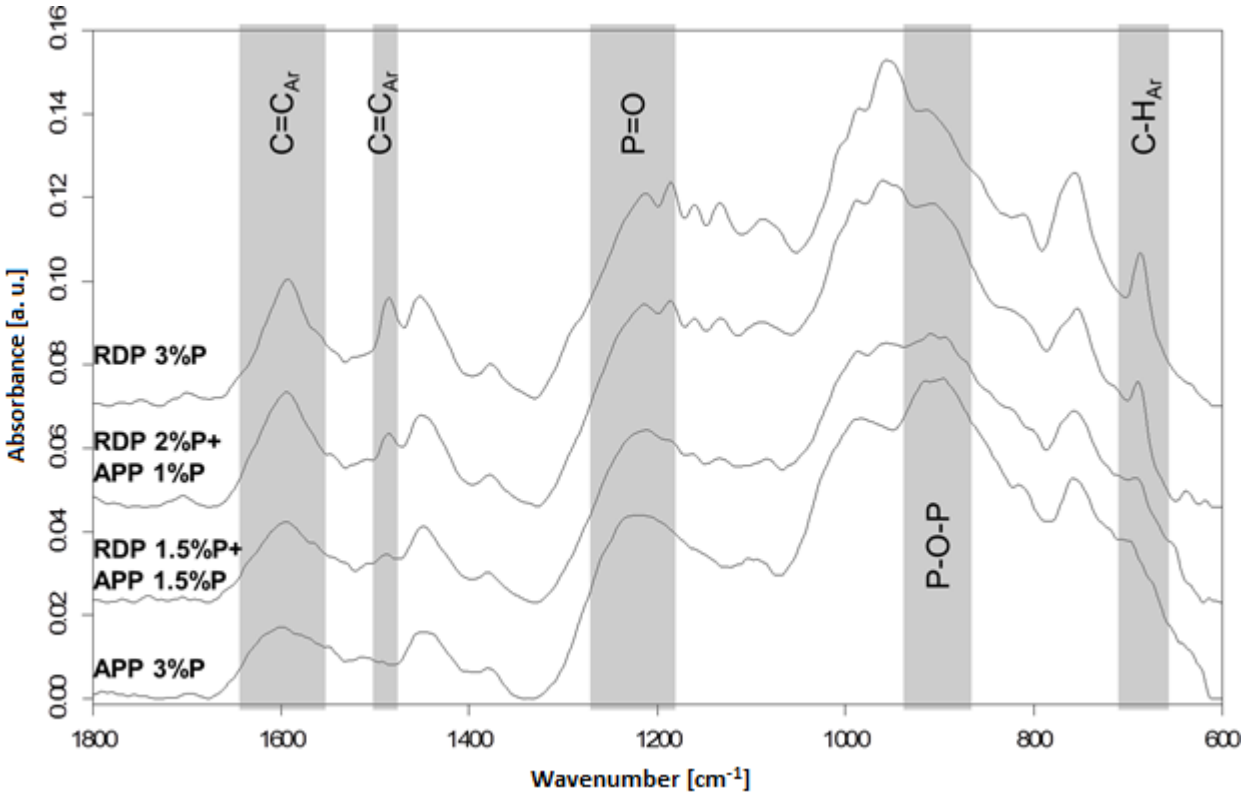

Figure 4.4.5 ATR-IR spectra of the charred residues from 3% P-containing SPE samples

Although in APP-containing samples the amount of charred residues is significantly higher, in their residues the peaks characteristic for aromatic C=C (1600 cm^{-1} and 1480 cm^{-1}) and C-H (690 cm^{-1}) vibrations have lower intensity than in the case of RDP-containing samples. The P-content of RDP is only 10.8%, thus to reach the same P-content much more additive is needed than in the case of APP (containing 31-32% P), and approx. 90% of the RDP's remaining mass is present in the form of phenol and resorcinol, increasing the aromatic content of the solid phase residue. On the other hand, the intensity of the P-O-P (910 cm^{-1}) and P=O (1215 cm^{-1}) bonds is higher in the case of the APP 3%P sample, and decreases with decreasing amounts of APP, which indicates the dominance of the solid phase mechanism of the APP.

Char strength

The mechanical resistance of the chars obtained after combustion in the mass loss calorimeter (set to 50 kW/m^2 heat flux) was examined through compression tests carried out in a rheometer. The average height of the charred residues is summarized in **Table 4.4.7** (for detailed results see [**220**]. After breaking the charred structure the normal force increases significantly because of the compression of the charred layer. The scattering of the normal force correlates with the diameter

of the formed bubbles in the char: small, uniform fluctuation refers to small bubble diameter and uniform, flexible char; while sudden decrease in normal force proves the presence of bubbles with big diameter, which causes the char to have an uneven, rigid structure.

Table 4.4.7 Average heights of the charred residues measured by compression test in the rheometer

sample	average char height [mm]
RDP 3%P	42±3
APP 3%P	11±1
RDP 1.5%P+APP 1.5%P	31±2
RDP 2%P+APP 1%P	27±2

The SPE RDP 3% P sample had the biggest char height, it can be assumed that the RDP entering the gas phase was capable to foam the upper layer of the polymer, forming a sponge like, elastic, microporous char. The sample flame retarded only with APP had the lowest char, which could be cracked with a minimal force. Significant scattering of the normal force was typical, which means that an uneven, rigid structure was formed. As APP acts mainly in the solid phase, and the gas formation was less significant than in the case of RDP, only the slight upper layer of the polymer was foamed, which was easily destructed in the weaker points by the applied pressure. In the case of combined FR system increasing tendency of normal force was detected similarly to the sample containing only RDP. However, scattering of the normal force was also detected similarly to the sample containing only APP. From the fire retardancy point of view neither the too rigid, nor the too elastic char structure is favourable. The behaviour of the char formed in the case of combined FR compositions lies between the two extremes, which provided adequate protection.

4.4.3. Flame retardancy of cycloaliphatic sugar based epoxy resins with combination of phosphorus-containing additives

Fire retardancy of a novel glucofuranoside based trifunctional epoxy monomer (GFTE) cured by aromatic amine hardener (DETDA) was tested using APP, RDP and their combination. Fire retardancy was evaluated by limiting oxygen index (LOI), UL-94 tests and mass loss calorimetry. The thermal stability was investigated by TGA, while the effect of FRs on the T_g and crosslinking process was studied by DSC [**221**].

Flame retardancy

Based on previous flame retardancy results with APP, RDP and their combinations in commercially available sorbitol polyglycidyl ether (SPE) bioepoxy matrix (see **4.4.2**), at first GFTE samples with 3% P were prepared. Although their LOI increased significantly, especially in samples containing

RDP, acting mainly in the gas phase, their UL-94 rate remained HB due to the flaming up to the holding clamp (**Table 4.4.8**). Increasing the amount of P to 4% resulted in significantly better UL-94 ratings: V-0 rate was reached both in RDP 2%P+APP 2%P and in APP 4%P samples. From these two samples the mixed FR formulation had 3 V/V% higher LOI, which means that the combined solid and gas phase FR action is more favourable than the sole solid phase action of APP in this bioepoxy system as well.

Table 4.4.8 LOI and UL-94 results of the reference and flame retarded GFTE matrix samples

sample	LOI [V/V%]	UL-94 (burning rate)
GFTE matrix	22	HB (25.6 mm/min)
RDP 3%P	30	HB (vertical 2nd ignition)
APP 3%P	25	HB (vertical 1st ignition)
RDP 1%P+APP 2%P	29	HB (vertical 2nd ignition)
RDP 2%P+APP 1%P	29	HB (vertical 2nd ignition)
RDP 4%P	31	V-1
APP 4%P	29	V-0
RDP 2%P+APP 2%P	32	V-0

Based on these results, in the followings only the reference and the 4% P-containing samples were subjected to further analysis. The HRR curves of the GFTE matrix samples can be seen in **Figure 4.4.6**, while numerical data obtained from mass loss calorimetry results are summarized in **Table 4.4.9**, best performances among the samples are highlighted with bold letters.

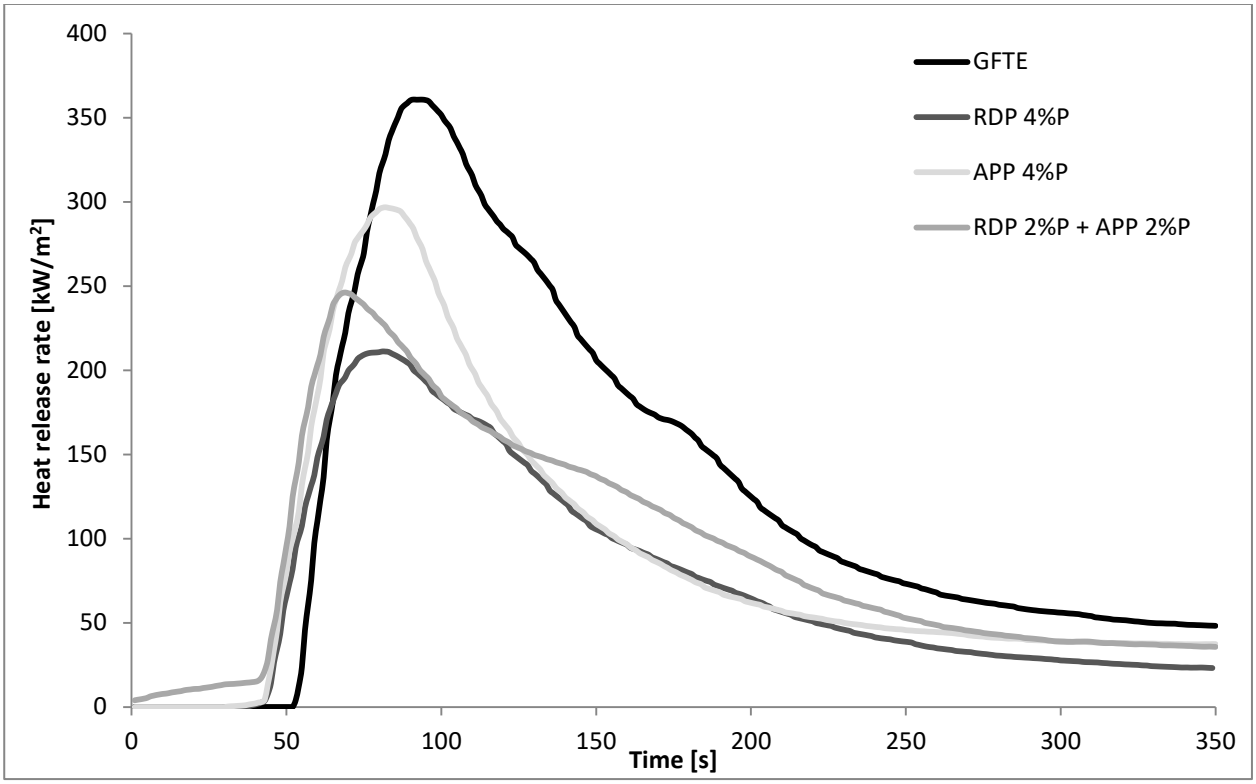

Figure 4.4.6 Heat release rate of reference and flame retarded GFTE samples

Table 4.4.9 Mass loss calorimetry results of reference and flame retarded GFTE samples

sample	TTI [s]	pHRR [kW/m^2]	time of pHRR [s]	FIGRA [kW/m^{2}s]	burning time [s]	THR [MJ/m^2]	EHC [MJ/kg]	MARHE [kW/m^2]	residue [%]
GFTE matrix	**54**	361	**93**	3.9	**155**	44.4	21.0	173.5	6
RDP 4%P	44	**211**	81	**2.6**	196	**26.0**	**14.5**	**110.5**	19
APP 4%P	44	297	82	3.6	472	31.2	17.8	138.9	23
RDP 2%P+APP 2%P	40	246	69	3.6	191	32.3	19	128.1	**25**

(TTI: time to ignition, pHRR: peak of heat release rate, FIGRA: fire growth rate, THR: total heat release, EHC: average effective heat of combustion, MARHE: maximum of average rate of heat emission)

In all flame retarded samples, the TTI decreased, which is in agreement with the lower thermal stability at the beginning of the thermal degradation (see TGA results in **Table 4.4.10**). As for the heat release rate, RDP 4%P showed the best overall performance, followed by the mixed formulation. Similarly to the LOI results, APP 4%P showed the most modest FR action, suggesting that the solid phase action alone is not sufficient in this bioepoxy resin to provide significant FR effect.

Thermogravimetric analysis

The thermal stability of the reference and flame retarded GFTE samples was examined by thermogravimetric analysis. **Table 4.4.10** shows the temperature at 5% and 50% mass loss ($T_{-5\%}$; $T_{-50\%}$), the maximum mass loss rate (dTG_{max}), the temperature belonging to this value (T_{dTGmax}) and the char yield at the end of the TGA test (at 800 °C). The TGA curves in the temperature range from 25-800 °C are displayed in **Figure 4.4.7.**

Table 4.4.10 TGA results of the reference and flame retarded GFTE matrix samples

sample	$T_{-5\%}$ [°C]	$T_{-50\%}$ [°C]	dTG_{max} [%/°C]	T_{dTGmax} [°C]	char yield at 800 °C [%]
GFTE matrix	348	373	5.21	323	11.8
RDP 4%P	269	373	0.97	277	29.9
APP 4%P	311	369	0.72	344	23.4
RDP 2%P+APP 2%P	300	409	2.81	322	33.4

$T_{-5\%}$: temperature at 5% mass loss, $T_{-50\%}$: temperature at 50% mass loss; dTG_{max}: maximum mass loss rate; T_{dTGmax}: the temperature belonging to maximum mass loss rate

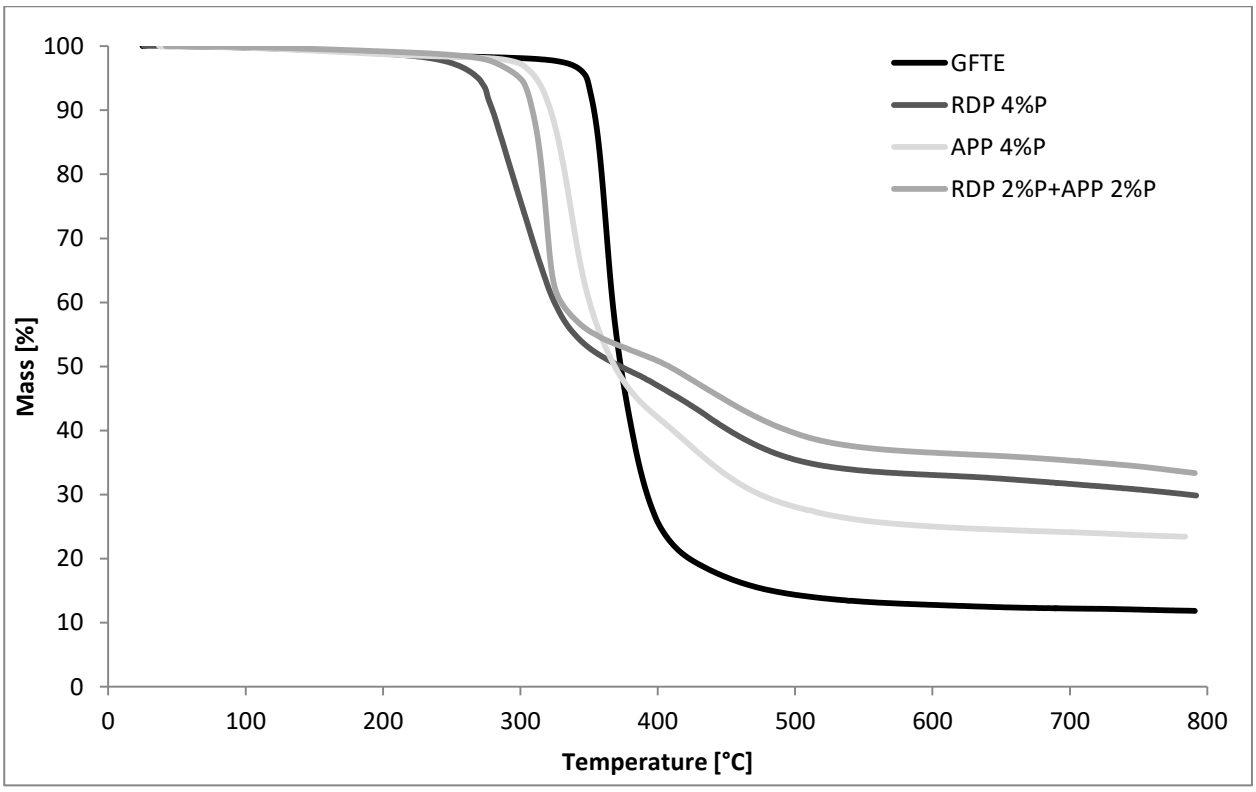

Figure 4.4.7 TGA curves of the reference and flame retarded GFTE samples

According to the TGA results, the beginning of the thermal degradation in the flame retarded samples is shifted to lower temperatures, especially in the case of samples containing RDP, acting mainly in the gas phase during the early stage of the degradation. On the other hand, the degradation of samples containing FRs is less intensive, with much lower mass loss rates and higher char yields. Above 350 °C, the mixed formulation has the best thermal stability along with the highest char yield.

Glass transition temperature and curing

In order to study the effect of the applied FRs on the glass transition temperature (T_g) and curing process, GFTE bioepoxy samples were subjected to DSC analysis, the results can be seen in **Table 4.4.11**.

Table 4.4.11 Effect of the additive flame retardants on the glass transition temperature, reaction enthalpy and temperature belonging to exothermic peak in the case of GFTE samples

sample	glass transition temperature [°C]	reaction enthalpy		temperature of exothermic peak [°C]
		[J/g]	[J/g epoxy]	
GFTE matrix	176	333	333	168
RDP 4%P	86	150	238	179
APP 4%P	175	264	302	167
RDP 2%P+APP 2%P	119	200	267	173

The plasticizing effect is more pronounced in the case of liquid RDP, by adding 4% P the T_g became half of the original value. The T_g of the APP-containing sample practically remained the same, which can be explained by two facts: Due to the higher P-content, less amount of APP is needed to reach the same P-content as in the case of RDP. Furthermore, well-dispersed rigid APP particles can block the segmental movements in the cross-linked epoxy resins and can consequently compensate the T_g decrease initiated by the presence of filler particles [**191**]. The T_g of the combined FR sample was between the values of the single FR formulations. As for the effect on the crosslinking process, the temperatures belonging to the exothermic peak of curing show no significant differences, in the case of RDP-containing samples the curing process is slightly shifted to higher temperatures. Again, due to the high amount needed from RDP to reach 4% P-content, RDP significantly reduces the reaction enthalpy of crosslinking, as expected. In order to have a clear comparison of the effect of APP and RDP on the curing process, reaction enthalpies related to g epoxy resin matrix (disregarding the mass of the added fillers) were compared as well. According to these results, the inclusion of RDP to reach 4% P-content resulted in approx. 30% reduction, while in the case of APP this reduction was only 10%.

4.4.4. Reactive flame retardancy of aromatic epoxy resins with phosphorus-containing epoxy monomer and cyanate ester

DGEBA, as benchmark aromatic epoxy monomer, was pre-reacted with DOPO to form an epoxy functional adduct (DGEBA-DOPO) (see **4.1.2**), and a novolac type CE, PT-30, having high T_g was reactively blended with it. The main advantage of the adduct formation is, that this way the highly intensive reaction between DOPO and PT-30, furthermore, carbamate and consequent CO_2 formation from CE (due to water traces present in DOPO despite careful drying) can be avoided. Due to controlled reaction conditions and stoichiometry, an oxirane functional adduct is formed, which reacts the same way as DGEBA with PT-30 [222]. As the inclusion of FRs usually decreases the T_g of EP systems, the hybrid system consisting of EP, CE and reactive FR would potentially provide higher T_g than in the case of flame retarded EP itself. In addition to the reference CE, EP samples, CE/EP blends containing 20% and 40% PT-30, as well as flame retarded EP and CE/EP blend samples with 2 and 3% P were prepared using the synthesized DGEBA-DOPO adduct. Effect of CE and FR ratio was determined on T_g, thermal stability and flammability [**189**].

Glass transition temperature

The T_g values of the CE and EP references and their blends determined by DSC are displayed in **Table 4.4.12**.

Table 4.4.12 Glass transition temperature values of CE and EP references and their blends determined by DSC method

sample	glass transition temperature [°C]
PT-30	387
DGEBA	149
20% PT-30 - 80% DGEBA	161
40% PT-30 - 60% DGEBA	214
DGEBA – DOPO 2% P	106
20% PT-30 - DGEBA – DOPO 2% P	129
30% PT-30 - DGEBA – DOPO 2% P	150
40% PT-30 - DGEBA – DOPO 2% P	162
20% PT-30 - DGEBA – DOPO 3% P	108
25% PT-30 - DGEBA – DOPO 3% P	113
40% PT-30 - DGEBA – DOPO 3% P	141

As expected, DOPO reduced the initial T_g values: the applied DOPO-DGEBA adduct has high epoxy equivalent and has only one free oxirane ring per molecule, therefore it reduces the crosslinking density of the polymers leading to lower T_g values. By increasing the amount of CE in the blends their T_g increases due to the rigid triazine structure present in CEs, consequently CEs can be used to increase the T_g of EPs and to compensate the T_g decreasing effect of DOPO. It would be desirable that the T_g of the flame retarded systems would approach the T_g of the benchmark systems they would eventually replace, i.e. in this case the T_g of DGEBA (149 °C measured by DSC). To reach this goal in the case of 2% P-containing systems at least 30% PT-30 is necessary, while in the case of 3% P-containing systems 40% PT-30 is necessary.

Thermogravimetric analysis

The effect of CE and FRs on the thermal stability of EP was determined by thermogravimetric analysis (**Table 4.4.13).** TGA curves of the CE and EP references and their2% P-containing blends are displayed in **Figure 4.4.8**.

Table 4.4.13 TGA results of CE and EP references and their blends

sample	$T_{-5\%}$ [°C]	$T_{-50\%}$ [°C]	dTG_{max} [%/°C]	T_{dTGmax} [°C]	char yield at 600 °C [%]
PT-30	415	-	0.64	435	69.6 (68.0 at 900 °C)
DGEBA	302	398	1.57	395	10.6
20% PT-30 - 80% DGEBA	377	426	1.90	422	20.0
40% PT-30 - 60% DGEBA	373	424	1.24	399	30.0
DGEBA – DOPO 2% P	311	387	1.43	383	10.3
20% PT-30 - DGEBA – DOPO 2%P	339	401	1.16	389	24.5
30% PT-30 - DGEBA – DOPO 2%P	346	411	1.12	398	26.2
40% PT-30 - DGEBA – DOPO 2%P	351	426	0.94	396	32.4
20% PT-30 - DGEBA – DOPO 3%P	306	399	0.72	379	26.5
25% PT-30 - DGEBA – DOPO 3%P	320	408	0.68	376	25.3
40% PT-30 - DGEBA – DOPO 3%P	347	443	0.68	384	35.4

$T_{-5\%}$: temperature at 5% mass loss $T_{-50\%}$: temperature at 50% mass loss; dTG_{max}: maximum mass loss rate; T_{dTGmax}: the temperature belonging to maximum mass loss rate

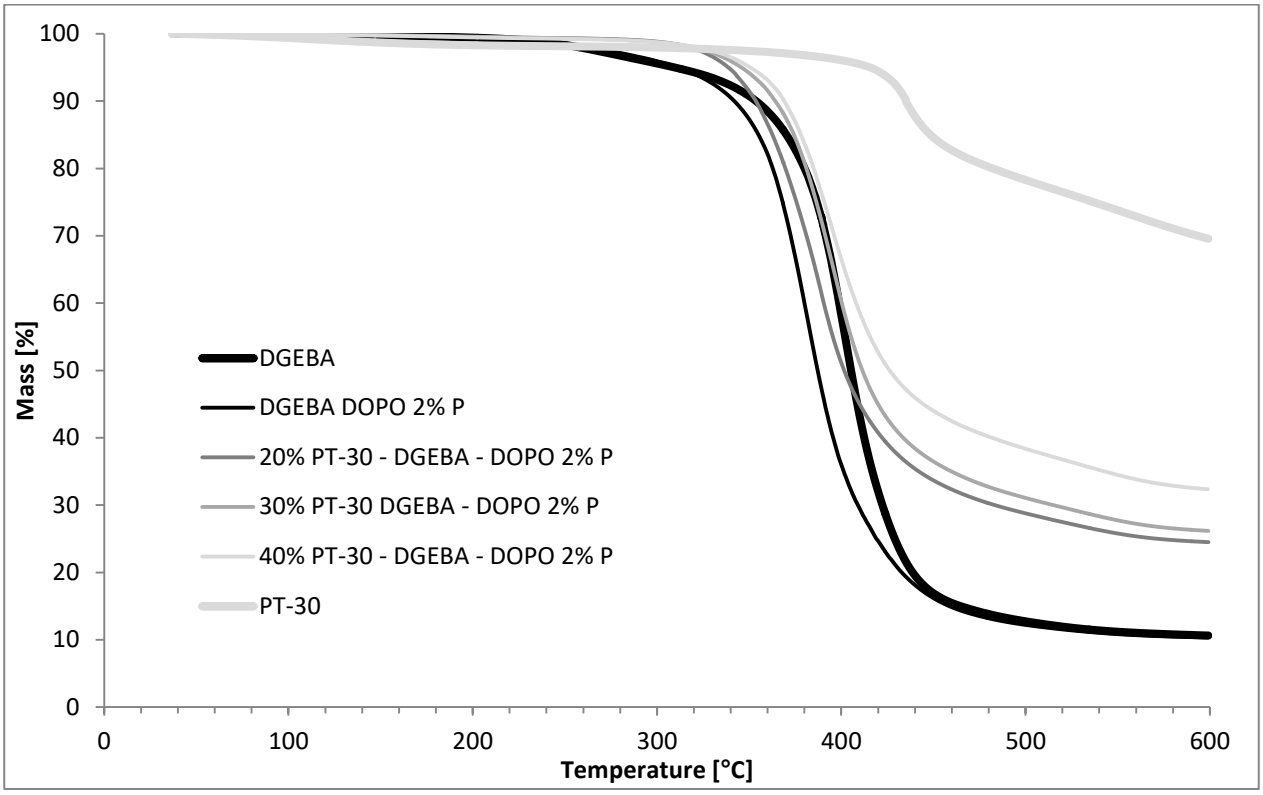

Figure 4.4.8 TGA curves of the CE and EP references and their 2% P-containing blends

The thermal stability of the CE reference is outstanding: its thermal degradation begins above 400 °C, with a moderate mass loss rate, and it loses only 30% of its mass by reaching 600 °C. By adding PT-30 to DGEBA the temperature belonging to 5% mass loss increases by 75 °C and the char yield increases from 10% up to 30% due to the rigid triazine structure in CE. On the other hand by increasing the amount of DOPO, the thermal degradation begins earlier and the maximum of mass loss rate was reached at lower temperatures, which can be explained by the gas phase FR mechanism of DOPO [110, 223]: during the initial phase of degradation P-containing radicals are

formed, which effectively delay the degradation process. DOPO decreases the mass loss rates as well, in 3% P-containing samples the mass loss rate is approx. the same as in the case of reference CE.

Flame retardancy

Limiting oxygen index (LOI), UL-94 and mass loss calorimetry results of the CE and EP references and their blends are summarized in **Table 4.4.14**. By adding PT-30 to DGEBA, its LOI value was increased from 23 up to 33 V/V%, however the UL-94 rate remained HB, as in the case of the reference PT-30 and DGEBA. By adding DOPO to DGEBA the UL-94 rate was ameliorated to V-1, however the LOI value was lower than in the case of PT-30 (28 vs. 30 V/V%). All blends consisting of EP, CE and P-containing FR reached the V-0 UL-94 classification, and their LOI values usually improved with increasing CE and FR content, reaching even LOI of 45 V/V% with 40% CE and 2% P. P-containing samples exhibited intensive intumescent charring.

As for the heat release rates (HRRs), by adding PT-30 to DGEBA the HRR curves were shifted in time by 10 s and the peak of heat release rate (pHRR) was lowered from 743 up to 238 kw/m^2 with 40% PT-30.

Table 4.4.14 LOI, UL-94 and mass loss calorimetry results of the CE and EP references and their blends

sample	LOI [V/V%]	UL-94*	TTI [s]	pHRR [kW/m^2]	time of pHRR [s]	FIGRA [kW/m^{2}s]	burning time [s]	THR [MJ/m^2]	EHC [MJ/kg]	MARHE [kW/m^2]	residue [%]
PT-30	30	HB	26	156	44	3.5	180	15.5	11.9	91.7	48
DGEBA	23	HB (17.1±2)	40	743	129	6.6	217	91.0	19.4	364.3	0
20% PT-30 - 80% DGEBA	33	HB	50	471	113	4.2	176	59.5	18.5	223.9	0
40% PT-30 - 60% DGEBA	28	HB	50	238	167	1.4	345	55.1	13.2	160.5	14
DGEBA – DOPO 2%P	29	V-1	32	477	134	3.6	226	65.1	13.5	252.6	0
20% PT-30 - DGEBA – DOPO 2% P	42	V-0	42	261	177	1.5	279	49.0	12.3	161.8	15
30% PT-30 - DGEBA – DOPO 2% P	40	V-0	50	207	207	1.0	309	42.0	11.4	130.8	18
40% PT-30 - DGEBA – DOPO 2% P	43	V-0	53	195	168	1.2	301	36.3	11.6	116.2	23
20% PT-30 - DGEBA – DOPO 3% P	40	V-0	27	218	156	1.4	380	50.3	11.8	150.5	14
25% PT-30 - DGEBA – DOPO 3% P	42	V-0	45	218	155	1.4	375	46.0	12.1	134.6	17
40% PT-30 - DGEBA – DOPO 3% P	45	V-0	44	234	179	1.3	315	47.5	13.3	142.9	22

* in parenthesis the horizontal burning rate is showed, where measurable

LOI: limiting oxygen index, TTI: time to ignition, pHRR: peak of heat release rate, FIGRA: fire growth rate, THR: total heat release, EHC: average effective heat of combustion, MARHE: maximum of average rate of heat emission

By adding DOPO to CE/EP blends, the pHRR and total heat release (THR) values decreased further. By comparing the heat release of the DGEBA reference and 2% P-containing samples (**Figure 4.4.9**), it can be concluded that by increasing the amount of PT-30, the pHRR and THR values decreased significantly. By increasing the P-content to 3% no further decrease was experienced,

which can be explained by the lower crosslinking density. The pHRR of the DOPO-containing CE/EP blends was in the range of 195-261 kW/m^2, not much higher than the pHRR value of 156 kW/m^2 of the CE reference. The time to ignition (TTI) and time of pHRR values significantly increased in DOPO-containing CE/EP blends (up to TTI of 53 s and time of pHRR of 207 in comparison to 26 s and 44 s, respectively, in case of CE reference). As for the fire growth rate (FIGRA) values, by blending 40% PT-30 to DGEBA FIGRA decreased to 1.4 kW/m^{2}s compared to 3.5 kW/m^{2}s in the case of PT-30 and 6.6 kW/m^{2}s in DGEBA. By adding DOPO adduct to this composition, FIGRA decreased further slightly. Effective heat of combustion (EHC) and maximum of average rate of heat emission (MARHE) values were the closest to the values of PT-30 in the case of 40% PT-30 - DGEBA – DOPO 2% P sample. Compared to the DGEBA DOPO 2%P sample the inclusion of 40% PT-30 significantly reduced the EHC and MARHE values.

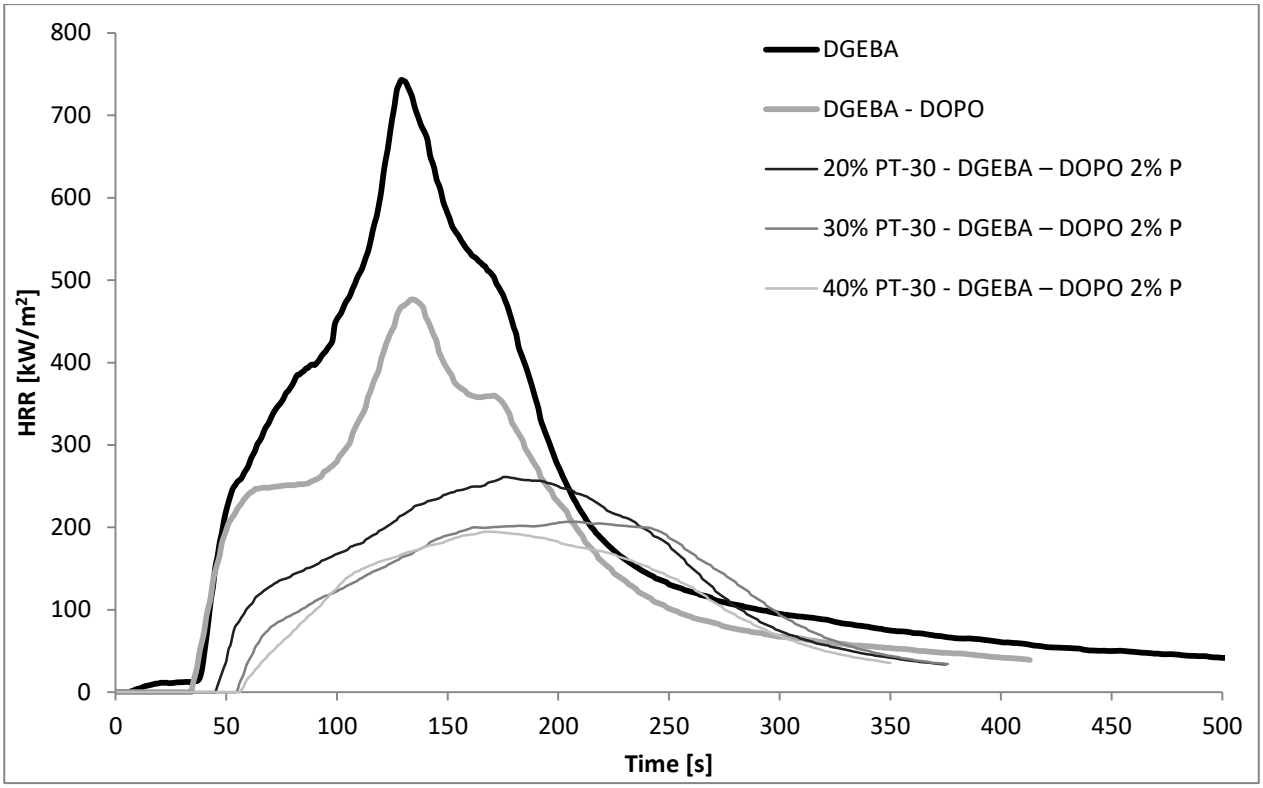

Figure 4.4.9 HRR curves of EP reference, flame retarded EP and CE/EP blends with 2% P-content

The inclusion of PT-30 and DOPO also increased the residual mass after cone calorimetry. The CE/EP blends exhibited slight charring, while the char thickness of the flame retarded CE/EP samples manifested a 10-fold increase due to the intumescent charring phenomena.

Storage modulus

Based on the flame retardancy results, the best performing samples (CE/EP blend containing 20% and 40% PT-30, flame retarded CE/EP blend containing 40% PT-30 and 2 or 3% P) along with CE

and EP references were subjected to dynamic mechanical analysis (DMA). The storage modulus curves of the CE and EP references and CE/EP blends are displayed in **Figure 4.4.10**, T_g determined from tan δ peaks and the storage modulus values at 25 and 75 °C are shown in **Table 4.4.15**.

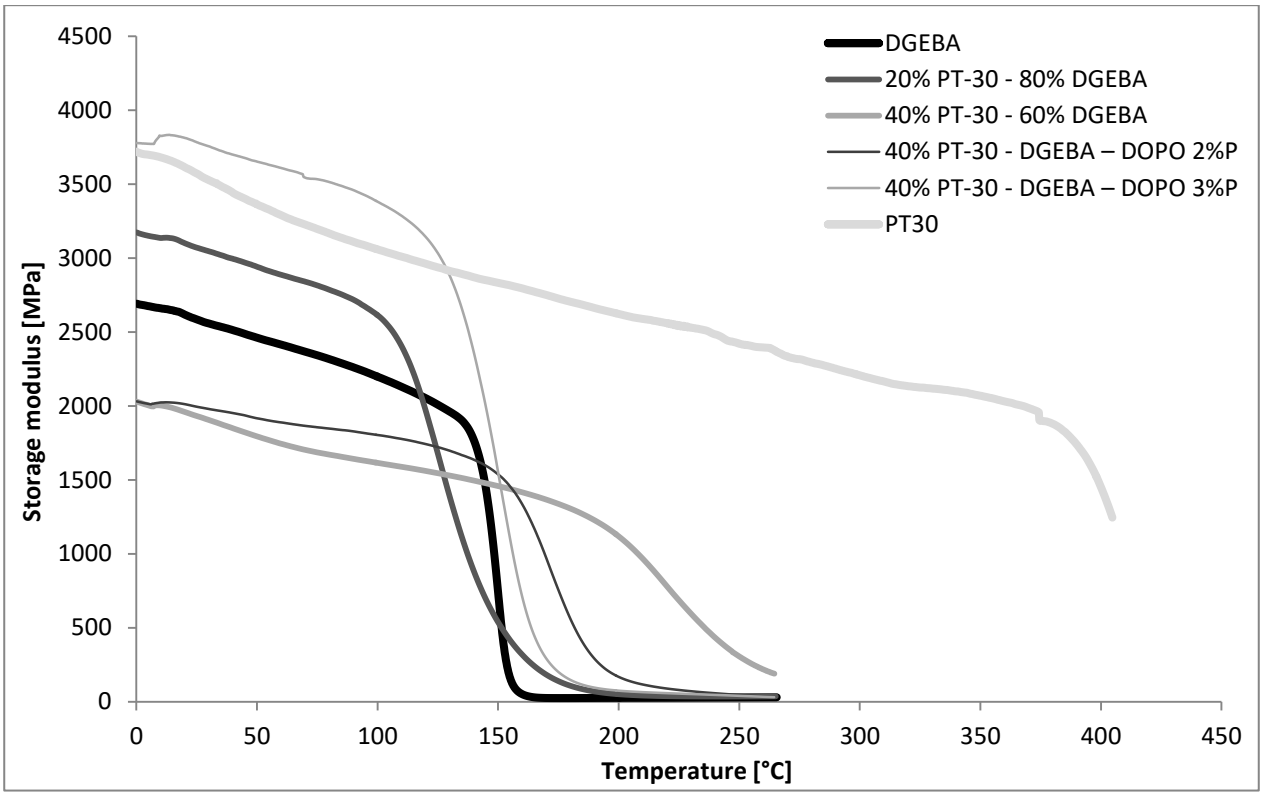

Figure 4.4.10 Storage modulus of the CE and EP references and CE/EP blends in the temperature range of 25-260 °C (in case of pure CE 25-400 °C)

Table 4.4.15 Glass transition temperature (T_g) and storage modulus values at 25 °C and 75 °C of CE/EP matrices determined by DMA

sample	glass transition temperature [°C]	storage modulus at 25 °C [MPa]	storage modulus at 75 °C [MPa]
PT-30	401	3572	3196
DGEBA	155	2585	2343
20% PT-30 - 80% DGEBA	172	3071	2815
40% PT-30 - 60% DGEBA	247	1932	1686
40% PT-30 - DGEBA – DOPO 2% P	188	1995	1856
40% PT-30 - DGEBA – DOPO 3% P	165	3784	3534

By increasing the temperature the storage moduli showed a decreasing tendency. As for the CE/EP blends, the 20% PT-30 - 80% DGEBA had higher storage modulus up to 115 °C, while the 40% PT-30 - 60% DGEBA showed better properties than DGEBA only above 140 °C, similarly to its flame retarded version with 2%P. However, the 40% PT-30 - DGEBA – DOPO 3%P matrix performed better than DGEBA in the whole temperature range, and had even higher storage modulus than CE

up to 125 °C, which may be explained by the relative stoichiometric excess of PT-30 (related to the amount of oxirane groups present in DGEBA and DOPO-DGEBA components in the sample).

As for the glass transition temperatures, the T_g of the blends increased with increasing amount of CE. Compared to 40% PT-30 - 60% DGEBA sample, the inclusion of FRs decreased the T_g, most probably due to lower crosslinking density , however it was still above the T_g of DGEBA.

4.4.5. Reactive flame retardancy of aliphatic and aromatic epoxy resins with phosphorus-containing crosslinking agent

As the synthesized TEDAP can act both as crosslinking agent and FR, reactively flame retarded aromatic DGEBA-based and aliphatic PER-based epoxy resins were prepared by substituting the original amine curing agents (TETA and T58) by TEDAP. In aromatic flame retarded samples 40% of DGEBA epoxy monomer was substituted by aliphatic PER reactive dilutant in order to reduce the viscosity of the system and to increase the compatibility of the aromatic component to TEDAP. The effect of TEDAP on the flammability and mechanical characteristics is summarized shortly below (for more detailed discussion see [**224**]).

Flame retardancy

Comparing the flame retardancy of the matrices in **Table 4.4.16**, one can conclude that the PER exhibits lower initial LOI value than DGEBA; however, the use of reactive FR results in higher LOI in the aliphatic system compared to the aromatic one. Due to TEDAP, time to ignition (TTI) increased by 53 s in the case of PER and by 36 s in DGEBA, the peak of heat release rate (pHRR) decreased by 70% and 84%, respectively (**Figure 4.4.11**), while the total heat release (THR) decreased by 71% and 54%, respectively. TEDAP increased the residual mass significantly, from practically no residue in case aliphatic PER to 36%, while in aromatic DGEBA to 25%.

Table 4.4.16 LOI, UL-94 and mass loss calorimetry results of PER, DGEBA reference and flame retarded epoxy resin matrices

sample	LOI [V/V%]	UL-94	TTI [s]	pHRR [kW/m^2]	time of pHRR [s]	THR [MJ/m^2]	burning time [s]	residue [%]
PER	21	HB	37	962	95	89.7	331	0
DGEBA	26	HB	32	1022	115	103.6	322	1
PER TEDAP	33	V-0	90	287	143	26.0	379	37
DGEBA TEDAP	31	V-0	68	166	125	48.1	484	25

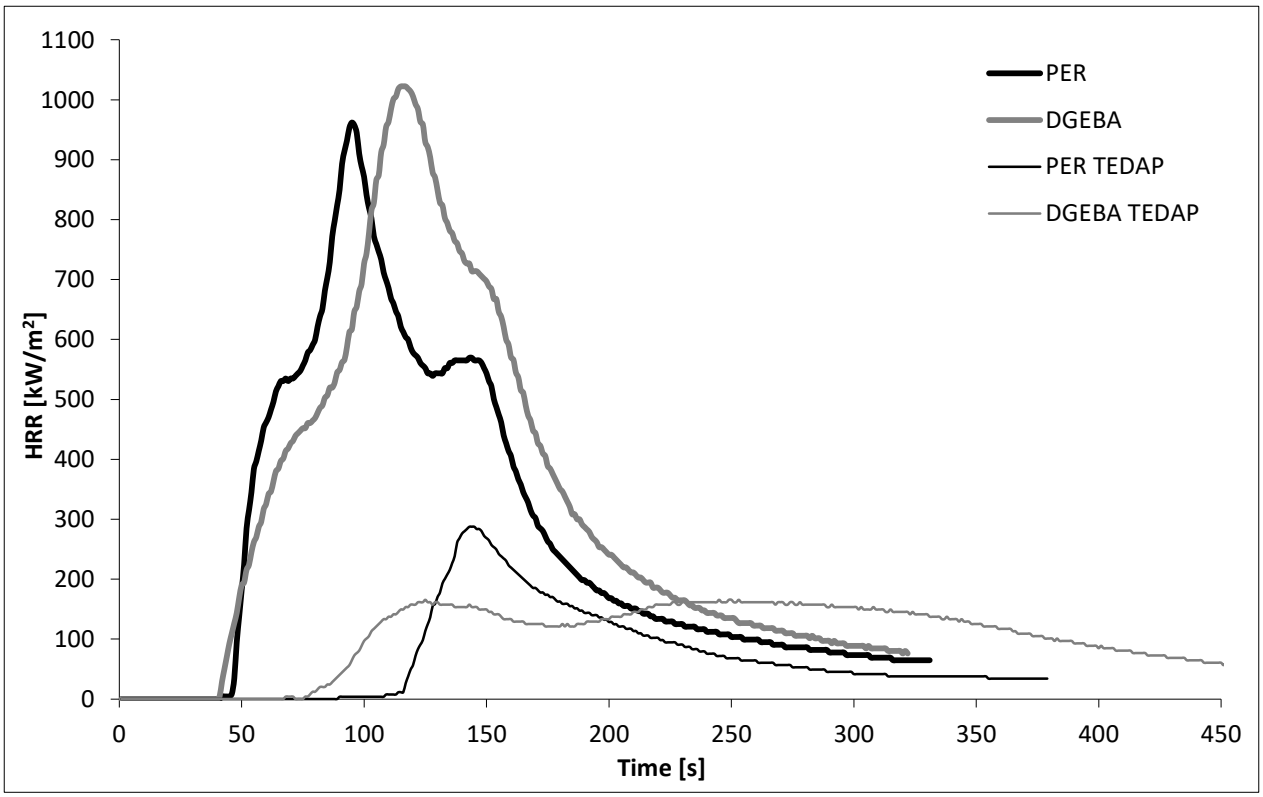

Figure 4.4.11 HRR curves of PER, DGEBA reference and flame retarded epoxy resin matrices

Mechanical characterisation

According to the tensile test results, both the tensile strength and the modulus values are higher in the case of aromatic epoxy resins. The inclusion of FR resulted in slight decrease both in aliphatic and aromatic matrices (**Table 4.4.17**).

Table 4.4.17 Tensile strength and modulus of reference and flame retarded epoxy resin matrices

sample	tensile strength [MPa]	tensile modulus [GPa]
PER	30.34±0.81	2.07±0.15
DGEBA	52.87±2.56	2.56±0.07
PER TEDAP	22.58±2.39	1.75±0.20
DGEBA TEDAP	46.10±1.24	2.36±0.15

4.4.6. Summary on flame retardancy of epoxy resins

P-based additive and reactive FRs were investigated in an **aliphatic, pentaerythritol-based model epoxy resin system (PER)**. The additive APP and the reactive TEDAP decreased the flammability of the resin: To reach V-0 rating, 5% of P (15% APP) was needed in the case of the additive FR, while with the application of TEDAP, 3% of P was enough for the same result. The **effectiveness of the reactive TEDAP, acting both in gas and solid phase,** was even more evident in the case of the cone calorimeter tests: the pHRR decreased by 85%, while the amount of the residual char was 40%. The application of reactive DOPO did not efficiently decrease the flammability of this system because of the molecular incompatibility of the condensed aromatic structured DOPO with the

aliphatic epoxy monomer. These findings emphasized the **significance of compatibility** in the flame retardancy process and the need **for tailoring the structure of the FRs to the polymer matrix** to be protected.

Systematic study was carried out on the flame retardancy mechanism of **combinations of solid and gas phase FRs** in commercially available **sorbitol polyglycidyl ether (SPE) bioepoxy resin** using resorcinol bis(diphenyl phosphate) (RDP) acting mainly in gas phase as radical scavenger and ammonium polyphosphate (APP) acting as intumescent FR in solid phase, and their combinations. **Synergistic effect** was found between the inorganic APP and the organophosphorus RDP, when applied in combination: Formulations applying RDP or APP alone showed increased limiting oxygen index (LOI) values, however, their UL-94 ratings remained HB. When the same amount of P originated from the two additives, V-0, self-extinguishing rating and LOI value of 34 V/V% was reached. By the combined approach the heat release rate of SPE could be lowered by approx. 60%. The assumed **balanced solid- and gas phase mechanism** was **confirmed** by thermogravimetric analysis, Fourier transform infrared spectrometry (FTIR) analysis of the gases formed during laser pyrolysis, attenuated total reflection-infrared spectrometry (ATR-IR) analysis of the charred residues, as well as by mechanical testing of the char obtained after combustion. In samples containing both RDP and APP the thermal degradation started at lower temperature when the amount of RDP was increased and the temperature belonging to 50% mass loss decreased. By increasing the amount of APP the maximum mass loss rate decreased and the char yield increased. The different phase mechanism of the two FRs could by clearly identified from the TGA results. LP-FTIR measurements indicated no gas phase effect in the case of sample containing only APP, while increasing the RDP content lead to increased amount of P species among the gas phase degradation products.

Fire retardancy of the synthesized novel **glucofuranoside based trifunctional bioepoxy monomer (GFTE)** was examined using the same additive FRs (RDP and APP) and their combination, as in the case of SPE. According to the flame retardancy results of the GFTE matrices, the **combined solid and gas phase FR action proved to be more favourable** than the sole solid phase action of APP in this bioepoxy: from the formulations reaching V-0 UL-94 rate (RDP 2%P+APP 2%P and APP 4%P), the mixed formulation had 3 V/V% higher LOI. The HB rated RDP 4%P sample had the lowest heat release rate, followed by the mixed formulation, while APP 4% P had the most modest FR performance, suggesting that the **solid phase action alone is not enough in this bioepoxy resin** to achieve effective flame retardancy. In terms of heat release rate, the mixed formulation showed slightly lower performance than the APP 4% sample, but as it has a V-0 UL-94 rating, compared to the HB rating of APP 4%P sample, the overall fire retardancy performance of the combined

formulation is better. RDP significantly reduced the reaction enthalpy of crosslinking and the T_g of the bioepoxy matrix. Addition of APP compensated the plasticizing effect of RDP, as well-dispersed rigid APP particles can block the segmental movements in the cross-linked epoxy resins, and resulted in **increased glass transition temperature and storage modulus values in mixed FR formulation**.

In order to compensate the T_g decreasing effect of DOPO in DGEBA epoxy monomer, a **hybrid system consisting of DGEBA, novolac type CE (PT-30) and reactive DGEBA-DOPO FR** was prepared and their T_g, thermal degradation and fire behaviour were tested. In order **to reach the T_g of the benchmark DGEBA** in hybrid systems at least 30% PT-30 is necessary at 2% P-content, while at 3% P-content 40% PT-30 is required. TGA measurements showed that the rigid structure of the **CE increased the thermal stability** of the CE/EP blends. By increasing the amount of DOPO, the thermal degradation begins earlier, due to the gas phase FR mechanism during the initial phase of degradation, but it effectively delays the degradation process, leading to lower mass loss rates as well. Addition of PT-30 to DGEBA **increased the LOI** value from 23 up to 33 V/V%, however it was not sufficient to improve the UL-94 rate, which remained HB, as in the case of CE and DGEBA reference samples. **All blends consisting of EP, CE and P-containing FR reached the V-0 UL-94 classification**, and their LOI values usually improved with increasing CE and FR content, reaching even LOI of 45 V/V%. P-containing samples exhibited **intensive intumescent charring** and increased residual mass. By adding PT-30 to DGEBA the **pHRR values were lowered** from 743 up to 238 kw/m^2 with 40% PT-30, which was further decreased to 195 kW/m^2 with 2% P from DOPO.

Finally, the effect of **P-containing, reactive FR, TEDAP** on the FR and mechanical performance **aromatic DGEBA-based and aliphatic PER-based epoxy resin** was compared. **Outstanding flame retardancy** results were achieved in both systems, accompanied by slight decrease in tensile strength and modulus.

4.5. Flame retardancy of epoxy resin composites

In this chapter the results on the flame retardancy of epoxy resin composites applying P-containing additive and reactive type FRs are summarized.

First, as an example for the additive approach, the flame retardancy of **carbon fibre reinforced** commercially available **sorbitol polyglycidyl ether (SPE)** and newly synthesized **glucofuranoside based trifunctional epoxy monomer (GFTE)** bioepoxy resin was investigated **using ammonium polyphosphate (APP)**, acting in the solid phase and **resorcinol bis(diphenyl phosphate) (RDP)**

acting mainly in the gas phase through flame inhibition, and **their combination**, which proved be synergistic in terms of fire retardancy in SPE polymer matrix (see **4.4.2**).

As an example for the reactive approach, **hybrid carbon fibre reinforced composite** system consisting of **diglycidyl ether of bisphenol A (DGEBA), novolac type cyanate ester (CE)** and **reactive DGEBA-DOPO FR** was prepared with the intention to compensate the plasticizing effect of FR in composites. To the extent of our knowledge, the **influence of P FRs on T_g and the mechanical properties** in hybrid CE/EP fibre reinforced composites were not yet examined, therefore our work aimed at filling in this gap.

Finally, the flame retardant effect of the synthesized **P-containing, reactive FR, TEDAP** was compared in **aromatic DGEBA-based and aliphatic PER-based epoxy resin composite reinforced with carbon fibres.** In order to combine the enhanced mechanical properties of fibre reinforced composites and the excellent FR properties of intumescent systems, and moreover to eliminate the negative effect of the fibres on the intumescence and of FR on the interlaminar adhesion, **multilayer carbon fibre reinforced composites with intumescent epoxy resin coating** were developed and investigated as well.

4.5.1. Flame retardancy of carbon fibre reinforced composites

Carbon fibre can be considered as a benchmark reinforcement in many structural composite applications, where its relatively higher price is balanced by technical advantages offered as high strength along with low density, durability, low moisture uptake, corrosion- and chemical resistance. Due to its high thermal stability it can be considered as non-flammable material, which usually reduces the flammability of the incorporating matrix in polymer composites. Despite the increased inert inorganic ratio, the organic polymer matrix will still require flame retardancy to meet the relevant standards of more demanding industrial sectors. Flame retardancy of polymers in the presence of carbon fibres however raises several issues to be addressed:

- Due to the high thermal conductivity of carbon fibres the ignition of the composites is facilitated (this phenomenon is known as candlewick effect).
- The sizing of the commercial carbon fibres is adapted to the polymer matrix, thus the use of FRs more polar than the polymer matrix to be flame retarded leads to decreased fibre-matrix adhesion, and consequent poorer mechanical properties. As FRs usually have a plasticizing effect, finding a balance between FR performance, T_g and mechanical properties means a real challenge.
- Last but not least, the incorporated carbon fibres interfere in the mode of action of solid phase FRs, which has to be addressed as well.

In the followings some possible solutions to these issues are presented.

4.5.1.1. *Flame retardancy of aliphatic sugar based carbon fibre reinforced composites with combination of phosphorus-containing additives*

Flame retardancy of carbon fibre reinforced sorbitol polyglycidyl ether (SPE) - cycloaliphatic amine (T58) composites was investigated applying ammonium polyphosphate (APP), acting in the solid phase, resorcinol bis(diphenyl phosphate) (RDP) acting primarily in the gas phase, and their combination, which proved be synergistic in terms of fire retardancy in SPE polymer matrix (see **4.4.2**). The fire retardant action of the additive FRs and their synergistic combinations was investigated in composites by limiting oxygen index (LOI), UL-94 tests and mass loss calorimetry. The effect of FRs on the T_g, storage modulus was evaluated by DMA test, while the fibre-matrix adhesion was investigated by interlaminar shear strength measurements [**225**].

Flame retardancy

The LOI and UL-94 results of the flame retarded composites can be seen in **Table 4.5.1.**

Table 4.5.1 LOI and UL-94 results of the flame retarded SPE composites

composite	**LOI [V/V%]**	**UL-94**
SPE composite	24	HB
RDP 1%P	26	HB
RDP 2%P	26	HB
RDP 3%P	27	V-1
APP 1%P	25	HB
APP 2%P	28	HB
APP 3%P	31	HB
RDP 1%P+APP 2%P	30	HB
RDP 1.5%P+APP 1.5%P	31	HB
RDP 2%P+APP 1%P	32	V-1

From the two FRs, the APP seemed to be more advantageous in terms of LOI: by adding 3% P from APP LOI of 31 V/V% was reached, while with the same P-content the RDP resulted only LOI of 27 V/V%. This may be explained by the different P-content of the additives: due to the relatively low P-content of RDP, higher amount is necessary to reach the same P-content, as in case of APP. The plasticizing effect of high amounts of RDP leads to lower LOI values. On the other hand, the UL-94 rate ameliorated only in 3%P RDP system among the composites flame retarded only with APP or RDP. According to this, at ambient oxygen concentrations the gas phase effect of RDP was indispensable to reduce the ignitability of the composite. As for the combined formulations containing both APP and RDP to reach 3% P-content, similar synergistic effects could be identified as in SPE bioepoxy matrix (see **4.4.2**). The balanced solid and gas phase FR mechanism lead to LOI of 32 V/V% and V-1 UL-94 rate in case of RDP 2%P+APP 1%P sample. In contrast to the combined

matrix formulations the self-extinguishing, V-0 UL-94 was not reached in composite specimens, most probably due to the so called candlewick effect of the introduced reinforcement fibres [**226**]. The heat release rate curves of samples containing 3% P (including the mixed formulations) obtained from mass loss calorimetry tests can be seen in **Figure 4.5.1**, while numerical data for all composites are summarized in **Table 4.5.2**, the best performances among the samples are highlighted with bold letters.

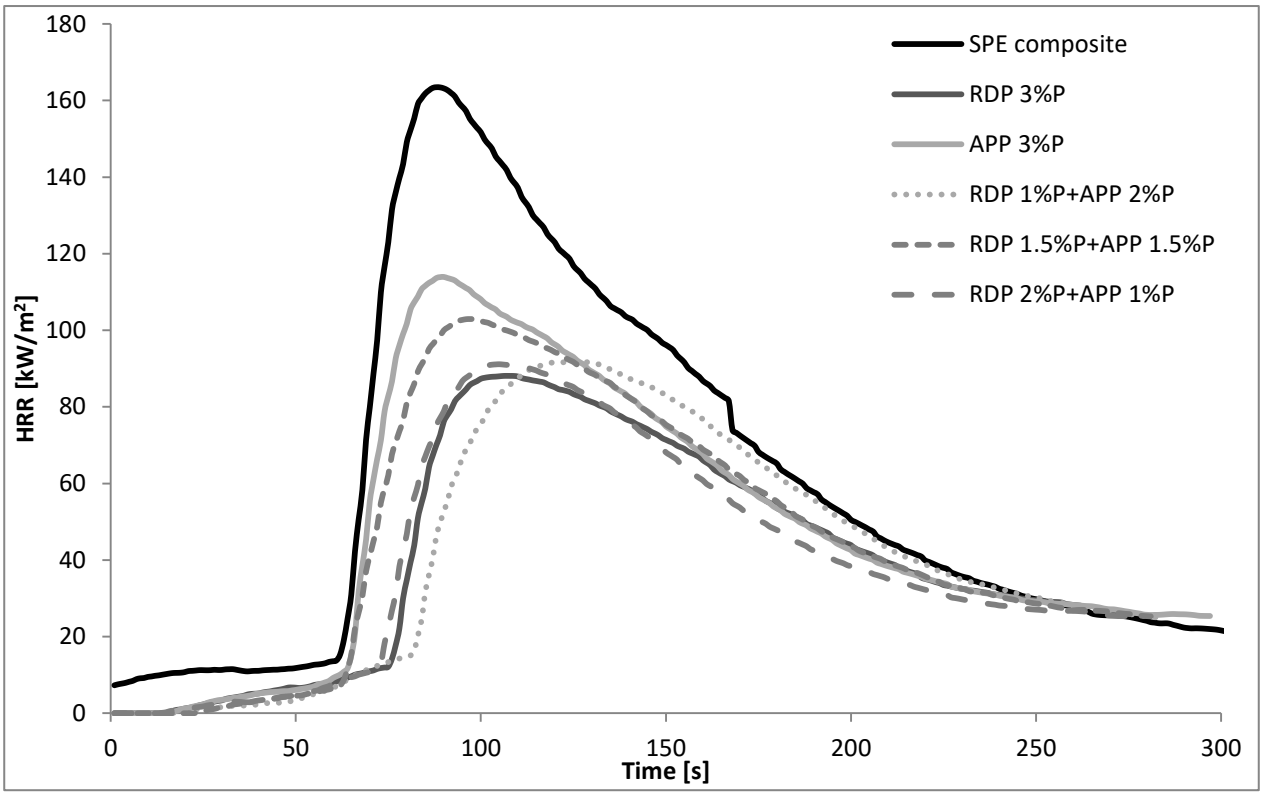

Figure 4.5.1 Heat release rate of reference and flame retarded SPE composites with 3% P

Table 4.5.2 Mass loss calorimetry results of reference and flame retarded SPE composites

composite	TTI [s]	pHRR [kW/m^2]	time of pHRR [s]	FIGRA [kW/m^{2}s]	burning time [s]	THR [MJ/m^2]	EHC [MJ/kg]	MARHE [kW/m^2]	residue [%]
SPE composite	61	163	88	1.9	163	16.9	16.4	77.4	60
RDP 1%P	57	127	72	1.8	137	14.4	15.7	66.3	63
RDP 2%P	66	100	91	1.1	149	11.9	13.2	51.4	65
RDP 3%P	77	**88**	107	**0.8**	136	10.6	12.3	44.3	67
APP 1%P	61	130	86	1.5	130	13.4	14.4	60.3	65
APP 2%P	58	124	81	1.5	**114**	13.3	14.1	61.7	64
APP 3%P	72	114	90	1.3	132	12.7	13.5	55.7	65
RDP 1%P+APP 2%P	**84**	92	**122**	**0.8**	127	10.9	**11.0**	45.2	63
RDP 1.5%P+APP 1.5%P	64	103	97	1.1	142	12.1	13.3	52.3	65
RDP 2%P+APP 1%P	72	91	105	0.9	150	**10.3**	12.2	**44.1**	**68**

(TTI: time to ignition, pHRR: peak of heat release rate, FIGRA: fire growth rate, THR: total heat release, EHC: average effective heat of combustion, MARHE: maximum of average rate of heat emission)

In the case of samples flame retarded by RDP, by increasing the amount of RDP, the pHRR gradually decreased, at 3% P-content from 163 to 88 kW/m^2. At 1% P-content, the sample ignited

earlier, but at higher concentrations the FR effect prevailed over the reduced thermal stability at early stage of degradation (see **Figure 4.4.3**), and the TTI increased (at 3% P-content by 16 s). In APP-containing samples the best results were also achieved at 3%P, but the decrease of flammability was less significant than in the case of RDP. According to the literature APP has pure solid phase mechanism, while RDP has some minor solid phase effect besides the main gas phase one, consequently by adding a FR acting in the other phase, major improvements were expected in the case of APP. All mixed formulations showed better performance than 3%P APP: by changing the origin of 1% P from APP to RDP, the TTI increased by 12 s, pHRR and EHC decreased by approx. 20% and FIGRA by approx. 40%. Comparing the combined formulations to the RDP 3% sample, only slight improvements could be achieved e.g. in RDP 2%P+APP 1%P THR, EHC and MARHE were slightly reduced. Regarding the overall fire retardancy performance of the composites, the combined RDP 2%P+APP 1%P formulations can be considered as an optimum.

Glass transition temperature and storage modulus of composites

The tan δ curves as a function of temperature are displayed in **Figure 4.5.2**, storage modulus curves of reference and flame retarded SPE composites are shown in **Figure 4.5.3**, while numerical results of dynamical mechanical analysis (T_g, storage modulus at 25 °C and 75 °C) of composites are shown in **Table 4.5.3**.

Similarly to SPE matrices (see **4.4.2**), the low P-containing RDP has a significant plasticizing effect in SPE composites as well: by increasing the amount of RDP, the T_g is gradually decreasing. At 3%P from RDP the decrease in T_g is 28 °C. In contrast to RDP, the T_g of the composites even increased by adding APP. This can be explained by the higher P-content of APP (meaning that less amount is needed to reach the same P-content than in case of RDP), and by well-dispersed rigid APP particles, which can block the segmental movements in the cross-linked epoxy resins matrix and can compensate the decrease in T_g [**191**]. In mixed FR formulations the T_g decrease caused by RDP was partially compensated by APP.

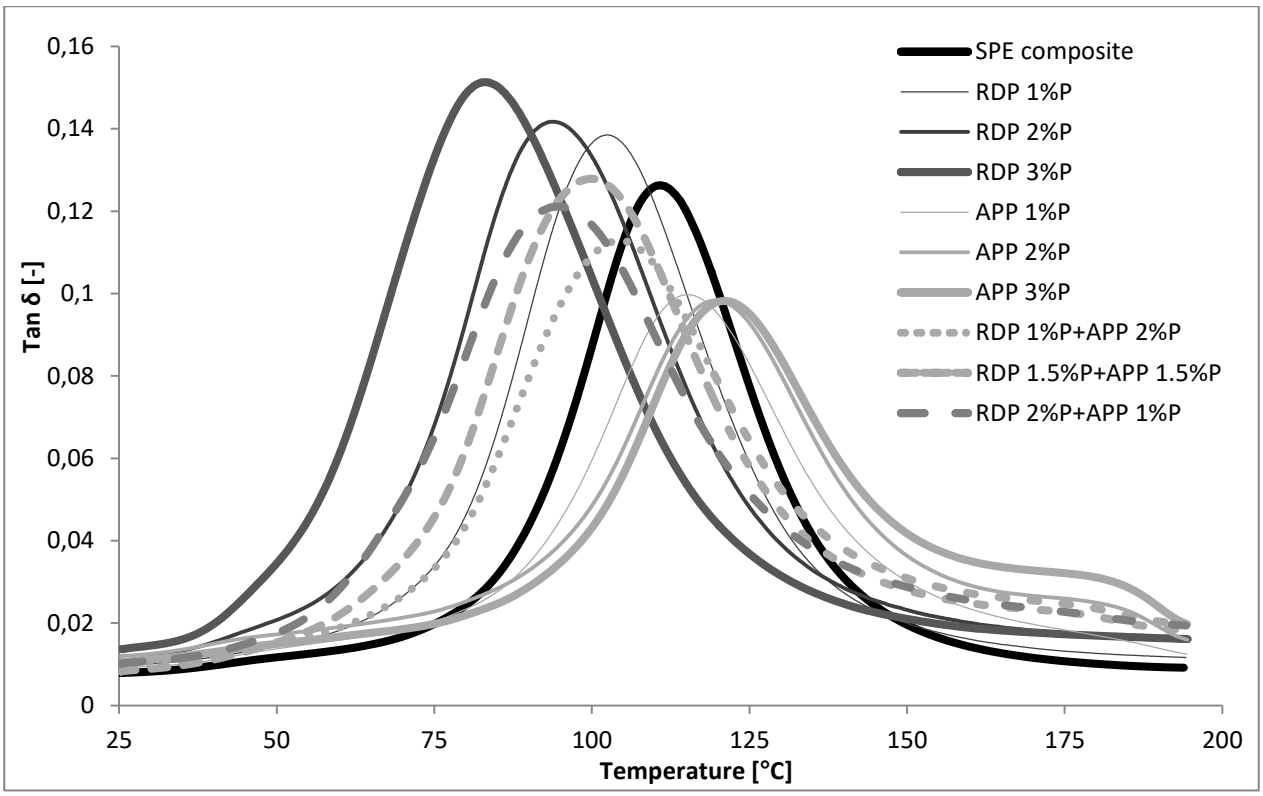

Figure 4.5.2 Tan δ curves of reference and flame retarded SPE composites

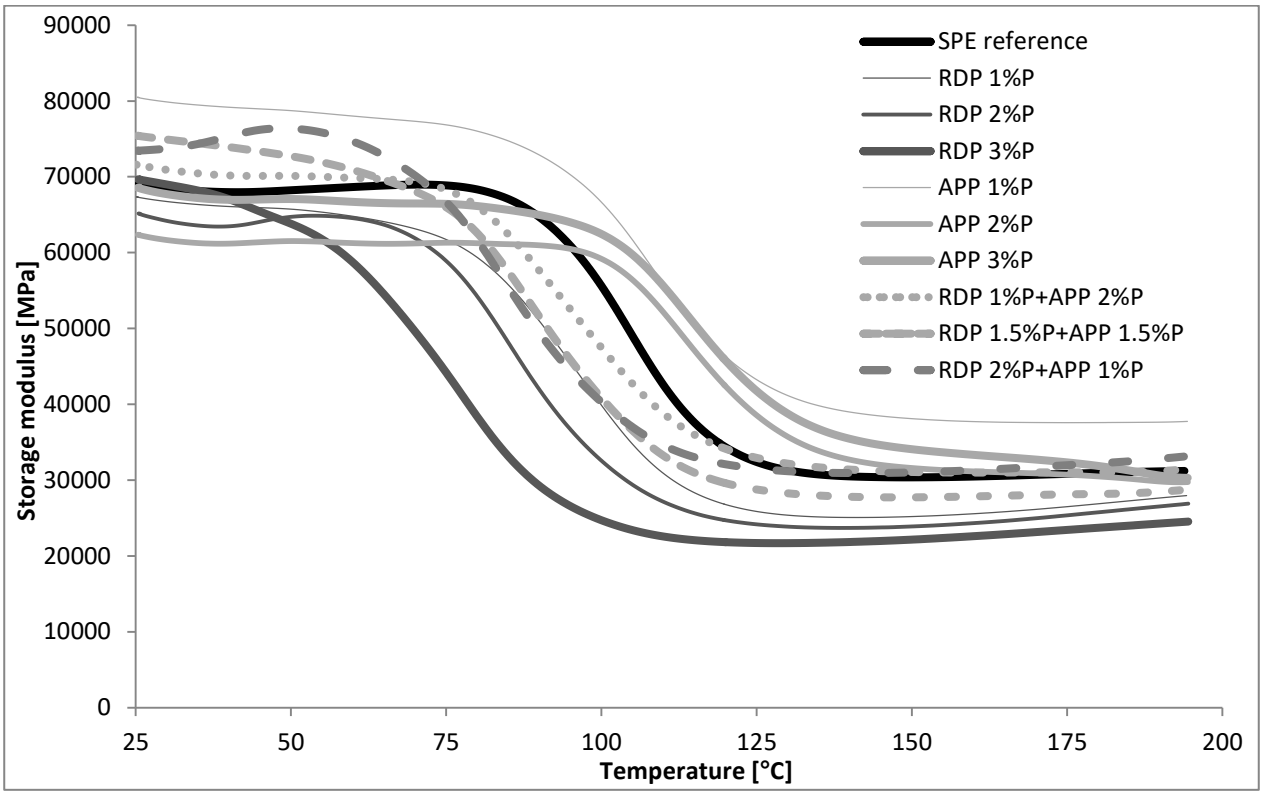

Figure 4.5.3 Storage modulus curves of reference and flame retarded SPE composites

Table 4.5.3 Glass transition temperature and storage modulus values of reference and flame retarded SPE composites

composite	glass transition temperature [°C]	storage modulus at 25 °C [MPa]	storage modulus at 75 °C [MPa]
SPE composite	111	68792	68863
RDP 1%P	102	67328	61755
RDP 2%P	94	65043	58929
RDP 3%P	83	69602	44233
APP 1%P	115	80328	76854
APP 2%P	120	62182	61307
APP 3%P	121	68404	66429
RDP 1%P+APP 2%P	104	71537	68330
RDP 1.5%P+APP 1.5%P	100	75344	65960
RDP 2%P+APP 1%P	95	73479	66697

By increasing the amount of RDP in SPE composites, the storage modulus decreases in the whole temperature region of the measurement, which can be explained by the significant plasticizing effect of RDP. Up to approx. 70 °C, the storage modulus of APP 1%P and of all combined formulations is higher than that of SPE reference, which may be interpreted with the well-dispersed rigid APP-particles, which compensated the plasticizing effect of the RDP.

Mechanical properties

Tensile, flexural, interlaminar shear and Charpy impact properties of the reference and flame retarded SPE composites are displayed in **Table 4.5.4**.

Table 4.5.4 Mechanical properties of the reference and flame retarded SPE composites

composite	tensile strength [MPa]	flexural strength [MPa]	interlaminar shear strength [MPa]	Charpy impact energy [kJ/m^2]
SPE composite	916.24±18.66	996.89±64.35	41.14±1.90	85.52±6.62
RDP 1%P	818.82±56.46	867.74±62.20	44.31±1.27	88.68±6.86
RDP 2%P	826.38±49.81	900.36±64.95	47.53±0.73	90.50±19.31
RDP 3%P	851.24±29.67	919.52±138.36	41.30±0.96	92.98±6.93
APP 1%P	795.59±123.04	895.03±41.31	42.66±1.49	75.13±8.95
APP 2%P	842.07±49.87	948.41±43.42	40.99±1.37	79.76±9.43
APP 3%P	914.33±76.64	927.40±74.43	42.71±1.21	102.17±33.61
RDP 1%P+APP 2%P	1024.98±23.40	1004.29±95.18	41.02±2.81	98.98±19.88
RDP 1.5%P+APP 1.5%P	951.06±37.26	956.05±98.55	41.02±1.10	95.02±17.60
RDP 2%P+APP 1%P	948.10±8.29	976.01±98.55	38.27±1.24	87.05±1.81

In the case of composites containing only one FR, by increasing the amount of the FR, the tensile strength showed a growing tendency, but all values were slightly below the value of the SPE composite. The tensile strength of the mixed FR formulations overperformed the SPE reference and showed a growing tendency with the increase of the APP ratio. Concerning the flexural strength results, the composites containing only APP or RDP had somewhat lower values than the

reference. The mixed FR samples had higher flexural strength than the composites with the same amount of P originating from one FR, and fell in the range of the standard deviation of the reference. The samples containing only RDP showed somewhat higher interlaminar shear strength values than the SPE composite, while the samples containing APP were in the same range as the reference, no clear tendencies could be observed. Concerning the dynamic properties, all composites with 3% P-content had higher values than the reference. In composites containing both RDP and APP, the Charpy impact energy increased by increasing the ratio of APP.

4.5.1.2. *Flame retardancy of cycloaliphatic sugar based carbon fibre reinforced composites with combination of phosphorus-containing additives*

The flame retardancy of carbon fibre reinforced glucofuranoside based trifunctional epoxy (GFTE) - aromatic amine hardener (DETDA) composites was investigated applying ammonium polyphosphate (APP), acting in the solid phase, resorcinol bis(diphenyl phosphate) (RDP) acting primarily in the gas phase, and their combination, which proved be synergistic in terms of fire retardancy in GFTE polymer matrix (see **4.4.3**). The fire retardant action of the additive FRs and their synergistic combinations was investigated in composites by limiting oxygen index (LOI), UL-94 tests and mass loss calorimetry. The effect of FRs on the T_g, storage modulus was evaluated by DMA test [**221**].

Flame retardancy

The LOI and UL-94 results of the flame retarded composites can be seen in **Table 4.5.5**. The heat release rate curves are displayed in **Figure 4.5.4**, while the numerical data obtained from mass loss calorimetry results are summarized in **Table 4.5.6**, best performances among the samples are highlighted with bold letters.

Table 4.5.5 LOI and UL-94 results of the reference and flame retarded GFTE composites

composite	**LOI [V/V%]**	**UL-94 (burning rate [mm/min])**
GFTE composite	22	HB (32.2 mm/min)
RDP 4%P	40	V-0
APP 4%P	30	HB
RDP 2%P+APP 2%P	30	V-0

According to the LOI and UL-94 results, despite the inclusion of inert carbon fibres, the GFTE composite had the same LOI as the matrix itself (see **4.4.3**), and even its burning rate increased, due to the so called candlewick effect of the fibres with good heat conductivity. As carbon fibre reinforcement also hinders the intumescent action of solid phase FRs, in this case the inclusion of

RDP was necessary to reach V-0 UL-94 rate. The RDP 4%P sample reached an outstanding LOI of 40 V/V% compared to the 22 V/V% value of the GFTE reference.

According to mass loss calorimetry results in the case of APP-containing samples the ignition occurred earlier than in the case of RDP-containing ones and the reference, which may be interpreted with the hindered intumescent action caused by carbon fibre reinforcement. However, once the protective coating is formed, the HRR is efficiently reduced, leading to the lowest pHRR, THR, EHC, MARHE values and highest amount of residue. The mixed formulation shows only a slightly lower performance, but taking into consideration, that it has a V-0 UL-94 rating, compared to the HB rating of APP 4%P sample, the overall performance of the combined formulation is better.

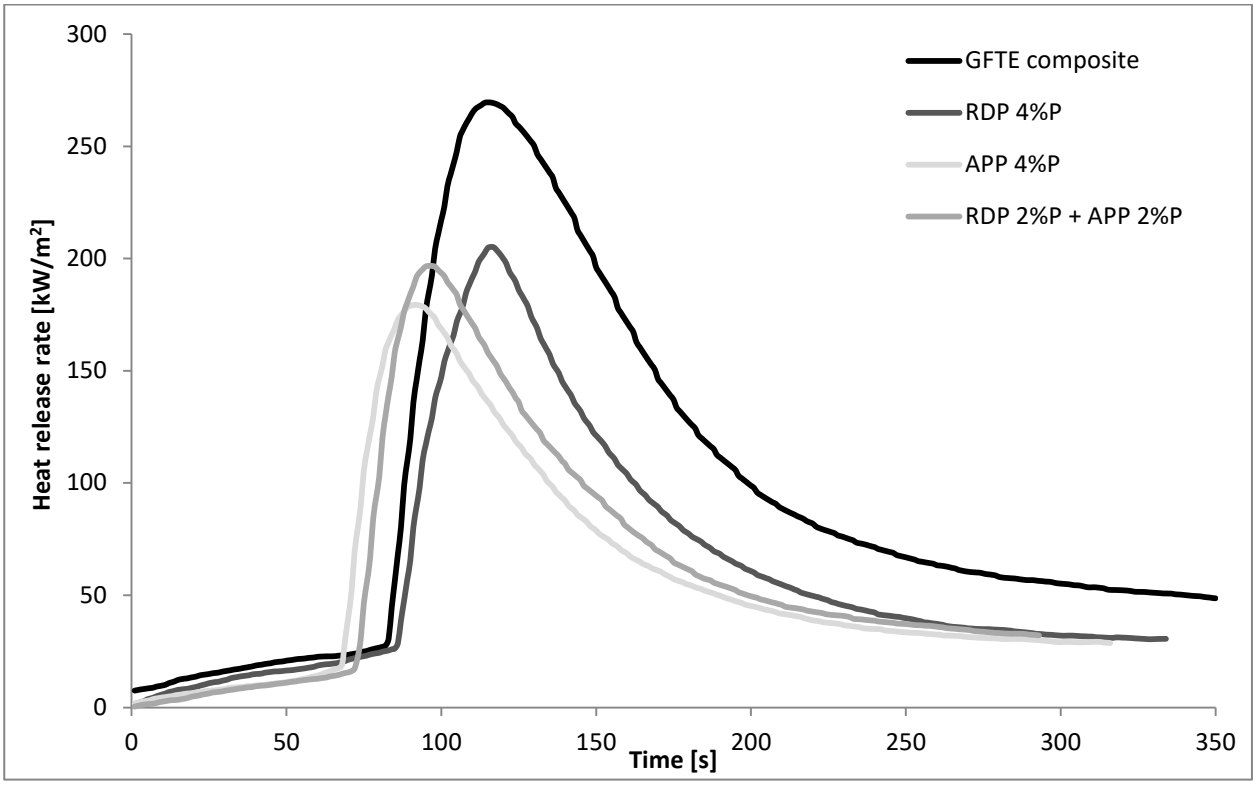

Figure 4.5.4 Heat release rate of reference and flame retarded GFTE composites

Table 4.5.6 Mass loss calorimetry results of reference and flame retarded GFTE samples

composite	TTI (s)	pHRR (kW/m^2)	time of pHRR (s)	FIGRA (kW/m^{2}s)	burning time (s)	THR (MJ/m^2)	EHC (MJ/kg)	MARHE (kW/m^2)	residue (%)
GFTE composite	83	270	115	2.3	108	32.6	25.5	116.0	42
RDP 4%P	**85**	205	**116**	**1.8**	104	20.6	17.3	77.8	49
APP 4%P	68	**179**	92	1.9	104	**18.0**	**16.3**	**74.1**	**54**
RDP 2%P+APP 2%P	71	197	96	2.0	**87**	18.4	**16.3**	77.4	53

(TTI: time to ignition, pHRR: peak of heat release rate, FIGRA: fire growth rate, THR: total heat release, EHC: average effective heat of combustion, MARHE: maximum of average rate of heat emission)

Glass transition temperature and storage modulus of composites

The storage modulus curves of the reference and flame retarded GFTE composites are displayed in **Figure 4.5.5**, while numerical results of dynamical mechanical analysis (T_g, storage modulus at 25 °C and 75 °C) of composites are shown in **Table 4.5.7**.

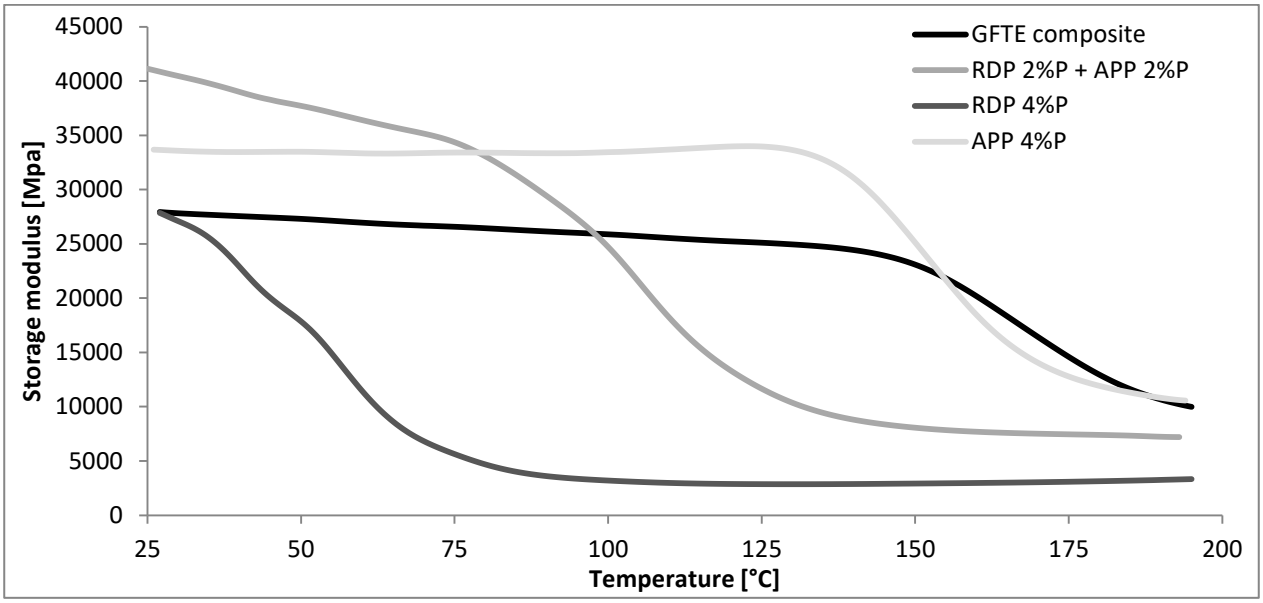

Figure 4.5.5 Storage modulus curves of reference and flame retarded GFTE composites

Table 4.5.7 Glass transition temperature, storage modulus of reference and flame retarded GFTE composites

composite	glass transition temperature [°C]	storage modulus at 25 °C [MPa]	storage modulus at 75 °C [MPa]
GFTE composite	172	27938	26576
RDP 4%P	56	27853	5638
APP 4%P	156	33666	33411
RDP 2%P+APP 2%P	104	41134	34363

In the case of APP-containing samples approx. up to their T_g, their storage modulus is higher than that of the GFTE reference composite, which may be explained by the stiffening effect of dispersed rigid APP particles in the matrix. On the other hand, it has to be noted that the RDP-containing samples are already in the transition state at the beginning of the measurement, which can be interpreted again by the low P-content of RDP and its high amount needed for appropriate flame retardancy, resulting in substantial plasticizing effect.

As for the T_g, the decreasing tendencies are similar to those observed in the matrices (see **4.4.3**), however the values are somewhat lower. The incorporation of the flame retardants more polar than the epoxy resin matrix itself decreases the fiber matrix adhesion, leading to the reduction of T_g as well.

4.5.1.3. *Reactive flame retardancy of aromatic epoxy resin based carbon fibre reinforced composites with phosphorus-containing epoxy monomer and cyanate ester*

Reactively flame retarded cyanate ester/epoxy resin (CE/EP) carbon fibre reinforced composites consisting of diglycidyl ether of bisphenol A (DGEBA), novolac type cyanate ester (CE) and an epoxy functional adduct of DGEBA and 9,10-dihydro-9-oxa-10-phosphaphenanthrene-10-oxide (DOPO) (see **4.1.2**) were prepared. Based on the flame retardancy results of the matrices (see **4.4.4**), only the best performing samples (CE/EP blend composites containing 20% and 40% PT-30, respectively, flame retarded CE/EP blend composites containing 40% PT-30 and 2 or 3% P from DGEBA-DOPO) were chosen for composite preparation along with the CE and EP references. Influence of cyanate ester and FR addition was determined on matrix viscosity, composite flame retardancy, T_g and storage modulus determined by DMA [**189**,**190**].

Viscosity of polymer matrices

One major aspect of the processing of resin systems is their viscosity, therefore prior to composite preparation viscosity of the polymer matrices was determined as a function of temperature (for detailed results see [**190**]). According to Hay [227] for resin injection 100-300 mPa·s, for pultrusion 400-800 mPa·s, while for filament winding viscosity of 800-2000 mPa·s is recommended. CEs are often processed by filament winding, where the filaments are immersed into a heatable resin bath allowing the reduction of the matrix viscosity by increasing its temperature. By increasing the amount of CE in the blends, the viscosity increased, as expected. The addition of solid DGEBA-DOPO adduct significantly increased the viscosity as well. According to the viscosity values at 80 °C (**Table 4.5.8**) the samples containing 3% P can be rather processed by hot pressing. Blends containing 2% P are suitable for filament winding as well. Based on these results hand lamination followed by hot pressing was chosen as composite preparation method, as it provides high fibre content and excellent reproducibility.

Table 4.5.8 Viscosity of the CE and EP references and CE/EP blends at 80° C

composite	viscosity [mPa·s]
PT-30	400
DGEBA	233*
20% PT-30 - 80% DGEBA	107
40% PT-30 - 60% DGEBA	113
40% PT-30 - DGEBA – DOPO 2%P	1623
40% PT-30 - DGEBA – DOPO 3%P	14780

* at 60 °C-on due to lower gel time

Flame retardancy

LOI, UL-94 and mass loss calorimetry results of the composites made of CE and EP references and their blends are summarized in **Table 4.5.9**. The higher LOI values in comparison to the neat matrices are the result of the decrease of the flammable matrix material due to the inclusion of approx. 60% of carbon fibre reinforcement (considered as inert material under these test conditions). By increasing the amount of PT-30 and DOPO, the LOI increases in the case of composites as well. As for the UL-94 results, in the case of composites 40% of PT-30 is already sufficient to reach the V-0 rate. As expected, the inclusion of carbon fibres significantly decreased the pHRR and THR values (**Figure 4.5.6**), and increased the residual mass. By increasing the amount of CE and P, the pHRR values showed further decrease. In contrast to matrix samples, where no further decrease in flammability was experienced when the P-content was increased to 3%, in the case of the composite samples the 40% PT-30 - DGEBA – DOPO 3%P sample showed the best performance: it had the same pHRR value, 84 kW/m^2 as the PT-30 reference composite. Its THR and MARHE values were still higher than that of the PT-30, however it had lower FIGRA and EHC values than PT-30. The increasing P-content slightly decreased the TTI values, which can be explained by the gas phase mechanism of DOPO [210, 223]: due to inclusion of DOPO the thermal stability of the system decreases, so it ignites earlier, on the other hand, the formed P-containing radicals effectively postpone the time of pHRR and reduce the pHRR values. These latter effects led to significant decrease in FIGRA values, as observed in the case of the matrices as well. The charring experienced at matrix samples was hindered by the included carbon fibre plies [**224**], no charring at all was detected on the surface of the mass loss calorimetry residual composite samples.

Table 4.5.9 LOI, UL-94 and mass loss calorimetry results of the composites made of CE and EP references and their blends

composite	LOI [V/V %]	UL-94	TTI [s]	pHRR [kW/m^2]	time of pHRR [s]	FIGRA [kW/m^{2}s]	burning time [s]	THR [MJ/m^2]	EHC [MJ/kg]	MARHE [kW/m^2]	residue [%]
PT-30	58	V-0	80	84	124	0.7	257	9.8	10.4	38.0	81
DGEBA	33	HB	55	176	197	0.9	355	37.9	13.8	112.2	50
20% PT-30 - 80% DGEBA	41	HB	51	162	156	1.0	301	29.9	14.7	95.8	61
40% PT-30 - 60% DGEBA	42	V-0	87	134	178	0.8	308	21.8	13.2	69.1	70
40% PT-30 - DGEBA – DOPO 2%P	46	V-0	72	101	195	0.5	401	20.1	11.2	61.1	67
40% PT-30 - DGEBA – DOPO 3%P	48	V-0	70	84	233	0.4	372	18.7	10.1	53.6	67

LOI: limiting oxygen index, TTI: time to ignition, pHRR: peak of heat release rate, FIGRA: fire growth rate, THR: total heat release, EHC: average effective heat of combustion, MARHE: maximum of average rate of heat emission

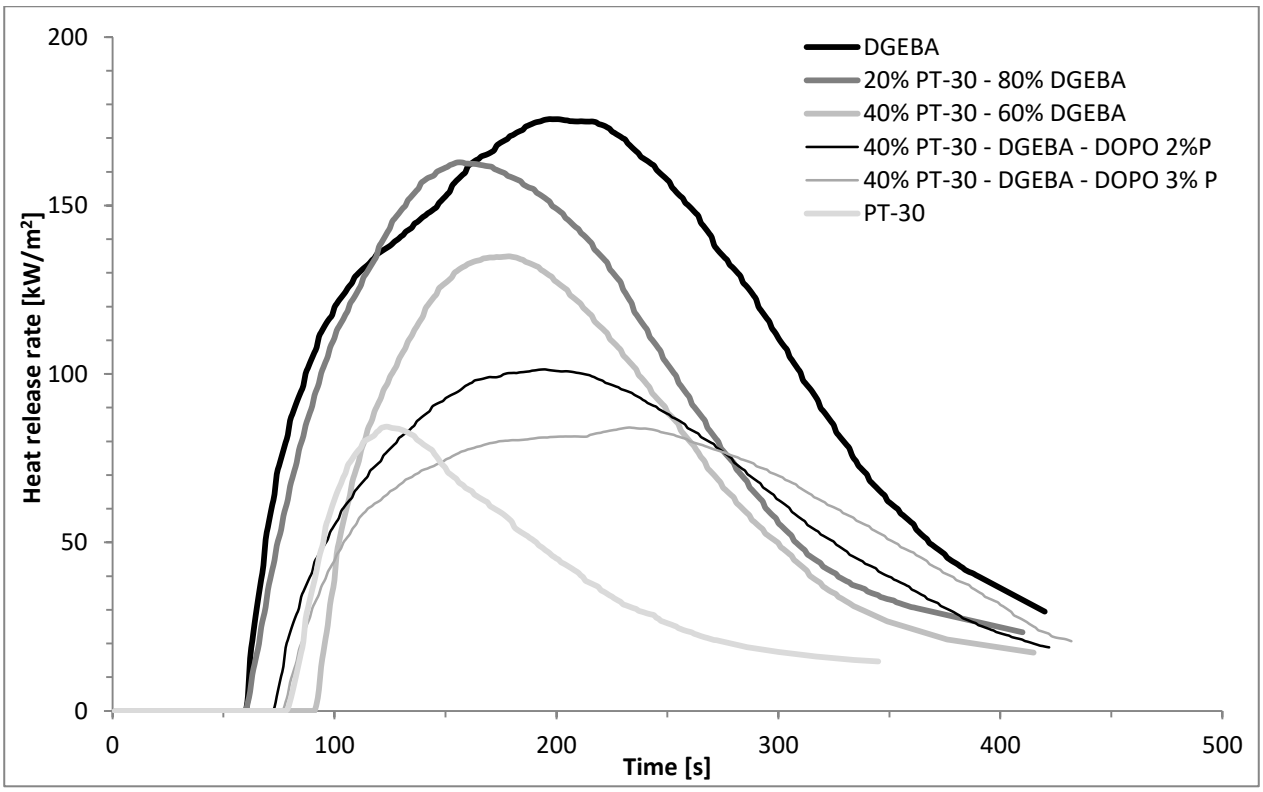

Figure 4.5.6 HRR curves of the composites made of CE and EP references and their blends

Storage modulus and glass transition temperature

The storage modulus curves of CE, EP reference and CE/EP blend composites are displayed in **Figure 4.5.7**. T_g and storage modulus values at 25 and 75 °C are shown in **Table 4.5.10**.

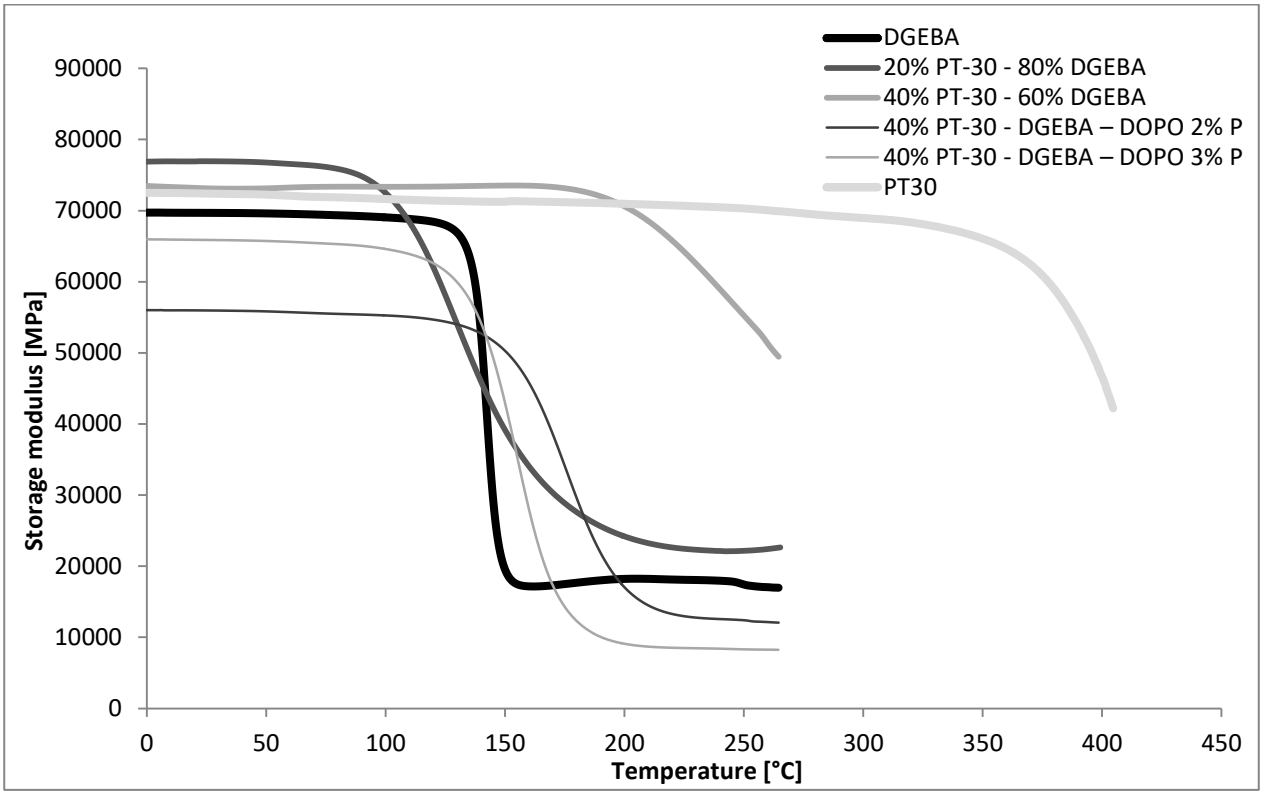

Figure 4.5.7 Storage modulus of CE, EP reference and CE/EP blend composites in the temperature range of 25-260° C (in the case of pure CE 25-400 °C)

Table 4.5.10 Glass transition temperature and storage modulus values at 25 and 75 °C of CE/EP composites determined by DMA

composite	glass transition temperature [°C]	storage modulus at 25 °C [MPa]	storage modulus at 75 °C [MPa]
PT-30	394	72407	71908
DGEBA	145	69691	69407
20% PT-30 - 80% DGEBA	145	92311	91420
40% PT-30 - 60% DGEBA	249	73150	73360
40% PT-30 - DGEBA – DOPO 2% P	187	55967	55537
40% PT-30 - DGEBA – DOPO 3% P	167	65882	65378

By increasing the temperature the storage moduli remained in the same range at least up to 75 °C. The 20% PT-30 - 80% DGEBA composite had higher storage modulus than CE up to 90 °C and higher than DGEBA up to 105 °C. The 40% PT-30 - 60% DGEBA composite performed similarly as CE up to 200 °C and overperformed DGEBA in the whole temperature range. The flame retarded composites showed somewhat lower storage modulus than DGEBA (except the 140-165 °C range in case of 40% PT-30 - DGEBA – DOPO 3%P composite, and the 140-190 °C range in case of 40% PT-30 - DGEBA – DOPO 2%P), most probably due to lower fibre-matrix adhesion (the interlaminar shear properties are discussed in details in **Table 4.5.13** in the following section).

As for the glass transition temperatures, the T_g decreased in CE and EP composites and in 20% PT-30 - 80% DGEBA sample, while in 40% PT-30 containing composites, including the flame retarded ones, practically it remained the same value as in case of the matrix samples (see **Table 4.4.15**). Compared to DGEBA, the 40% PT-30 - DGEBA – DOPO 2%P composite showed 42 °C increase, while the 40% PT-30 - DGEBA – DOPO 3%P composite had still 22 °C higher T_g.

Mechanical characterization

The tensile properties of the CE and EP reference composites and CE/EP blend composites are shown in **Table 4.5.11**. The inclusion of EP significantly increased the tensile strength of the rigid CE. More surprisingly, by adding DOPO-DGEBA adduct to the 40% PT-30 - 60% DGEBA, the tensile strength of the 2% P-containing composite increased even further, and in the case of 3% P-containing sample it still remained over the value of the CE reference. This amelioration may be attributed to better fibre-matrix adhesion and to the reactive nature of the FR: by incorporating it by primary chemical bonds to the matrix itself, it does not migrate to the matrix surface either during high temperature processing or application. The strain at break increased to some extent in all blends containing DGEBA in comparison to the reference CE, decreasing the rigidity of it. The highest tensile modulus was reached in case of 20% PT-30 - 80% DGEBA, higher than the moduli of the blend components themselves. By adding DOPO-DGEBA adduct to the system, the tensile modulus slightly decreased.

Table 4.5.11 Tensile properties of the CE, EP reference and CE/EP blend composites

composite	tensile strength [MPa]	strain at break [%]	tensile modulus [GPa]
PT-30	689.20±100.91	4.43±0.60	27.68±0.72
DGEBA	912.64±45.67	5.35±0.43	26.78±2.38
20% PT-30 - 80% DGEBA	1040.94±43.02	5.66±0.22	28.81±0.20
40% PT-30 - 60% DGEBA	844.14±40.32	5.06±0.16	25.14±2.09
40% PT-30 - DGEBA – DOPO 2%P	861.25±54.71	5.73±0.47	24.95±0.45
40% PT-30 - DGEBA – DOPO 3%P	715.23±32.41	5.06±0.19	23.37±0.24

The flexural properties of the CE and EP reference composites and CE/EP blend composites are shown in **Table 4.5.12**. According to the results the addition of CE into EP resulted in slightly higher flexural strength than in case of the reference CE and EP itself. The inclusion of DGEBA-DOPO adduct decreased the flexural strength and modulus, and increased the deformation at break, however taking into account the standard deviation values, the flexural strength and modulus of 40% PT-30 - DGEBA – DOPO 3% remained in the same range as in case of CE and EP references.

Table 4.5.12 Flexural properties of the CE, EP reference and CE/EP blend composites

composite	flexural strength [MPa]	deformation at break [%]	flexural modulus [GPa]
PT-30	1226.96±271.12	1.36±0.03	103.20±19.51
DGEBA	1203.02±115.92	1.36±0.09	98.24±4.28
20% PT-30 - 80% DGEBA	1240.14±114.31	1.36±0.04	100.11±10.92
40% PT-30 - 60% DGEBA	1238.53±79.23	1.37±0.04	98.24±8.82
40% PT-30 - DGEBA – DOPO 2%P	1056.18±54.07	1.43±0.02	79.48±4.98
40% PT-30 - DGEBA – DOPO 3%P	1149.05±96.71	1.45±0.09	95.96±10.93

In accordance with the tensile and flexural properties, the interlaminar shear strength values (**Table 4.5.13**) of the CE/EP blends were higher than in case of the CE and EP references. The inclusion of the polar P-containing FR decreased the interlaminar shear strength, however these values were still well above the value of the reference CE composite.

Table 4.5.13 Interlaminar shear strength of the CE, EP reference and CE/EP blend composites

composite	interlaminar shear strength [MPa]
PT-30	40.01±1.34
DGEBA	61.34±1.95
20% PT-30 - 80% DGEBA	66.83±3.7
40% PT-30 - 60% DGEBA	68.26±3.59
40% PT-30 - DGEBA – DOPO 2%P	53.38±1.97
40% PT-30 - DGEBA – DOPO 3%P	47.86±2.12

The results of the instrumented Charpy unnotched impact tests are given in **Table 4.5.14**. The impact strength of the 20% PT-30 - 80% DGEBA blend was practically the same as in the case of DGEBA, however, the 40% PT-30 - 60% DGEBA blend had even higher impact strength than CE. By increasing the amount of FRs, the fracture toughness showed further increase in comparison to CE, meaning that the FR composites are less brittle than the CE/EP blends and CE, EP references.

Table 4.5.14 Charpy impact strength of the CE and EP reference and CE/EP blend composites

composite	Charpy impact strength [J/mm^2]
PT-30	90.09±8.03
DGEBA	84.28±5.25
20% PT-30 - 80% DGEBA	84.57±2.91
40% PT-30 - 60% DGEBA	98.33±32.04
40% PT-30 - DGEBA – DOPO 2%P	99.12±15.12
40% PT-30 - DGEBA – DOPO 3%P	113.68±14.01

4.5.1.4. *Reactive flame retardancy of carbon fibre reinforced epoxy resin composites with phosphorus-containing crosslinking agent*

Reactively flame retarded aromatic DGEBA-based and aliphatic PER-based epoxy resin composites were prepared by substituting the original amine curing agents (TETA and T58, respectively) by TEDAP. In aromatic flame retarded samples 40% of DGEBA epoxy monomer was substituted by PER reactive dilutant to reduce the viscosity of the system and to increase the compatibility of aromatic component to TEDAP. The effect of carbon fibre and TEDAP inclusion on flammability and mechanical characteristics is summarized shortly below (for more details see [**224**,**228**]).

Flame retardancy

The LOI, UL-94 and mass loss calorimetry results of PER, DGEBA reference and flame retarded epoxy resin composites are summarized in **Table 4.5.15**, HRR curves are showed in **Figure 4.5.8**.

Table 4.5.15 LOI, UL-94 and mass loss calorimetry results of PER, DGEBA reference and flame retarded epoxy resin composites

composite	LOI [V/V%]	UL-94	TTI [s]	pHRR [kW/m^2]	time of pHRR [s]	THR [MJ/m^2]	burning time [s]	residue [%]
PER	29	HB	43	445	121	46.5	428	53
DGEBA	33	HB	48	363	189	49.5	420	50
PER TEDAP	33	V-0	56	195	115	16.0	404	59
DGEBA TEDAP	31	V-0	88	307	152	39.1	336	55

LOI: limiting oxygen index, TTI: time to ignition, pHRR: peak of heat release rate, THR: total heat release

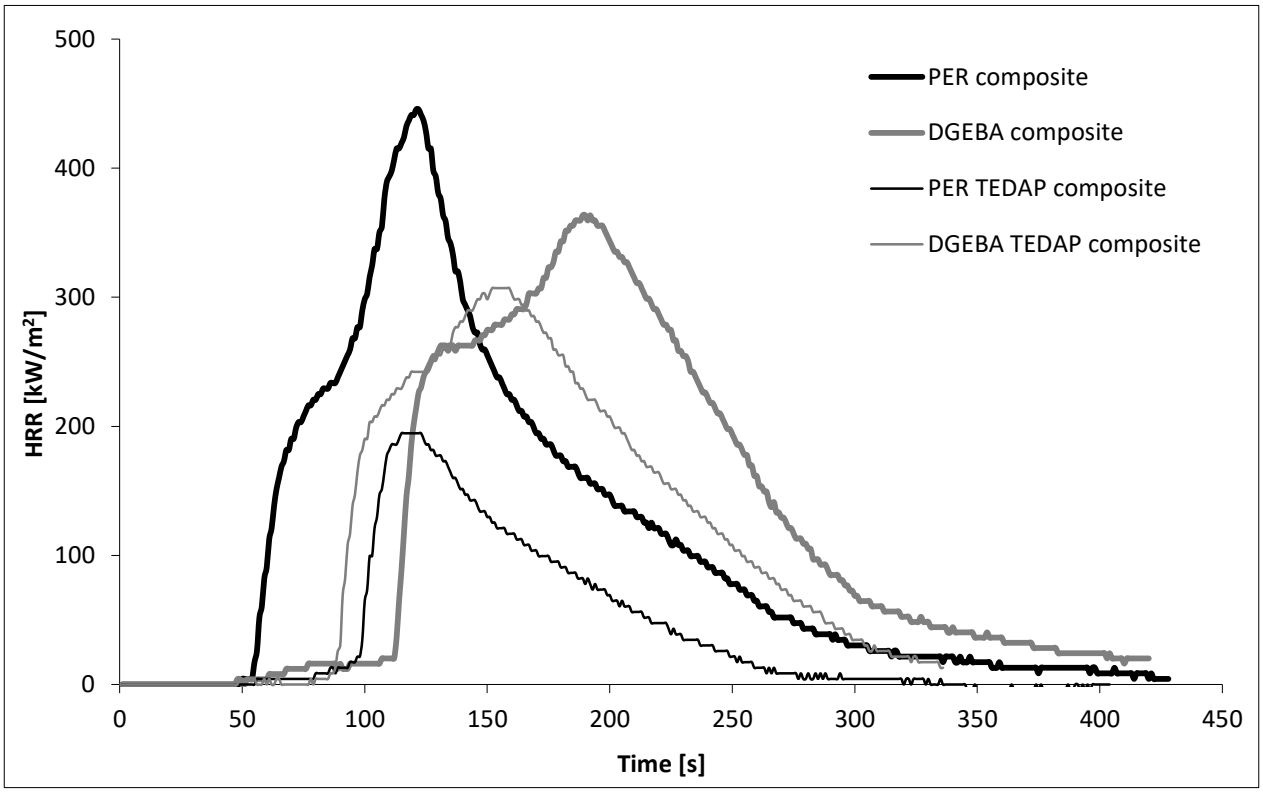

Figure 4.5.8 HRR curves of the reference and flame retarded PER and DGEBA composites

The aliphatic composite has lower LOI value than the aromatic one; however, the use of reactive FR leads to higher LOI in the PER-based system compared to the DGEBA-based one. In the case of reference matrices the LOI shows significant increase when carbon fibres (acting as inert material under test conditions), are incorporated, while in the case of FR samples no further improvement could be achieved this way (see the flame retardancy results of the related matrices in **Table 4.4.16**). Although the inclusion of carbon fibres increased significantly the LOI of PER and DGEBA, the UL-94 rating of the not flame retarded composites remained HB, and similarly to the matrices the application of TEDAP was necessary to reach the V-0 rate. According to the mass loss calorimetry results in PER and DGEBA the peak of heat release rate (pHRR) and the total heat release (THR) decreased significantly due to the introduction of carbon fibres. The time to ignition (TTI) increased in some extent, particularly in the case of DGEBA. Comparing the amount of residues after combustion, the introduction of 40% of carbon fibres led to an additional increase in

residual mass: disregarding the mass of carbon fibres in the aliphatic system, there was a 12.2% increase compared to the aliphatic reference, while in the aromatic system this quantity was 9.3%. The combined phase FR action of TEDAP [**211**] resulted in significant reduction in flammability of PER and DGEBA, especially in non-reinforced matrices. However, in the case of composites the improvement of FR performance achieved by TEDAP is less than expected from the additivity of effects of TEDAP and carbon fibres, especially in aromatic composite. The residual mass amounts also increased, but much less than calculated on the basis of additivity. These results suggest that the reinforcing carbon fibre fabric plies in the composite hinder the solid phase intumescent FR effect of TEDAP and instead of forming a well-developed char only thin char layers are formed between the carbon fibre plies slightly delaminating them (**Figure 4.5.9**) (still leading to catastrophic deterioration of residual mechanical properties in case of accidental fire). Accordingly the decrease in THR may be attributed mainly to the gas phase effect of the P-containing FR.

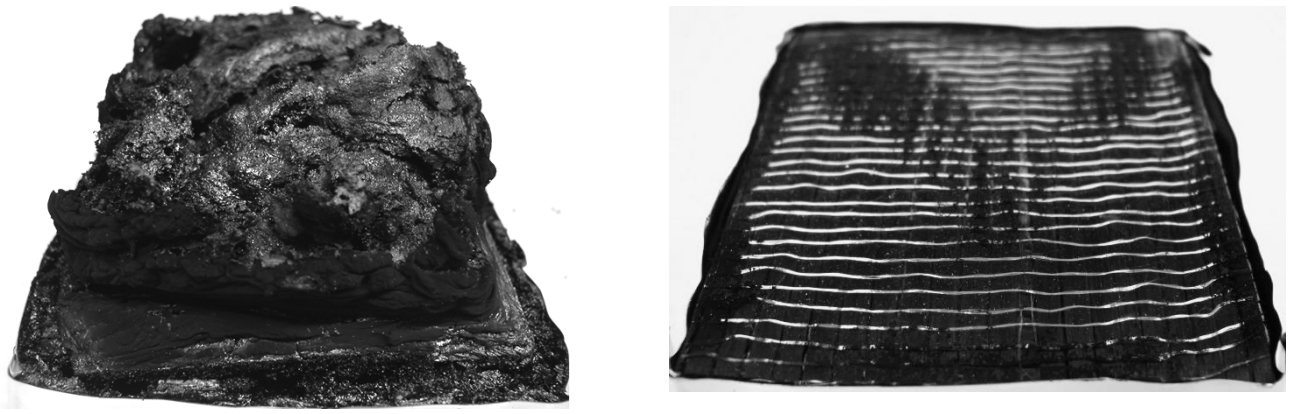

DGEBA TEDAP **DGEBA TEDAP composite**

Figure 4.5.9 Photos of calorimetry residues of DGEBA TEDAP matrix and composite samples

Mechanical characterization

Tensile, bending and interlaminar shear strength test results of PER, DGEBA reference and flame retarded carbon fibre reinforced composites are summarized in **Table 4.5.16**.

Table 4.5.16 Tensile, bending and interlaminar shear strength test results of PER, DGEBA reference and flame retarded composites

composite	tensile strength [MPa]	tensile modulus [GPa]	flexural strength [MPa]	flexural modulus [GPa]	interlaminar shear strength [MPa]
PER	523.02±22.70	21.38±0.42	578.68±22.88	55.35±0.88	22.00±2.84
DGEBA	424.28±13.79	18.49±0.82	725.71±42.02	52.78±0.92	25.52±4.55
PER TEDAP	393.75±16.93	16.67±0.58	318.89±19.72	45.80±1.90	9.82±0.88
DGEBA TEDAP	375.26±16.44	16.13±0.81	434.36±9.64	36.95±2.42	9.98±1.69

Both in terms of tensile strength and modulus the aliphatic reference composite had superior properties than the aromatic one. In flame retarded composites no significant difference was

observed, meaning that the tensile strength and modulus decreasing effect of TEDAP was larger in PER. As for the flexural properties, the reference DGEBA composite had 25% higher flexural strength, while the flexural modulus values were similar in DGEBA and PER. The application TEDAP significantly decreased the flexural strength in both matrices. In order to explain the decreasing effect of FR modification on the mechanical properties interlaminar shear strength tests were performed. In the case of the FR composites the interlaminar shear strength decreased significantly compared to the composites without FR. This phenomenon can be explained by the more polar character of the FR component, which does not fit to the sizing of the reinforcing fibre designed for the unmodified epoxy resin.

4.5.1.5. *Multilayer carbon fibre reinforced composites with intumescent epoxy resin coating*

In order to combine the enhanced mechanical properties of fibre reinforced composites and the outstanding FR properties of intumescent systems, and moreover to eliminate the negative effect of the fibres on the intumescence and of the FR on the interlaminar adhesion, respectively, two kinds of coated systems were developed. Both of them consisted of 2 mm thick DGEBA aromatic reference composite core; one of them had a 2 mm thick PER TEDAP aliphatic intumescent coating on the top, while the other had two 1 mm thick PER TEDAP aliphatic intumescent coatings – one above and one below the core composite [**224**].

In these combinations the core was the load bearing element, while the coating was responsible for the flame retardancy. According to the mechanical tests, the coating did not affect the mechanical properties of the core, therefore in structural design the values of the core should be considered and the coating can be disregarded.

As for the flame retardancy results (**Table 4.5.17** and **Figure 4.5.10**), this combination seemed to be synergistic in both cases: an increase of LOI from 33 to 37 was measured in both coated composites compared to their constituent layers. The differences between the two types of coated systems became obvious at mass loss calorimeter tests. In the case of the composite with 2x1 mm layers the pHRR remained between the values of the constituent layers, while the TTI increased by 100 s compared to aliphatic FR layer. In the case of 2 mm coating the result was even more evident: the HRR value fluctuated around zero as no ignition occurred at all at 50 kW/m^2 heat flux. The total absence of ignition can be explained by two reasons: in the coated composite the intumescence was not hindered, therefore the P-containing FR could act both in gas and solid phase, furthermore the carbon fibre reinforced layer lead away the accumulated heat from the char and distributed it in the core, so the 50 kW/m^2 proved to be not enough to cause ignition in this coated composite system.

Table 4.5.17 Comparison of the flame retardant properties of coated composites and their constituent layers alone

	LOI [V/V%]	UL-94	TTI [s]	peak of HRR [kW/m^2]	THR [MJ/m^2]	residue [%]
DGEBA composite	33	HB	48	363	49.5	50
PER TEDAP	33	V-0	90	287	26.0	37
2 mm DGEBA composite + 2x1 mm PER TEDAP coating	37	V-0	190	318	26.4	53
2 mm DGEBA composite + 2 mm PER TEDAP coating	37	V-0	no ignition	no ignition	no ignition	44

LOI: limiting oxygen index, TTI: time to ignition, pHRR: peak of heat release rate, THR: total heat release

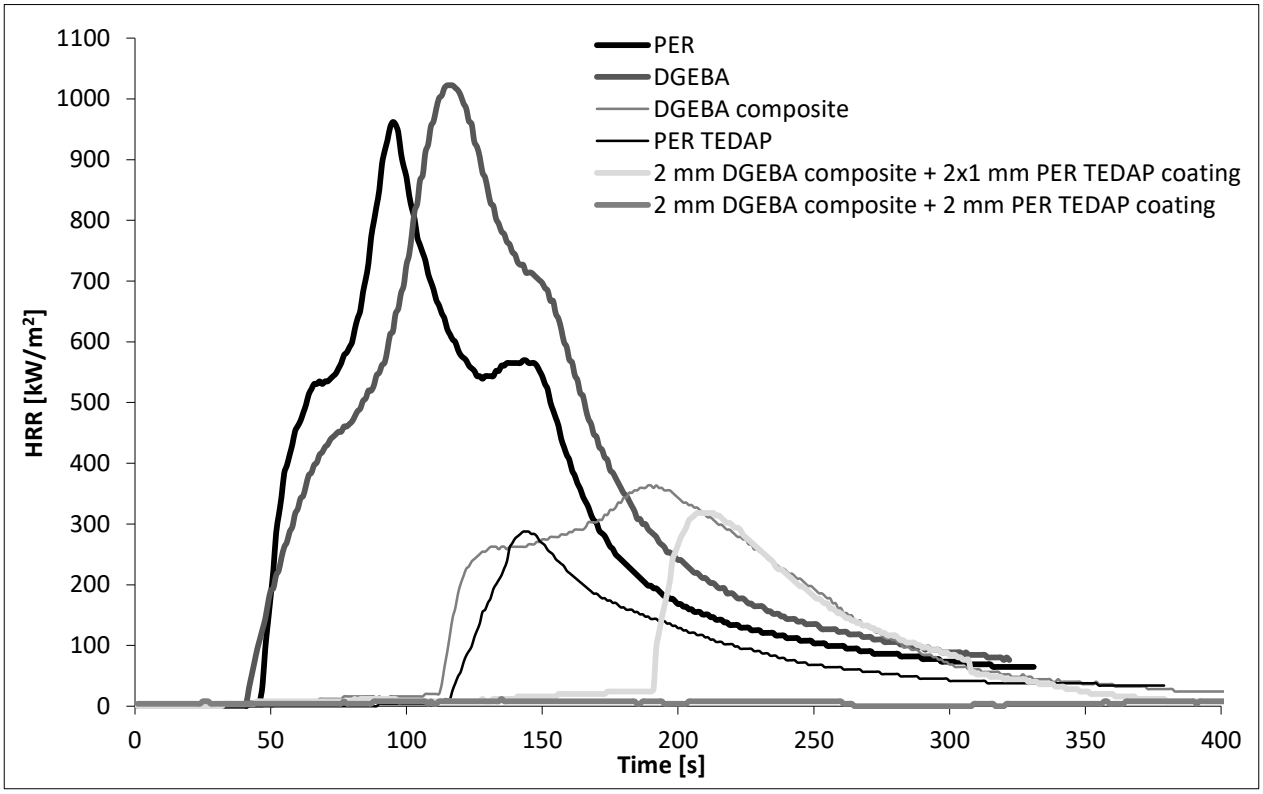

Figure 4.5.10 Comparison of HRR curves of coated composites, their constituent layers alone and reference epoxy resin matrices

4.5.2. Flame retardancy of natural fibre reinforced composites

Natural fibres offer various advantages over commonly applied man-made reinforcements, as lower density, renewability and biodegradability, however their low thermal stability and flammability represents a major drawback, especially in more demanding structural composite applications. The high amount of functionalizable groups on their surface offers various possibilities for rendering them FR (as summarized in **2.3.4**). Nevertheless, it is still a challenging task to be solved due the so called candlewick effect of natural fibres in polymer composites, as well as because of their low thermal stability and susceptibility to various chemicals.

In the followings results on FR modifications of twill woven hemp fabrics, as well as reference and flame retarded composites made thereof, will be presented.

4.5.2.1. *Fire retardant modification of biofibres*

The effects of thermotex procedure (i.e. removal of adsorbed water from the capillaries and then filling the micro/nano-voids with phosphoric acid [171]) and sol-gel treatment with amine-type silanes followed by thermotex treatment were compared on the flammability of hemp fibres used for the reinforcement of epoxy resins. The effect of the applied modifications (THF: thermotex-treated hemp fabric and SiTHF: silane and thermotex-treated hemp fabric) on the thermal stability and flammability of the fibres, compared to the unmodified fabric (NHF: non-modified hemp fabric), was tested by TGA and mass loss calorimetry. The effect of surface modification on the tensile properties of the fabrics was evaluated by strip tensile tests [**229**].

Thermal stability, flammability and strip tensile strength of modified fabrics

The most important thermal, flammability and mechanical characteristics of the untreated and surface treated hemp fabrics are summarized in **Table 4.5.18** (for detailed results see [**229**]).

Table 4.5.18 Thermal, flammability and mechanical characteristics of the modified hemp fabrics

fibre	$T_{-5\%}$ [°C]	$T_{-50\%}$ [°C]	dTG_{max} [%/°C]	T_{dTGmax} [°C]	char yield at 500 °C [%]	TTI [s]	pHRR [kW/m^2]	time of pHRR [s]	THR [MJ/m^2]	F_{max} [N]
NHF	278.0	362.5	1.71	360.7	29.6	3	68	35	5.5	1140
THF	210.0	361.3	1.38	269.6	42.2	4	18	14	2.0	739
SiTHF	239.5	426.7	1.08	287.5	45.7	15	9	62	1.4	708

$T_{-5\%}$: temperature at 5% mass loss; $T_{-50\%}$: temperature at 50% mass loss, dTG_{max}: maximum mass loss rate; T_{dTGmax}: temperature belonging to dTG_{max}; TTI: time to ignition; pHRR peak of heat release rate; THR: total heat release; F_{max}: maximal force measured during the strip tensile test of the fabrics

Concerning the thermal stability, the thermotex procedure decreased the initial degradation temperature of the hemp fabric by more than 60 °C, as anticipated [**229**]. In the case of SiTHF fabric the sol-gel treatment partially protected the cellulose structure from the acidic hydrolysis [230,231], and thus increased the decomposition temperature by 30 °C compared to THF. The temperatures belonging to maximal mass loss rates showed similar tendency: the main degradation of the treated fabrics occurred at approx. 90° C and 70 °C lower temperatures in case of THF and SiTHF, respectively. On the other hand, the surface treatments considerably decreased the decomposition rates: in the case of the combined treatment the synergism between P and Si [163] resulted in a decrease from 1.71%/°C to 1.08%/°C. The surface treatment also increased the amount of the residue significantly, but no remarkable difference (only 3.5%) was detected between the two treatments by TGA measurements.

In order to determine the macroscopic flammability of the fabrics, single fabric plies were subjected to mass loss calorimetric measurements. The application of the combined treatment was the most beneficial: it increased the time to ignition from 3 s to 15 s, decreased the heat release rate from 68 kW/m^2 to 9 kW/m^2 and led to the formation of consistent char instead of fluffy, light ash as in the case of untreated fabrics and thermotex treated fabrics.

According to the maximal forces measured during the strip tensile test of the fabrics, the strength of the treated fabrics decreased by about 35%. In this apect there was no significant difference between the two different surface treatments. These results also confirm that the acidic degradation of cellulose deteriorates the tensile properties of the natural fabrics.

4.5.2.2. *Reactive flame retardancy of aliphatic epoxy resin based composites reinforced with flame retarded natural fibre*

Reference and flame retarded composites were prepared from pentaerythritol-based epoxy resin (PER) and T58 curing agent with natural (NHF), thermotex treated (THF) and sol-gel and thermotex treated (SiTHF) twill woven hemp fabrics. In combination with the surface treated fabrics amine-type P-containing curing agent (TEDAP) was used as FR. The P-content of the flame retarded matrix was chosen for 2.5%, to reach V-0 rating in UL-94 tests, according to previous studies [**173**,**220**].

A possible synergistic effect was described in terms of composite mechanical properties: when both the matrix and the reinforcement contained P, despite the inferior mechanical performance of the FR matrix itself and the decreased strength of the surface treated fabrics, the mechanical properties for the FR samples reached the level of the reference composite almost in all cases.

Flame retardancy

The flame retardancy results of the hemp fibre reinforced composites are summarized in **Table 4.5.19**.

Table 4.5.19 LOI, UL-94 and cone calorimetry results of hemp fibre reinforced composites

sample	P-content [%]	LOI [V/V%]	UL-94*	TTI [s]	pHRR [kW/m^2]	pHRR time [s]	THR [MJ/m^2]	residue [%]
PER NHF	0	22	HB (18.2)	41	1342	113	84.9	2
PER THF	0.51	26	HB	40	994	109	62.6	7
PER SiTHF	0.51 (+1.47% Si)	28	HB	31	1005	107	77.1	10
PER TEDAP NHF	1.75	32	V-1	33	778	107	45.9	20
PER TEDAP THF	2.26	32	V-0	30	674	123	45.6	20
PER TEDAP SiTHF	2.26 (+1.47% Si)	32	V-0	30	621	153	49.5	23

LOI: limiting oxygen index, TTI: time to ignition, pHRR: peak of heat release rate, THR: total heat release
*in parenthesis the horizontal burning rate is showed in mm/min, where measurable

Due to the well-known candle-wick effect of the natural fibres [160] the application of untreated NHF reinforcement slightly reduced the LOI value of PER from 23 to 22 V/V%. This effect was compensated by flame retarded hemp fabrics: by applying THF the LOI increased by 4 V/V% compared to the NHF reinforced composite, while when applying the combined treatment, an LOI value of 28 V/V% was reached. The application of NHF slowed the horizontal burning of the HB rated PER from 32 mm/min to 18.2 mm/min. When treated fabrics were used, no horizontal burning rates could be measured, however due to flaming up to the holding clamp, the samples did not reach the V-categories.

In TEDAP-containing matrices, the LOI value was increased by 3 V/V% by the use of reinforcement, independently from the surface treatment, which can be attributed to the intense charring of the FR. The effect of the P-Si synergism, observed in the case of the LOI values in PER-based non flame retarded composites, was overwhelmed by the effect of the FR curing agent. As a general rule, the use of at least 2% P is necessary to reach V-0 [103,104]. As the application of 30% untreated fabric as reinforcement decreased the overall P-content of the composite below 2%, so the UL-94 rating was only V-1 in PER TEDAP NHF composite. When treated fabrics were applied, the P-content of the composite increased and V-0 rating was reached again.

Considering the heat release rates, when flame retarded fabrics were applied in PER, pHRR was reduced by about 25%, compared to the NHF reinforced specimen, independently of the surface treatment.

The application of FR matrix decreased the pHRR values by about 32-42%, compared to the reference matrix composites. Comparing them to each other, the effect of the different surface treatments (THF and SiTHF) is more pronounced. In the case of THF, the pHRR appeared 15 s later than in the case of NHF, and its value decreased by 15%. Using SiTHF further 10% pHRR decrease was observed, while the maximum was reached 45 s later, compared to the NHF. The application of the treated fabrics decreased the THR of the reference matrix composites. In flame retarded

matrix composites no significant difference was found between the effects of the fabrics. The amount of the residues increased when treated fabrics were applied in the reference matrix. In the case of PER TEDAP composites, the highly charring character of the applied FR matrix overwhelmed the effect of the fabric treatment, therefore the quantity of the charred residue was almost the same for all samples, approx. 10 times higher than in case of PER NHF composite.

Mechanical characterization

The tensile, bending and interfacial shear strength test results of hemp fibre reinforced composites are presented in **Table 4.5.20**.

Table 4.5.20 Tensile, bending and interfacial shear strength test results of hemp fibre reinforced composites

sample	tensile strength [MPa]	tensile modulus [GPa]	flexural strength [MPa]	flexural modulus [GPa]	interfacial shear strength [MPa]
PER NHF	66.50±3.21	3.26±0.36	92.79±10.11	4.91±0.64	13.21±2.20
PER THF	48.36±2.24	3.56±0.46	81.15±8.58	4.09±0.55	6.78±3.00
PER SiTHF	35.87±4.93	3.09±0.36	71.04±8.96	3.41±0.46	n. a.
PER TEDAP NHF	55.31±2.53	3.43±0.28	69.01±5.29	3.03±0.58	5.33±2.80
PER TEDAP THF	62.47±4.9	4.87±0.21	69.87±4.40	4.51±0.29	n. a.
PER TEDAP SiTHF	64.98±2.43	3.94±0.35	87.41±5.82	5.20±0.56	n. a.

As expected from the mechanical properties of the fabrics (see **4.5.2.1**) the tensile strength of the composites decreased in PER reference composites, if the reinforcing fabric was surface treated. Taking into account these results and the poorer mechanical properties of the FR matrix itself (see **4.4.5**), it was unanticipated that the tensile strength of the FR composites with FR treated fabrics reached that of the PER NHF reference, not only in the case of the combined treatment, but also when thermotex treatment was applied alone. Similar trend was observed comparing the flexural strengths of the different composites, indicating increased fibre-matrix adhesion in composites, where both the matrix and the fibres were flame retarded.

Comparing the tensile modulus of the reference PER composites, no significant difference was observed between the different fabrics. When both the matrix and the reinforcing fabrics were flame retarded, slightly increased values were measured. Comparing the flexural modulus values, the PER reference composites showed decreasing values with the surface treatment, while in PER TEDAP composites the values increased when the fibres were flame retarded.

In order to explain the possible synergistic effect of flame retarding both the matrix and the natural fibres with P-containing FRs, the fibre matrix adhesion was determined by means of interfacial shear strength (IFSS) measurements applying microbond test (in the case of SiTHF fabric, elemental fibres could not be prepared as the fibres were attached to each other). Among

the measurable IFSS values, the highest one was measured in the case of untreated NHF fibres with PER reference matrix. In all other cases it decreased significantly. However, when both the matrix and the fibre were flame retarded, the method was not applicable because the droplets placed on the fibres were partially absorbed by the fibre, therefore the diameter of the spread droplets became too small to be caught by the blades of the microbond device. Consequently, no pull-outs could be detected at all. This phenomenon suggests considerably increased fibre-matrix adhesion, which explains the improved tensile and flexural properties of the composites consisting of matrix and natural fibres both flame retarded with P-containing species.

4.5.3. Summary on the flame retardancy of epoxy resin composites

The flame retardancy of **sorbitol polyglycidyl ether (SPE) bioepoxy composites** was investigated applying liquid **resorcinol bis(diphenyl phosphate) (RDP)**, **solid ammonium polyphosphate (APP)**, and their **combinations**. As APP acts only in solid phase, while RDP has some minor solid phase effect as well, by adding a FR acting in the other phase, major improvements were expected in the case of APP. At ambient oxygen concentrations the **gas phase effect of RDP was essential to reduce the ignitability of the composite**: The self-extinguishing, **V-0 was not reached** in composites contrary to matrix formulations, probably due to the so called **candlewick effect** of the introduced **carbon fibres with good heat conductivity**. **In mixed FR formulations** the addition of RDP resulted in the **best overall fire performance due to the balanced gas and solid phase mechanisms.** On the other hand, as well-dispersed rigid APP particles can block the segmental movements in the cross-linked epoxy resins, the addition of **APP reduced the plasticizing effect of RDP**, compensating the decrease in T_g and storage modulus values caused by RDP.

The flame retardancy of **glucofuranoside based trifunctional epoxy monomer (GFTE) bioepoxy composites** was examined using two additive FRs (**RDP** acting mainly in gas phase and **APP** acting in solid phase), and **their combination**. As in **carbon fibre** reinforced composite the reinforcement **hinders the intumescent action of APP**, the **addition of RDP**, acting in gas phase as well, **was necessary to reach V-0 UL-94** rate in composites. In terms of heat release rate, the mixed formulation showed slightly lower performance than the APP 4% sample, but as it has a V-0 UL-94 rating, compared to the HB rating of APP 4%P sample, the **overall fire retardancy performance** of the **combined formulation** is **better**. APP compensated the plasticizing effect of low P-containing RDP, resulting in increased T_g and storage modulus values in this bioepoxy system as well.

Reactively flame retarded **cyanate ester/epoxy resin (CE/EP) carbon fibre reinforced composites** consisting of diglycidyl ether of bisphenol A (DGEBA), novolac type CE and an epoxy functional adduct of DGEBA and 9,10-dihydro-9-oxa-10-phosphaphenanthrene-10-oxide (DOPO) were

prepared and tested. The addition of **CE compensated the T_g decreasing effect of DOPO**. Reactively flame retarded CE/EP carbon fibre reinforced composites had **LOI of 48 V/V%, V-0 UL-94 rate and peak of heat release rate of 84 kW/m^2**. The addition of EP considerably increased the tensile and flexural strength of the rigid CE, which can be interpreted by the **better fibre-matrix adhesion**. Although the inclusion of the polar P-containing FR decreased the interlaminar shear strength, their values were still high above the value of the CE composite. The impact strength also increased in comparison to CE, from all composites the flame retarded ones were the least brittle.

The FR and mechanical performance of **reactively flame retarded aliphatic PER and aromatic DGEBA carbon fibre reinforced composites** was compared to their reference systems. The inclusion of carbon fibres into the resin resulted in significant increase of FR performance, though the simultaneous application of FR and carbon fibres did not lead to the improvement that could be expected on the basis of additivity, due to the **hindered intumescence caused by the plies of the reinforcing carbon fibres**. Concerning the mechanical properties, it could be concluded that the inclusion of the carbon fibres resulted in a significant amelioration, as expected. However, the application of the **polar FR** in composites **deteriorated** in most cases the **mechanical properties** in some extent.

The solution for the **simultaneous increase both in FR and mechanical performance** was the formation of **multilayer composite** consisting of reference composite core and intumescent epoxy resin coating layer. This synergistic combination lead to a composite, which **does not ignite** when subjected to 50 kW/m^2 heat flux during cone calorimeter measurements owing to the **gas and solid phase effect of the FR coating** (not hindered by the reinforcement) and **heat distribution effect of the carbon fibre reinforcement**.

Twill woven **hemp fabric reinforced PER-based epoxy resin composites** were prepared and flame retarded twofold: The curing agent was replaced by a recently synthesized **P-containing amine, TEDAP**, and the **hemp fabric was surface treated** in order **to decrease its flammability**. The modification of the fabrics led to increased LOI values and heat release rate decreased by 25% in PER composite, however **to reach V-0** UL-94 **rating** , the **flame retardancy of both the matrix and the fabrics was necessary**. Regarding the **mechanical properties** of the composites, a **possible synergistic effect** was found **when both the matrix and the fabrics contained P**: despite the poorer mechanical performance of the flame retarded matrix and the reduced strength of the surface treated fabrics, the mechanical properties of the twofold flame retarded composites reached the values of the reference composites almost in all cases. These unexpected results can be explained by the **increased fibre-matrix adhesion between the FR matrix and the treated fabrics**, as well as by their **easier wetting** in the case of more polar P-containing matrix.

5. SUMMARY OF THE RESULTS

Novel trifunctional bioepoxy monomers with high glass transition temperature were synthesized from a renewable and easily available starting material, D-glucose. The carbon fibre reinforced bioepoxy composites had better mechanical properties, than the mineral oil based ones, therefore they offer an alternative to the latter ones. It was shown that the combined gas and solid phase flame retardant mechanism is a key factor in efficient flame retardancy of epoxy resins by phosphorus-containing flame retardants. The complex gas and solid phase mechanism was reached both by the reactive flame retardant developed and by the combination of two additive flame retardants. It was demonstrated that cyanate esters can be used as multifunctional reactive modifiers acting as crosslinking agent, compensating the glass transition temperature decreasing effect of flame retardants and improving the thermal stability and mechanical properties of epoxy resins. It was found that the flammability of carbon fibre reinforced epoxy resin composites can be effectively reduced, maintaining the mechanical properties as well, with the formation of a multilayer composite consisting of a load-bearing reference composite core and an intumescent epoxy resin coating layer. The synergistic effect of the common application of phosphorus and silicone was demonstrated on the flammability of natural fibres. It was stated that for effective flame retardancy of natural fibre reinforced epoxy resin composites both the fibre and the matrix have to be flame retarded. Synergistic effect was found both in terms of flame retardancy and mechanical properties, when both the epoxy resin matrix and the natural reinforcement contained phosphorus.

The results on synthesis of polymer components (4.1.4), development and characterization of bio-based polymer matrices (4.2.3) and composites (4.3.3), as well as on flame retardancy of epoxy resins (4.4.6) and their composites (4.5.3) are summarized in more details at the end of each main chapter in the experimental results section, therefore this chapter focuses on the exploitation of these results, accompanied by the novel results summarized in the form of theses, and last but not least the further tasks are discussed.

5.1. Exploitation of the results

The results summarized in this work were achieved in the frame of Hungarian and international projects listed in **chapter 6**. During the work carried out the industrial applicability of the results was considered to be essential, both in the case of new polymer components developed and novel composite materials investigated.

There is a continuous demand on P-containing flame retardants and consequently novel and improved methods for their synthesis are also of great industrial importance. The novel simple, cost-effective and environmentally friendly method for preparation amine functional phosphoric amides, elaborated by the author and her co-workers was protected by PCT patent in 2009, after the Hungarian patent filed in 2007 [**133**]. The synthesis of the P-containing amine type hardeners was optimized and scaled up in a computer controlled 1L reactor. Among the P-containing amines synthesized using this patented method, *N,N',N''*-tris(2-aminoethyl)phosphoric triamide (TEDAP) found its use not only as FR and crosslinking agent for epoxy resins [**211**, **224**], but also as base material for pH-reversible supramolecular hydrogels [232] and for preparation and stabilization of gold nano- and microcrystals [233].

As according to the literature [126,134], it is not trivial that the reaction between a tertiary phosphoric ester and diamines, in particular, in the case of TEDAP the reaction of triethyl phosphate and ethylene diamine would take place, the Fourier transform infrared (FT-IR) vibrational spectra of TEDAP were modelled to support the identification of this novel compound [**192**]. The molecular geometry and vibrational wavenumbers of TEDAP in its ground state have been calculated by using Density Functional Theory/B3LYP and Hartree-Fock functionals with 6-31++G (d,p) basis set. The obtained vibrational wavenumbers and optimized geometric parameters were seen to be in good agreement with the experimental data. The calculated results also serve as a basis for the identification of other amine functional phosphoric amide derivatives synthesized with this method.

Concerning the FR effect of TEDAP, a mathematical model was developed to describe the degradation of reference and flame retarded epoxy resins initiated by a constant heat flux under mass loss calorimeter test conditions [**234**,**235**]. The applied model describes both the heat and mass changes of a polymer layer with finite thickness and predicts the whole temperature and pressure profiles of the system. It is assumed that the polymer degrades to a fixed mass of char and volatile gas in an instantaneous step, at the moment when the temperature reaches a critical value. The most important heat transport mechanism is conduction, which dominates the temperature profile. The mass transport of gas is described by Darcy's law, with a simplifying condition that the overall solid volume is constant during degradation. The transport processes have been modelled in one spatial dimension. Experiments in mass loss calorimeter and computer simulations have been carried out to establish the effects of critical parameters such as layer thickness, heat flux and material properties. The predicted ignition times and critical temperatures were in good agreement with the experimental data. Furthermore it could be concluded that the heat capacity of polymer does not have any effect on the temperature profile of the preheating

process, it determines the preheating time instead. The effect of re-radiated combustion heat was established and it has been found that the amount of absorbed pyrolysis heat is an important factor in the degradation model.

The results achieved in the field of bioepoxy composites were used in prototype development for Dassault Aviation in the relevant Clean Sky EU7 project. As composite sandwich structures play important role in aeronautical applications, especially in case of indoor elements (e.g. aircraft floors, ceilings, sidewalls and storage compartments), our aim was to compare the properties of sandwich composite structures prepared from polymethacrylimide foam, a core material preferred in aeronautical applications, using DGEBA and GFTE as matrices, cured with AR917 anhydride type curing agent. Jute fibre reinforcement was used to reach as high as possible renewable ratio in composite sandwich structures. In case of indoor elements the flexural strength and modulus are the most important properties; therefore three point bending tests were carried out on the sandwich composites.

According to the test results [**204**] both in the case of 6.5 and 20 mm thick core, after the bending stress value reached a maximum, it started to decrease due to the failure of the upper composite layer of the sandwich composite structure. After that two different phenomena took place: In the case of the 6.5 mm core, the bending stress decreased further, while with 20 mm core, the bending stress increased until the breaking of the specimen. Two different types of failure occurred: in the case of the 6.5 mm core, when the sandwich structure broke, the specimen stayed together (non-catastrophic failure), while in the case of the 20 mm core, the failure of the specimens was catastrophic. In the case of the 6.5 mm core, the thin core had higher force intermediary and low damping properties, than the 20 mm core. It lead to a decreasing force, resulting in non-catastrophic failure at the end of the bending tests. GFTE sandwich composites with 6.5 mm core had significantly better average flexural properties than the DGEBA composites (flexural strength: GFTE – 55.07±1.20 MPa; DGEBA – 44.22±3.94 MPa, flexural modulus: GFTE – 33.93±0.10 GPa; DGEBA – 3.67±0.09 GPa). In the case of the GFTE composites, the average flexural strength was 24%, and the average flexural modulus was 7% higher than with DGEBA, respectively. With 20 mm core the DGEBA composite had 15% higher flexural strength, the modulus values were in the same range (flexural strength: GFTE – 13.48±0.36 MPa; DGEBA – 15.90±0.32 MPa, flexural modulus: GFTE – 0.68±0.02 GPa; DGEBA – 0.70±0.03 GPa).

The reason behind these results is the different polarity of DGEBA and GFTE epoxy matrices. As the applied polymethacrylimide core material is polar, the more polar epoxy resin leads to better impregnation at the phase boundary of the foam. The polarity of the epoxy resins was quantified by the topological polar surface area (TPSA) method according to Ertl et al. [236]. This method was

developed for quantitative characterization of the polarity of potential drug candidate molecules in order to predict if they can pass the blood-brain barrier, however, it proved to be suitable for the comparison of the polarity of polymer components as well. According to TPSA calculations GFTE has twice as much TPSA as DGEBA (92.99 vs. 43.52), therefore in the case of the thinner core material with better load transfer capabilities, the better impregnation lead to better flexural properties in the case of the GFTE sandwich composite.

Based on these results, the bio-based GFTE can replace the DGEBA EP component in the sandwich composite structures, with jute fibre reinforcement, especially in the case of the thinner cores, for example the 6.5 mm one. No interfacial failure between the composite layers and the core material was observed, which indicates a good adhesion between the composite resin system and the core foam.

The prepared GFTE sandwich composites were used for Falcon business jet cabin applications by Dassault Aviation (**Figure 5.1.2**).

Figure 5.1.2 Aircraft cabinet prototype prepared by Dassault Aviation using GFTE bioepoxy sandwich composites

5.2. Theses

The new scientific achievements of the experimental work, categorized into new bio-based epoxy resins and composites, and new green flame retardancy solutions, are the followings:

NEW BIO-BASED EPOXY RESINS AND COMPOSITES:

Thesis 1. Synergistic combination of epoxidized soybean oil with aliphatic epoxy resins [195,198]

In contrast to aromatic diglycidyl ether of bisphenol-A (DGEBA) epoxy resin, in aliphatic triglycidyl ether of glycerol (GER) and tetraglycidyl ether of pentaerythritol (PER) resins the addition of epoxidized soybean oil (ESO) proved to be synergistic in terms of glass transition temperature and storage modulus. Aliphatic resins cure at lower temperatures than ESO, therefore the already

cured aliphatic parts apply pressure on the uncured ESO parts, shifting the beginning of the segmental movements in the cured ESO parts to higher temperature, which leads to higher glass transition temperature in ESO-aliphatic resin blends. The mechanical properties of jute fibre reinforced aliphatic epoxy resin composites containing 25% ESO approach the properties of the reference DGEBA composite. In those applications where the glass transition temperature of the blends - lower than in the case of DGEBA, but higher than that of ESO and aliphatic resins itself - is appropriate; DGEBA can be replaced by 25% ESO-containing aliphatic epoxy resin blends in jute fibre reinforced composites.

Thesis 2. Sugar based bioepoxy monomers [175,196]

Glucopyranoside-based bi-, tri- and tetrafunctional, as well as glucofuranoside-based trifunctional bioepoxy monomers were synthesized from an inexpensive, renewable and easily available starting material, D-glucose. The applicability of the synthesized compounds as epoxy monomers was confirmed by differential scanning calorimetry (DSC) curing probes with a model aromatic amine type hardener (4,4'-diamino diphenyl methane). Based on the determined degree of cure, glass transition temperature and thermal stability, the glucopyranoside- and glucofuranoside-based trifunctional ones proved to be the most promising, therefore their extensive characterization was carried out using methyltetrahydrophthalic anhydride and diethyl-methylbenzene-diamine crosslinking agents, commonly used in high-tech applications. By systematically altering the crosslinking conditions, the heat treatment cycle necessary to obtain the highest possible degree of curing was determined. Due to their higher functionality, the trifunctional bioepoxy monomers provided higher glass transition temperature than the benchmark diglycidyl ether of bisphenol A (DGEBA) resin both with methyltetrahydrophthalic anhydride and diethyl-methylbenzene-diamine crosslinking agent. Both bioresins had lower tensile and flexural strength, and similar modulus values as DGEBA. In applications where bending stresses are dominant over the tensile ones, and outstanding glass transition temperature is required, the developed sugar based resins offer a feasible renewable choice.

Thesis 3. Sugar based bioepoxy composites [204]

Jute and carbon fibre reinforced glucofuranoside-based trifunctional bioepoxy (GFTE) composites were prepared and characterized. When diethyl-methylbenzene-diamine, providing high glass transition temperature, was used as crosslinking agent, in the case of jute fibres similar, while with carbon fibres better mechanical properties were achieved in bioepoxy composites than in DGEBA composites, used as benchmark material in aeronautical applications. Based on the results, it can

be stated that the new glucose-based epoxy monomer may be a renewable alternative to DGEBA both in the case of jute and carbon fibre reinforcement, even in high temperature applications up to 160 ° C. For the first time, the topological polar surface area method was used for the numerical characterization of the polarity of polymer monomers as DGEBA and GFTE. In the case of a jute fibre reinforced sandwich composite structure containing a polar core material, the higher polarity of GFTE lead to better impregnation of the core and thus greater flexural strength and modulus than in the case of the less polar DGEBA.

Thesis 4. Alkali treatment of jute fibres [198,199]

Based on a systematic study, it was found, that due to the alkali treatment the maximal force values, necessary to break the elemental fibres during the strip tensile test of jute fabrics, mostly decreased or only increased within the scattering range, therefore, the alkali treatment of jute fibres, generally applied before composite preparation, can be omitted. Although the removal of hemicellulose and lignin leads to a rougher and bigger fibre surface, consequently better interfacial properties and higher glass transition temperatures in composites reinforced with treated fibres; the lower tensile strength of the fibres and the thermal degradation of the cellulose fraction shifted to lower temperatures due to the residual alkali ions, make the application of the treated fibres altogether less favourable than that of the untreated ones.

GREEN FLAME RETARDANCY SOLUTIONS

Thesis 5. Epoxy resins: combined gas and solid phase action of flame retardants [191,193,220,221,225]

It was demonstrated that the combined gas- and solid phase flame retardant mechanism is a key factor in efficient flame retardancy of epoxy resins by phosphorus-containing flame retardants. The complex gas- and solid phase mechanism was reached both by a reactive flame retardant, *N,N',N''*-tris(2-aminoethyl) phosphoric triamide, and by the combination of two additive flame retardants: resorcinol bis(diphenyl phosphate) (RDP), acting mainly in the gas phase as radical scavenger and ammonium polyphosphate (APP), acting as intumescent type flame retardant in the solid phase. Synergistic effect in terms of flame retardancy was proved between the inorganic APP and the organophosphorus RDP, when applied in combination both in aliphatic and cycloaliphatic bioepoxy resins and their carbon fibre reinforced composites, respectively. In sorbitol polyglycidyl ether bioepoxy resin formulations applying RDP or APP alone showed increased limiting oxygen index (LOI) values, however, their UL-94 ratings remained HB. When the same amount of P originated from the two additives, V-0, self-extinguishing rating and LOI value of 34 V/V% was

reached and the peak heat release rate of SPE could be lowered by approx. 60%. The assumed balanced gas- and solid phase mechanism was confirmed by thermogravimetric analysis, Fourier transform infrared spectrometry of the gases formed during laser pyrolysis, attenuated total reflection-infrared spectrometry of the charred residues, as well as by mechanical testing of the char obtained after combustion.

Thesis 6. Flame retarded epoxy resins: cyanate esters as multifunctional reactive modifiers [189,190]

It was demonstrated that cyanate esters can be used as multifunctional reactive modifiers acting as crosslinking agent, compensating the glass transition temperature decreasing effect of flame retardants and improving the thermal stability and mechanical properties of epoxy resins. In a hybrid system consisting of DGEBA (diglycidyl ether of bisphenol A), novolac type cyanate ester and a reactive DGEBA - 9,10-dihydro-9-oxa-10-phosphaphenantrene-10-oxide (DOPO) adduct, at 2% P-content 30%, while at 3% P-content 40% of cyanate ester was necessary to compensate the glass transition temperature decreasing effect of DOPO. All flame retarded hybrid blends exhibited intensive intumescent charring, reached the V-0 UL-94 classification, as high LOI as 45 V/V%, and their peak heat release rate (pHRR) values were lowered by 75% and in carbon fibre reinforced composites by 90%.

Thesis 7. Carbon fibre reinforced epoxy resin composite with intumescent coating [224]

It was demonstrated that the flammability of carbon fibre reinforced epoxy resin composites can be effectively reduced, maintaining the mechanical properties as well, with the formation of a multilayer composite consisting of a load-bearing reference composite core and an intumescent epoxy resin coating layer. It was stated, that by the application of the polar flame retardant in a separate layer, the decrease of fibre-matrix adhesion and consequent reduction of mechanical properties can be avoided; the catastrophic deterioration of the residual mechanical properties due to the delamination caused by intumescence in case of accidental fire can be prevented; furthermore, unlimited charring is assured at the surface of the composite during the solid phase flame retardancy. This multilayer approach proved to be synergistic in terms of flame retardancy: the composite consisting of carbon fibre reinforced diglycidyl ether of bisphenol A core and tetraglycidyl ether of pentaerythritol - N,N',N"-tris(2-aminoethyl)-phosphoric triamide intumescent coating did not ignite at all under standard mass loss calorimeter test conditions. The total absence of ignition was explained by the combined gas- and solid phase effect of flame

retardant coating, the latter one not hindered by the reinforcement, and the heat distribution effect of the carbon fibre reinforcement.

Thesis 8. Combined surface treatment of natural fibres [229]

By comparing the effects of thermotex procedure (i.e. removal of adsorbed water from the capillaries and then filling the micro/nano-voids with phosphoric acid) and sol-gel treatment with amine-type silanes followed by thermotex treatment on the flammability of hemp fibres, the synergistic effect of the common application of phosphorus and silicone was demonstrated. The combined treatment increased the time to ignition from 3 s to 15 s, decreased the peak heat release rate from 68 kW/m^2 to 9 kW/m^2 and led to the formation of consistent char instead of fluffy, light ash in case of untreated fabrics and thermotex treated fabrics. Furthermore, as the sol-gel treatment partially protected the cellulose structure from the acidic hydrolysis, it increased the initial decomposition temperature by 30 °C and decreased the maximal decomposition rate by 20% compared to thermotex treatment applied alone. Based on these results, not only the flame retardancy, but also of the low thermal stability and susceptibility to various chemicals of natural fibres was successfully addressed by the combined treatment.

Thesis 9. Natural fibre reinforced epoxy resin composites: combined flame retardancy of matrix and natural fibres [229]

It was demonstrated that for effective flame retardancy of natural fibre reinforced epoxy resin composites both the fibre and the matrix have to be flame retarded. Synergistic effect was found both in terms of flame retardancy and mechanical properties, when both the epoxy resin matrix and the natural reinforcement contained phosphorus. In hemp fabric reinforced tetraglycidyl ether of pentaerythritol (PER) based composites, when the curing agent was replaced by *N,N′,N″*-tris(2-aminoethyl)-phosphoric triamide and the hemp reinforcement was sol-gel and thermotex treated, self-extinguishing V-0 UL-94 rate was reached, furthermore, despite the poorer mechanical performance of the flame retarded matrix and the reduced strength of the surface treated fabrics, the mechanical properties of the twofold flame retarded composites reached the values of the reference composites almost in all cases. These results can be explained by the increased fibre-matrix adhesion between the flame retarded matrix and the treated fabrics, as well as by their easier wetting in the case of more polar phosphorus-containing matrix.

5.3. Further tasks

The work presented raised several further questions to be answered and initiated further research tasks, which may contribute to the utilization of the elaborated solutions.

After up-scaling of the synthesis of the developed sugar based bioepoxy resins, their more detailed characterization (including e.g. water uptake, UV-stability, biodegradability) will be possible. Also, more detailed mechanical characterization of carbon fibre and jute fibre reinforced sugar based bioepoxy composites will be feasible (including e.g. interlaminar shear strength, instrumented falling weight impact).

In the case of all-bio jute fibre reinforced bioepoxy composites also the use of bio-based hardeners, as itaconic acid anhydride is foreseen. Preliminary experiments were also performed to synthesize amine functional counterparts of the prepared sugar based resins, so that fully sugar based epoxy resin systems could be established. A further step forward would be the synthesis of phosphorus-containing sugar based amine type compounds, which would act both as hardener and flame retardant in epoxy resins.

In the case of these all-bio composites the potential biodegradability is an important feature to be examined. On the one hand it would provide a clear advantage, but it also raises several issues to be addressed as optimal relationship between biodegradability and recyclability, as well as accurate design and prediction of lifetime, furthermore risks of applying common additives, as flame retardants in biodegradable composites.

Concerning the manufacturing techniques of composites, mainly hand-layup followed by hot pressing was used to ensure reproducibility and high fibre content. In order to increase the competitiveness, other advanced techniques as resin transfer moulding (RTM) and vacuum-assisted transfer moulding (VRTM) are considered. In the case of these processing methods, however, it has to be taken into consideration that solid additives, as some usual additive type flame retardants can be filtered out by the reinforcing fabric, therefore application of liquid flame retardants can be more flawlessly integrated into the manufacturing process. Liquid phase additives are also preferred from viscosity point of view.

6. RESEARCH PROJECTS CONNECTED TO THE TOPIC OF THE THESIS

The scientific achievements summarized in this thesis greatly contributed to the successful accomplishment of the Hungarian and international research projects listed below.

6.1. Hungarian research projects

2015 - 2018 Multifunctional Bio-based Hybrid Thermosets: Synthesis, Characterization and Potential Use in Composites Hungarian project (identification number: 114547)

2013 - 2016 Development of flame retarded composites of reduced additive content for upgrading of recycled PET Hungarian project (identification number: 109224)

2011 - 2014 Development and characterization of epoxy resin-based shape memory polymer (SMP) systems Hungarian project (identification number: 83421)

2009 - 2011 Development of polymer nano- and biocomposites of designed stability and controlled technology for their production Hungarian project (identification number: 76346)

2009 - 2011 Development of a novel polymer composite of advanced recyclability for large series production Hungarian project (identification number: 75117)

2009 - 2011 Development of technologies for utilization of organic materials from car and electronic waste for avoiding future landfill dumping project in Jedlik Ányos Program (identification number: OM-00278/2008)

2008 - 2011 Preparation and realization of transport safety innovations in production of prototype of new 4 person composite aircraft project in Jedlik Ányos Program (identification number: OM-00168/2008)

2005 - 2008 Investigation of new synthetic pathways for environmental flame retardants and their mechanism of action Hungarian project (identification number: 49121)

6.2. International research projects

2012 - 2014 Development of an innovative bio-based resin for aeronautical applications (Clean Sky) EU7 project (identification number: 298090), topic manager: Dassault Aviation

2010 - 2012 Resin, Laminate and Industrial Nanoparticles Concept and Application. Industrialization (Clean Sky) EU7 project (identification number: 270599), topic manager: Airbus Defence and Space

2009 - 2010 Recycling of polymer and polymer composites for industrial applications Polish-Hungarian project (identification number: PL-9/08)

2008 - 2012 Magnetic sorting and ultrasound sensor technologies for production of high purity secondary polyolefins from waste (W2PLASTICS) EU7 project (identification number: 212782)

2008 - 2009 Development of Natural Fibre based Composites for Automotive Applications Indian-Hungarian project (identification number: IND-7/2006)

2007 - 2010 Innovative sensor-based processing technology of nanostructured multifunctional hybrids and composites (MULTIHYBRIDS) EU6 project (identification number: IP 026685-2)

2004 - 2007 Environmentally friendly multifunctional fire retardant polymer hybrids and nanocomposites (NANOFIRE) EU6 project (identification number: IP 026685-2)

2000 - 2003 New surface modified flame retarded polymeric systems to improve safety in transportation and other areas (FLAMERET) EU5 project (identification number: G5RD-CT-1999-00120)

7. REFERENCES

In the list of references the publications belonging to the author of this thesis are highlighted with bold numbers.

[1] Bruins PF. Epoxy resin technology. New York: Interscience; 1968.

[2] May CA. Epoxy resins. New York: Dekker; 1988.

[3] Ellis B. Chemistry and Technology of Epoxy Resins, London: Blackie, Academic and Professional; 1993.

[4] Mohanty AK, Misra M, Drzal LT, Selke SE, Harte BR, Hinrichsen G. Natural fibers, biopolymers, and biocomposites: An Introduction. In: Mohanty AK, Misra M, Drzal LT, editors. Natural fibers, biopolymers, and biocomposites, Boca Raton: Taylor & Francis Group; 2009, 1–36.

[5] Soroudi A, Jakubowicz I. Recycling of bioplastics, their blends and biocomposites: A review. European Polymer Journal 2013;49:2839–58. http://doi.org/10.1016/j.eurpolymj.2013.07.025.

[6] Pickering SJ. Recycling technologies for thermoset composite materials—current status. Composites Part A: Applied Science and Manufacturing 2006;37:1206–15. http://doi.org/10.1016/j.compositesa.2005.05.030.

[7] Boyle MA, Martin CJ, Neuner JD. Epoxy resins. In: Miracle DB, Donaldson SL, editors. ASM Handbook Volume 21: Composites. Materials Park: ASM International; 2001.

[8] Directive 2002/95/EC on Restriction of certain hazardous Substances in Electric and Electronic Equipment. Official Journal of the European Union 2003;37:19-23. http://eur-lex.europa.eu/LexUriServ/LexUriServ.do?uri=CELEX:32002L0095:EN:HTML

[9] van der Veen I, de Boer J. Phosphorus flame retardants: Properties, production, environmental occurrence, toxicity and analysis. Chemosphere 2012;88:1119–53. http://doi.org/10.1016/j.chemosphere.2012.03.067.

[10] Auvergne R, Caillol S, David G, Boutevin B, Pascault J-P. Biobased Thermosetting Epoxy: Present and Future. Chemical Reviews 2014;114:1082–115. http://doi.org/10.1021/cr3001274.

[11]Chapin RE, Adams J, Boekelheide K, Gray LE, Hayward SW, Lees PSJ, et al. NTP-CERHR expert panel report on the reproductive and developmental toxicity of bisphenol A. Birth Defects Research Part B: Developmental and Reproductive Toxicology 2008;83:157–395. http://doi.org/10.1002/bdrb.20147.

[12] Raquez J-M, Deléglise M, Lacrampe M-F, Krawczak P. Thermosetting (bio)materials derived from renewable resources: A critical review. Progress in Polymer Science 2010;35:487–509. http://doi.org/10.1016/j.progpolymsci.2010.01.001.

[13] Wang R. Schuman TP. Vegetable oil-derived epoxy monomers and polymer blends: A comparative study with review. Express Polymer Letters 2013;7:272–92. http://doi.org/10.3144/expresspolymlett.2013.25.

[14] Sarwono A, Man Z, Bustam MA. Blending of Epoxidised Palm Oil with Epoxy Resin: The Effect on Morphology, Thermal and Mechanical Properties. Journal of Polymers and the Environment 2012;20:540–9. http://doi.org/10.1007/s10924-012-0418-5.

[15] Seniha Güner F, Yağcı Y, Tuncer Erciyes A. Polymers from triglyceride oils. Progress in Polymer Science 2006;31:633–70. http://doi.org/10.1016/j.progpolymsci.2006.07.001.

[16] Guenter S, Rieth R, Rowbotton KT. Ullmann's Encyclopedia of Industrial Chemistry, New York: Wiley, 2003;12:269–284

[17] Rangarajan B, Havey A, Grulke EA, Culnan PD. Kinetic parameters of a two-phase model forin situ epoxidation of soybean oil. Journal of the American Oil Chemists' Society 1995;72:1161–9. http://doi.org/10.1007/bf02540983.
[18] Kim JR, Sharma S. The development and comparison of bio-thermoset plastics from epoxidized plant oils. Industrial Crops and Products 2012;36:485–99. http://doi.org/10.1016/j.indcrop.2011.10.036.
[19] Ratna D. Mechanical properties and morphology of epoxidized soyabean-oil-modified epoxy resin. Polymer International 2001;50:179–84. http://doi.org/10.1002/1097-0126(200102)50:2<179::aid-pi603>3.3.co;2-5.
[20] Zhu J, Chandrashekhara K, Flanigan V, Kapila S. Curing and mechanical characterization of a soy-based epoxy resin system. Journal of Applied Polymer Science 2004;91:3513–8. http://doi.org/10.1002/app.13571.
[21] Earls JD, White JE, López LC, Lysenko Z, Dettloff ML, Null MJ. Amine-cured ω-epoxy fatty acid triglycerides: Fundamental structure–property relationships. Polymer 2007;48:712–9. http://doi.org/10.1016/j.polymer.2006.11.060.
[22] Li J, Du Z, Li H, Zhang C. Porous epoxy monolith prepared via chemically induced phase separation. Polymer 2009;50:1526–32. http://doi.org/10.1016/j.polymer.2009.01.049.
[23] Mustata F, Tudorachi N, Rosu D. Curing and thermal behavior of resin matrix for composites based on epoxidized soybean oil/diglycidyl ether of bisphenol A. Composites Part B: Engineering 2011;42:1803–12. http://doi.org/10.1016/j.compositesb.2011.07.003.
[24] Park S-J, Jin F-L, Lee J-R. Thermal and mechanical properties of tetrafunctional epoxy resin toughened with epoxidized soybean oil. Materials Science and Engineering: A 2004;374:109–14. http://doi.org/10.1016/j.msea.2004.01.002.
[25] Park S-J, Jin F-L, Lee J-R. Effect of Biodegradable Epoxidized Castor Oil on Physicochemical and Mechanical Properties of Epoxy Resins. Macromolecular Chemistry and Physics 2004;205:2048–54. http://doi.org/10.1002/macp.200400214.
[26] Gerbase AE, Petzhold CL, Costa APO. Dynamic mechanical and thermal behavior of epoxy resins based on soybean oil. Journal of the American Oil Chemists' Society 2002;79:797–802. http://doi.org/10.1007/s11746-002-0561-z.
[27] Miyagawa H, Misra M, Drzal LT, Mohanty AK. Fracture toughness and impact strength of anhydride-cured biobased epoxy. Polymer Engineering & Science 2005;45:487–95. http://doi.org/10.1002/pen.20290.
[28] Altuna FI, Espósito LH, Ruseckaite RA, Stefani PM. Thermal and mechanical properties of anhydride-cured epoxy resins with different contents of biobased epoxidized soybean oil. Journal of Applied Polymer Science 2010;120:789–98. http://doi.org/10.1002/app.33097.
[29] Gupta AP, Ahmad S, Dev A. Modification of novel bio-based resin-epoxidized soybean oil by conventional epoxy resin. Polymer Engineering & Science 2011;51:1087–91. http://doi.org/10.1002/pen.21791.
[30] Karger-Kocsis J, Grishchuk S, Sorochynska L, Rong MZ. Curing, gelling, thermomechanical, and thermal decomposition behaviors of anhydride-cured epoxy (DGEBA)/epoxidized soybean oil compositions. Polymer Engineering & Science 2013;54:747–55. http://doi.org/10.1002/pen.23605.

[31] Lora JH, Glasser WG. Recent industrial applications of lignin: a sustainable alternative to nonrenewable materials. Journal of Polymers and the Environment 2002;10:39–48. http://doi.org/10.1023/a:1021070006895.
[32] Effendi A, Gerhauser H, Bridgwater A V. Production of renewable phenolic resins by thermochemical conversion of biomass: A review. Renewable and Sustainable Energy Reviews 2008;12:2092–116. http://doi.org/10.1016/j.rser.2007.04.008.
[33] Pan H. Synthesis of polymers from organic solvent liquefied biomass: A review. Renewable and Sustainable Energy Reviews 2011;15:3454–63. http://doi.org/10.1016/j.rser.2011.05.002.
[34] Sun G, Sun H, Liu Y, Zhao B, Zhu N, Hu K. Comparative study on the curing kinetics and mechanism of a lignin-based-epoxy/anhydride resin system. Polymer 2007;48:330–7. http://doi.org/10.1016/j.polymer.2006.10.047.
[35] Feng P, Chen F. Preparation and characterization of acetic acid lignin-based epoxy blends, BioResources 2012; *7(3)*:2860-2870.
[36] Zhao B, Chen G, Liu Y, Hu K, Wu R. Synthesis of lignin base epoxy resin and its characterization. Journal of Materials Science Letters 2001;20:859–62. http://doi.org/10.1023/a:1010975132530.
[37] Kishi H, Fujita A, Wood-based epoxy resins and the ramie fiber reinforced composites, Environmental Engineering and Management Journal 2008;7(5):517-523.
[38] Kishi H, Fujita A, Miyazaki H, Matsuda S, Murakami A. Synthesis of wood-based epoxy resins and their mechanical and adhesive properties. Journal of Applied Polymer Science 2006;102:2285–92. http://doi.org/10.1002/app.24433.
[39] Asano T, Kobayashi M, Tomita B, Kajiyama M. Syntheses and properties of liquefied products of ozone treated wood/epoxy resins having high wood contents. Holzforschung 2007;61. http://doi.org/10.1515/hf.2007.003.
[40] Kishi H, Akamatsu Y, Noguchi M, Fujita A, Matsuda S, Nishida H. Synthesis of epoxy resins from alcohol-liquefied wood and the mechanical properties of the cured resins. Journal of Applied Polymer Science 2010;120:745–51. http://doi.org/10.1002/app.33199.
[41] Hofmann K, Glasser WG. Engineering Plastics from Lignin. 21. 1 Synthesis and Properties of Epoxidized Lignin-Poly (Propylene Oxide) Copolymers . Journal of Wood Chemistry and Technology 1993;13:73–95. http://doi.org/10.1080/02773819308020508.
[42] Haettenschwiler S, Hagerman AE, Vitousek PM, Polyphenols in litter from tropical montane forests across a wide range in soil fertility. Biogeochemistry 2003;64:129-148. http://doi.org/10.1023/A:1024966026225
[43] Khanbabaee K, van Ree T. ChemInform Abstract: Tannins: Classification and Definition. ChemInform 2010;33. http://doi.org/10.1002/chin.200213268.
[44] Benyahya S, Aouf C, Caillol S, Boutevin B, Pascault JP, Fulcrand H. Functionalized green tea tannins as phenolic prepolymers for bio-based epoxy resins. Industrial Crops and Products 2014;53:296–307. http://doi.org/10.1016/j.indcrop.2013.12.045.
[45] Aouf C, Benyahya S, Esnouf A, Caillol S, Boutevin B, Fulcrand H. Tara tannins as phenolic precursors of thermosetting epoxy resins. European Polymer Journal 2014;55:186–98. http://doi.org/10.1016/j.eurpolymj.2014.03.034.

[46] Nouailhas H, Aouf C, Le Guerneve C, Caillol S, Boutevin B, Fulcrand H. Synthesis and properties of biobased epoxy resins. part 1. Glycidylation of flavonoids by epichlorohydrin. Journal of Polymer Science Part A: Polymer Chemistry 2011;49:2261–70. http://doi.org/10.1002/pola.24659.
[47] Boutevin B, Caillol S, Burguiere C, Rapior S, Fulcrand H, Nouailhas H, Novel methods for producing thermosetting epoxy resins, US 20120165429 A1, 2012.
[48] Aouf C, Nouailhas H, Fache M, Caillol S, Boutevin B, Fulcrand H. Multi-functionalization of gallic acid. Synthesis of a novel bio-based epoxy resin. European Polymer Journal 2013;49:1185–95. http://doi.org/10.1016/j.eurpolymj.2012.11.025.
[49] Sultania M, Rai JSP, Srivastava D. Process modeling, optimization and analysis of esterification reaction of cashew nut shell liquid (CNSL)-derived epoxy resin using response surface methodology. Journal of Hazardous Materials 2011;185:1198–204. http://doi.org/10.1016/j.jhazmat.2010.10.031.
[50] Vasapollo G, Mele G, Del Sole R. Cardanol-Based Materials as Natural Precursors for Olefin Metathesis. Molecules 2011;16:6871–82. http://doi.org/10.3390/molecules16086871.
[51]Voirin C, Caillol S, Sadavarte N V, Tawade B V, Boutevin B, Wadgaonkar PP. Functionalization of cardanol: towards biobased polymers and additives. Polymer Chemistry 2014;5:3142–62. http://doi.org/10.1039/c3py01194a.
[52] Devi A, Srivastava D. Studies on the blends of cardanol-based epoxidized novolac type phenolic resin and carboxyl-terminated polybutadiene (CTPB), I. Materials Science and Engineering: A 2007;458:336–47. http://doi.org/10.1016/j.msea.2006.12.081.
[53] Unnikrishnan KP, Thachil ET. Synthesis and Characterization of Cardanol-Based Epoxy Systems. Designed Monomers & Polymers 2008;11:593–607. http://doi.org/10.1163/156855508x363870.
[54] Ionescu M, Petrovic Z. Phenolation of vegetable oils. Journal of the Serbian Chemical Society 2011;76:591–606. http://doi.org/10.2298/jsc100820050i.
[55] Kim YH, An ES, Park SY, Song BK. Enzymatic epoxidation and polymerization of cardanol obtained from a renewable resource and curing of epoxide-containing polycardanol. Journal of Molecular Catalysis B: Enzymatic 2007;45:39–44. http://doi.org/10.1016/j.molcatb.2006.11.004.
[56] Braddock RJ. Handbook of Citrus By-Products and Processing Technology, Ocala: Florida Science Source, 2000.
[57] Sellers RF. Epoxy resins from polyhydric phenol-terpene addition products. U.S. 3378525, 1968
[58] Xu K, Chen M, Zhang K, Hu J. Synthesis and characterization of novel epoxy resin bearing naphthyl and limonene moieties, and its cured polymer. Polymer 2004;45:1133–40. http://doi.org/10.1016/j.polymer.2003.12.035.
[59] Liu XQ, Huang W, Jiang YH, Zhu J, Zhang CZ. Preparation of a bio-based epoxy with comparable properties to those of petroleum-based counterparts. Express Polymer Letters 2012;6:293–8. http://doi.org/10.3144/expresspolymlett.2012.32.
[60] Mantzaridis C, Brocas A-L, Llevot A, Cendejas G, Auvergne R, Caillol S, et al. Rosin acid oligomers as precursors of DGEBA-free epoxy resins. Green Chemistry 2013;15:3091. http://doi.org/10.1039/c3gc41004h.

[61] Kricheldorf HR. “Sugar Diols” as Building Blocks of Polycondensates. Journal of Macromolecular Science, Part C: Polymer Reviews 1997;37:599–631. http://doi.org/10.1080/15321799708009650.
[62] Varela O, Orgueira HA. Synthesis of chiral polyamides from carbohydrate-derived monomers. Advances in Carbohydrate Chemistry and Biochemistry 2000:137–74. http://doi.org/10.1016/s0065-2318(00)55005-7.
[63] Okada M. Molecular design and syntheses of glycopolymers. Progress in Polymer Science 2001;26:67–104. http://doi.org/10.1016/s0079-6700(00)00038-1.
[64] Varma AJ, Kennedy JF, Galgali P. Synthetic polymers functionalized by carbohydrates: a review. Carbohydrate Polymers 2004;56:429–45. http://doi.org/10.1016/j.carbpol.2004.03.007.
[65] Galbis JA, García-Martín MG. Synthetic Polymers from Readily Available Monosaccharides. Carbohydrates in Sustainable Development II 2010:147–76. http://doi.org/10.1007/128_2010_57.
[66] Wang Q, Dordick JS, Linhardt RJ. Synthesis and Application of Carbohydrate-Containing Polymers. Chemistry of Materials 2002;14:3232–44. http://doi.org/10.1021/cm0200137.
[67] Huijbrechts AML, Huang J, Schols HA, van Lagen B, Visser GM, Boeriu CG, et al. 1-allyloxy-2-hydroxy-propyl-starch: Synthesis and characterization. Journal of Polymer Science Part A: Polymer Chemistry 2007;45:2734–44. http://doi.org/10.1002/pola.22029.
[68] Huijbrechts AML, Haar R ter, Schols HA, Franssen MCR, Boeriu CG, Sudhölter EJR. Synthesis and application of epoxy starch derivatives. Carbohydrate Polymers 2010;79:858–66. http://doi.org/10.1016/j.carbpol.2009.10.012.
[69] Burton SC, Harding DRK. Bifunctional etherification of a bead cellulose for ligand attachment with allyl bromide and allyl glycidyl ether. Journal of Chromatography A 1997;775:29–38. http://doi.org/10.1016/s0021-9673(97)00130-1.
[70] Katz M, Reese ET. Production of glucose by enzymatic hydrolysis of cellulose, Applied Microbiology 1968;16(2):419-420
[71] Onda A, Ochi T, Yanagisawa K. Selective hydrolysis of cellulose into glucose over solid acid catalysts. Green Chemistry 2008;10:1033. http://doi.org/10.1039/b808471h.
[72] Nagamori M, Funazukuri T. Glucose production by hydrolysis of starch under hydrothermal conditions. Journal of Chemical Technology and Biotechnology 2004;79:229–33. http://doi.org/10.1002/jctb.976.
[73] Kearsley MW, Dziedzic SZ. Handbook of Starch Hydrolysis Products and their Derivatives, Heidelberg: Springer Science & Business Media; 1995.
[74] Shibata M, Yoshihara S, Yashiro M, Ohno Y. Thermal and mechanical properties of sorbitol-based epoxy resin cured with quercetin and the biocomposites with wood flour. Journal of Applied Polymer Science 2012;128:2753–8. http://doi.org/10.1002/app.38438.
[75] Shibata M, Nakai K. Preparation and properties of biocomposites composed of bio-based epoxy resin, tannic acid, and microfibrillated cellulose. Journal of Polymer Science: Part B: Polymer Physics 2010;48:425–33. http://doi.org/10.1002/polb.21903.
[76] Shimasaki T, Yoshihara S, Shibata M. Preparation and properties of biocomposites composed of sorbitol-based epoxy resin, pyrogallol-vanillin calixarene, and wood flour. Polymer Composites 2012;33:1840–7. http://doi.org/10.1002/pc.22327.
[77] Feng X, East AJ, Hammond WB, Zhang Y, Jaffe M. Overview of advances in sugar-based polymers. Polymers for Advanced Technologies 2010;22:139–50. http://doi.org/10.1002/pat.1859.

[78] Chrysanthos M, Galy J, Pascault J-P. Preparation and properties of bio-based epoxy networks derived from isosorbide diglycidyl ether. Polymer 2011;52:3611–20. http://doi.org/10.1016/j.polymer.2011.06.001.
[79] East A, Jaffe M, Zhang Y., Catalani LH. Thermoset epoxy polymers from renewable resources, US 7619056 B2. 2009.
[80] Hong J, Radojčić D, Ionescu M, Petrović ZS, Eastwood E. Advanced materials from corn: isosorbide-based epoxy resins. Polymer Chemistry 2014;5:5360. http://doi.org/10.1039/c4py00514g.
[81] Dicker MPM, Duckworth PF, Baker AB, Francois G, Hazzard MK, Weaver PM. Green composites: A review of material attributes and complementary applications. Composites Part A: Applied Science and Manufacturing 2014;56:280–9. http://doi.org/10.1016/j.compositesa.2013.10.014.
[82] Faruk O, Bledzki AK, Fink H-P, Sain M. Biocomposites reinforced with natural fibers: 2000–2010. Progress in Polymer Science 2012;37:1552–96. http://doi.org/10.1016/j.progpolymsci.2012.04.003.
[83] Saha P, Manna S, Chowdhury SR, Sen R, Roy D, Adhikari B, Enhancement of tensile strength of lignocellulosic jute fibers by alkali-steam treatment. Bioresource Technology 2010;101:3182-3187. http://doi.org/10.1016/j.biortech.2009.12.010
[84] Roy A, Chakraborty S, Kundu SP, Basak RK, Basu Majumder S, Adhikari B. Improvement in mechanical properties of jute fibres through mild alkali treatment as demonstrated by utilisation of the Weibull distribution model. Bioresource Technology 2012;107:222–8. http://doi.org/10.1016/j.biortech.2011.11.073.
[85] Gassan J, Bledzki AK. Possibilities for improving the mechanical properties of jute/epoxy composites by alkali treatment of fibres. Composites Science and Technology 1999;59:1303–9. http://doi.org/10.1016/s0266-3538(98)00169-9.
[86] Doan TTL, Brodowsky H, Mäder E. Jute fibre/epoxy composites: Surface properties and interfacial adhesion. Composites Science and Technology 2012;72:1160–6. http://doi.org/10.1016/j.compscitech.2012.03.025.
[87] Pinto MA, Chalivendra VB, Kim YK, Lewis AF. Effect of surface treatment and Z-axis reinforcement on the interlaminar fracture of jute/epoxy laminated composites. Engineering Fracture Mechanics 2013;114:104–14. http://doi.org/10.1016/j.engfracmech.2013.10.015.
[88] Hossain MR, Islam MA, Van Vuurea A, Verpoest I. Tensile Behavior of Environment Friendly Jute Epoxy Laminated Composite. Procedia Engineering 2013;56:782–8. http://doi.org/10.1016/j.proeng.2013.03.196.
[89] Mishra V, Biswas S. Physical and Mechanical Properties of Bi-directional Jute Fiber Epoxy Composites. Procedia Engineering 2013;51:561–6. http://doi.org/10.1016/j.proeng.2013.01.079.
[90] Jawaid M, Abdul Khalil HPS, Abu Bakar A. Mechanical performance of oil palm empty fruit bunches/jute fibres reinforced epoxy hybrid composites. Materials Science and Engineering: A 2010;527:7944–9. http://doi.org/10.1016/j.msea.2010.09.005.
[91] Jawaid M, Abdul Khalil HPS, Abu Bakar A. Woven hybrid composites: Tensile and flexural properties of oil palm-woven jute fibres based epoxy composites. Materials Science and Engineering: A 2011;528:5190–5. http://doi.org/10.1016/j.msea.2011.03.047.

[92] Jawaid M, Khalil HPSA, Bakar AA, Khanam PN. Chemical resistance, void content and tensile properties of oil palm/jute fibre reinforced polymer hybrid composites. Materials & Design 2011;32:1014–9. http://doi.org/10.1016/j.matdes.2010.07.033.
[93] Jawaid M, Abdul Khalil HPS, Hassan A, Dungani R, Hadiyane A. Effect of jute fibre loading on tensile and dynamic mechanical properties of oil palm epoxy composites. Composites Part B: Engineering 2013;45:619–24. http://doi.org/10.1016/j.compositesb.2012.04.068.
[94] Boopalan M, Niranjanaa M, Umapathy MJ. Study on the mechanical properties and thermal properties of jute and banana fiber reinforced epoxy hybrid composites. Composites Part B: Engineering 2013;51:54–7. http://doi.org/10.1016/j.compositesb.2013.02.033.
[95] Santulli C, Sarasini F, Tirillò J, Valente T, Valente M, Caruso AP, et al. Mechanical behaviour of jute cloth/wool felts hybrid laminates. Materials & Design 2013;50:309–21. http://doi.org/10.1016/j.matdes.2013.02.079.
[96] Ramesh M, Palanikumar K, Reddy KH. Comparative Evaluation on Properties of Hybrid Glass Fiber- Sisal/Jute Reinforced Epoxy Composites. Procedia Engineering 2013;51:745–50. http://doi.org/10.1016/j.proeng.2013.01.106.
[97] Ramnath BV, Kokan SJ, Raja RN, Sathyanarayanan R, Elanchezhian C, Prasad AR, Manickavasagam VM. Evaluation of mechanical properties of abaca-jute-glass fibre reinforced epoxy composite. Materials and Design 2013;51:357–66. http://doi.org/10.1016/j.matdes.2013.03.102.
[98] Avancha S, Behera AK, Sen R, Adhikari B. Physical and mechanical characterization of jute reinforced soy composites. Journal of Reinforced Plastics and Composites 2013;32:1380–90. http://doi.org/10.1177/0731684413485979.
[99] Ramamoorthy SK, Di Q, Adekunle K, Skrifvars M. Effect of water absorption on mechanical properties of soybean oil thermosets reinforced with natural fibers. Journal of Reinforced Plastics and Composites 2012;31:1191–200. http://doi.org/10.1177/0731684412455257.
[100] Manthey NW, Cardona F, Francucci G, Aravinthan T. Thermo-mechanical properties of epoxidized hemp oil-based bioresins and biocomposites. Journal of Reinforced Plastics and Composites 2013;32:1444–56. http://doi.org/10.1177/0731684413493030.
[101] Campaner P, D'Amico D, Ferri P, Longo L, Maffezzoli A, Stifani C, et al. Cardanol Based Matrix for Jute Reinforced Pipes. Macromolecular Symposia 2010;296:526–30. http://doi.org/10.1002/masy.201051069.
[102] Jain P, Choudhary V, Varma IK. Flame retarding epoxies with phosphorus. Journal of Macromolecular Science, Part C: Polymer Reviews 2002;42:139–83. http://doi.org/10.1081/mc-120004762.
[103] Levchik SV, Weil ED. Thermal decomposition, combustion and flame-retardancy of epoxy resins - a review of the recent literature. Polymer International 2004;53:1901–29. http://doi.org/10.1002/pi.1473.
[104] Rakotomalala M, Wagner S, Döring M. Recent Developments in Halogen Free Flame Retardants for Epoxy Resins for Electrical and Electronic Applications. Materials 2010;3:4300–27. http://doi.org/10.3390/ma3084300.
[**105**] Toldy A. Chemically modified flame retardant polymers, Express Polymer Letters 2009;3(5):267. http://doi.org/10.3144/expresspolymlett.2009.33

[**106**] Marosi G, Szolnoki B, Bocz K, Toldy A. Reactive and additive phosphorus-based flame retardants of reduced environmental impact. In: Papaspyrides CD, Kiliaris P, editors. Polymer Green Flame Retardants. A Comprehensive Guide to Additives and their Applications. Amsterdam: Elsevier. 2014;5:181-221. http://doi.org/10.1016/b978-0-444-53808-6.00005-6.
[107] Wang CS, Lin CH. Synthesis and properties of phosphorus-containing epoxy resins by novel method. Journal of Polymer Science: Part A: Polymer Chemistry 1999;37:3903–9. http://doi.org/10.1002/(sici)1099-0518(19991101)37:21<3903::aid-pola4>3.0.co;2-x.
[108] Schäfer A, Seibold S, Walter O, Döring M. Novel high Tg flame retardancy approach for epoxy resins. Polymer Degradation and Stability 2008;93:557-560. http://doi.org/10.1016/j.polymdegradstab.2007.11.016
[109] Gao L-P, Wang D-Y, Wang Y-Z, Wang J-S, Yang B. A flame-retardant epoxy resin based on a reactive phosphorus-containing monomer of DODPP and its thermal and flame-retardant properties. Polymer Degradation and Stability 2008;93:1308–15. http://doi.org/10.1016/j.polymdegradstab.2008.04.004.
[110] Schäfer A, Seibold S, Lohstroh W, Walter O, Döring M. Synthesis and properties of flame-retardant epoxy resins based on DOPO and one of its analog DPPO. Journal of Applied Polymer Science 2007;105:685–96. http://doi.org/10.1002/app.26073.
[111] Ho T-H, Hwang H-J, Shieh J-Y, Chung M-C. Thermal, physical and flame-retardant properties of phosphorus-containing epoxy cured with cyanate ester. Reactive and Functional Polymers 2009;69:176–82. http://doi.org/10.1016/j.reactfunctpolym.2008.12.019.
[112] Ho T-H, Hwang H-J, Shieh J-Y, Chung M-C. Thermal and physical properties of flame-retardant epoxy resins containing 2-(6-oxido-6H-dibenz〈c,e〉〈1,2〉oxaphosphorin-6-yl)-1,4-naphthalenediol and cured with dicyanate ester. Polymer Degradation and Stability 2008;93:2077–83. http://doi.org/10.1016/j.polymdegradstab.2008.09.002.
[113] Ren H, Sun J, Wu B, Zhou Q. Synthesis and properties of a phosphorus-containing flame retardant epoxy resin based on bis-phenoxy (3-hydroxy) phenyl phosphine oxide. Polymer Degradation and Stability 2007;92:956–61. http://doi.org/10.1016/j.polymdegradstab.2007.03.006.
[114] Spontón M, Mercado LA, Ronda JC, Galià M, Cádiz V. Preparation, thermal properties and flame retardancy of phosphorus- and silicon-containing epoxy resins. Polymer Degradation and Stability 2008;93:2025–31. http://doi.org/10.1016/j.polymdegradstab.2008.02.014.
[115] Spontón M, Ronda JC, Galià M, Cádiz V. Cone calorimetry studies of benzoxazine–epoxy systems flame retarded by chemically bonded phosphorus or silicon. Polymer Degradation and Stability 2009;94:102-106. http://dx.doi.org/10.1016/j.polymdegradstab.2008.10.005
[116] Hergenrother PM, Thompson CM, Smith JG, Connell JW, Hinkley JA, Lyon RE, et al. Flame retardant aircraft epoxy resins containing phosphorus. Polymer 2005;46:5012–24. http://doi.org/10.1016/j.polymer.2005.04.025.
[117] El Gouri M, El Bachiri A, Hegazi SE, Rafik M, El Harfi A. Thermal degradation of a reactive flame retardant based on cyclotriphosphazene and its blend with DGEBA epoxy resin. Polymer Degradation and Stability 2009;94:2101–6. http://doi.org/10.1016/j.polymdegradstab.2009.08.009.

[118] Liu R, Wang X. Synthesis, characterization, thermal properties and flame retardancy of a novel nonflammable phosphazene-based epoxy resin. Polymer Degradation and Stability 2009;94:617-624. http://doi.org/10.1016/j.polymdegradstab.2009.01.008
[119] Sudhakara P, Kannan P. Diglycidylphenylphosphate based fire retardant liquid crystalline thermosets. Polymer Degradation and Stability 2009;94:610–6. http://doi.org/10.1016/j.polymdegradstab.2009.01.005.
[120] Liu W, Varley RJ, Simon GP. A phosphorus-containing diamine for flame-retardant, high-functionality epoxy resins. I. Synthesis, reactivity, and thermal degradation properties. Journal of Applied Polymer Science 2004;92:2093–100. http://doi.org/10.1002/app.20145.
[121] Liu W, Varley RJ, Simon GP. Understanding the decomposition and fire performance processes in phosphorus and nanomodified high performance epoxy resins and composites. Polymer 2007;48:2345–54. http://doi.org/10.1016/j.polymer.2007.02.022.
[122] Ananda Kumar S, Denchev Z, Alagar M. Synthesis and thermal characterization of phosphorus containing siliconized epoxy resins. European Polymer Journal 2006;42:2419–29. http://doi.org/10.1016/j.eurpolymj.2006.06.010.
[123] Jeng R, Wang J, Lin J, Liu Y, Chiu Y, Su W. Flame retardant epoxy polymers using phosphorus-containing polyalkylene amines as curing agents. Journal of Applied Polymer Science 2001;82:3526–38. http://doi.org/10.1002/app.2215.abs.
[124] Jeng R-J, Shau S-M, Lin J-J, Su W-C, Chiu Y-S. Flame retardant epoxy polymers based on all phosphorus-containing components. European Polymer Journal 2002;38:683–93. http://doi.org/10.1016/s0014-3057(01)00246-4.
[125] Zhao ZP. Synthesis and thermal degradation characterization of novel poly(phosphazene-aryl amides). Express Polymer Letters 2012;6:308–17. http://doi.org/10.3144/expresspolymlett.2012.34.
[126] Mauerer O. New reactive, halogen-free flame retardant system for epoxy resins. Polymer Degradation and Stability 2005;88:70-73. http://doi.org/10.1016/j.polymdegradstab.2004.01.027
[127] Braun U, Balabanovich AI, Schartel B, Knoll U, Artner J, Ciesielski M, et al. Influence of the oxidation state of phosphorus on the decomposition and fire behaviour of flame-retarded epoxy resin composites. Polymer 2006;47:8495–508. http://doi.org/10.1016/j.polymer.2006.10.022.
[128] Wu CS, Liu YL, Chiu Y-S. Synthesis and characterization of new organosoluble polyaspartimides containing phosphorus. Polymer 2002;43:1773–9. http://doi.org/10.1016/s0032-3861(01)00751-0.
[129] Sun D, Yao Y. Synthesis of three novel phosphorus-containing flame retardants and their application in epoxy resins. Polymer Degradation and Stability 2011;96:1720–4. http://doi.org/10.1016/j.polymdegradstab.2011.08.004.
[130] Wu CS, Liu YL, Chiu YS. Epoxy resins possessing flame retardant elements from silicon incorporated epoxy compounds cured with phosphorus or nitrogen containing curing agents. Polymer 2002;43:4277–84. http://doi.org/10.1016/s0032-3861(02)00234-3.
[131] Schartel B, Braun U, Balabanovich AI, Artner J, Ciesielski M, Döring M, et al. Pyrolysis and fire behaviour of epoxy systems containing a novel 9,10-dihydro-9-oxa-10-phosphaphenanthrene-10-oxide-(DOPO)-based diamino hardener. European Polymer Journal 2008;44:704–15. http://doi.org/10.1016/j.eurpolymj.2008.01.017.

[132] Wang X, Hu Y, Song L, Xing W, Lu H. Preparation, mechanical properties, and thermal degradation of flame retarded epoxy resins with an organophosphorus oligomer. Polymer Bulletin 2011;67:859–73. http://doi.org/10.1007/s00289-011-0473-4.
[**133**] Toldy A, Anna P, Marosi GJ. Process for the preparation of amine functional phosphoric amides and their use as flame retardant and curing agent for epoxy resins. Hungarian Patent: P0700792; 2007, PCT patent: WO2009/077796, 2009
[134] Michaelis A. Ueber die organischen Verbindungen des Phosphors mit dem Stickstoff. Justus Liebigs Annalen der Chemie 1903;326:129–258. http://doi.org/10.1002/jlac.19033260107.
[135] Das G, Karak N. Vegetable oil-based flame retardant epoxy/clay nanocomposites. Polymer Degradation and Stability 2009;94:1948–54. http://doi.org/10.1016/j.polymdegradstab.2009.07.028.
[136] Zhan M, Wool RP. Design and evaluation of bio-based composites for printed circuit board application. Composites Part A: Applied Science and Manufacturing 2013;47:22–30. http://doi.org/10.1016/j.compositesa.2012.11.014.
[137] Lligadas G, Ronda JC, Galià M, Cádiz V. Novel Silicon-Containing Polyurethanes from Vegetable Oils as Renewable Resources. Synthesis and Properties. Biomacromolecules 2006;7:2420–6. http://doi.org/10.1021/bm060402k.
[138] Pillai CKS, Prasad VS, Sudha JD, Bera SC, Menon ARR. Polymeric resins from renewable resources. II. Synthesis and characterization of flame-retardant prepolymers from cardanol. Journal of Applied Polymer Science 1990;41:2487–501. http://doi.org/10.1002/app.1990.070410947.
[139] Lligadas G, Ronda JC, Galià M, Cádiz V. Synthesis and properties of thermosetting polymers from a phosphorous-containing fatty acid derivative. Journal of Polymer Science Part A: Polymer Chemistry 2006;44:5630–44. http://doi.org/10.1002/pola.21691.
[140] Lligadas G, Ronda JC, Galià M, Cádiz V. Development of novel phosphorus-containing epoxy resins from renewable resources. Journal of Polymer Science Part A: Polymer Chemistry 2006;44:6717–27. http://doi.org/10.1002/pola.21794.
[141] Ma S, Liu X, Jiang Y, Fan L, Feng J, Zhu J. Synthesis and properties of phosphorus-containing bio-based epoxy resin from itaconic acid. Science China Chemistry 2013;57:379–88. http://doi.org/10.1007/s11426-013-5025-3.
[142] Sithique MA, Nagendiran S, Alagar M. Synthesis and Characterization of Bismaleimide-modified, Soy-based Epoxy Matrices for Flame-retardant Applications. High Performance Polymers 2009;22:328–44. http://doi.org/10.1177/0954008308101724.
[143] Moreno M, Lligadas G, Ronda JC, Galià M, Cádiz V. Phospha-Michael addition to enone-containing triglyceride derivatives as an efficient route to flame retardant renewable thermosets, Journal of Polymer Science Part A: Polymer Chemistry 2012;50:3206–13. http://doi.org/10.1002/pola.26106.
[144] Moreno M, Lligadas G, Ronda JC, Galià M, Cádiz V. Flame retardant high oleic sunflower oil-based thermosetting resins through aza- and phospha-Michael additions, Journal of Polymer Science Part A: Polymer Chemistry 2013;51:1808–15. http://doi.org/10.1002/pola.26562.
[145] Dittenber DB, GangaRao HVS. Critical review of recent publications on use of natural composites in infrastructure. Composites Part A: Applied Science and Manufacturing 2012;43:1419–29. http://doi.org/10.1016/j.compositesa.2011.11.019.

[146] Rudnik E. Thermal properties of biocomposites. Journal of Thermal Analysis and Calorimetry 2007;88:495–8. http://doi.org/10.1007/s10973-006-8127-8.
[147] Chapple S, Anandjiwala R. Flammability of Natural Fiber-reinforced Composites and Strategies for Fire Retardancy: A Review. Journal of Thermoplastic Composite Materials 2010;23:871–93. http://doi.org/10.1177/0892705709356338.
[148] Mngomezulu ME, John MJ, Jacobs V, Luyt AS. Review on flammability of biofibres and biocomposites. Carbohydrate Polymers 2014;111:149–82. http://doi.org/10.1016/j.carbpol.2014.03.071.
[149] Yang H, Yan R, Chen H, Lee DH, Zhen Ch. Characteristics of hemicelluloses, cellulose and lignin pyrolysis. Fuel 2007;86:1781–1788. http://doi.org/10.1016/j.fuel.2006.12.013
[150] Liodakis S, Fetsis IK, Agiovlasitis IP. The fire-retarding effect of inorganic phosphorus compounds on the combustion of cellulosic materials. Journal of Thermal Analysis and Calorimetry 2009;98:285–91. http://doi.org/10.1007/s10973-009-0307-x.
[151] Gaan S, Sun G. Effect of phosphorus flame retardants on thermo-oxidative decomposition of cotton. Polymer Degradation and Stability 2007;92:968–74. http://doi.org/10.1016/j.polymdegradstab.2007.03.009.
[152] Suardana NPG, Ku MS, Lim JK. Effects of diammonium phosphate on the flammability and mechanical properties of bio-composites. Materials and Design 2011;32:1990–9. http://doi.org/10.1016/j.matdes.2010.11.069.
[153] Nam S, Condon BD, Parikh D V, Zhao Q, Cintrón MS, Madison C. Effect of urea additive on the thermal decomposition of greige cotton nonwoven fabric treated with diammonium phosphate. Polymer Degradation and Stability 2011;96:2010–8. http://doi.org/10.1016/j.polymdegradstab.2011.08.014.
[**154**] Bocz K, Szolnoki B, Wladyka-Przybylak M, Bujnowicz K, Harakály Gy, Bodzay B, Zimonyi E, Toldy A, Marosi Gy. Flame retardancy of biocomposites based on thermoplastic starch. Polimery 2013;58:385–94. http://doi.org/10.14314/polimery.2013.385.
[155] Nam S, Condon BD, White RH, Zhao Q, Yao F, Cintrón MS. Effect of urea additive on the thermal decomposition kinetics of flame retardant greige cotton nonwoven fabric. Polymer Degradation and Stability 2012;97:738–46. http://doi.org/10.1016/j.polymdegradstab.2012.02.008.
[156] Xie Y, Hill CAS, Xiao Z, Militz H, Mai C. Silane coupling agents used for natural fiber/polymer composites: A review. Composites Part A: Applied Science and Manufacturing 2010;41:806–19. http://doi.org/10.1016/j.compositesa.2010.03.005.
[157] Arbelaiz A, Fernández B, Ramos JA, Mondragon I. Thermal and crystallization studies of short flax fibre reinforced polypropylene matrix composites: Effect of treatments. Thermochimica Acta 2006;440:111–21. http://doi.org/10.1016/j.tca.2005.10.016.
[158] Srikulkit K, Iamsamai C, Dubas ST. Development of flame retardant polyphosphoric acid coating based on the polyelectrolyte multilayers technique. Journal of Metals, Materials and Minerals 2006;16(2):41-45.
[159] Alongi J, Carosio F, Malucelli G. Current emerging techniques to impart flame retardancy to fabrics: An overview. Polymer Degradation and Stability 2014;106:138–49. http://doi.org/10.1016/j.polymdegradstab.2013.07.012.

[160] Le Bras M, Duquesne S, Fois M, Grisel M, Poutch F. Intumescent polypropylene/flax blends: a preliminary study. Polymer Degradation and Stability 2005;88:80–4. http://doi.org/10.1016/j.polymdegradstab.2004.04.028.
[161] Chen D, Li J, Ren J. Combustion properties and transference behavior of ultrafine microencapsulated ammonium polyphosphate in ramie fabric-reinforced poly(L-lactic acid) biocomposites. Polymer International 2010;60:599–606. http://doi.org/10.1002/pi.2986.
[162] Shumao L, Jie R, Hua Y, Tao Y, Weizhong Y. Influence of ammonium polyphosphate on the flame retardancy and mechanical properties of ramie fiber-reinforced poly(lactic acid) biocomposites. Polymer International 2009:n/a-n/a. http://doi.org/10.1002/pi.2715.
[163] Bocz K, Szolnoki B, Marosi A, Tábi T, Wladyka-Przybylak M, Marosi G. Flax fibre reinforced PLA/TPS biocomposites flame retarded with multifunctional additive system. Polymer Degradation and Stability 2014;106:63–73. http://doi.org/10.1016/j.polymdegradstab.2013.10.025.
[164] Alongi J, Ciobanu M, Malucelli G. Novel flame retardant finishing systems for cotton fabrics based on phosphorus-containing compounds and silica derived from sol–gel processes. Carbohydrate Polymers 2011;85:599–608. http://doi.org/10.1016/j.carbpol.2011.03.024.
[165] Brancatelli G, Colleoni C, Massafra MR, Rosace G. Effect of hybrid phosphorus-doped silica thin films produced by sol-gel method on the thermal behavior of cotton fabrics. Polymer Degradation and Stability 2011;96:483–90. http://doi.org/10.1016/j.polymdegradstab.2011.01.013.
[166] Yousif BF, Shalwan A, Chin CW, Ming KC. Flexural properties of treated and untreated kenaf/epoxy composites. Materials and Design 2012;40:378–85. http://doi.org/10.1016/j.matdes.2012.04.017.
[167] Lavorgna M, Romeo V, Martone A, Zarrelli M, Giordano M, Buonocore GG, Qu MZ, Fei GX, Xial HS. Silanization and silica enrichment of multiwalled carbon nanotubes: Synergistic effects on the thermal-mechanical properties of epoxy nanocomposites. European Polymer Journal 2013;49:428–38. http://doi.org/10.1016/j.eurpolymj.2012.10.003.
[168] Kuo P-Y, Yan N, Sain M. Influence of cellulose nanofibers on the curing behavior of epoxy/amine systems. European Polymer Journal 2013;49:3778–87. http://doi.org/10.1016/j.eurpolymj.2013.08.022.
[169] Godshall MA. Future directions for the sugar industry. International Sugar Journal, 2001;103:378-384.
[170] Legendre BL, Burner DM. Biomass production of sugarcane cultivars and early-generation hybrids. Biomass and Bioenergy 1995;8:55–61. http://doi.org/10.1016/0961-9534(95)00014-x.
[171] Rusznák I. Finishing of Textile Fabrics by the Thermotex Process. Textile Research Journal 1973;43:128–32. http://doi.org/10.1177/004051757304300302.
[172] Bodzay B, Marosfoi BB, Igricz T, Bocz K, Marosi G. Polymer degradation studies using laser pyrolysis-FTIR microanalysis. Journal of Analytical and Applied Pyrolysis 2009;85:313–20. http://doi.org/10.1016/j.jaap.2008.11.016.
[173] Toldy A, Anna P, Csontos I, Szabó A, Marosi G. Intrinsically flame retardant epoxy resin – Fire performance and background – Part I. Polymer Degradation and Stability 2007;92:2223–30. http://doi.org/10.1016/j.polymdegradstab.2007.04.017.
[174] Ratna D. Epoxy resins In: Handbook of Thermoset Resins. Shawbury: Smithers Rapra Technology. 2009.

[**175**] Rapi Z, Szolnoki B, Bakó P, Niedermann P, Toldy A, Bodzay B, Keglevich G, Marosi G. Synthesis and characterization of biobased epoxy monomers derived from d-glucose. European Polymer Journal 2015;67:375–82. http://doi.org/10.1016/j.eurpolymj.2014.09.025.
[176] Whistler RL, Wolfrom ML. Methods in Carbohydrate Chemistry. New York: Academic Press. 1963;2:326.
[177] Richtmeyer NK. Methods in Carbohydrate Chemistry 1962, New York: Academic Press. 1962;1:107.
[178] Laidler DA, Stoddart JF. Chiral asymmetrical crown-ethers. Carbohydrate Research 1977;55:C1–4. http://doi.org/10.1016/s0008-6215(00)84460-2.
[179] Holmberg L, Lindberg B, Lindqvist B. The reaction between epichlorohydrin and polysaccharides: Part 2, synthesis of some model substances, with cyclic substituents. Carbohydrate Research 1995;268:47–56. http://doi.org/10.1016/0008-6215(94)00293-o.
[180] Namme R, Mitsugi T, Takahashi H, Shiro M, Ikegami S. Synthesis of 1-deoxyhept-2-ulosyl-glycono-1,5-lactone utilizing α-selective O-glycosidation of 2,6-anhydro-1-deoxy-d-hept-1-enitols. Tetrahedron 2006;62:9183–92. http://doi.org/10.1016/j.tet.2006.07.032.
[181] Ohta K, Miura M, Sakaguchi K, Sugawara F, Sato N, Sahara H, Takahashi N, Mori Y, Yamazuki T, Masaki K, Murata H. US Patent 2009/0209475 A1. 2009.
[182] Huang C-Y, Cabell LA, Anslyn E V. Molecular Recognition of Cyclitols by Neutral Polyaza-Hydrogen-Bonding Receptors: The Strength and Influence of Intramolecular Hydrogen Bonds between Vicinal Alcohols. Journal of the American Chemical Society 1994;116:2778–92. http://doi.org/10.1021/ja00086a011.
[183] Wing RE, Doane WM, Rist CE. Sugars with reactive substituents: preparation of several epoxypropyl-derivatized sugars. Carbohydrate Research 1970;14:267–71. http://doi.org/10.1016/s0008-6215(00)80496-6.
[184] Indurugalla D, Bennet AJ. A Kinetic Isotope Effect Study on the Hydrolysis Reactions of Methyl Xylopyranosides and Methyl 5-Thioxylopyranosides: Oxygen versus Sulfur Stabilization of Carbenium Ions. Journal of the American Chemical Society 2001;123:10889–98. http://doi.org/10.1021/ja011232g.
[185] S. Hanessian. Preparative Carbohydrate Chemistry. New York: CRC Press. 1997.
[186] Bullock AL, Cirino VO, Rowland SP. Mono-O-(methylsulfonylethy)-d-glucoses. Canadian Journal of Chemistry 1967;45(3):255-260. http://doi.org/10.1139/v67-047
[187] Rozenberg BA. Kinetics, thermodynamics and mechanism of reactions of epoxy oligomers with amines. In Dušek K, editor, Advances in Polymer Science, Epoxy Resins and Composites II. Berlin Heidelberg: Springer-Verlag. 1986;75(4):113-165.
[188] Swier S, Van Mele B. Reaction thermodynamics of amine-cured epoxy systems: Validation of the enthalpy and heat capacity of reaction as determined by modulated temperature differential scanning calorimetry. Journal of Polymer Science Part B: Polymer Physics 2003;41:594–608. http://doi.org/10.1002/polb.10413.
[**189**] Toldy A, Szlancsik Á, Szolnoki B. Reactive flame retardancy of cyanate ester/epoxy resin blends and their carbon fibre reinforced composites. Polymer Degradation and Stability 2016;128:29–38. http://doi.org/10.1016/j.polymdegradstab.2016.02.015.

[**190**] Toldy A, Niedermann P, Szebényi G, Szolnoki B. Mechanical properties of reactively flame retarded cyanate ester/epoxy resin blends and their carbon fibre reinforced composites. Express Polymer Letters 2016;10:1016-1025. http://doi.org/10.3144/expresspolymlett.2016.94.
[**191**] Szolnoki B, Toldy A, Konrád P, Szebényi G, Marosi G. Comparison of additive and reactive phosphorus-based flame retardants in epoxy resins. Periodica Polytechnica Chemical Engineering 2013;57:85. http://doi.org/10.3311/ppch.2175.
[**192**] Unsalan O, Szolnoki B, Toldy A, Marosi G. FT-IR spectral, DFT studies and detailed vibrational assignment on N,N′,N″-tris(2-aminoethyl)-phosphoric acid triamide. Spectrochimica Acta Part A: Molecular and Biomolecular Spectroscopy 2012;98:110–5. http://doi.org/10.1016/j.saa.2012.08.050.
[**193**] Toldy A, Szolnoki B, Csontos I, Marosi G. Green synthesis and characterization of phosphorus flame retardant crosslinking agents for epoxy resins. Journal of Applied Polymer Science 2014;131:40105. http://doi.org/10.1002/app.40105.
[194] Mahmoud E, Watson DA, Lobo RF. Renewable production of phthalic anhydride from biomass-derived furan and maleic anhydride. Green Chemistry 2014;16:167–75. http://doi.org/10.1039/c3gc41655k.
[**195**] Niedermann P, Szebényi G, Toldy A. Effect of Epoxidized Soybean Oil on Curing, Rheological, Mechanical and Thermal Properties of Aromatic and Aliphatic Epoxy Resins. Journal of Polymers and the Environment 2014;22:525–36. http://doi.org/10.1007/s10924-014-0673-8.
[**196**] Niedermann P, Szebényi G, Toldy A. Novel high glass temperature sugar-based epoxy resins: Characterization and comparison to mineral oil-based aliphatic and aromatic resins. Express Polymer Letters 2015;9:85–94. http://doi.org/10.3144/expresspolymlett.2015.10.
[197] Le Bras M, Camino G, Bourbigot S, Delobel R. Fire retardancy of polymers: the use of intumescence. Cambridge: The Royal Chemical Society. 1998.
[**198**] Niedermann P, Szebényi G, Toldy A. Effect of epoxidized soybean oil on mechanical properties of woven jute fabric reinforced aromatic and aliphatic epoxy resin composites. Polymer Composites 2017. http://doi.org/10.1002/pc.23650.
[**199**] Niedermann P, Toldy A. Juta erősítés alkáli kezelésének hatása epoxigyanta kompozitok mechanikai tulajdonságaira. Műanyag és Gumi 2014;51(3):109-111. http://www.muanyagesgumi.hu/images/stories/pdf/2014/M518_2014.pdf
[200] Kabir MM, Wang H, Lau KT, Cardona F. Effects of chemical treatments on hemp fibre structure. Applied Surface Science 2013;276:13–23. http://doi.org/10.1016/j.apsusc.2013.02.086.
[201] Van de Weyenberg I, Chi Truong T, Vangrimde B, Verpoest I. Improving the properties of UD flax fibre reinforced composites by applying an alkaline fibre treatment. Composites Part A: Applied Science and Manufacturing 2006;37(9): 1368-1376. http://doi.org/10.1016/j.compositesa.2005.08.016.
[202] Fiore V, Di Bella G, Valenza A, The effect of alkaline treatment on mechanical properties of kenaf fibers and their epoxy composites. Composites Part B: Engineering, 2015;68:14-21. https://doi.org/10.1016/j.compositesb.2014.08.025.
[203] Sebestyén Z, May Z, Réczey K, Jakab E. The effect of alkaline pretreatment on the thermal decomposition of hemp. Journal of Thermal Analysis and Calorimetry 2011;105:1061-1069 http://doi.org/10.1007/s10973-010-1056-6.

[**204**] Niedermann P, Szebényi G, Toldy A. Characterization of high glass transition temperature sugar-based epoxy resin composites with jute and carbon fibre reinforcement. Composites Science and Technology 2015;117:62–8. http://doi.org/10.1016/j.compscitech.2015.06.001.
[205] Davis DC, Wilkerson JW, Zhu J, Hadjiev VG. A strategy for improving mechanical properties of a fiber reinforced epoxy composite using functionalized carbon nanotubes. Composites Science and Technology 2011;71:1089–97. http://doi.org/10.1016/j.compscitech.2011.03.014.
[206] Laoutid F, Bonnaud L, Alexandre M, Lopez-Cuesta J-M, Dubois P. New prospects in flame retardant polymer materials: From fundamentals to nanocomposites. Materials Science and Engineering: R: Reports 2009;63:100–25. http://doi.org/10.1016/j.mser.2008.09.002.
[207] Wang J-S, Liu Y, Zhao H-B, Liu J, Wang D-Y, Song Y-P, et al. Metal compound-enhanced flame retardancy of intumescent epoxy resins containing ammonium polyphosphate. Polymer Degradation and Stability 2009;94:625–31. http://doi.org/10.1016/j.polymdegradstab.2009.01.006.
[208] Wu K, Zhang Y-K, Zhang K, Shen M-M, Hu Y. Effect of microencapsulation on thermal properties and flammability performance of epoxy composite. Journal of Analytical and Applied Pyrolysis 2012;94:196–201. http://doi.org/10.1016/j.jaap.2011.12.009.
[209] Salmeia KA, Gaan S. An overview of some recent advances in DOPO-derivatives: Chemistry and flame retardant applications. Polymer Degradation and Stability 2015;113:119–34. http://doi.org/10.1016/j.polymdegradstab.2014.12.014.
[210] Schartel B. Phosphorus-based Flame Retardancy Mechanisms—Old Hat or a Starting Point for Future Development? Materials 2010;3:4710–45. http://doi.org/10.3390/ma3104710.
[**211**] Toldy A, Anna P, Novák Cs, Madarász J, Tóth A, Marosi Gy. Intrinsically flame retardant epoxy resin - fire performance and background - Part 2. Polymer Degradation and Stability 2008;93(11): 2007-2013. http://dx.doi.org/10.1016/j.polymdegradstab.2008.02.011
[212] Howell BA. Development of additives possessing both solid-phase and gas-phase flame retardant activities. Polymer Degradation and Stability 2008;93:2052–7. http://doi.org/10.1016/j.polymdegradstab.2008.02.019.
[213] Levchik S V. A Review of Recent Progress in Phosphorus-based Flame Retardants. Journal of Fire Sciences 2006;24:345–64. http://doi.org/10.1177/0734904106068426.
[214] Pawlowski KH, Schartel B. Flame retardancy mechanisms of triphenyl phosphate, resorcinol bis(diphenyl phosphate) and bisphenol A bis(diphenyl phosphate) in polycarbonate/acrylonitrile–butadiene–styrene blends. Polymer International 2007;56:1404–14. http://doi.org/10.1002/pi.2290.
[215] Bright DA, Dashevsky S, Moy PY, Williams B. Resorcinol bis(diphenyl phosphate), a non-halogen flame-retardant additive. Journal of Vinyl and Additive Technology 1997;3:170–4. http://doi.org/10.1002/vnl.10184.
[216] Walters RN, Lyon RE. Fire-resistant cyanate ester-epoxy blends. Fire and Materials 2003;27:183–94. http://doi.org/10.1002/fam.827.
[217] Hamerton I, Hay JN. Recent developments in the chemistry of cyanate esters. Polymer International 1998;47:465–73. http://doi.org/10.1002/(sici)1097-0126(199812)47:4<465::aid-pi88>3.0.co;2-s.

[218] Martin MD, Ormaetxea M, Harismendy I, Remiro PM, Mondragon I. Cure chemo-rheology of mixtures based on epoxy resins and ester cyanates. European Polymer Journal 1999;35:57–68. http://doi.org/10.1016/s0014-3057(98)00095-0.

[**219**] Toldy A. Cyanate ester resins – 'old newcomers' among high performance composite materials. Express Polymer Letters, 2013;7(9):722-722. http://doi.org/10.3144/expresspolymlett.2013.69

[**220**] Szolnoki B, Bocz K, Marosi G, Toldy A. Flame Retardancy of Sorbitol Based Bioepoxy via Combined Solid and Gas Phase Action. Polymers 2016;8:322. http://doi.org/10.3390/polym8090322.

[**221**] Toldy A, Niedermann P, Szolnoki B**,** Flame retardancy of glucofuranoside based bioepoxy and composites made thereof. Polymer Degradation and Stability, 2017;142:62. http://dx.doi.org/10.1016/j.polymdegradstab.2017.05.024

[222] Bauer M, Bauer J. Co-reactions of cyanate esters with epoxies, In: Hamerton I, editor. Chemistry and Technology of Cyanate Ester Resins. London: Blackie Academic & Professional (Chapman & Hall), 1994;77-82.

[223] Zhang W, He X, Song T, Jiao Q, Yang R. The influence of the phosphorus-based flame retardant on the flame retardancy of the epoxy resins. Polymer Degradation and Stability 2014;109:209–17. http://doi.org/10.1016/j.polymdegradstab.2014.07.023.

[**224**] Toldy A, Szolnoki B, Marosi G. Flame retardancy of fibre-reinforced epoxy resin composites for aerospace applications. Polymer Degradation and Stability 2011;96:371–6. http://doi.org/10.1016/j.polymdegradstab.2010.03.021.

[**225**] Toldy A, Niedermann P, Pomázi Á, Marosi Gy, Szolnoki B. Flame retardancy of carbon fibre reinforced sorbitol based bioepoxy composites. Materials 2017;10:467. http://dx.doi.org/10.3390/ma10050467

[**226**] Marosi Gy, Szolnoki B, Bocz K, Toldy A. Fire retardant recyclable and bio-based polymer composites. In: Wang D-Y, editor. Novel Fire Retardant Polymers and Composite Materials: Technological Advances and Commercial Applications. Cambridge: Woodhead Publishing Ltd. 2016;5:117-146.

[227] Hay JN. Processing and cure schedules for cyanate esters. In: Hamerton I, editor. Chemistry and Technology of Cyanate Ester Resins. London: Blackie Academic & Professional (Chapman & Hall), 1994;151-192.

[**228**] Toldy A, Szolnoki B, Czeller A. Égésgátolt szénszálerősítésű epoxigyanta-kompozitok fejlesztése repüléstechnikai alkalmazásokhoz. Műanyag és Gumi 2010;47(10):384-386. http://www.muanyagesgumi.hu/images/stories/pdf/2010/M123.pdf

[**229**] Szolnoki B, Bocz K, Sóti PL, Bodzay B, Zimonyi E, Toldy A, Morlin B, Bujnowicz K, Wladyka-Przybylak M, Marosi G. Development of natural fibre reinforced flame retarded epoxy resin composites. Polymer Degradation and Stability 2015;119:68–76. http://doi.org/10.1016/j.polymdegradstab.2015.04.028.

[230] Zhang J, Zhang B, Zhang J, Lin L, Liu S, Ouyang P. Effect of phosphoric acid pretreatment on enzymatic hydrolysis of microcrystalline cellulose. Biotechnology Advances 2010;28:613–9. http://doi.org/10.1016/j.biotechadv.2010.05.010.

[231] Wei S. Phosphoric acid mediated depolymerization and decrystallization of cellulose: Preparation of low crystallinity cellulose — A new pharmaceutical excipient. International Journal of Pharmaceutics 1996;142:175–81. http://doi.org/10.1016/0378-5173(96)04673-x.
[232] Zhang L, Choi EJ, Kim MH, Lee GM, Suh H, Kim I. pH-reversible supramolecular hydrogels based on aminoalkyl phosphoamide compounds. Supramolecular Chemistry 2012;24:189–96. http://doi.org/10.1080/10610278.2011.638382.
[233] Zhang L, Zheng S, Kim KH, Kim I. Simple and environmentally friendly preparation and stabilization of gold nano- and microcrystals using N,N′,N″-tris(2-aminoethyl)phosphoric triamide. Current Applied Physics 2012;12:104-111. http://doi.org/10.1016/j.cap.2012.02.030.
[**234**] Farkas E, Meszena ZG, Toldy A, Matkó S, Marosfői BB, Marosi G. Modelling of transport processes in a developing char. Polymer Degradation and Stability 2008;93:1205–13. http://doi.org/10.1016/j.polymdegradstab.2008.02.010.
[**235**] Farkas E, Toldy A, Matkó S, Marosfõi BB, Marosi G, Meszena ZG. Degradation of Neat and Flame Retarded Polymer - Comparison of Simulation and Experimental Results. Chemie Ingenieur Technik 2008;80:1430. http://doi.org/10.1002/cite.200750619.
[236] Ertl P, Rohde B, Selzer P. Fast Calculation of Molecular Polar Surface Area as a Sum of Fragment-Based Contributions and Its Application to the Prediction of Drug Transport Properties Journal of Medicinal Chemistry 2000;43:3714–7. http://doi.org/10.1021/jm000942e.

ISBN 978-963-313-262-3